**File No. 39-832/2010 (SR)**

A Final Report on

Major Research Project entitled

# "Synthesis of nanostructured mono and bimetallic cluster of Cu and Mo and their application as catalyst in various organic reactions."

***Submitted to,***

**University Grants Commission,**
**Bahadur Shah Zafar Marg, New Delhi-110 002**

***Submitted by,***

**Dr. Anjali S. Rajbhoj**

Principal Investigator
Professor & Head
Department of Chemistry
Dr. Babasaheb Ambedkar Marathwada University,
Aurangabad, 431 004 (M.S.) India

# Index


| Chapter | Title | Page no. |
|---|---|---|
| **1** | **Introduction** | **1-31** |
| *1.1* | *Nanotechnology* | *1* |
| *1.2* | *Properties of nanoparticles* | *5* |
| *1.3* | *Methods of Synthesis* | *9* |
| *1.4* | *Characterization Techniques* | *13* |
| *1.5* | *Application of Nanoparticles* | *20* |
| *1.6* | *Literature survey* | *24* |
| *1.7* | *Aim and Objective of the project* | *25* |
| *1.8* | *Reference* | *27* |
| **2** | **Experimental** | **32-65** |
| *2.0* | *Experimental* | *32* |
| *2.1* | *Synthesis of monometallic nanoparticles* | *34* |
| *2.1.1* | *Variation of process parameters* | *36* |
| *2.2* | *Synthesis of bimetallic nanoparticles* | *37* |
| *2.2.1* | *Variation of process parameters* | *38* |
| *2.3* | *Sample Preparation For Characterization Techniques* | *38* |
| **Section I** | **Copper Nanoparticles** | **39-45** |
| *2.4.1* | *Introduction* | *39* |
| *2.4.2* | *Visual Inspection* | *40* |
| *2.4.3* | *UV-Visible Spectroscopic Study* | *40* |
| *2.4.4* | *Infrared Spectroscopic Study* | *42* |
| *2.4.5* | *X-Ray Diffraction Study* | *42* |
| *2.4.6* | *Scanning Electron Microscopic Study and Energy Dispersive Spectroscopic Study* | *44* |
| *2.4.7* | *Transmission Electron Microscopic Study* | *45* |
| **Section II** | **Molybdenum oxide Nanoparticles** | **46-53** |
| *2.5.1* | *Introduction* | *46* |
| *2.5.2* | *Visual Inspection* | *46* |
| *2.5.3* | *UV-Visible Spectroscopic Study* | *47* |
| *2.5.4* | *Infrared Spectroscopic Study* | *48* |
| *2.5.5* | *X-Ray Diffraction Study* | *49* |
| *2.5.6* | *Scanning Electron Microscopic Study and Energy Dispersive Spectroscopic Study* | *50* |
| *2.5.7* | *Transmission Electron Microscopic Study* | *52* |
| **Section III** | **Cu-Mo Bimetallic Nanoparticles** | **54-65** |
| *2.6.1* | *Introduction* | *54* |
| *2.6.2* | *Visual Inspection* | *54* |
| *2.6.3* | *UV-Visible Spectroscopic Study* | *55* |

| | | |
|---|---|---|
| *2.6.4* | *Infrared Spectroscopic Study* | *56* |
| *2.6.5* | *X-Ray Diffraction Study* | *57* |
| *2.6.6* | *Scanning Electron Microscopic Study and Energy Dispersive Spectroscopic Study* | *58* |
| *2.6.7* | *Transmission Electron Microscopic Study* | *60* |
| *2.6.8* | *Reference* | *62* |
| **3** | **Study of catalytical activity of monometallic & bimetallic nanoparticles** | **66-135** |
| *3.1* | *Scope and application* | *66* |
| **Section A** | **Copper nanoparticles catalyzed organic transformation reactions** | ***68-83*** |
| *3.2* | **Solvent free green synthesis of 5-arylidine barbituric acid derivatives catalyzed by copper oxide NPs** | |
| *3.2.1* | *Introduction* | *68* |
| *3.2.2* | *Literature reviews* | *68* |
| *3.2.3* | *Present work* | *69* |
| *3.2.4* | *Experimental* | *69* |
| *3.2.5* | *Spectral data of representative compound* | *69* |
| *3.2.6* | *Result and Discussion* | *70* |
| *3.2.7* | *Conclusion* | *72* |
| *3.3* | **Synthesis of 2-benzylidenemalononitrile catalyzed by copper oxide nanoparticles** | |
| *3.3.1* | *Introduction* | *73* |
| *3.3.2* | *Literature reviews* | *73* |
| *3.3.3* | *Present work* | *74* |
| *3.3.4* | *Experimental* | *74* |
| *3.3.5* | *Spectral data of representative compound* | *75* |
| *3.3.6* | *Result and Discussion* | *75* |
| *3.3.7* | *Conclusion* | *76* |
| *3.4* | **Synthesis of 1, 2-dibenzylidenehydrazine derivatives catalyzed by copper oxide nanoparticles** | |
| *3.4.1* | *Introduction* | *78* |
| *3.4.2* | *Literature reviews* | *78* |
| *3.4.3* | *Present work* | *79* |
| *3.4.4* | *Experimental* | *80* |
| *3.4.5* | *Spectral data of representative compound* | *80* |
| *3.4.6* | *Result and Discussion* | *81* |
| *3.4.7* | *Conclusion* | *82* |
| **Section B** | **$MoO_3$ nanoparticles catalyzed organic transformation reactions** | ***84-105*** |
| *3.5* | **Synthesis of 2, 6-bis (benzylidene) cyclohexanones** | |

| | | |
|---|---|---|
| | **derivatives catalyzed by $MoO_3$ nanoparticles** | |
| *3.5.1* | *Introduction* | *84* |
| *3.5.2* | *Literature reviews* | *84* |
| *3.5.3* | *Present work* | *85* |
| *3.5.4* | *Experimental* | *85* |
| *3.5.5* | *Spectral data of representative compound* | *86* |
| *3.5.6* | *Result and Discussion* | *86* |
| *3.5.7* | *Conclusion* | *88* |
| *3.6* | **Synthesis of (1E,4E)-1,5-diphenylpenta-1,4-dien-3-one derivatives catalyzed by $MoO_3$ nanoparticles** | |
| *3.6.1* | *Introduction* | *90* |
| *3.6.2* | *Literature reviews* | *90* |
| *3.6.3* | *Present work* | *91* |
| *3.6.4* | *Experimental* | *92* |
| *3.6.5* | *Spectral data of representative compound* | *92* |
| *3.6.6* | *Result and Discussion* | *92* |
| *3.6.7* | *Conclusion* | *94* |
| *3.7* | **Green synthesis of 2-phenylbenzo[d]thiazole derivatives catalyzed by $MoO_3$ nanorods** | |
| *3.7.1* | *Introduction* | *96* |
| *3.7.2* | *Literature reviews* | *96* |
| *3.7.3* | *Present work* | *96* |
| *3.7.4* | *Experimental* | *97* |
| *3.7.5* | *Spectral data of representative compound* | *97* |
| *3.7.6* | *Result and Discussion* | *98* |
| *3.7.7* | *Conclusion* | *99* |
| *3.8* | **Synthesis of 2-phenylbenzo[d]oxazole derivatives catalyzed by $MoO_3$ nanoparticles** | |
| *3.8.1* | *Introduction* | *101* |
| *3.8.2* | *Literature reviews* | *101* |
| *3.8.3* | *Present work* | *102* |
| *3.8.4* | *Experimental* | *102* |
| *3.8.5* | *Spectral data of representative compound* | *103* |
| *3.8.6* | *Result and Discussion* | *103* |
| *3.8.7* | *Conclusion* | *104* |
| **Section C** | **Cu-Mo nanoparticles catalyzed organic transformation** | **105-135** |
| *3.9* | **Synthesis of 2-phenylbenzo[d]imidazole derivatives catalyzed by Cu-Mo nanoparticles** | |
| *3.9.1* | *Introduction* | *106* |

| | | |
|---|---|---|
| *3.9.2* | *Literature reviews* | *106* |
| *3.9.3* | *Present work* | *107* |
| *3.9.4* | *Experimental* | *107* |
| *3.9.5* | *Spectral data of representative compound* | *108* |
| *3.9.6* | *Result and Discussion* | *108* |
| *3.9.7* | *Conclusion* | *110* |
| *3.10* | **Synthesis of 2-phenylbenzo[d]oxazole derivatives catalyzed by Cu-Mo nanoparticles** | |
| *3.10.1* | *Introduction* | *112* |
| *3.10.2* | *Literature reviews* | *112* |
| *3.10.3* | *Present work* | *113* |
| *3.10.4* | *Experimental* | *113* |
| *3.10.5* | *Spectral data of representative compound* | *114* |
| *3.10.6* | *Result and Discussion* | *114* |
| *3.10.7* | *Conclusion* | *116* |
| *3.11* | **Green synthesis of 2-phenylbenzo[d]thiazole derivatives catalyzed by Cu-Mo nanoparticles** | |
| *3.11.1* | *Introduction* | *118* |
| *3.11.2* | *Literature reviews* | *118* |
| *3.11.3* | *Present work* | *118* |
| *3.11.4* | *Experimental* | *119* |
| *3.11.5* | *Spectral data of representative compound* | *119* |
| *3.11.6* | *Result and Discussion* | *120* |
| *3.11.7* | *Conclusion* | *121* |
| *3.12* | **Synthesis of (Z)-5-benzylidenethiazolidine-2,4-dione derivatives catalyzed by Cu-Mo nanoparticles** | |
| *3.12.1* | *Introduction* | *123* |
| *3.12.2* | *Literature reviews* | *124* |
| *3.12.3* | *Present work* | *125* |
| *3.12.4* | *Experimental* | *125* |
| *3.12.5* | *Spectral data of representative compound* | *126* |
| *3.12.6* | *Result and Discussion* | *126* |
| *3.12.7* | *Conclusion* | *127* |
| *3.13* | *Reference* | *129-135* |
| | **Summary and Conclusion** | **136-139** |
| | **List of Publication** | **140** |

## 1.0 Introduction

Nanoscience and nanotechnology is implanting its footprint in the present decade very rapidly. The twenty-first century is in many ways the century of nanotechnology. Nanotechnology represents a rather broad interdisciplinary field of research and industrial activities involving particles less than 100 nanometer (nm) in diameter. Nanomaterials have evoked wide interest in science mainly due to their unpredictable properties and the ability to control design and fabricate materials at nanoscale.

In recent years, research work in the area of particles of smaller size (1-10 nm) has received greater attention [1]. Exhaustive study has been carried out in methodology of preparation and stabilization of these nanocrystalline materials, as well as in studying their physical and chemical properties. The nanomaterials are designed at the molecular (nanometer) level to take advantage of their small size and possessing novel properties which are generally not seen in their conventional, bulk counterparts. The two main reasons why materials at the nanoscale can have different properties such as increased relative surface area and new quantum size effects. Nanomaterials have a much greater surface area to volume ratio than their conventional forms which can lead to greater chemical reactivity and affect their strength. At the nano scale, quantum effects can become much more important in determining the material properties and characteristics leading to novel optical, electrical and magnetic behavior.

## 1.1 Nanotechnology

"Nanotechnology" is the manipulation of atoms, molecules and materials to form structures on the scale of nanometers (billionths of a meter). These nanostructures typically exhibit new properties or behaviors different from that of bulk materials. In 1974 Taniguchi [2] Japan first introduced the word "Nanotechnology". In Greek nanotechnology is derived from "nano" which means dwarf and "technologies" which means systematic treatment of an art or craft. It can also be said to be a science and engineering of making material, functional structures and devices on the nanometer scale. In scientific terms "nano" means $10^{-9}$ meter.

Material chemists are recently focusing on entities with atomic and molecular dimensions ranging from 0.1 to 10 nm, whereas solid-state chemists and material chemists have traditionally been concerned with solid materials with dimensions greater than 100 nm [3]. Nanomaterials are of interest because at this scale these materials show unique optical, magnetic, electrical, and

other properties. These emergent properties have the potential for great impacts in electronics, medicine, and other fields [4-7].

Richard P. Feynman (Nobel Laureate in Physics, 1965) is often credited for introducing the concept of nanotechnology. Nanotechnology is the creation of useful/functional materials, devices and systems through control of matter on the nanometer length scale and exploitation of novel phenomena and properties (chemical, physical, biological) at that length scale. Nanotechnology as defined by size is naturally very broad, including fields of science as diverse as surface science, organic chemistry, molecular biology, semiconductor physics, micro electronics, Information Technology etc. The associated research and applications are equally diverse, ranging from extensions of conventional device physics to completely new approaches based upon molecular self-assembly, from developing new materials with dimensions on the nanoscale to direct control of matter on the atomic scale.

### 1.1.1 Nanoparticles

Today, nanomaterials show an emerging, interdisciplinary science that deals with the synthesis of nanomaterials with scientific investigations. Overall, the nanomaterials has tremendous prospective in commercial and technological advances. The nanomaterials possess one or more dimensions of the order of 100 nanometer (nm) or less [8-11]. Nanomaterials are larger than single atom but smaller than bacteria and cells. It is useful to use a scale like the as shown in **Fig.1.1** where we can visualize the relationship between bulk materials like ant and nanomaterials. Nanomaterial and nanodevices that are of interest in nanotechnologies are in the lower end of the scale.

There are naturally occurred nanomaterials and synthetically prepared nanomaterials. The wax crystals covering a lotus or nasturtium leaf, some butterfly wing scales, spider and spider-mite silk [12], natural colloids (milk, blood), bone matrix, horny materials (skin, claws, beaks, feathers, horns, hair) are the examples of natural organic nanomaterials. Natural inorganic nanomaterials occur through crystal growth in the diverse chemical conditions of the earth's crust. Fullerenes, carbon nanotubes are some of the examples of synthetic organic nanomaterials. Inorganic nanomaterials are based on other elements, such as silicon. Solids and molecules have been studied and understood quite well, however nanomaterials exhibit properties that are entirely different from either of the two. If the physical size of the material is reduced below the nanometer length scale, all its properties like mechanical strength, thermal, optical, magnetic,

electrical conducting etc. change and become sensitive to its size and shape. The reason for the variation in properties with size of the materials stems from extremely large surface-to-volume ratio. The number of surface atom increases with decreasing particle size.

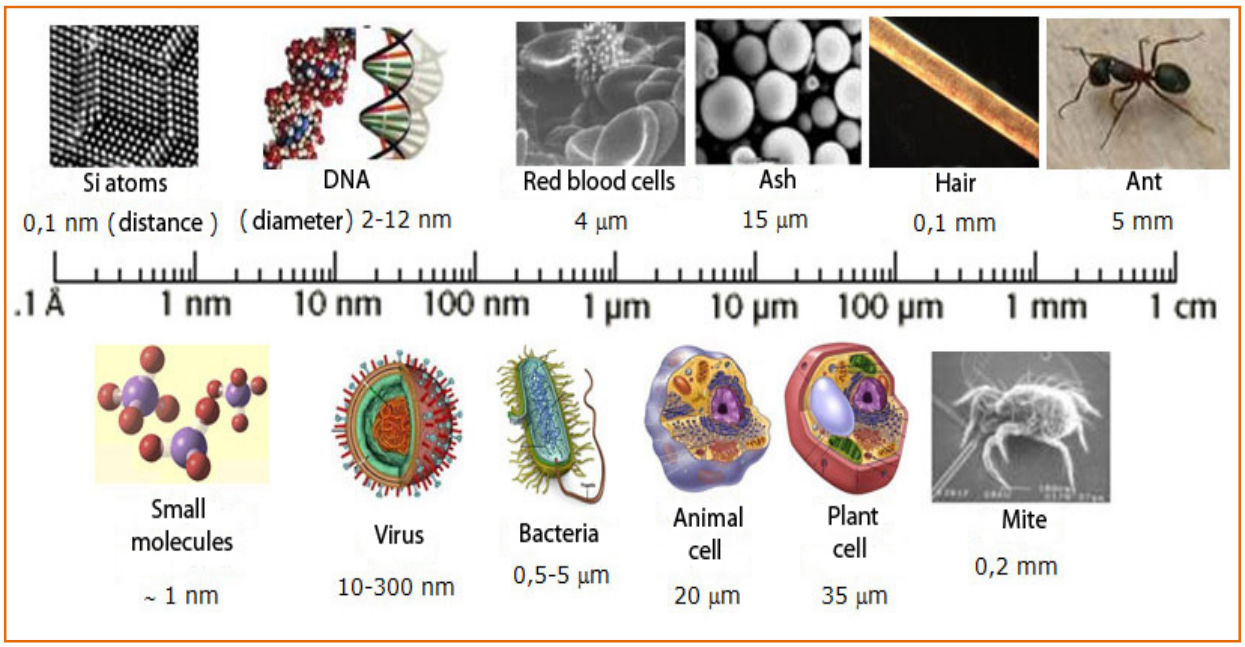


**Fig.1.1** Relative size of macro material to atom

Nanomaterials can be synthesized by growing and shaping the materials by variety of physical, chemical, biological or hybrid methods. All the nanomaterial synthesis methods are often divided into two categories: *top down* and *bottom up* approach [13]. In *top down* approach materials are brought down from a larger size to nanometer dimensions. This approach involves milling, machining and lithographic techniques. On the other hand, it is also possible to start with atoms or molecules, bring them together to make the required particles or assemblies of nanometer size. This is known as *bottom up* approach. The *bottom up* approach consists of physical as well as chemical methods. One classification of nanomaterials is according to the number of dimensions which lie within the nanometer range of 1 to 100 nm**.** According to Siegel nanomaterials are classified **(Fig.1.2)** into 0-dimension (clusters), 1-dimension (nanorods, fibres and rods), 2-dimensions (nanosheets, films) or 3-dimensions (polycrystals). Any changes in the dimensions of the system influence the electronic density of state which in turn will affect the optical and electronic properties of nanomaterials [13].

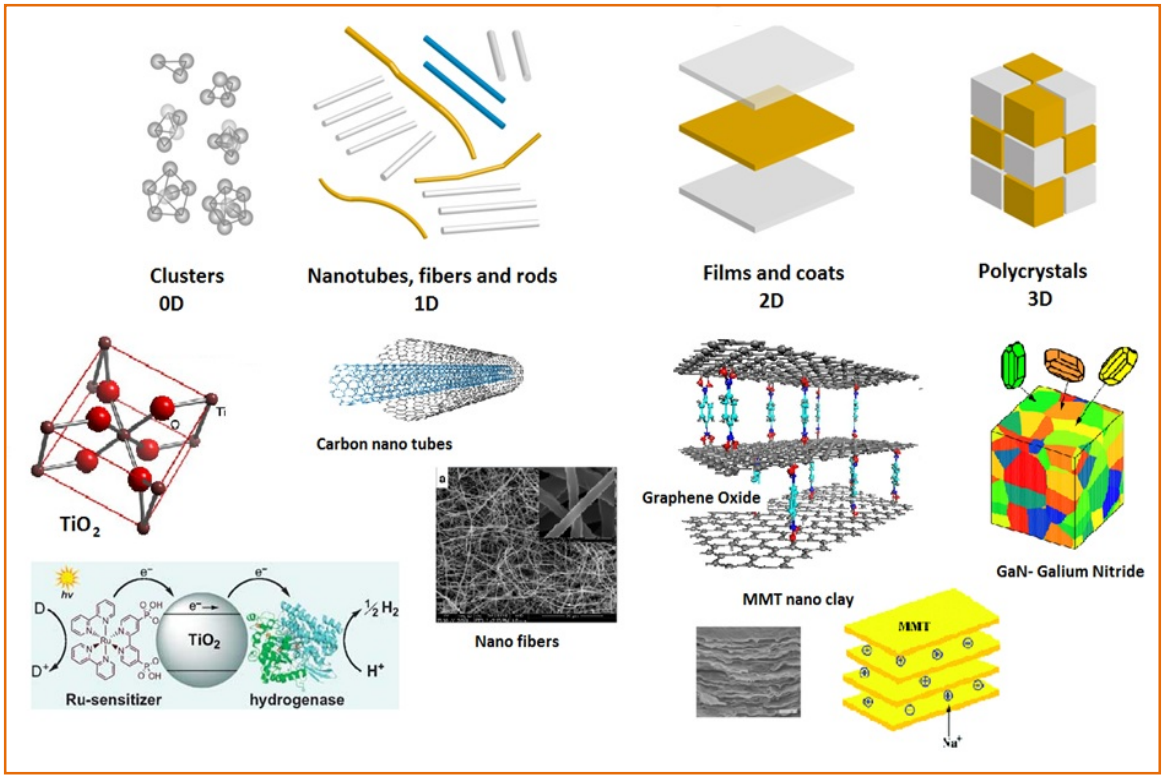


**Fig. 1.2** Classification of Nanomaterials

### 1.1.2 History of Nanoparticles

Roman people had experienced nanotechnology in 4$^{th}$ century A.D. They were incorporating the gold nanoparticles in the cup when the glass was molten and were calling it as 'Lycurgus Cup', named after a king 'Lycurgus' which is an outstanding example of ancient nanotechnology. This cup is preserved in British Museum and looks red when light is transmitted and green if light is reflected from it (unique red-green dichroism).Vibrant stained glass windows in 6$^{th}$-15$^{th}$ centuries in European cathedrals owed their rich colors to nanoparticles of gold chloride and other metal oxides and chlorides. The glaziers who created gold-painted stained glass windows for mediaeval churches in Europe developed a solar-powered nanotech air-purification system. The gold paint used in mediaeval-era stained glass windows purified the air when heated by sunlight. For centuries people appreciated only the beautiful works of art, and long life of the color, but little did they realize that these works of art are also, in modern language, photocatalytic air purifier with nanostructured gold catalyst.

In 1831, Michael Faraday investigated the ruby red colloids of gold and made public that the color was due to the small size of the metal particles [14]. Gold and silver have found their way into glasses for over 200 years as nanoparticles. Beautiful examples of this can be found in glass

windows of many Gothic European cathedrals. These vivid colors which were observed controlled by the size and the form or shape of the nanoparticles of gold and silver. The relation between particles size, shape and their associated colors has been discussed recently by Jin and coworkers [15-16].

The first time the idea of nanotechnology was introduced was in 1959 when Richard Feynman, a physicist at Caltech gave a talk called "There's Plenty of Room at the Bottom"[17]. Though he never explicitly mentioned "nanotechnology," Feynman suggested that it will eventually be possible to precisely manipulate atoms and molecules. Specifically, he suggested that as the scale got smaller and smaller gravity would become more negligible while both Van Der Waals attraction and surface tension would become very important.

## 1.2 Properties of nanoparticles

Nanoparticles are defined very generally as objects whose three spatial dimensions are confined to less than 100nm, intermediately between the molecular state and the bulk state show chemical and physical properties different from those of the bulk materials. It has even been suggested that they are a new state of matter.

The physical and chemical properties of metal nanoparticles depend upon several factors such as a) large surface atom, b) large surface energy, c) spatial confinement d) particle size, e) structure, f) organization of the particles and their dispersity. Numerous studies [18-22] on size and shape dependent properties have been carried out in the last two decades. The size dependent physical and chemical properties have been studied extensively by many scientists [23-25]. The few properties of nanomaterials are discussed as follows:

**a) Mechanical properties:**

The clusters interact fully with one another, yet the effect of cluster size is still important. Clusters of metals and ceramics in the size range of 5 - 25 nm have been consolidated to form ultrafine grained polycrystals that have mechanical properties remarkably different from and frequently better than those of their conventional coarse grained counterparts [26]. The mechanical properties of nanomaterials increase with the decrease in size. Most of the studies have been focused on the mechanical properties of one dimensional structure such as nanowire. The enhanced mechanical strength of nanowires or nanorods is ascribed to the high internal perfection of the nanowires.

b) **Color:**

One of the many applications that take advantage of the unique optical properties of metal nanoparticles is color engineering - where custom nanoparticle formulations are designed to absorb and scatter specific wavelengths of light to generate a color. Plasmonically generated colors are unique in that the optical properties of metal nanoparticles can be tuned by changing size, shape and material composition. As the size decreases, band gap increases and thus the position of the fluorescence band is shifted to the shorter wavelength [27]. Since ancient time gold was used to stain glass with beautiful colours such as red, purple and burgundy [28]. Gold nanospheres have a characteristic red colour, while silver nanospheres are yellow. The color is due to the electron cloud at the surface of a gold nanoparticle which resonates with different wavelengths of light depending upon their frequency. Depending on the size of the nanoparticle, the electron cloud will be in resonance with a particular wavelength of light and absorb that wavelength [29]. The colour of the metal nanoparticles in suspended state changes with the size. As the size decreases band gap increases and thus the position of the fluorescence band is shifted to the shorter wave length [30].

**c) Optical Properties:**

Nanoparticles have a surface plasmon resonance absorption in the UV–Visible region. The surface plasmon band arises from the coherent existence of free electrons in the conduction band due to the small particle size effect [31]. The band shift is dependent on the particle size, surrounding chemical and dielectric constant [32]. Metal nanoparticles [33] which are of particular interest in this work are optically active in the visible range of the spectrum. For last few decades, metallic nanoparticles have fascinated researchers due to their colorful colloidal solutions. Mie was the first to explain the red color of gold nanoparticles in 1908 by solving Maxwell's equation for an electromagnetic light wave interacting with small metallic spheres.

When the crystal size becomes smaller than the wavelength of the visible light, nanoparticles partially transmit the light which results in changes of the color of the dispersion. The reason for this modification is the presence of a strong optical absorption in the visible region arising from the surface plasmon excitation in response to the external electromagnetic field. As nanocluster size decreases, there is a dramatic increase in the surface plasmon resonance band width accompanied by a shift in the resonance position

(generally a red-shift). As an example, gold particles of 30-500nm in size changes their color from blue to red. For the smaller Au nanoparticles there is broad surface plasma absorption between the green and yellow wavelengths allowing only red light to be transmitted. This is one reason for the typical red color of stained glasses containing a dispersion of gold nanoparticles [34-37].

**d) Thermal Properties:**

As compared to the study of other well known properties of the nanomaterials, this study has seen slower progress. This is partially due to the difficulties of experimentally measuring and controlling the thermal transport in nanoscale dimensions. Atomic Force Microscope [38] (AFM) has been introduced to measure the thermal transport of nanostructures with nanometer scale having a high special resolution providing for a promising way to probe the thermal properties with nanostructures. Recent advances in experiments have showed that certain nanomaterials have extraordinary thermal properties as compared to their macroscopic counterparts. This is attributed due to several factors such as the small size, special shape; the large interfaces modified the thermal properties of the nanomaterials rendering them to quite different behavior. As the dimension goes down to nanoscales, the size of the nanomaterial is comparable to the wavelength and the mean free path of the photons. Due to the photon confinement and quantization of photon transport, the phototransfer within the materials will be changed significantly resulting in modified thermal properties. For e.g. nanowires [39] from silicon have a much smaller thermal conductivity as compared to bulk silicon. Carbon nanotubes [40] have extreme high thermal conductivity in axial direction leaving high anisotropy in the heat transports in the materials. Metal and semiconductor nanoparticles are found to have significantly lower melting point or phase transition temperature as compared to their bulk counterparts. The decrease in the phase transition temperature can be ascribed to the changes in the ratio of surface energy to volume energy as a function of size. The lowering of the melting points is observed when the particle size is >100 nm and is attributed to increase in surface energy with a reduction of size.

**e) Electronic Properties:**

In the nano-regime the electronic, structural, magnetic and thermodynamic properties are essentially size-dependent [41,42]. A root cause for this behavior is that the electronic energy levels in a quantum dot are not continuous as in the bulk but are discrete, due to the

confinement of the electron wave function in finite physical dimensions of the particle. The average electronic energy level spacing of successive quantum levels ($\delta$) known as the so called Kubo gap, is given by, $\delta = 4E_f/3n$, where $E_f$ is the Fermi energy of the bulk material and n is the total number of valence electrons in the nanocrystal. Thus, for an individual silver nanoparticle of 3 nm diameter containing approximately one thousand silver atoms, the value of $\delta$ would be 5–10 MeV [43]. Tunnelling measurements by Thomas [44] et al. have shown that clusters containing few tenths of atoms with diameters ~ 1 $nm^3$ are essentially non-metallic at room temperature while clusters with slightly larger diameters are metallic. It may be noted that a $Pd_{561}$ nanocrystal with its metal-core diameter of 2.5 nm exists virtually at the metal–non metal boundary.

f) **Specific Surface Area:**

Nanoscale materials have far larger surface areas than similar masses of large-scale materials. As surface area per mass of a material increases, a greater amount of the material can come into contact with surrounding materials thus enhancing reactivity. When a metal particle decreases in size to become a nanoparticle or a nanocrystal, a greater proportion of atoms are found at the surface [45]. Specific surface area is relevant for unique catalytic reactivity; physical, chemical and biological properties of nanomaterials originate from these two features. If a bulk material is subdivided into an ensemble of individual nanomaterials, the total volume remains the same but the collectively surface area is greatly increased. This is schematically shown in **Fig. 1.3.** The consequence is that the surface to volume ratio of the material is increased compared to that of parent bulk material. Surface area is a property of immense importance in the nano-world, especially in the area of heterogeneous catalysis [46-49]. A solid catalyst works with its active sites binding to the reactants and hence for a given active site reactivity, the higher the number of active sites available, the faster the reaction will occur.

In heterogeneous catalysis, if the catalyst is in the form of spherical nanoparticles, most of the active sites are believed to be present on the outer surface. Large surface area also makes nanostructured membranes and materials ideal candidates for water treatment and desalination among other uses.

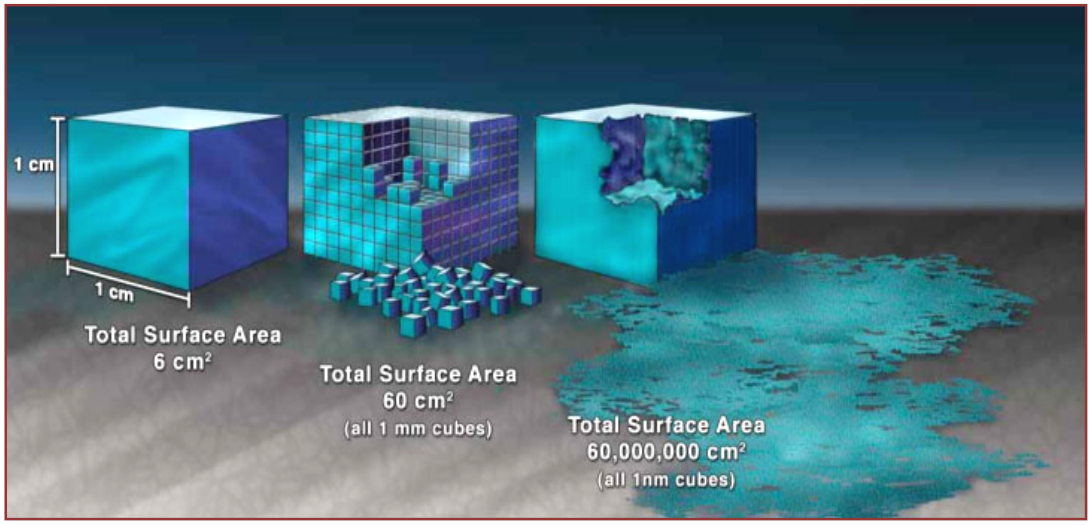


**Fig. 1.3** Schematic diagram showing how surface to volume ratio increases as the size decreases.

## 1.3 Synthesis Method

Nanoparticles are being viewed as fundamental building blocks of nanotechnology. They are the starting point for preparing many nanostructured materials and devices. Their synthesis is an important component of rapidly growing research efforts in nanoscale science and engineering. The nanoparticles of a wide range of materials can be prepared by number of methods. In synthesis and assembly strategies of nanoparticles or nanomaterials, precursors from liquids, solid or gas phase are used. They employ both chemical and physical deposition approach. They rely on either chemical reactivity or physical compaction to integrate nanostructure building blocks.

Generally the manufacturing techniques fall under two categories: 'bottom-up' and 'top-down' approach. The bottom-up approach refers to the buildup of a material from the bottom, i.e. atom-by-atom, molecule-by-molecule or cluster-by-cluster. The colloidal dispersion is a good example of bottom up approach in the synthesis of nanoparticles. Nanolithography and nanomanipulation techniques are also a bottom-up approach. These techniques have been widely used in the formation of structural composite nanomaterials. The top-down approach involves designing or milling of block bulk material to the desired shape. Both approaches play very important roles in modern industry and in nanotechnology as well.

A number of specific methods have been developed such as milling, co-precipitation, sol-gel, micro-emulsion, solvothermal, template method, chemical vapor deposition, multiple pulsed laser deposition, spray pyrrolysis, microwave synthesis, sonochemical method etc. The

different methods for the synthesis of nanoparticles will be discussed under the following categories:

**a) Synthesis of Nanoparticles by Sol-Gel Process:**

The sol-gel method is based on inorganic polymerization reactions. The sol-gel process includes four steps: hydrolysis, polycondensation, drying and thermal decomposition. The size of the sol particles depends on the solution composition, pH and temperature. By controlling these factors, one can tune the size of the particles. This method has been used to synthesize metal oxide nanostructures, such as $TiO_2$ [50], $UO_2$ [51], $ZrO_2$ [52], $CeO_2$ [53], $SnO_2$ [54], $SiO_2$ [55], CuO [56], $SnO_2$ [57] ZnO [58], $Al_2O_3$ [59], $Sc_2O_3$ [60], $ZnTiO_3$ [61], $SrTiO_3$ [62], $BaZrO_3$ [63], $CaSnO_3$ and other nanostructures [64].

**b) Synthesis of Nanoparticles by Hydrothermal Method:**

Hydrothermal synthesis is a common method to synthesize zeolite/molecular sieve crystals. This method exploits the solubility of almost all inorganic substances in PbS and water at elevated temperatures and pressures and subsequent crystallization of the dissolved material from the fluid. Water at elevated temperatures plays an essential role in the precursor material transformation because the vapor pressure is much higher and the structure of water at elevated temperatures is different from that at room temperature. The properties of the reactants including their solubility and reactivity also change at high temperatures. The changes mentioned above provide more parameters to produce different high-quality nanoparticles and nanotubes which are not possible at low temperatures. During the synthesis of nanocrystals, parameters such as pressure, temperature, reaction time and the respective precursor product system can be tuned to maintain quite high rate of simultaneous nucleation and narrow particle size distribution. Different types of nanostructures have also been obtained by solvothermal synthesis using supercritical fluids as solvents. Ag [65] Cu [66], Ni [67], Co, Pt, Ge [68], ZnS [69] and CdS [70], nanowires and carbon nanotubes have also been synthesized. In addition, various shapes of nanostructures have been synthesized including $Cu_2S$ nanoparticles, nanorods, nanodisks, nanoplates, NiS nanorods [71] and triangular nanoprisms [72] by a new method named solventless synthesis.

**c) Synthesis of Nanoparticles by Pyrolysis:**

Pyrolysis is a chemical process in which chemical precursors decompose into solid compound and unwanted waste evaporates away. Upon completion, the desired new

substance is obtained. Generally the pyrolytic synthesis of compounds leads to powders with a wide size distribution in the micrometer regime. To get a uniform nanosized material, some modifications or revisions of the pyrolytic preparation procedure and reaction conditions need to be changed such as slowing of the reaction rate or decomposition of the precursor in the inert solvent. Pyrolysis can be used to prepare different kinds of nanoparticles including metals, metal oxides, semiconductors and composite materials such as Ag [73], Au [74], $Al_2O_3$ [75], $TiO_2$ [76], Ni [77] and carbon nanotubes [78].

**d) Microwave assisted synthesis:**

Microwave assisted method is another novel method for the synthesis of mixed metal oxides and has been gaining significance in the synthesis of oxide nanomaterials [79-80]. The microwave processing of nanoparticles results in rapid heating of the reaction mixture, particularly containing water. As a consequence, the precipitation of particles from such solutions tends to be rapid and nearly instantaneous, leading to very small particle size and narrow size distribution within the product. The method offers additional benefit of very short reaction time and is used for the synthesis of Ag and Au nanoparticles and transition metal oxides. Various metal oxides were synthesized using this method. This is one of the good method used for the synthesis of mixed metal oxides.

**e) Sonochemical Co-Precipitation:**

In recent years, ultrasound irradiation has been extensively used for the preparation of novel materials with unusual properties [81-83]. Ultrasound irradiation can induce the formation of particles with much smaller size and higher surface area. It involves precipitation of metal which exits in solution when exposed to high intensity ultrasound irradiation under ambient air for a particular time period with a varying pulse of the order of one or two seconds. It is accomplished with a high intensity ultrasonic probe immersed directly in the solutions. The sonochemical method has been found useful in many areas of material science, right from the preparation of amorphous products through the insertion of nanomaterials into mesoporous materials to deposition of nanoparticles on ceramic and polymeric surfaces.

**f) Electrochemical Method:**

This method was developed by Reetz in the 1990s [84-85]. Pure and size selective nanoparticles can be prepared by electrochemical method. The process makes the use of an

inexpensive two electrode set up for 25 to 50 ml electrolyte solution. The overall process includes five steps.

- Oxidative dissolution of the sacrificial metal bulk anode.
- Migration of metal ions to the cathode.
- Reductive formation of zero valent metal atoms at the cathode.
- Nucleation and growth of metal particles.
- Arresting the growth process and stabilizing the Nps with protecting agents, eg. Tetra alkyl ammonium ions.

A controlled current electrolysis is used throughout the synthesis process. Solvent selection is made (either single or mixture) depending on the solubility of the ligand or surfactant. The basic principle is simple viz. electrochemical reduction of metal ion in the presence of surfactants serves as an electrolyte and also as a stabilizer. The salient features of the process includes high yield, absence of any side products, easy isolation of the nanoparticles, variation of ligands and control of particle size by controlling current density. The metal aggregates synthesized do not coalesce during the process.

All of the methodologies developed for the production of metal nanoparticles, the electrochemical method offers simple alternative means within reverse micelles in organic solvent systems. We have now successfully applied it in the preparation of Cu, $MoO_3$ mono and Cu-Mo bimetallic nanoclusters within a suitable mixture of organic solvents and have developed a unique synthetic route in preparing sufficient yield of these nanoparticles. Our synthetic approach is to control the growth and particle size by introducing size control reagent into the electrochemical systems in which appropriate surfactants or ligands are employed. These act as a supporting electrolyte and a stabilizer for the resulting nanoparticles. It allows size-selective particle formation by tunning the current density; ie. High current densities lead to small NPs and vice versa. The particle size can also be controlled by adjusting the distance between the electrodes, the reaction time and temperature or the solvent polarity.

Quaternary ammonium compounds are a group of ammonium salt in which organic groups are substituted for all the four hydrogen of the original ammonium cation. They have central nitrogen atom which is joined to four organic groups. The organic group is mainly alkyl or aryl and the nitrogen can be a part of the ring system. They show a variety of

physical, chemical and biological properties and most compounds are soluble in water and act as strong electrolyte. The surfactant used for synthesis of nanoparticles are tetra ethyl ammonium bromide (TEAB), tetra propyl ammonium bromide (TPAB) and tetra butyl ammonium bromide (TBAB) in the present work.

## 1.4Characterization technique

The fascinating properties of the nanoparticles have triggered a massive advance in material science and nanotechnology and its commercial applications in last twenty years. It is thus necessary to establish an understanding and control of nanoparticles synthesis and applications. The applications of the nanoparticles are dependent upon their principle parameters like shape, size, surface characteristics, inner structure, porosity, homogeneity, conductivity, processablity and solubility. Thus characterizations of nanoparticles for knowledge of principle parameters are very essential. Different techniques are generally in use to examine the structural, surface and physical properties of nanocomposites. These techniques are used to identify the materials, crystallinity, morphology, purity, homogeneity, particle size, porosity, electrical conductivity etc. which are discussed below.

### 1.4.1 UV-Visible (UV-vis) Spectrometry

The electromagnetic radiation in the UV/Visible wavelength range interacts with a sample, four results are possible: the radiation is absorbed, transmitted, reflected or scattered. Typically UV-Vis spectrometers are equipped to measure the transmittance or absorbance of a transparent solid or homogenous solution. However, when equipped with the proper accessories, UV-Vis instruments can measure the reflected and scattered energy from a sample. In case of reflected energy, the spectrophotometer measures the intensity of light reflected from a sample and compares it to the intensity of light reflected from a reference material. This ratio is called the reflectance and is usually expressed as a percentage (%R).

Electronic transitions within molecules are often induced by excitation with electromagnetic radiation, whereby a photon interacts with the molecule to promote an electron from a bonding or non-bonding orbital to an anti-bonding orbital [86]. The quantum of energy of a photon that can be exchanged with the molecule and is therefore a measure of the separation of the energy levels of the transition concerned and is dependent on the frequency of the incident radiation [86-87] described by ν in the following equation:

$$E = h\nu = hc/\lambda$$

Where E is the change in energy of the molecule in an electronic transition, h is the Planck constant (h = 6.626 x $10^{-34}$ J.s), c is the speed of light (~3 x $10^{8}$ $ms^{-1}$) and λ describes the wavelength of the incident photon. Simply, one photon excitation follows the *Beer-Lambert* law relating the intensity of the incident photon ($I_0$) to the intensity of the photon transmitted through a sample (I) by the equation:

$$\log_{10}\left(\frac{I_0}{I}\right)=\varepsilon cl=A$$

Where ε is the molar extinction coefficient of the sample, c is the molar concentration, l is the sample thickness (usually 1 cm) and $\log_{10}(I_0/I)$ is referred to as the absorbance or the optical density and is simplified to A.

However, in the field of nanotechnology when one is predominantly dealing with inorganic materials (metals and semi-metals) of nanoscale size, the photon absorbance due to surface plasmons has the effect of masking the majority of electronic transitions that occur [88]. As the surface plasmon resonance is the result of the collective oscillations of the surface electrons, the number and positions of the absorbance bands observed in a UV-visible spectrum are determined by the size of the axis along which electrons that can resonate [89-90]. As a spherical particle is homogenous in all directions and has continuous rotational symmetry, all axes along which electrons may oscillate are the same length and as a result spherical nanoparticles will possess a single absorbance peak in a UV-visible spectrum. Conversely, anisotropic nanoparticles possess multiple axes of different lengths along which electrons can resonate and as such will possess multiple absorbance bands in an absorbance spectrum [90-91]. By studying the changes in absorption maxima using UV-visible spectroscopy, the changes in the surface plasmon resonances of nanomaterials and nanocomposites materials can be observed and followed through the interpretation of the absorption maxima, the observed features can be related to a specific nanoparticle size, shape and composition [92].

### 1.4.2 Fourier Transform Infra Red (FTIR) Spectroscopy

Fourier transforms infrared (FTIR) spectroscopy deals with the infrared region of the electromagnetic spectrum. It covers a range of techniques mostly based on absorption of IR radiations. As with all spectroscopic techniques it can be used to identify and study chemicals. The FTIR spectroscopy is one of the most commonly used techniques by organic and

inorganic chemists. It is the technique in which absorption measurement of different IR frequencies by a sample positioned in the path of an IR beam is monitored and recorded.

The application of infra red spectroscopy is to identify unknown organic compound is well established and widely used. It deals with vibration of chemical bonds in a molecule at various frequencies depending on elements and type of bonds. After absorbing electromagnetic radiation, the frequency of vibration of a bond increases leading to transition between ground state and several excited states. These absorption frequencies represent excitations of vibrations of chemical bonds and thus are specific to the type of bond and the group of atoms involved in vibration. Energy corresponding to these frequencies corresponds to infrared region (4000-400 $cm^{-1}$) of electromagnetic spectrum.

The main goal of FTIR spectroscopic analysis is to determine the chemical functional groups in the sample. Different functional groups absorb characteristic frequencies of incident IR radiations. Using various sampling accessories, FTIR spectrometers can accept a wide range of sample types such as gases, liquids and solids. Thus, IR spectroscopy is an important and popular tool for structural elucidation and compound identification of conducting polymer, metal oxides, metal nanocomposites, metal-oxygen-metal bonding (M-O-M) in metal oxides (stretching and bending modes of vibrations) and hydroxyl (OH) groups adsorbed on the surface of mixed metal oxides [93-94].

### 1.4.3 X-Ray Diffractometer:

The structure of the crystal can be determined using X-ray diffraction (XRD) technique. The technique is used to identify bulk phases, degree of crystallinity, unit cell or lattice parameters and particle size. The analyzed material is finely ground, homogenized and average bulk composition is determined. X-ray diffractometer technique is used to confirm the single-phase nature of the samples to determine the structural parameters such as lattice constant, X-ray density, particle size etc.

In the method of X-ray diffraction the powder material is placed in a beam of monochromatic X-rays. Copper (Cu) X-ray tube is most commonly used for X-ray diffraction of inorganic materials. The wavelength of the strongest Cu radiation (Kα) is approximately 1.54 Å. Other anodes commonly used in X-ray generating tubes include Cr (Kα 2.29 Å), Fe (Kα 1.94 Å), Co (Kα 1.79 Å), and Mo (Kα 0.71 Å). Each particle of the powder is a tiny crystallite oriented at random with respect to the incident beam. In crystals atoms are arranged

in a pattern periodic in three dimensions. It may be possible that some of the particles are correctly oriented to (100) planes and can reflect the incident beam while other particles can reflect for (hkl). As X-ray has electric field associated with it, this field interacts with electron clouds of atoms due to its short wavelength and it is scattered by adjacent atoms in crystals. If the interference between these scattered rays is constructive, diffraction phenomenon is observed. The condition for constructive interference in terms of inter planar spacing d and the diffraction angle θ is,

$$n\lambda = 2d\sin\theta.$$

Where, λ is wavelength of X-ray radiation, d is inter planar spacing and θ is the glancing angle measured from the position of Bragg's peak. X-ray diffraction pattern is unique for each crystalline substance and therefore is currently of prime importance in elucidating the structures of metals, polymeric materials and complex natural products such as steroids, vitamins and antibiotics. A crystalline substance produces a good X-ray diffraction pattern if the size of the particles lies in the range $10^{-3}$ to $10^{-5}$ cm.

**Estimation of crystallite size from X-ray diffraction**:

The crystallite or particle size and shape in finely divided powdered solid often helps to correlate many physical properties of system undergoing transformation in a solid state reaction. X-ray line broadening analysis provides a method of finding bulk average size of coherently diffracting domains. The average crystallite size (T) of solid material can be estimated from X-ray line broadening using the Debye-Scherrer equation [95].

$$T = \frac{0.94\lambda}{\beta cos\,\theta}$$

Where, T = average particle size, λ = wavelength, θ = diffraction angles, β= FWHM (Full width half maximum).

### 1.4.4 Scanning Electron Microscopy (SEM):

Scanning electron microscope is useful for morphological examination with direct visualization. The techniques based on electron microscopy offer several advantages in morphological and sizing analysis; however they provide limited information about the size distribution and true population average. For SEM characterization nanoparticles and nanocomposites solution should be first converted into a dry powder which is then mounted on a sample holder followed by coating with a conductive metal such as gold using a sputter

coater. The sample is then scanned with a focused fine beam of electrons [96]. The surface characteristics of the sample are obtained from the secondary electrons emitted from the sample surface presented in SEM. The nanoparticles must withstand vacuum and the electron beam can damage the nanoparticles. The mean size obtained by SEM is comparable with results obtained by dynamic light scattering. Moreover, these techniques are time consuming, costly and frequently need complementary information about sizing distribution [97].

### 1.4.5 Energy Dispersive Spectrophotometer (EDS):

Often used in parallel to scanning electron microscopy (SEM) is the microanalysis technique known as energy dispersive X-ray analysis (EDX) or energy dispersive X-ray spectroscopy (EDS).

Electrons generated in the scanning electron microscope that interact with the sample surface with enough energy can force the ejection of electrons from the innermost orbitals of atoms on the surface and eject them all the way to the conduction band. Ejecting an electron from the inner orbitals creates a momentary vacancy within the atom into which an electron form a higher energy shell (relative to the ejected electron) will fall into lower energy shell [98]. As two shells possess different energy, the excess energy of the electron transition is released as a quantum of energy, generally in the X-ray region of the spectrum. If an electron ejected from the K shell is replaced by an electron from the L shell, the photon generated by the electronic transition will be designated Kα, whereas if an electron from the M shell falls into the vacancy the photon generated will be designated Kβ and so on [99]. As all elements possess unique electronic configurations, all elements will generate unique X-ray spectra. Therefore, elements within a sample can be easily be determined it must be quantitatively are obtaining percentage of elements using EDX. Additionally, by studying the collected X-rays EDX can be used to semi-quantitatively determine the abundance of particular elements within a composite material through comparison with internal standards.

### 1.4.6 Transmission Electron Microscope (TEM):

Transmission electron microscope (TEM) refers to a technique where a beam of electrons, typically emitted from a tungsten cathode using accelerating voltages on the order of 100 kV are directed through the use of magnetic condenser lenses to interact with a thin sample [100-101]. Samples prepared for TEM analysis are generally very thin to allow the electron beam to transmit through the sample (generally a sample thicker than 300 nm will be

completely opaque to electrons). As the electron beam passes through the sample the incident electrons have several different fates; the electron may pass through the sample and remain undeflected, it may be elastically scattered or it may be inelastically scattered. If these three types of interactions are allowed to contribute to the obtained image, all regions would look identical, in essence there would be no contrast [100]. By removing the scattered electrons through the insertion of an aperture after interaction with the sample the image formed will therefore be a direct correlation to the thickness and type of the material that the electron beam has passed through [100-101]. Heavier and denser elements scatter more electrons and therefore appear darker while materials of the same composition with different thicknesses will also display a contrast due to the thicker material deflecting more electrons. Consider a sample consisting of two regions of carbon of different thicknesses and a single region of gold. If the thin region of carbon scatters only 9% of the electrons and the thicker region scatters 22% of the electrons there will exist a faint contrast between the two regions. If the gold region scatters >90% of the electrons it will be clearly visible as a dark region in the electron image showing great contrast against the carbon regions.

### 1.4.7 Selected Area Electron Diffraction (SAED):

It is a crystallographic experimental technique that can be performed inside a transmission electron microscope (TEM). By adjusting the magnetic lenses, the back focal plane of the lens rather than the imaging plane is placed on the imaging apparatus and diffraction pattern can be generated. For thin crystalline samples, this produces an image that consists of a pattern of dots in the case of a single crystal or a series of rings in the case of a polycrystalline or amorphous solid material. For the single crystal case the diffraction pattern is dependent upon the orientation of the specimen and the structure of the sample illuminated by the electron beam. This image provides the investigator with information about the space group symmetries in the crystal and the crystal's orientation to the beam path. As a result, the image on the screen of the TEM will be a series of spots called the selected area electron diffraction (SAED) pattern, each spot corresponding to a satisfied diffraction condition of the sample's crystal structure. As a diffraction technique, SAED can be used to identify crystal structures and examine crystal defects. Indexing is often possible to index an electron diffraction pattern by noting its symmetry. A reciprocal lattice has the same symmetry as its real lattice.

The Bragg Law for small angles approximates to:

$n\lambda = 2d\sin\theta.$ Where n=1 then,

If $\frac{r}{L} = 2\theta$

Therefore: $\frac{r}{L} = \frac{\lambda}{d}$

Or $r = \lambda L \times \frac{1}{d}$

The distance (r) of a diffraction spot from the direct beam spot on the diffraction pattern varies inversely with the spacing of the planes (*d*) that generate that spot. No lenses have been shown. They merely alter the effective camera length (*L).* Often the value of $\lambda L$ is referred to as the camera constant of the microscope [102].

**1.4.8 Nuclear Magnetic Resonance Spectroscopy:**

Nuclear Magnetic Resonance Spectroscopy is a research technique that exploits the magnetic properties of certain atomic nuclei to determine physical and chemical properties of atoms or the molecules in which they are contained. It relies on the phenomenon of nuclear magnetic resonance and can provide detailed information about the structure, dynamics and chemical environment of molecules [102].

Most frequently, NMR spectroscopy is used by chemists and biochemists to investigate the properties of organic molecules though it is applicable to any kind of sample that contains nuclei possessing spin. Suitable samples range from small compounds analyzed with 1-dimensional proton or carbon-13 NMR spectroscopy to large proteins or nucleic acids using 3 or 4-dimensional techniques. The most commonly studied nuclei are $^{1}H$ and $^{13}C$ by high-field NMR spectroscopy as well. The chemical shift provides information about the structure of the molecule.

**1.4.9 Mass Spectrometry:**

Mass Spectrometry (MS) is an analytical technique that measures the mass-to-charge ratio of charged particles. It is used for determining masses of particles for determining the elemental composition of a sample or molecule and for elucidating the chemical structures of molecules. MS works by ionizing chemical compounds to generate charged molecules or molecular fragments and measuring their mass-to-charge ratios [103].

The technique has both qualitative and quantitative uses. These include identifying unknown compounds, determining the isotopic composition of elements in a molecule and

determining the structure of a compound by observing its fragmentation. Other uses include quantifying the amount of a compound in a sample or studying the fundamentals of gas phase ion chemistry. MS is now very commonly used in analytical laboratories that study physical, chemical or biological properties of a great variety of compounds.

## 1.5 Application of nanoparticles

The prefix "nano" has found in last decade an ever-increasing application to different fields of the knowledge. The nanoparticles are classified as two types i.e. Engineered or Non-Engineered. Engineered nanoparticles are intentionally designed and created with physical properties tailored to meet the need of specific application. They can be end product in themselves as in the case of quantum dots or pharmaceutical drugs, sensors for special purpose or they can be later incorporated, such as carbon black in rubber products. Metal nanoparticles have many unique properties which include large surface to volume ratio, high surface reaction reactivity, high catalytic efficiency and strong adsorption ability. Thus nanomaterials have broad applications in variety of fields like electronics, optical communications and biological systems to new smart materials. Some of the applications of nanostructures and nanomaterials are highlighted in the following ways:-

### 1.5.1 Catalysis:

A catalyst can be defined as a reactant that is essential to the pathway or mechanisum of a reaction and often appears in the rate law, but not in the overall stoichiometry of the reaction. The materials used as a catalyst can be classified in to five categories, i.e. (1) metals, (2) metal oxides, (3) metal complexes, (4) other chemicals, (5) biocatalyst. Metals are one of the most important materials for catalysis. The catalytic activity and selectivity depends on their composition and structure. The particle size is one of the factors affecting the catalytic properties. Since the catalysis occurs only on the surface of metal, the small metal particle is favored as the catalyst.

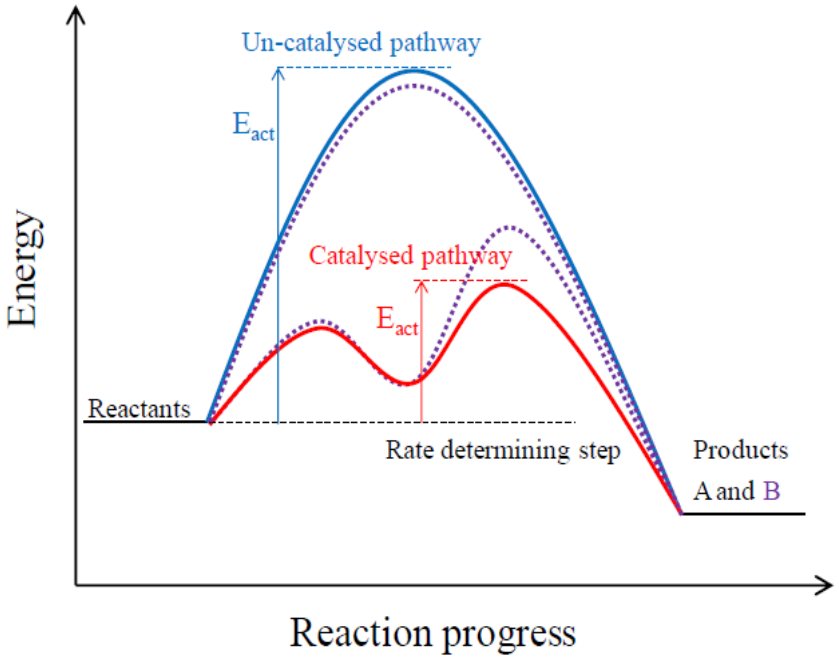


**Fig. 1.4** Reduction of activation energy by catalyst

Catalytic reactions have a lower rate-limiting free energy of activation than the corresponding uncatalyzed reaction, resulting in higher reaction rate at the same temperature shown in **Fig. 1.4**. However, the mechanistic explanation of catalysis is complex. Catalysts may affect the reaction environment favorably or bind to the reagents to polarize bonds, e.g. acid catalysts for reactions of carbonyl compounds.

Catalysts can be either heterogeneous or homogeneous, depending on whether it exists in the same or different phase as the substrate.

**i) Homogeneous catalysis:**

Homogeneous catalysis includes all reactions in which the substrate and the catalyst are in the same state. The catalyst is usually in solution and so access to the reagents is easier so there is improved activity and milder reaction conditions. Another advantage of the catalysts being in solution is that the heat transfer for highly exothermic or endothermic reactions is not a problem. Although homogeneously catalyzed reactions are highly selective, their major limitations are difficulties in reuse, troublesome work-up, disposal of spent catalysts and/or high toxicity.

**ii) Heterogeneous catalysis:**

Heterogeneous catalysis includes all reactions in which the substrate and the catalyst are in the different phase. Most heterogeneous catalysts are solids that act on substrates in a liquid or gaseous reaction mixture. Diverse mechanisms for reactions on surfaces are known, depending on how the adsorption takes place. The total surface area of solid has an important effect on the reaction rate. Smaller the catalyst particle size, larger the surface area for a given mass of particles. Hence, efforts are being made to replace homogeneous catalysts by heterogeneous ones in organic synthesis. Also, heterogeneous catalysis is gaining increasing importance in the production of fine chemicals and pharmaceuticals due to its definite technical advantages like production process, competitiveness and economy. The main advantage of a heterogeneous catalyst is that it can be operated in a fixed bed reactor by which reactants flow continuously without interruption. Since the catalyst is present in a phase different from that of the reactants as well as products and can be separated easily from the reaction mass.

Heterogeneous catalysts offer several intrinsic advantages over their homogeneous counterparts such as easy removal of catalyst materials and possible use of high temperatures, suffered for a long time from lack of selectivity and understanding of the mechanistic aspects that are indispensable for parameter improvements. Green catalysis aspects now obviously require that environmentally friendly catalysts be designed for easy removal from the reaction media and recycling many times with very high efficiency. These demanding conditions bring a new research impetus for catalyst development at the interface between homogeneous and heterogeneous catalysis.

In the case of metal nanoparticle they can be used as heterogeneous catalyst as colloidal dispersion in solution. When metal nanoparticles are used in a colloidal state in solution, the stability of the colloid is a key factor to get active catalyst. The use of metal nanoparticles in the field of catalysis is of great interest, since they have a large surface-to-volume ratio compared to bulk materials [104-107].

Normally, because of the synergetic effect bimetallic nanoparticles show better catalytic activity compared with the single pure metallic nanoparticles. Bimetallic core/shell nanoparticles especially Au/Pd[108], Au/Ag[109], Au/Pt[110], Ag/Pt[110], Co/Pt and Pd-Co[111] are used as catalysts in a range of reactions.

### 1.5.2 Cosmetics:

ZnO nanoparticles [112] have received considerable attention due to their unique properties. They are well known as UV blocking materials especially of light in the UV region and as such are used widely in cosmetics, paints and fibers. But their high catalytic activity in oxidation and photochemical reactions restrict their application as UV blocking materials. Particle surface modification is regarded as an effective way to restrain the ultrafine particles from high oxidative and photochemical activity.

### 1.5.3 Industrial applications

Silver is amongst the widely used metal in the world. Its metallic properties make it a great conductor. Its antimicrobial property has also been exploited in several applications. Reducing silver to nonosized particles helps to make the element highly effective, making it more in demand for several uses in the industry of medicine and technology. Currently there are many uses of silver nanoparticles in industries that have resulted in a boost in its demand and production. Silver nanoparticles can be used as an ingredient for water purifiers and even as an ingredient for inks used in inkjets. A potential industrial use of silver nanoparticles is making it as coating on polyurethane foams. The material is ideal as it can be washed, dried and stored for long period of time and yet retains same number of nanoparticles. The material is also tested as an element for water filtration to eliminate bacteria. It is also possible to use it in the air filtration, air quality management and industrial settings as well as antibacterial packing semiconductor nanoparticles.

### 1.5.4 Solar Cells:

Electrochemical studies have demonstrated the electron storing properties of gold nanoparticles and their ability to act as an electric relay on a nanotemplate structure. Beneficial role of gold nanoparticles in photocurrent generation has been reported by Kuwahara [113] in tris 2, 8 bipyridilede ruthenium (II) vilogen linked thiol.

### 1.5.5 Drug Delivery:

In recent years nanocapsusles and nanospheres surrounded by a polymer matrix into which the drug is physically and uniformly dispersed are used as drug delivery devices. These have the ability to circulate for a prolonged period of time, target a particular organ as carriers [114] of DNA in gene therapy and have the ability to deliver proteins, particles and genes. Some of the challenges facing conventional therapies are poor bioavailability and intrinsic

toxicity. These have seriously compromised the therapeutic efficiency of many otherwise beneficial drugs. Thus innovative nanodevices and nanostructures have been developed for applications [115] in the fields of diagnostics, biosensing, therapeutics, drug delivery and targeting.

## 1.6 Literature survey

Catalysis is a central field of nanoscience and nanotechnology [116] and the interest in catalysis by metal nanoparticles is increasing dramatically as reflected by the large number of publications in the last ten years. It can be seen that transition metal nanoparticles are very attractive to use as catalysts due to their high surface-to-volume ratio and their high surface energy, which makes their surface atoms very active [117-119]. The first use of nanoparticles in the field of catalysis catalysis appeared in the $19^{th}$ century with photography (Ag nanoparticles) and the decomposition of hydrogen peroxide [120]. A breakthrough of catalytic applications of nanoparticles came with Haruta's seminal studies on oxide-supported Au nanoparticle-catalyzed CO oxidation by $O_2$ at low temperatures [121-122] and olefin hydrogenation reactions [123]. Since these studies, there have been numerous types of reactions that have been catalyzed using colloidal nanoparticles. For example, oxidations of alcohols and alkenes [124], carbon cross-coupling reactions [125], electron-transfer reactions [126-127], hydrogenations of unsaturated substrates [128] and many others.

The use of metal and mixed metal nanoparticles in the field of catalysis is of great interest, because these are utilized both for their acid-base and redox properties. Depending upon the nature of metal and hence which belongs to the largest family of heterogeneous catalyst, which are widely used for organic transformation reactions [129]. Generally, organic reactions are carried out using mineral acids such as $H_2SO_4$, HCl and $HNO_3$. These homogeneous classical acid catalysts offer several drawbacks such as high toxicity, corrosive nature, generate maximum waste, difficult to recover and reuse. In view of environmental and economic aspects, it is necessary to replace these toxic acid catalysts by newer solid heterogeneous catalyst as an excellent alternative source over these conventional acid catalysts.

Heterogeneous catalysts offer several advantages over their homogeneous catalysis such as easy separation of product by simple filtration, easy recovery and reusability of the catalyst,

better selectivity, safe, less toxic, more stable reagents, long life of catalyst, high thermal stability, good heat resistant and environmentally friendly. Thus the mixed metal oxides are excellent alternative to use as heterogeneous catalyst for organic transformation reactions [130-131]. Copper nanoparticles/oxide/salts were used as heterogeneous catalyst in various organic transformation reactions such as cycloaddition of azides and acetylenes, condensation, one pot multicomponant reactions and coupling reactions [132-136]. Much research has been focused on Mo-based catalysts which can be active and selective for many reactions. Selective oxidation [137-138], hydrogenation and dehydrogenation [139-140] are a few examples of the important applications of these catalysts. The Cu-Mo bimetallic catalysts have also been studied for the catalytic wet oxidation of dye wastewater [141].

## 1.7 Aim and objective of the project.

On the overlook at the literature survey, it has been observed that metal oxide and mixed metal oxide play an important role in catalytic processes to speed up chemical reactions in an ecofriendly manner, cost effective, efficient and clean processes. The main objectives of the present work are:

- ✓ Synthesis of Cu, Mo monometallic and Cu-Mo bimetallic nanoparticles by electrochemical method.
- ✓ To study the effect of surfactants and current density on the morphologies such as particle size, crystal structures and surface properties of metal nanoparticles.
- ✓ To study the catalytic applications of both monometallic and bimetallic nanoparticles.
- ✓ To replace the toxic, conventional/classical acid catalysts by means of solid heterogeneous catalyst ie. mono/bimetallic nanoparticles.
- ✓ To develop a clean, efficient and environmentally benign processes for the synthesis of pharmacologically and biologically important heterocyclic compounds.

The important aspect of electrochemical method is simple, easy to operate, cost effective, allows high purity of the products, allows reproducible results and is environment friendly since it does not make use of toxic chemicals and that the particle size can be controlled in a simple manner by the variation in the current density. Thus electrochemical method is used for the synthesis of the nanoparticles in the non polar organic solvent in the form of a mixture of acetonitirile and tetrahydrofuran (4:1). The advantages in using the non polar organic solvent include control over the size of the nanoparticles, monodispersity and the chemical

nature of the nanoparticles surface (via capping agent). Synthesized metal nanoparticles are characterized by different characterization techniques like UV-Visible spectrophotometer, FTIR spectroscopy, XRD, SEM-EDS, TEM etc.

In the preparation of nanoclusters, capping agents are required to stabilize them and prevent their agglomeration. The surfactants used in the present study are a group of tetra alkyl ammonium salts, which include TPAB and TBAB. The tetra alkyl ammonium ion forms a monolayer around the nanoparticles and is weakly bonded with it.

In order to facilitate the nanoparticles loading and reduce health risks, the bacterial effectiveness of metal nanoparticles has been suggested to be due to both their size and high surface-to-volume ratio. There lies a strong challenge in preparing nanoparticles of metal oxides stable enough to significantly restrict bacterial growth. Thus the present work can be pursued in a systematic and result oriented manner with definite information being obtained for the monometallic and bimetallic nanoclusters of copper, molybdenum capped with different capping agents like TEAB, TPAB and TBAB. Successful utilization of prepared monometallic and bimetallic nanoparticles was tested as catalysts for various organic transformation reactions.

## 1.8 References:


1. John F. Sargent Jr., *The National Nanotechnology Initiative: Overview, Reauthorization, and Appropriations Issues.* (**2011**)
2. Altavilla C., *Advance Materials: Research Trends, ed. L. A. Basbanes New York: Nova Science Publishers* **(2007)** pp.217-236.
3. Dowling A., *Nanoscience and Nanotechnology: Opportunities and Uncertainties, A Report by The Royal Society & The Royal Academy of Engineering, London* **(2004)**.
4. Taniguchi N. *In book Nano: The Next Revolution* (**2004)**, 27.
5. Rao C.N.R., Muller A., Cheetham A. K. (Eds.), *The Chemistry of Nanomaterials: Synthesis, Properties and Applications, Wiley-VCH, Weinheim*, (**2004)**, 1.
6. Faraday M., *Philos. Trans. R. Soc. London* (**1857),** 147**,** 145 – 181.
7. Jin R., Cao Y., Mirkin C.A., Kelly K.L., Schatz G.C., Zheng J.G., *Science* **(2001)**, 294 , 1901 – 1903.
8. The New York Times publishing article of February 22, 2005. http://www.nytimes.com/magepages/2005/02/21/science/20050222_NANO1_GRAPHIC .html .
9. Feynmann R.P., *Miniaturization Reinhold*, New York, (**1961)**.
10. Kim D.H. et al., *Epidermal electronics. Science* **(2011)** 333(6044), 838–843.
11. Breunig M. et al., *Eur. J. Pharm. Biopharm*. **(2008)** 68, 112–128.
12. Sachiko Kaihara Nitta and Keiji Numata, *Int. J. Mol. Sci.* **(2013)** 14,1629-1654.
13. Koo O.M., Rubinstein I., Onyuksel H., *Nanomed. Nanotechnol. Biol. Med.* **(2005)** 1, 193–212.
14. McAteer M.A. et al., *Nat. Med.* **(2007)** 13, 1253–1258.
15. Wang X., Yang L., Chen Z., Shin D.M., *CA Cancer J. Clin***. (2008)** 58, 97–110.
16. Rahmani M.B., Keshmiri S.H., Yu J., Sadek A.Z., Al-Mashat L., Moafi A., Latham K., Li Y.X., Wlodarski W. and Kalantarzadeh K., *Sens. actuators, B* **(2010)**, 145, 13.
17. Altavilla C., Ciliberto E., *Inorganic Nanoparticles: Synthesis, Applications and perspectives, Taylor and francis* **(2011)**.
18. Haberland H., *Clusters of Atoms and molecules, Springer-Verblag, New-York* **(1994)**.
19. Burda C., Chen X., Narayanan R. and Ei-Sayed, *Chem.Rev*. **(2005)**, 105, 1025-1102.
20. Arthur D, et al., *MRS Bull* **(2012)**, 37(12), 1297–1306.
21. Yu Z.B., Niu X.F., Liu Z.T., Pei Q.B., *Adv Mater* **(2011)**, 23(34), 3989–3994.
22. Bolotin K.I., Kuemmeth F., Pasupathy A.N., Ralpha D.C., *App. Phy.Lett.* **(2004)**, 84(16), 3154-3156.
23. Gubin S. P., *Magnetic nanoparticles, Wiley-VCH, Weinheim* **(2009)**, 5.
24. Kecob B., Garik P., *Nature* **(1990)**, 343.
25. Meakin P., *Phys. Rev. Lett*. **(1983)**, 51.
26. Nieman G.W., Weertman J.R., Siegel R.W., *Scripta Metall* **(1989)**, 23, 2013.

27. Weller H., Angew, *Chem. Int. Ed. Engl*. **(1993)**, 32, 41.
28. Daniel M.C., Astruc D., *Chem. Rev*. **(2004)**, 104, 293.
29. Liz-Marzan L.M., *Langmuir* **(2006)**, 22, 32.
30. Daniel M.C., Astruc D., *Chem. Rev*. (**2004)**, 104, 293.
31. Smith A.M., Duan H., Rhyner M.N., Ruan G., Nie S.A., *Phys. Chem.,* **(2006)**, 8, 3895.
32. Kittel, C., *Introduction to solid state physics*. *John Wiley & Sons,* **(2005)**.
33. Paul M., *Nanoscale materials in chemistry, ch. 5: "Metal nanoparticles: double layers, optical properties, and electrochemistry"*, p. 121. John Wiley & Sons, **(2001)**.
34. Kaszkur Z., *J.Applied crystallography* **(2000)**, 33, 1262.
35. Moriarty P.M., *Progress in Physics* **(2001)**, 64, 297.
36. De Heer W.A., *Reviews of modern physics* **(1993)**, 65, 611.
37. Luis M., Liz-Marzan, "*Nanomaterials: formation and color", Materialstoday,* **(2004)**, 26.
38. Uchic M.D., Dimiduk D.M., Florando J.N. and Nix W.D., *Science* **(2004)**, 305, 986-989.
39. Deyu L., Yiying W., Philip K., Li S., Peiodong Y., Arun M., *Applied Physics Letters* **(2003)**, 83, 2934.
40. Chen Y., Shaw D.T., Bai X.D., Wang E.G., Lund C, Lu W.M. and Chung D.D.L., *Appl. Phys. Lett.* **(2001)**, 78, 2128–2130.
41. Wiley B., Sun Y., Mayers B. and Xia Y., *Chem.Eur. J.*, **(2005)**, 11, 454.
42. Rao C.N.R., Müller A. and Cheetham A.K., *Chemistry of Nanotechnologies*,W*iley VCH, Weinheim* **(2004)**.
43. Vinod C.P., Kulkarni G.U. and Rao C.N.R., *Chem. Phys. Lett.*, **(1998)**, 289, 329.
44. Edwards P.P., Johnston R.L. and Rao C.N.R., *Metal Clusters in Chemistry (eds Braunstein P., Oro G. and Raithby P.R.), Wiley-VCH, Weinham,* **(1999)**.
45. H-S D., G-G M.B., Garcia A.C., *Electroanalysis* **(2002)**, 14, 1225.
46. Cuenya B.R., *Thin Solid Films* **(2010)**, 518, 3127–3150.
47. Chintareddy V. R., Lakshmi Kantam M., *Catal Surv Asia* **(2011)**, 15, 89–110.
48. Yuen W., Dingsheng W., Peng Zhao., Zhiqiang N., Qing P. and Yadong Li, *Inorg. Chem.* **(2011)**, 50, 2046–2048.
49. Safaei-Ghomi J, Ziarati A, and Teymuri R, *Bull. Korean Chem. Soc*. **(2012)**, 33(8), 2679.
50. Li, Y.; White, T.; Lim, S. H. *Rev. Adv. Mater. Sci.* **2003**, *5*, 211.
51. Lackey, W. *J. Nucl. Technol.* **1980**, *49*, 321.
52. Woodhead, J. L. *Sci. Ceram.* **1983**, *12*, 179.
53. Gao, J.; Qi, Y.; Yang, W.; Guo, X.; Li, S.; Li, X. *Mater. Chem. Phys.* **2003**, *82*, 602.
54. Kiss,K.; Magder, J.; Vukasovich, M. S.; Lockhart, R. J. *J. Am. Ceram. Soc.* **1966**, *49*, 291.
55. Shen,J.; Zhang, Z.; Wu, G. *J. Chem. Eng. Jpn.* **2003**, *36*, 1270.

56. Viano, A.; Mishra, S. R.; Lloyd, R.; Losby, J.; Gheyi, T. *J. Non-Cryst. Solids* **2003**, *325*, 16.

57. Jitianu, A.; Altindag, Y.; Zaharescu, M.; Wark, M. *J. Sol-Gel Sci. Technol.* **2003**, *26*, 483.

58. Mondelaers, D.; Vanhoyland, G.; Van den Rul, H.; D'Haen, J.; Van Bael,; Mullens, M. K. J.; Van Poucke, L. C. *Mater. Res. Bull.* **2002**, *37*, 901.

59. Pathak,L. C.; Singh, T. B.; Verma, A. K.; Ramachandrarao, P. *J. Metall. Mater. Sci.* **2000**, *42*, 93.

60. Grosso, D.; Sermon, P. A. *J. Mater. Chem.* **2000**, *10*, 359.

61. Chang, Y. S.; Chang, Y. H.; Chen, I. G.; Chen, G. J.; Chai, Y. L. *J. Cryst. Growth* **2002**, *243*, 319.

62. Wang, X.; Zhang, Z.; Zhou, S. *Mater. Sci. Eng. B* **2001**, *86*, 29.

63. Veith, M.; Mathur, S.; Lecerf, N.; Huch, V.; Decker, T.; Beck, H. P.; Eiser, W.; Haberkorn, R. *J. Sol-Gel Sci. Technol.* **2000**, *17*, 145.

64. Sharma, N.; Shaju, K. M.; Rao, G. V. S.; Chowdari, B. V. R. *Electrochem. Commun.* **2002**, *4*, 947.

65. Ji, M.; Chen, X.; Wai, C. M.; Fulton, J. L. *J. Am. Chem. Soc.* **1999**, *121*, 2631.

66. McLeod, M. C.; McHenry, R. S.; Beckman, E. J.; Roberts, C. B. *J. Phys. Chem. B* **2003**, *107*, 2693.

67. Sun, Y. P.; Rollins, H. W.; Guduru, R. *Chem. Mater.* **1999**, *11*, 7.

68. Shah, P. S.; Hanrath, T.; Johnston, K. P.; Korgel, B. A. *J. Phys. Chem. B* **2004**, *108*, 9574.

69. Ohde, H.; Ohde, M.; Bailey, F.; Kim, H.; Wai, C. M. *Nano Lett.* **2002**, *2*, 721.

70. Holmes, J. D.; Bhargava, P. A.; Korgel, B. A.; Johnston, K. P.; *Langmuir* **1999**, *15*, 6613.

71. Larsen, T. H.; Sigman, M.; Ghezelbash, A.; Doty, R. C.; Korgel, B. A. *J. Am. Chem. Soc.* **2003**, *125*, 5638.

72. Ghexelbash, A.; Sigman, M.; Korgel, B. A. *Nano Lett.* **2004**, *4*, 537.

73. Cai, W.; Zhang, L. *J. Phys. Condensed Matter* **1997**, *9*, 7257.

74. Maya, L.; Paranthaman, M.; Thundat, T.; Bauer, M. L. *J. Vac. Sci. Technol. B* **1996**, *14*, 15.

75. Indackers, D.; Janzen, C.; Rellinghaus, B. *Nanostruct. Mater.* **1998**, *10*, 247.

76. Depero, L. E.; Bonzi, P.; Musci, M.; Casale, C. *J. Solid State Chem.* **1994**, *111*, 247.

77. Valentini, A.; Carreno, N. L. V.; Probst, L. F. D.; Leite, E. R.; Longo, E. *Microporous Mesoporous Mater.* **2004**, *68*, 151.

78. Jou, S.; Hsu, C. K. *Mater. Science Eng. B* **2004**, *106*, 275.

79. A.A. Taherpour, M. Faraji, *Molbank*, (**2008**), M 577.

80. M. Nuchter, B. Ondrusehka, W. Bonreth, A. Gum, *Green Chem.* (**2004**), 6, 128.
81. W.T. Richards, A.L. Loomis, *J. Am. Chem. Soc.* (**1927)**, 49, 3086.
82. M. Blaskovicova, A. Gaplovsky, J. Blasko, *Molecules,* (**2007**), 11, 188.
83. X.K. Wang, G.H. Chen, W.L. Guo, *Molecules,* (**2003**), 8, 40.
84. Reetz M.T., Helbig W., Quaiser S.A., in *Active metals VCH: Weinheim,* (**1996)**, 279.
85. Kiwi J., Gratzen M.*J., Am. Chem. Soc.* **(1979)**, *101,* 7214.
86. Williams D.H., Fleming I., *Spectroscopic Methods in Organic Chemistry*; 5th ed.; McGraw-Hill Publishing Company: London, **(1995)**.
87. Liang W., Shores M.P., Bockrath M., Long J.R., Park H., *Nature* **(2002)**, 417, 725
88. Montalti M., *Handbook of Photochemistry, CRC/Taylor & Francis,* **(2006)**.
89. Mie G., *Annalen der Physik* **(1908)**, 25, 377-445.
90. Pileni M., *J. Phys. Chem. B* **(1998)**, 102, 2114-2220.
91. Thomas K.G., In *Nanomaterials Chemistry*; Rao C.N.R., Muller A., Cheetham A. K., Eds.;Wiley-VCH: **(2007)**.
92. Dhanasankar M., Purushothaman K.K., Muralidharan G., *Appl. Surf. Sci.,* **(2011)**, 257, 2074.
93. Cheng T., Fang Z., Zou G., Hu Q., Hu B., Yang X., Zhang Y., *Bull. Mater. Sci.,* **(2006)**, 29, 701.
94. Scherrer P., *Göttinger Nachrichten Gesell.,* (**1918**), 2, 98.
95. Jores K., Mehnert W., Drecusler M., Bunyes H., Johan C., Mader K. *J. Control Release.* **(2004)**, 17, 217- 227.
96. Molpeceres J., Aberturas M.R., Guzman M., *J Microencapsul.* **(2000)**, 17, 599-614.
97. Russ J.C., *Fundamentals of Energy Dispersive X-Ray Analysis*; *Butterworths and Co.Ltd.,* **(1984)**.
98. Lee R.E., *Scanning Electron Microscopy and X-Ray Microanalysis*; *P TR Prentice-Hall, Inc,* **(1993).**
99. Chescoe D., Goodhew P.J., *The operation of the transmission electron microscope*; *Oxford University Press,* **(1984)**.
100. Rochow T.G., Tucker P.A., *Introduction to Microscopy by Means of Light, Electrons, X-Rays, or Accoustics*; *2nd ed.; Plenum Press: New York,* **(1994)**.
101. Kircher M.F., Mahmood U., King R.S., Weissleder R., Josephson L., *Cancer Res.* **(2003)**, 63, 8122.
102. Richards S.A., Hollerton J.C., *Essential Practical NMR for Organic Chemistry,* (**2010**).
103. Gross J.H., *Mass Spectrometry, A Textbook,* 2nd ed., **(2011)**.
104. Kidwai M., Bhardwaj S., Poddar R., *Beilstein Journal of Organic Chemistry* **(2010)**, 6, 35.
105. Mitsudome T., Mikami Y., Mori H., Arita S., Mizugaki T., Jitsukawa K., Kaneda, K.,*Chem. Commun.* **(2009)**, 22, 3258.
106. Singh P., Kumari K., Katyal A., Kalra R., Chandra R., *Catal. Lett.* **(2009)**, 127, 119.

107. Khurana J.M., Vij K., *J. Chem. Sci*. **(2012)**, 124, 4.
108. (a) Zhao D., Chen X., Liu Y., Wu C., Ma R., An Y., Shi L., *J. Colloid Interface Sci.* **(2009)**, 331, 104. (b) Wang L., Yamauchi Y., *J. Am. Chem. Soc.* **(2010)**, 132, 13636.
109. Feng L., Gao G., Huang P., Wang K., Wang X., Luo T., Zhang C., *Nano Biomed. Eng.* **(2010)**, 2, 258.
110. (a)Fan F.R., Liu D.Y., Wu Y.F., Duan S., Xie Z.X., Jiang Z.Y., Tian Z.Q., *J. Am. Chem. Soc.* **(2008)**, 130, 6949. (b) Hui Liu, Feng Ye, Qiaofeng Yao, Hongbin Cao, Jianping Xie, Jim Yang Lee, Jun Yang, *Scientific Report*, **(2014)**, 4, 3969.
111. Feng Yi-Si, Lin Xin-Yan, Jian Hao, Hua-Jian Xu, *Tetrahedron*, **(2014)**, 70, 5249-5253.
112. Hotchandani, S.; Kumar, P. V. *J. Electrochem. Soc*. **1991**, *113*, 2826.
113. Kuwahara, Y.; Akiyam, T. Yamada, S. *Langmuir* **2001**, *17*, 5714.
114. Mohanraj, V. J.; Chen, Y. *Tropical Journal of Pharmaceutical Research* **2006**, *5*, 561.
115. Baron, R.; Willner, B.; Willner, I. *Chem. Commun*. **2007**, *28*, 323.
116. Grunes J., Zhu J., Somorjai G.A., *Chem. Commun.*, **(2003)**, 2257 – 2260.
117. Toshima N. and Yonezawa T., *New J. Chem.*, **(1998)**, 22, 1179-1201.
118. Moreno-Mañas M. and Pleixats R., *Acc. Chem. Res.*, **(2003)**, 36, 638.
119. Roucoux A., Schulz J., Patin H., *Chem. Rev.*, **(2002)**, 102, 3757–3778.
120. Bradley J.S., *Clusters and Colloids: From Theory to Applications*. *Vol. 6., VCH: Weinheim.* 459, **(1994)**.
121. Schmid G. and Corain B., *Eur. J. Inorg. Chem.*, (**2003)**, 3081-3098.
122. Haruta M., Tsubota S., *J. Catal.*, **(1993)**, 144, 175-192.
123. Hirai H., Nakao Y., Toshima N., *J. Macromol. Sci. Chem.*, (**1979)**, 13, 727-750.
124. Hou W., Dehm N.A., Scott R.W.J., *J. Catal.*, **(2008)**, 253, 22-27.
125. Littke A.F., Dai C., Fu G.C., *J. Am. Chem. Soc.*, (**2000)**, 122, 4020.
126. Kamat P.V., *J. Phys. Chem. C*, **(2007)**, 111, 2834–2860.
127. Luo X., A. Morrin., *Electroanal.*, (**2006)**, 18, 319-326.
128. Wilson O.M., Knecht M.R., *J. Am. Chem. Soc.*, **(2006)**, 128, 4510-4511.
129. C. Kappe, A. Stadler, *Org. React.*, (**2004**), 63, 1.
130. B. Stefane, *Org. Lett.*, (**2010**), 12, 2900.
131. G. Guillena, D.J. Raman, M. Yus, *Chem. Rev.*, (**2010**), 110, 1611.
132. Díez-González, S.; Correa, A.; Cavallo, L.; Nolan, S. P. *Chem. Eur. J.* **2006**, 7558.
133. Nolte, C.; Mayer, P.;Straub, B. F. *Angew. Chem. Int. Ed.* **2007**, *46*, 2101.
134. Guerreiro, E. D.; Gorriz, O. F.; Rivarola, J. B.;Arrua, L. A. *Appl. Catal. A* **1997**, *165*, 259.
135. Carniti, P.;Gervasini, A.; Modica, V. H.; Ravsio, N. *Appl. Catal. B* **2000**, *28*,175
136. Gervasini, A.; Carniti, P.; Bennici, S.; Messi, C. *Chem. Mater*. **2007**, *19*, 1319
137. A. Rezaeifard, I. Sheikhshoaie, N. Monadi and M. Alipour, Polyhedron, 2010, 29, 2703–2709.
138. A. Rezaeifard, M. Jafarpour, H. Raissi, M. Alipour and H. Stoeckli-Evans, Z. Anorg. Allg. Chem., 2012, 638, 1023.
139. K. D. Chen, A. T. Bell and E. Iglesia, *J. Phys. Chem. B*, 2000,104, 1292.
140. M. D. Argyle, K. D. Chen, A. T. Bell and E. Iglesia, *J. Catal.*, 2002, 208, 139.
141. H. M a, Q. Zhuo, B. Wang, *Environ. Sci. Technol*. **2007**, 41, 7491-7496

## 2.0 Experimental:

Nanoparticles of a wide range of materials can be prepared by a variety of techniques. These techniques include physical methods such as mechanical milling [1], inert gas condensation [2] along with chemical methods such as chemical reduction [3], photochemical reduction [4], electrodeposition [5], hydrothermal [6] and sol-gel synthesis [7]. Among them chemical methods [8-9] are generally based on the reduction of metal salts by variety of reducing agents such as citrate, hydrazine, ferric ions, formaldehyde, ethanol, boron hydrides and ascorbic acid. Depending upon the reducing power of these reagents, the synthesis reactions were carried out at various temperature and other conditions to achieve reasonable rates. To prevent undesired agglomeration with formation of large particles in the range of micrometer or metal powders, stabilizers such as special ligands, polymers [10-11] or tetra alkyl ammonium salts generally need to be used. In the physical method metal nanoparticles were formed through free radical mechanism. These methods have been discussed in details in Chapter I.

Of all the methodologies developed for the production of metal nanoparticles, the electrochemical method offers an simple alternative means within reverse micelles in organic solvent systems. We have successfully applied it to the preparation of transition metal mono and bimetallic nanoclusters within suitable mixture of organic solvents and have developed a unique synthetic route in preparing sufficient yields of these nanoparticles. Our synthetic approach is to control the growth and particle size by introducing 'size control' reagent in to the electrochemical system in which appropriate surfactants or ligands are employed as both supporting electrolyte and the stabilizer for the resulted nanoparticles. Other parameter for controlling the size of nanoparticles is current density in electrochemical reduction method.

Pure and size selective nanoparticles can be prepared by electrochemical reduction method. This process makes use of an inexpensive two electrode set up for 25-30ml electrolyte solution. A sacrificial anode consisting of the bulk metal is transformed into metal nanocluster. Inert platinum sheet is used as a cathode. The supporting electrolyte used is tetra alkyl ammonium salt which also serves as stabilizer for metal clusters. Organic solvents are used to prevent possible metal hydride formation.

During the synthesis, the bulk metal anode is oxidized and converted into metal cations. These cations migrate to the cathode and reduction takes place with the formation of metal in zero oxidation state.

Anode – M bulk→ $Mn^+ + ne^-$

Cathode– $Mn^+ + ne^- +$ stabilizer→ M coll/Stabilizer

M bulk + stabilizer →Mcoll/stabilizer

Where, M bulk = metal bulk sheet,

M coll/stabilizer = ammonium salt stabilized colloidal metal cluster.

The transition metal cluster in the range 1-20 nm range has been prepared by this method for fundamental and practical reason. The particle size of nanostructured metal clusters can be controlled by varying parameters such as types of ligands, their concentration, solvent and current density in electrochemical synthesis.

Quaternary ammonium compounds, a group of ammonium salts in which organic radicals are substituted for all four hydrogen of the original ammonium cation have a central nitrogen atom which is joined to four organic radicals and one acid radical. The organic radicals may be alkyl or aryl and the nitrogen can be part of a ring system. They are prepared by treatment of an amine with an alkylating agent. They show a variety of physical, chemical and biological properties and most compounds are soluble in water and act as a strong electrolyte. In electrochemical synthesis, the choice of tetra alkyl ammonium surfactant is governed by following constraints:

i) It should be absorbed on the metal oxide surface to stabilize the synthesized nanoparticles.

ii) It should be highly soluble and dissociated in the solvent to play the role of electrolyte.

iii) The hydrophilic–lipophilic balance of the chosen surfactant should be sufficiently high to prevent any precipitation.

The surfactants that satisfy the above constraints are tetra ethyl ammonium bromide (TEAB), tetra propyl ammonium bromide (TPAB) and tetra butyl ammonium bromide (TBAB) etc. These were used in the present work.

A controlled current electrolysis is used throughout the synthesis process. The basic working principle is simple viz. the electrochemical reduction of metal salts in presence of surfactants which serves as the electrolyte as well as the stabilizer.

The salient features of these types of metal colloids are

i) High yield,

ii) Absence of undesired side products such as metal hydrides or boron impurities,

iii) Easy isolation,

iv) Variation of solubility of proper choice of ammonium salt,

v) Control of particle size by adjustment of the current density

Metal oxide (MOx) nanoparticles are promising materials as they can be prepared with highly ionic and extremely high surface areas that can possess unusual crystallography which can demonstrate numerous surface reaction sites [12]. The highly ionic natures of many MOx nanoparticles allow the formation of many stable surface defect sites. Many MOx systems are considered hard acids or bases and therefore possess reaction sites capable of catalyzing acid/base chemistry. For these reasons, MOx nanoparticles are often employed directly as catalysts or as a very high surface area catalytic support [13-16]. As there are a significant number of MOx's available the properties of metal oxide nanoparticles can vary greatly depending on the elements present.

Bimetallic nanoparticles are considered the next generation of nanocatalysts with increased stability and catalytic activity. Combination of two metals into single bimetallic nanoparticles lead to higher physical stability and unique optical, magnetic and catalytic properties compared to monometallic particles. Synthesis of bimetallic nanoparticles is therefore receiving much attention due to the many exciting applications of such particles. For example, bimetallic Pd-Au particles have been applied as catalysts for different reactions such as hydrogen peroxide synthesis [17], oxidation of benzyl alcohol [18], oxidation of alcohol to aldehydes [19] or removal of contaminants in groundwater. Bimetallic nanoparticles have previously been prepared by chemical and physical methods [20-21]. However these methods are generally expensive, energy consuming, environmentally hazardous [22-23] and relatively few methods [24-25] produce true alloy nanoparticles due to phase separation at the atomic level leading to the formation of core shell particles

## 2.1 Synthesis of Monometallic Copper and Molybdenum Nanoparticles:

The electrochemical reduction method for the size selective preparation of tetra-alkyl ammonium salt stabilized transition metal clusters in the size range of 1-50 nm has been reported [26-27]. The tetra-alkyl ammonium salts are very effective phase transfer catalysts which are used as stabilizers in the synthesis of nanoclusters of transition and noble metals. They have

weak interaction with the nanoparticles and can be exchanged. They also help to prevent oxidation of the metal atoms.

In the present work we have prepared tetra-alkyl ammonium salt stabilized copper and molybdenum (oxide) monometallic nanoparticles separately using the electrochemical reduction method of Reetz [27]. The mechanism proposed for this method is shown in Fig. 2.1. In this work we have also verified the effect of concentration and nature of tetra-alkyl ammonium salt and the effect of the current density on the particle size.

The electrolysis cell designed for electrolysis process is of 25-30 ml. The sacrificial anode of pure bulk metal sheet (Cu/Mo) 1cm x 1cm and an inert cathode of platinum sheet 1cm x 1cm were arranged parallel to one another 1cm apart from each other in the electrolysis cell. Dry oxygen free solvent consisting of a mixture of acetonitrile (ACN) and tetra hydro furan (THF) in the ratio of 4:1 respectively was used for preparing the solution of supporting electrolyte cum stabilizer which is either TBAB or TPAB or TEAB. Trials were conducted to determine the optimum concentration to be used during electrolysis. It was observed that a concentration of 0.01M was most effective for better synthesis. This 30 ml solution of supporting electrolyte was taken in a vessel and electrolysis was carried out at room temperature by passing the current of constant current densities (for Cu 6 & 10 $mA/cm^2$ and for Mo 14 & 18 $mA/cm^2$) for two hours in each experiment set.

In the electrolysis process whatever physical changes that were produced in the solutions were carefully recorded and the formation of metal nanoparticles was observed by monitoring the change of color. The electrolysis duration was kept constant for 2 hours. After allowing the suspension to settle for another two hours the tetra-alkyl ammonium bromide stabilized metal nanoparticles formed agglomerates and settled at the bottom of the electrolysis vessel. The solid particles settled at the bottom of the bottle were separated from the solution by simple decantation and the decanted solid product was washed with dry THF for three to four times to remove excess tetra-alkyl ammonium bromide. The supernatant was also collected and preserved for further analysis. The products were then dried under vacuum in desiccators. The samples were preserved in air tight capsule for further analysis. The supernatant solution after first decantation was used for UV- visible spectroscopic analysis and the optical properties were observed as a function of current density. The solid obtained as metal nanoparticles were preserved for further characterization.

**Reaction Mechanism for Electrochemical Synthesis of Metal Clusters:**

$$M^0 \text{ Anode} \rightarrow M^{n+} + ne^-$$

$$M^{n+} + ne^- + \text{stabilizer} \rightarrow M^0 \text{ (Nanoparticles)}$$

$$M^0 \text{ Anode} + \text{stabilizer} \rightarrow M^0 \text{ (Nanoparticles)}$$

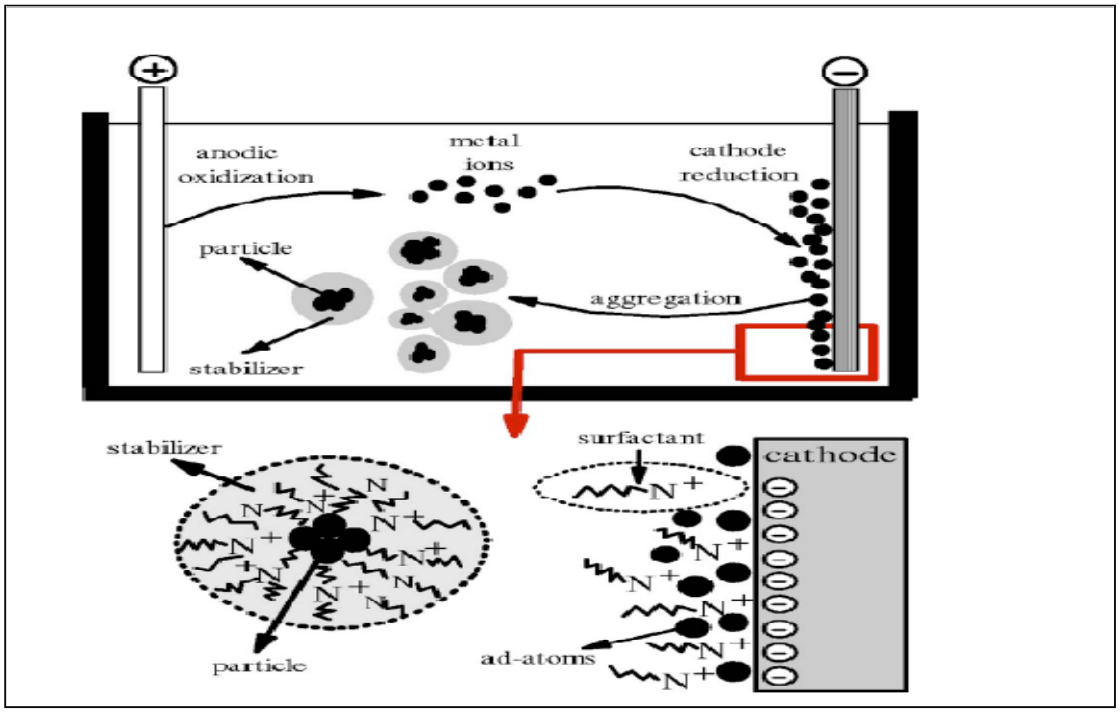


**Fig. 2.1** Mechanism for the electrochemical reduction synthesis of metal colloids and nanoparticles

### 2.1.1 Variation of Parameters in Synthesis of Cu and Mo Monometalic Nanoparticles

***a) Effect of nature of stabilizer:-***

In order to study the effect of nature of stabilizer, the electrolysis process was carried out using different quaternary ammonium salts like TBAB, TPAB and TEAB. Nanoclusters prepared by using these quaternary ammonium salts were characterized by different analytical techniques.

***b) Effect of concentration of stabilizer:-***

The concentration of each stabilizer was varied to study the concentration effect on the particle size and effective formation of copper, silver and molybdenum (oxide) nanoclusters. Optimization of concentration of the stabilizer was made and it was found that 0.01 M solution of each stabilizer is proper for efficient formation of metal oxide nanoclusters.

***c) Effect of current density:-***

In order to study the effect of current density on particle size, the current in the electrolysis process was varied for each stabilizer from at 10 to 14 $mA/cm^2$. At optimum concentration

(0.01M) of each stabilizer, the effect of current density was studied by characterizing the samples, using different analytical techniques such as UV visible spectroscopy, FTIR, XRD, SEM-EDS and TEM. It was found that variation in current density influences the potential at cathode and ultimately it affects the particle size of nanoclusters in the electrolysis process.

## 2.2 Synthesis of Cu-Mo Bimetallic Nanoparticles

Electrochemical reduction method has been adopted for synthesis of bimetallic nanoparticles in the present study. The method employed was similar to the one used for the monometallic nanoparticles as discussed earlier.

Electrolysis cell (for solution volume of 25-30 ml) was designed to carry out electrolysis process. In this cell, two anodes (Cu-Mo) were positioned in such a way that they lie parallel to each other and apart from each other by a distance of 1x1 cm. The inert cathode, platinum foil was placed between the two anodes and it was perpendicular to both of them.

In typical procedure, the above electrolysis vessel having anode (Cu-Mo) 1 x 1cm and a platinum cathode (1 x 1cm) were employed in the preparation of Cu-Mo bimetallic nanoclusters. A mixture of acetonitrile and tetrahydrofuran (4:1) was used as solvent. The supporting electrolyte consisted of solution of ligand, tetra-alkyl ammonium bromide (TEAB/TPAB/TBAB) at 0.01M. The supporting electrolyte used also act as stabilizer in the formation of bimetallic nanoclusters.

Electrolysis was carried out at room temperature by passing the current of various current densities (10 or 14 $mA/cm^2$) for two hours in each experimental set. The colour changes were observed and noted during the electrolysis process. After two hours of electrolysis process the concentration of the nanoparticles increased sufficiently and the solid particles of the nanoparticles settled at the bottom of the vessel. The reaction mixture was transferred into the clean and dry bottle along with solid particles and then after 15 to 20 minutes the nanoparticles were separated by decantation process. The solid as well as the supernatant were collected separately. The solid sample was washed 2 to 3 times with THF to remove the excess ligand. The samples were then dried in vacuum desicator and further stored in airtight capsules for characterization. The supernatant obtained after first step of decantation was preserved for UV visible analysis.

### 2.2.1 Variation of process parameters in synthesis of Cu-Mo Bimetallic Nanoparticles

In the preparation of the bimetallic nanoparticles, a number of parameters have been varied in order to observe the effect on the synthesis of nanoparticles. These parameters are same as those studied in the synthesis of monometallic nanoparticles. They include,

a) Effect of stabilizer

b) Effect of concentration of stabilizer

c) Effect of current density

## 2.3 Sample Preparation for Characterization Techniques:

**a)** ***UV visible spectroscopic analysis:***

Supernatant samples were used to record colour and study surface plasmon absorption in the UV-visible region using Jasco UV-Visible Spectroscopy (UV 540).

**b)** ***Fourier Transform Infrared Spectroscopy:***

The synthesized solid nanoclusters were mixed with KBr and FTIR spectra were recorded in the range of 400 to 4000 cm-1 on Jasco FTIR 8400 Spectrophotometer.

**c)** ***X-ray Diffractometry:***

The powdered X-ray diffraction patterns were obtained out on X-ray powder diffractometer PW-1840, using CuKα radiation (λ = 1.54 A0). The samples were scanned from 20-820 at the scan rate of 5 x 104 CPS. The study was carried out at the Department of Physics, Pune University, Pune.

**d)** ***Scanning Electron Microscopy:***

The scanning electron microscopy study was carried out on JEOL make JSM 63608A microscope at the Department of Physics, Pune University, Pune.

**e)** ***Transmission Electron Microscopy:***

The synthesized nanoclusters were ultrasonicated in ethanol and then a drop of the dispersed nanoparticles was placed onto a carbon coated 400 mesh copper grid with format coating over it, followed by natural evaporation. HR-Transmission electron microscopic study and electron diffraction were carried out on Philips CM 200kv at the Indian Institute of Technology, Mumbai.

## 2.4 SECTION-I Copper Nanoparticles

### 2.4.1 Introduction

Metallic nanoparticles are of great interest due to their excellent chemical, physical and catalytic properties [28]. Among the metal nanoparticles, Cu NPs have received considerable public interest, which may be due to their good optical, electrical and thermal properties. Cu NPs are cost-effective as compared to noble metals like Ag, Au, and Pt. Hence, they are potentially applied in the fields of catalysis [29]. Comparatively Cu NPs have wide range of applications than traditional catalysts because copper has low cost, easy availability, soft reaction conditions to produces high yields in less reaction time. The Cu NPs have also been reported as suitable heterogeneous recyclable catalyst in various environmental problems like hazardous wastes and toxic water pollutants [28].

Metal-catalyzed Coupling reactions (C-C, C-O, C-N etc.) have been hot research topics in recent years because these reactions are very important in organic synthesis. Based on coupling reactions, some complex compounds can be obtained through fewer steps compared with conventional methods. Pd and Cu are widely used in coupling reactions because of their good activity and wide reaction scopes. For Cu, because of its low cost and easy availability, Cu-catalyzed coupling reactions have received tremendous attention in organic synthesis. Actually, Cu-catalyzed coupling reactions have been applied to industrial applications long time ago [30]. C-X coupling reactions using Cu-based catalysts are widely studied in recent years since the discovery of the application of diamine ligands that enabling the coupling of aryl halides and amides (the Goldberg reaction) to be performed under much milder conditions [31]. Since then, Cu-based catalysts for C-X coupling reactions have attracted much attention due to the wide scope of C-X coupling reactions when we use Cu-based catalysts.

In the present study, we have prepared tetra alkyl ammonium salts protected copper oxide nanoparticles by electrochemical reduction method. We have also studied the effect of current density, concentration of ammonium salt, and nature of tetra alkyl ammonium salt on the particle size. These synthesized nanoparticles were used as organic transformation reactions.

### 2.4.2 Visual Inspection

The inset of Fig.2.2 shows sample bottles (1-4) of the colloids of copper oxide nanoparticles after the reaction at different interval of time. After 10 min. the gradual change of color from

colorless to brown black is the clear indicative of the formation of copper nanoparticles and after 2 hrs. the dark black copper oxide nanoparticles were formed in colloidal form.

**Fig.2.2** Visual inspection of copper oxide nanoparticles

### 2.4.3 UV-Visible spectroscopy

Metallic nanoparticles exhibit optical absorption originated from the collective oscillation of the conduction electrons when they are excited by light. It is named as surface plasmon resonance (SPR) and is not observed in bulk metal. The optical response depends upon several factors like local refractive index, the dielectric constant of the medium, morphology (size and shape) and the state of aggregation of the nanoparticles. Any change in these physical features will alter the peak position, intensity optical response [32].

The electrochemical synthesis of Cu nanoparticles capped with different capping agents (TEAB/TPAB/TBAB) at 6 and 10mA/cm$^2$ current density has been carried out in the present study. As the electrochemical reduction proceeds, the change in colour of the reaction mixture with time is monitored. It was seen that between 15 to 20 minutes a change in colour usually took place. In order to obtain the UV-Visible spectrum of the copper nanoparticles about 3.0 ml of the reaction mixture was withdrawn after 20 min. of electrolysis. The spectrum was thus recorded for individual samples. The overlay spectra of the copper nanoparticles obtained at 10 mA/cm$^2$ of current density of each ligand have been presented in Fig.2.3.a-c.

The reduction of copper ions visibly evident from color change associated with it. **Fig. 2.3** shows the copper(II) oxide nanoparticles showed a peak at about 640nm. The greenish colour obtained gradually changed to brownish black indicating copper being oxidized to zero to 2+ oxidation state. Copper(II) oxide nanoparticles exhibits maximum absorption at 638-642nm. This absorption band can be attributed to the surface plasmon resonance peak of copper(II) oxide

nanoparticles. The SPR of colloidal copper oxide nanoparticles reported previously [33] with a broad peak at 590-640nm is in agreement with the present result. A broad peak around 640nm can be attributed to agglomeration and wide size distribution of nanoparticles in the solution. The particles showed hardly any change in the absorption spectra even after a month of ageing time, which indicates the highly stable nature of copper(II) oxide nanoparticles.

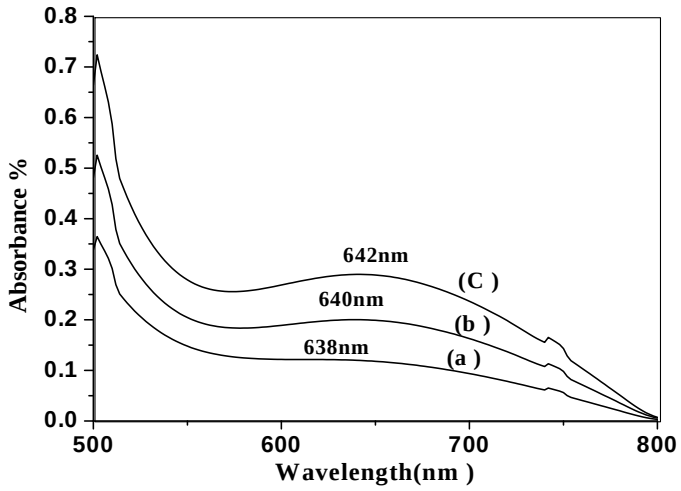


Fig. 2.3 UV-Visible spectrum of CuO NPs a) TEAB b)TPAB & c) TBAB 10mA of 0.01M solution at 10mA current density

Reetz [27] has reported that in the electrochemical reduction method for the preparation of the metal nanoparticles, the size of the nanoparticles decreases with the increase in the current density. It can thus be said that the colloidal Cu nanoparticles prepared at a current density at 6 $mA/cm^2$ are bigger in size as compared to the colloidal Cu nanoparticles prepared at a current density of 10 $mA/ cm^2$, which are thus comparatively small in size. Thus in the present study the colloidal copper nanoparticles prepared at a current density of 6 $mA/cm^2$ show the absorption band at 650-700nm in range over the entire visible range. These results have been well correlated to the reports and can thus be said to be confirmed.

**2.4.4 FTIR Spectroscopy**

In the present work, copper nanoparticles are synthesized by the electrochemical reduction method in which tetra alkyl ammonium bromide salts (TEAB, TPAB and TBAB) were used as capping agents. These capping agents are organic in nature and possess C-N, C-H, and C-C bonds, which are IR active. Hence IR spectroscopic study of the prepared samples will provide important information regarding the capping of the nanoparticles samples.

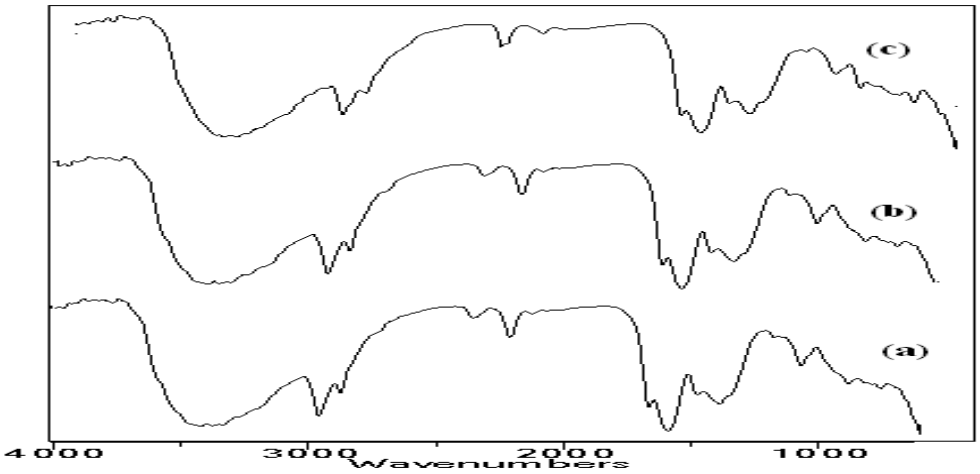


Fig. 2.4 FT-IR Spectra of CuO Nps a) TEAB b) TPAB c) TBAB at 10 mA current density.

Fig. 2.4 represents IR spectra of copper(II)oxide nanoparticles capped with a) TEAB b) TPAB and C) TBAB of 0.01 M solution at 10mA/cm$^2$ current density. In IR spectrum peak appears at 3424-3437 cm$^{-1}$ which can be attributed to the hydroxyl groups, which indicate hygroscopic nature of copper oxide nanoparticles. Peaks at 2962- 2975 cm$^{-1}$, 2872-2885 cm$^{-1}$ & 1587 cm$^{-1}$ are due to the C-H stretching & bending respectively. 1664 cm$^{-1}$ is peak due to $N^+R_4$ symmetrical ion. Peak at 1386-1399 cm$^{-1}$ can be attributed to the C-C stretching and at 1069 cm$^{-1}$ to C-N stretching. Some of the peaks reflect in the range of 752-880 cm$^{-1}$ that are due to bending mode of vibrations of M-O-M bending (M=Cu) and the peak at 659-690 cm$^{-1}$ are the stretching of mode of vibration of Cu-O. In general change in capping agents from TEAB to TBAB showed increase in wave number was noticed from 3424 to 3437, 2962 to 2975, 2872 to 2885, 752 to 760 and 659-690 cm$^{-1}$.

**2.4.5 X-ray diffraction pattern**

In order to understand the phase symmetry of copper(II)oxide nanoparticles a systematic study on the XRD studies was undertaken. Fig. 2.5 shows XRD pattern of copper(II)oxide nanoparticles capped with 0.01M concentration a) TEAB b) TPAB c) TBAB at 10 mA/cm$^2$ current density. The lattice parameters a = 4.653, b = 3.410, c = 5.4089 at $\beta$ = 99.480. The strong and sharp peaks were obtained at planes (-111), (111), (012), (020), (120) & (121) indicating the monoclinic structure of copper(II)oxide nanoparticles which were found to be highly crystalline in nature. The diffraction is in good co-ordination with the ASTM card No. 74-1021. The average particles size calculated were in the range of 5-25 nm using Debye Scherrer equation (1), indicating high surface area. The surface area to volume ratio of nano-crystals [34] is given by

$$d = \frac{K\lambda}{\beta \cos \theta} \qquad (1)$$

Where K known as Scherrer's constant (shape factor), ranging from 0.9 to 1.0, λ the wavelength of the X-ray radiation source is 1.5418, β is the full width of the peak at half height and θ is Bragg angle.

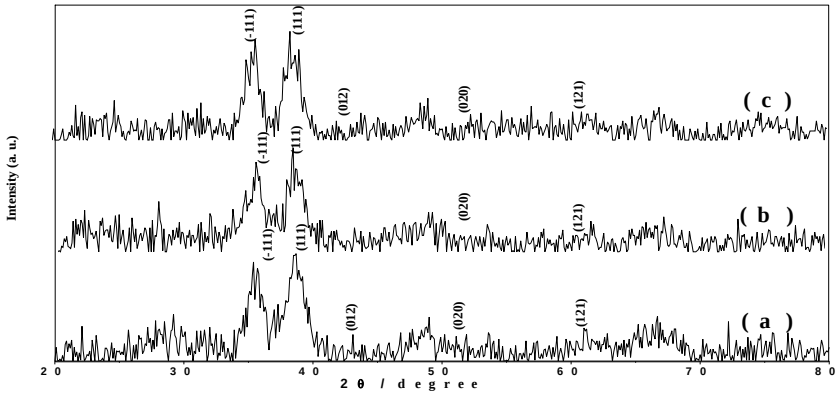


Fig.2.5 XRD pattern of copper(II)oxide nanoparticles a) TEAB b) TPAB c) TBAB at 10 mA/cm$^2$ current density.

XRD plots show the intense peaks of TEAB, TPAB, TBAB for (111) plane the full width of half maximum (FWHM) value were 1.3818, 1.4097 & 1.5609 increases with decreasing the particle in size 6.04nm, 5.92nm & 5.34nm respectively as shown in Table 2.1.

**Table 2.1** The effect of stabilizer on size of copper(II)oxide nanoparticles

| **Cu NPs** | **2θ** | **h k l** | **FWHM** | **Size (nm)** |
|---|---|---|---|---|
| Cu-TEAB | 38.37 | 111 | 1.3818 | 6.04 |
| Cu-TPAB | 38.56 | 111 | 1.4097 | 5.92 |
| Cu-TBAB | 38.65 | 111 | 1.5609 | 5.34 |

### 2.4.6 Scanning Electron microscopy

The evaluated morphology of copper nanoparticles capped with TEAB TPAB and TBAB by SEM is shown in Fig. 2.6 a-c. The scanning electron micrograph and the particle size distribution for the sample of copper nanoparticles capped with TEAB, TPAB and TBAB at current density of 10 mA/cm$^2$ is obtained for various resolutions.

To study the surface morphology and elemental composition, the SEM with EDS were investigated systematically. Fig. 2.6a-c shows that nanoparticles have irregular shape and the

distribution was not uniform, which was probably due to the partial solubility of the surfactant in the solvent in experimental condition. Fig.2.6a-b shows presence of porous nanoparticles that agglomerated irregularly. Fig.2.6c shows SEM microstructure of copper oxide nanoparticles capped with TBAB with dense agglomerations.

This is probably due to the partial solubility of the surfactant in the solvent under the given experimental conditions. The shapes of the copper nanoparticles [35-36] on the SEM micrographs of copper nanoparticles were studied.

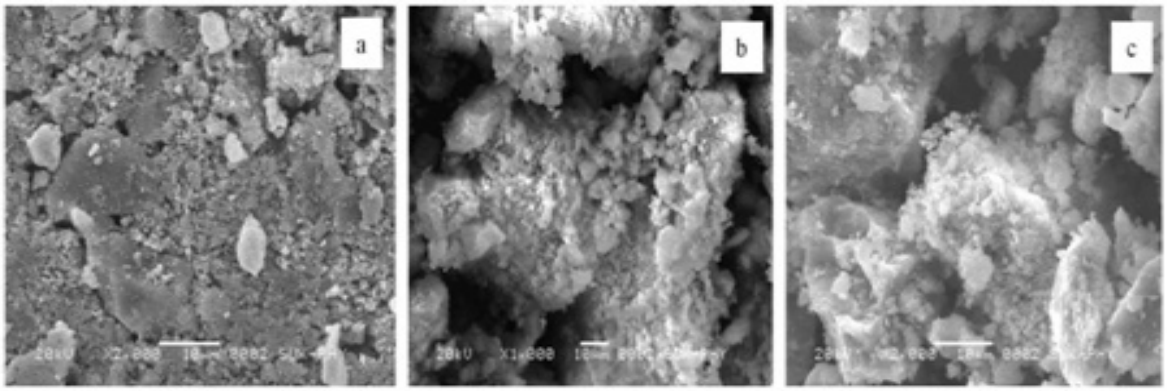


Fig.-2.6 SEM images of Copper oxide Nps a) TEAB b) TPAB c) TBAB at 10 mA current density

**Energy dispersive spectroscopy**

Copper nanoparticles sample was analyzed qualitatively and quantitatively by EDS. Fig.2.7 shows that copper, oxygen and bromine are present in the sample and its composition is given in Table 2.2. According to the atomic % and mass % of elements clearly shows that the copper oxide nanoparticles are formed. Br is present in trace amount because of TBAB used as capping agent. The EDS spectra (Fig. 2.7) of copper nanoparticles excited by electron beam (20 kv) show peaks for the elements of C, O, Br and Cu as observed in Table 2.2 Br present in trace amount is an impurity present in capping agents.

**Table -2.2** Elemental compositions of CuO nanoparticles capped with TBAB

| **Elements** | **KeV** | **Mass%** | **Atom%** |
|---|---|---|---|
| C K | 0.277 | 7.64 | 26.80 |
| O K | 0.525 | 6.24 | 16.43 |
| CuK 1 | 8.840 | 84.02 | 55.67 |
| BrL | 1.480 | 2.10 | 01.11 |

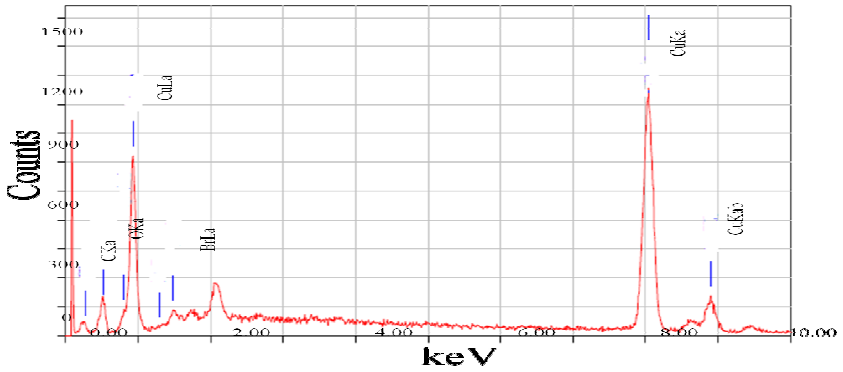


Fig.2.7 EDS spectrum of copper nanoparticles

### 2.4.7 Transmission electron microscope

Transmission electron microscopic study has been done for evaluate, particle shape and size distribution of copper oxide nanoparticles as shown in Fig.2.8 synthesized with capping agents TBAB and TPAB respectively. Micrograph also showed particles of various sizes and some clusters have been observed in Fig.2.8a-c. In Fig. 2.8c clear anisotropy is observed with the particles in size range of less than 5nm and greater up to about 10nm which isin coordination with the XRD results.

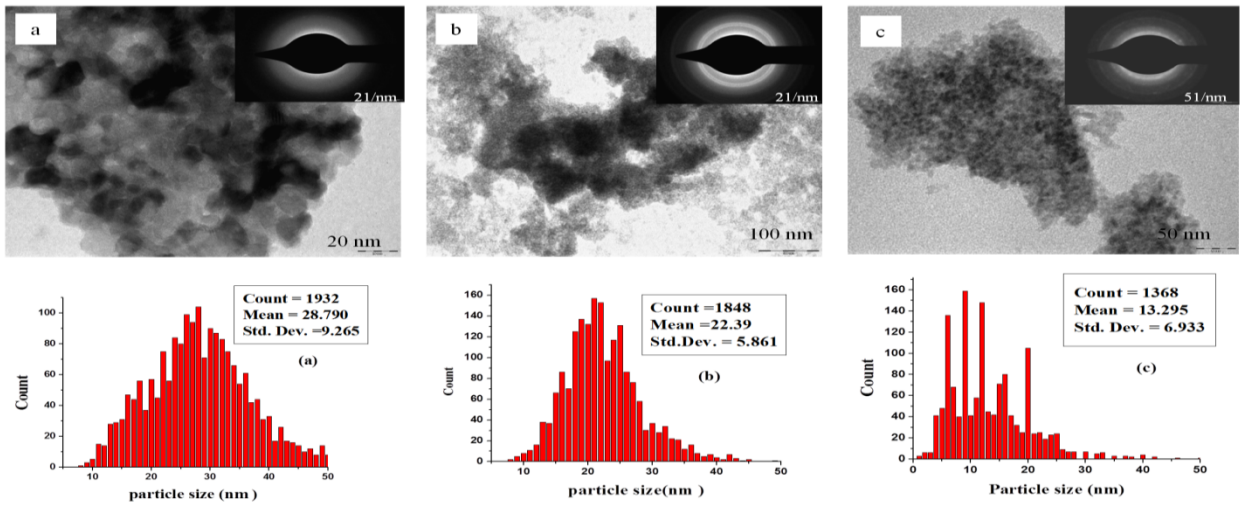


Fig. 2.8 TEM images inset with SAED pattern & respective histogram of copper oxide Nps a) TEAB b) TPAB c) TBAB at 10 mA current density

In the micrograph of Fig. 2.8a-c, the product consists of spherical nanoparticles with a regular morphology and average size of the particles in the range of 5-30 nm, which showed good agreement with crystalline size from XRD. The histogram in Fig.2.8a-c showed that the average mean size & standard deviation of copper oxide NPs capped with a) TEAB b) TPAB & c) TBAB as 28.79 ± 9.26 nm, 22.39 ± 5.86 nm & 13.29 ± 6.93 nm respectively, which represent the

aggregated copper nano-crystals. The SAED images inset of Fig 2.8 a-c show that the CuO NPs showed good crystallinity. The difraction rings on picture correspond to (-111) and (111) respectively which is in accordance with (-111) and (111) peaks in XRD pattern.

## 2.5 Section II Molybdenum nanoparticles

### 2.5.1 Introduction

In recent years, much effort has been devoted to the study of molybdenum oxide and related materials. Molybdenum oxides posses unique catalytic and electronic properties and have potential applications in chemical synthesis, petroleum refining, recording media and sensors [37-40]. They are also used in the optical device applications [41-43] and are promising material for photoelectrochemical energy production with high surface area having higher photo efficiencies [44-45].

### 2.5.2 Visual inspection

The inset in Fig.2.9 shows sample bottles (1-4) of the colloids of molybdenum oxide nanoparticles after the reaction at different interval of time. After 10 min. the color of reaction mixture changes from colorless to yellow and after 2 hr. the bright yellow appears indicating formation of molybdenum oxide nanoparticles.

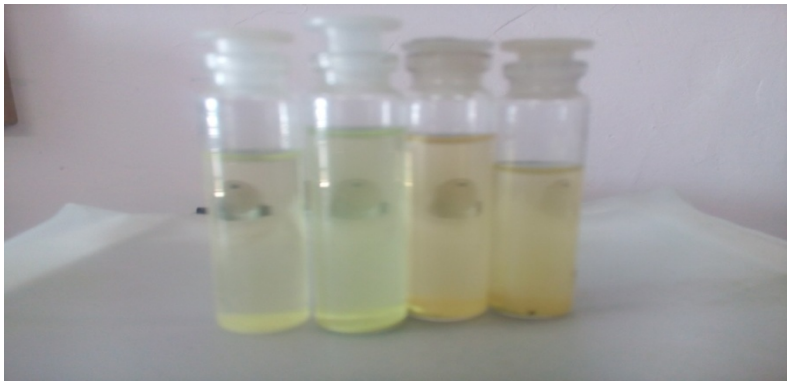

Fig. 2.9 Visual inspection of Molybdenum oxide nanoparticles

### 2.5.3 UV visible spectroscopy

Molybdenum oxides are photochromic materials, which change colour upon going from one oxidation state to another by absorption of light [47-48]. The yellow molybdenum oxide nanoparticles are stable nature they do not change their color even after the sample is stored under ambient conditions.

The dependence of the UV-Visible absorption spectra of the molybdenum oxide nanoparticles are shown in Fig.2.10a-b capped with TPAB at 14mA and 18mA current density. The absorbance seen across the visible range from 600 to 850nm confirms the formation of $MoO_3$ nanoparticles [49].

The UV-visible absorption spectrum recorded for molybdenum oxide nanoparticles is shown in Fig 2.10a & 2.10b which exhibits maximum absorption at 634nm & 642nm for TPAB and TBAB at 14 mA respectively. The metal nanoparticles exhibit absorption bands or broad regions of absorption in the UV–visible range due to the excitation of surface plasmon resonances (SPR) or interband transitions; these SPR are characteristic properties for the metallic nature of particles. The prominent peak observed at 634nm & 642 nm, in the visible wavelength is due to the absorption of surface Plasmon. This absorption band can be attributed to the surface Plasmon resonance (SPR) peak of molybdenum oxide nanoparticles Red shift from 634 to 642 was observed as the particle size decreased because of increase in intensity of absorption peaks and current density respectively. A broad peak around 634nm & 642nm can be attributed to wide size distribution of particles form in the solution. The particles showed hardly any change in the absorption spectra even after a month of ageing time indicating highly stable nature of particles. The broadening of SPR peak was due to the agglomeration of the nanoparticles in the sample and high width of these particles distribution

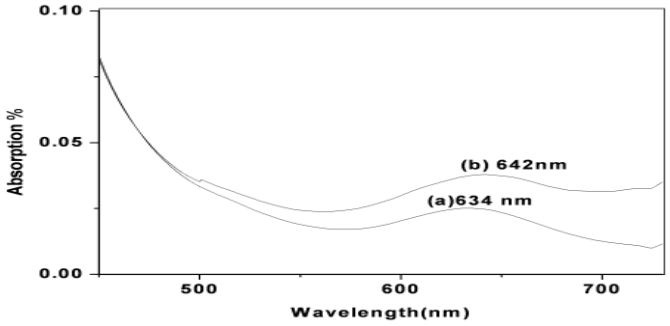


Fig. 2.10 UV-vis spectrum of $MoO_3$ NPs a) TPAB and b) TBAB at 14 mA current density

**2.5.4 FTIR spectroscopy**

In IR Spectrum of molybdenum oxide nanoparticles shown in Fig. 2.11a-b show broad peaks appearing at 3432 $cm^{-1}$ & 1633 $cm^{-1}$ due to the stretching and bending vibration of hydroxyl groups adsorbed on molybdenum oxide nanoparticles. The peak at 949 $cm^{-1}$ is due to the terminal Mo=O bond which indicate the layered orthorhombic phase[50] and absorption at

848 $cm^{-1}$ & 597 $cm^{-1}$ are of the stretching and bending mode of vibration Mo-O-Mo. The spectrum also contains distinct peaks at 496 $cm^{-1}$ & 669 $cm^{-1}$ which correspond to the mixed phase that contains molybdenum and molybdenum oxide.

The IR spectra of nanorods obtained after heated at 500°C in Fig. 2.11c-d show the peak at 989 $cm^{-1}$ due to the terminal Mo=O bond which indicate the layered orthorhombic $MoO_3$ phase. Absorption at 848 $cm^{-1}$ is attributed to the stretching vibration of the oxygen atom in the Mo-O-Mo unit and at 580 $cm^{-1}$ is due to bending mode of the Mo-O-Mo unit which reveals that the oxygen ion is shared by three molybdenum ions. Absorption of $H_2O$ on the sample takes place due to contact of sample with environment which give rise to hydrogen bonding of all surface O-H groups, the broad peak around 3424 $cm^{-1}$ is the stretching mode of vibration of O-H groups & peak at 1633 $cm^{-1}$ can be assigned to the bending mode of O-H groups of absorbed water. Hydrogen bonded O-H groups show (H…O-H) bending vibration at 1420 $cm^{-1}$ and 2974 $cm^{-1}$ for O-H stretching.

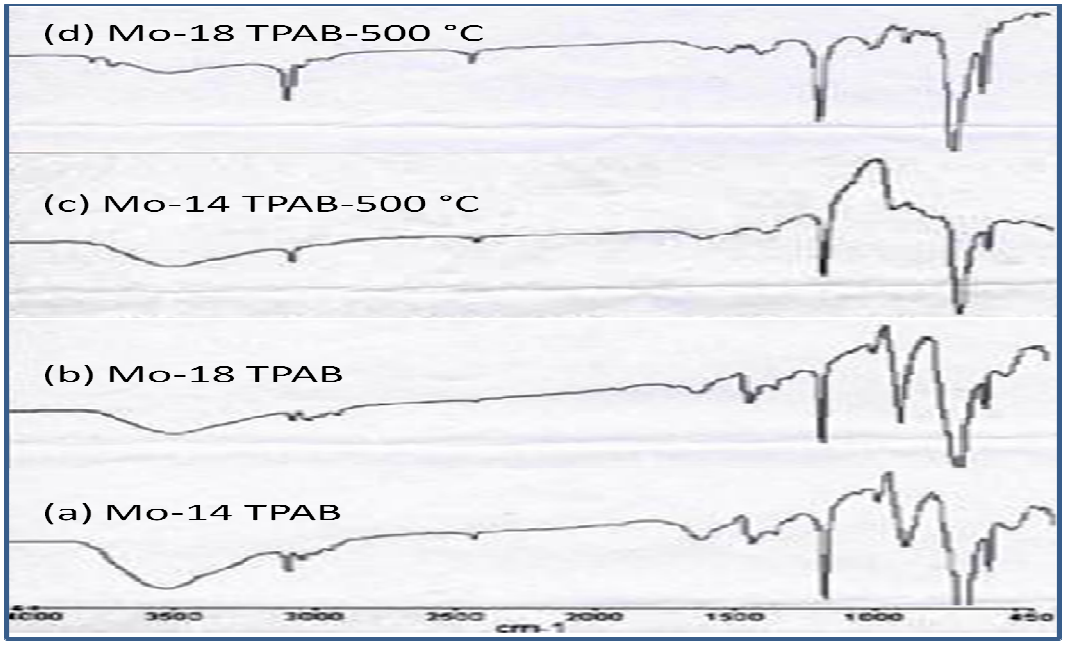


Fig.2.11 IR spectra of $MoO_3$ at 14mA & 18 mA current density (a), (b) before and (c), (d) after heated at 500ºC.

### 2.5.5 X-Ray Diffraction pattern

The X- ray diffraction pattern shown in Fig.2.12 explains the crystal structure and phase composition of $MoO_3$ nanocrystalline materials. The sharp diffraction peaks suggest crystalline nature of nanomaterials. It can be observed in Fig.2.12a-b that orthorhombic lattice system with lattice parameter a=3.966 A°, b=13.82 A°, c= 3.703A°(JCPDS: 05-0506) and strong peaks at

(001) & (011) show crystalline nature of molybdenum oxide nanoparticles. Few peaks of other phase occur due to the presence of capping agent. The effect of heating temperature at 500°c as observed in XRD spectrum Fig.2.12c-d revels that $MoO_3$ nanorods have orthorhombic lattice system with lattice parameter a=3.96A°, b= 13.85A°, c=3.696A°,(JCPDS: 35-0609). Interestingly, no peaks of any other phases or impurities were detected, indicating high purity of $MoO_3$ nanorods.

When compared with the standard XRD results, most of the peaks matched at (0k0), a strong peak appears for nanorods. Considering these results with regard to the crystal structure of bulk $MoO_3$ the (010) & (100) planes encloses the nanorods facets along the longitudinal direction & the (001) planes enclose the growth direction (Fig. 2.12e). In Fig.2.12c-d observed that (040), (060) are very strong peaks respectively, that means all the strong diffraction peaks correspond to (0k0) planes compared to the other (hkl) planes of the $MoO_3$ nanorods indicating the highly anisotropic growth as well as the preferred orientation of the nanorods. In Fig.2.12c-d (110), (021), (130) & (002) are weak peaks, which show that crystal growth is slow in these directions, causing decrease in the crystal diffraction line intensity. The surface area to volume ratio of nano-crystals is given by

$$d = \frac{K\lambda}{\beta \cos \theta} \quad (1)$$

Where K known as Scherrer's constant (shape factor), ranging from 0.9 to 1.0, λ=1.5418 is the wavelength of the X-ray radiation source, β is the width of the XRD peak at half height and θ is Bragg angle. The average particle size of the powder was calculated by using Debye-Scherrer formula (1). In Table 2.3(entries a-d) shows the decrease in particle size with increasing current density and also calcinate temperature is given.

From Table 2.3, intense peaks appear at 24.273, 24.246, 25.723 & 25.723 for hkl plane 001, 001, 040 & 040 respectively. The change of current density from 14mA to 18mA decreases the crystalline size from 182.57 nm to 59.41nm. The effect of heating at 500ºC also decreases the crystalline size from 40.11nm to 31.44nm

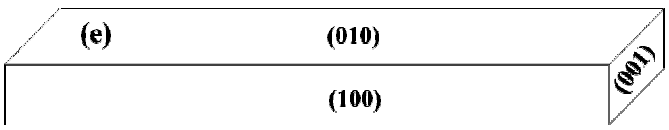

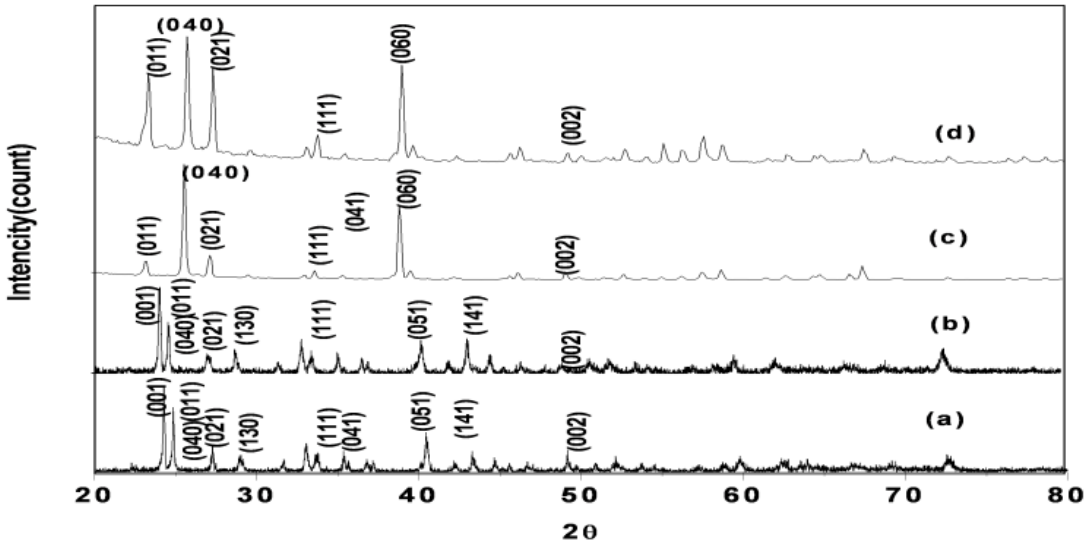


Fig. 2.12 XRD pattern of $MoO_3$ nanoparticles at 14mA & 18 mA current density (a), (b)before heated, (c), (d) after heated at 500ºC and (e) Orientation of nanorod.

Table 2.3 Change in particle size with change in current density and calcination temperature

| SN | $MoO_3$ nano | 2θ | h k l | FWHM | Size (nm) |
|---|---|---|---|---|---|
| 1 | Mo-14 TPAB | 24.273 | 001 | 0.1106 | 182.57 |
| 2 | Mo-18 TPAB | 24.246 | 001 | 0.1763 | 59.41 |
| 3 | Mo-14 TPAB-500°C | 25.723 | 040 | 0.2366 | 40.11 |
| 4 | Mo-18 TPAB-500°C | 25.723 | 040 | 0.2913 | 31.44 |

### 2.5.6 Scanning Electron microscopy

The morphology of product were examined by scanning electron microscope. Fig.2.13a-b reveals sample before calcination ie. ununiform crystals are observed with square and cubical like structures. The effect of current density reduces the size of nanomaterials as shown in morphology in Fig. 2.13a-b. The effect of calcining at 500°C changes the morphology from particles to nanorods as shown in Fig.2.13c-d which show flat or belt like and few cylindrical wire like nanorods of $MoO_3$. Energy dispersive X-ray spectra were also recorded to determine the chemical composition of $MoO_3$ nanorods. Result from the EDX spectra show that the nanorods contain only molybdenum and oxygen elements.

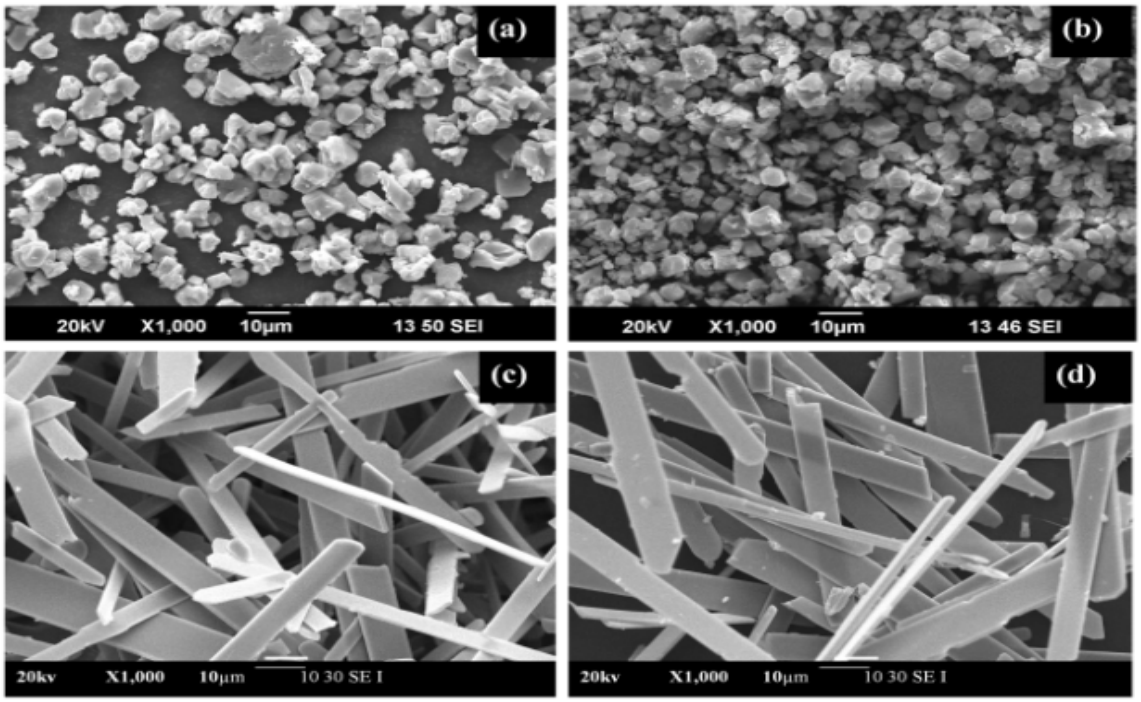


Fig. 2.13 SEM micrograph of $MoO_3$ nanoparticles at 14mA & 18 mA current density(a), (b) before heated and (c), (d) after heated at 500ºC.

**Energy dispersive spectroscopy**

Elemental compositions of $MoO_3$ nanoparticles before calcination are represented in the EDS spectrum shown in Fig.2.14a. The Mo & O peaks were found in spectrum which indicates formation of $MoO_3$ nanoparticles. In addition to that C & Br peaks were found in trace amount indicating $MoO_3$ nanoparticles capped with TPAB capping agent. The elemental quantitative analysis is also shown in Table 2.4a shows that according to the atomic % and mass % of elements the $MoO_3$ nanoparticles were formed. Br presented in trace is an impurity from capping agent.

Elemental compositions of after heated at 500°C $MoO_3$ nanoparticles are represented in the EDS spectrum shown in Fig.2.14b. Only Mo & O peaks were found in spectrum which indicates formation of pure $MoO_3$ nanoparticles. The elemental quantitative analysis is also shown in Table 2.4b shows that according to the atomic % and mass % of elements the elements present are Mo and oxygen only.

**Table 2.4 a** The elemental quantitative analysis of before heated $MoO_3$ nanoparticles.

| Constituents | Mass (%) | Atom (%) |
|---|---|---|
| C | 22.18 | 46.86 |
| O | 24.56 | 38.96 |
| Br | 1.62 | 0.51 |
| Mo | 51.65 | 13.66 |
| Total | 100.00 | 100.00 |

**Table 2.4b** The elemental quantitative analysis of after heated at 500°C $MoO_3$ nanoparticles.

| Constituents | Mass (%) | Atom (%) |
|---|---|---|
| O | 12.47 | 46.08 |
| Mo | 87.53 | 53.92 |
| Total | 100.00 | 100.00 |

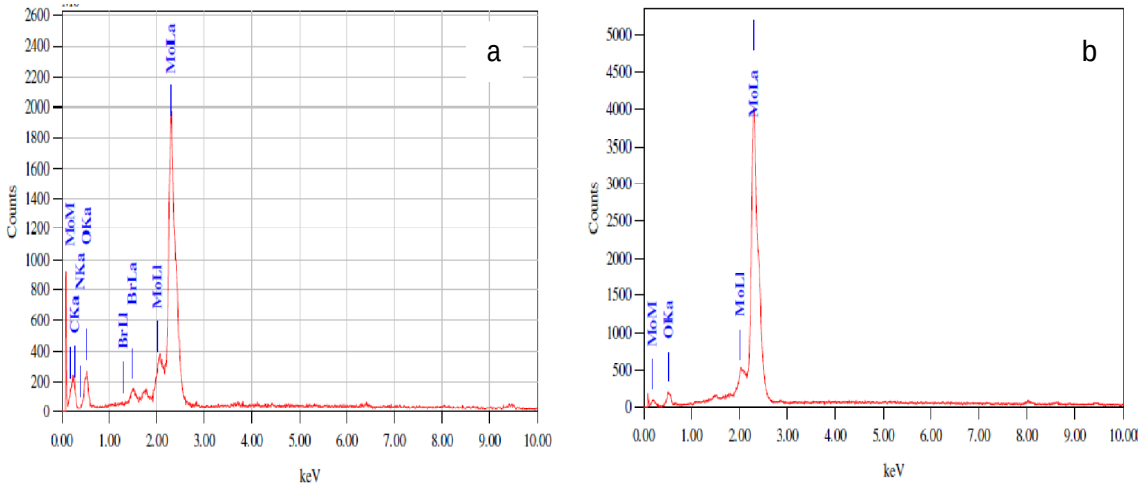


Fig. 2.14 EDS patterns of $MoO_3$ NPs at 14mA current density (a) before (b) after heated at 500ºC

### 2.5.7 Transmission electron microscope

The size and morphology of product were examined by transmission electron microscope (TEM) micrograph of $MoO_3$ crystal. Before heating (Fig. 2.15a-b) square & few irregular shape crystallites occured with size of few tens of micron. Fig. 2.15c-f show the effect of heating at 500ºC in which change in the morphology from irregular shape to uniform nanorods with 20-120 nm width and length of few tens of micron. In fig. 2.15e-f cylindrical wire nanorods, mostly flat or belt nanorods were present. The selected area electron diffraction (SAED) pattern recorded perpendicular to the growth axis of individul nanorods could be indexed to the [010] zone axis of

diffraction of orthorhombic $MoO_3$( Fig. 2.15g-h). The spot pattern of SAED confirms that the compounds are single crystalline nanorods.

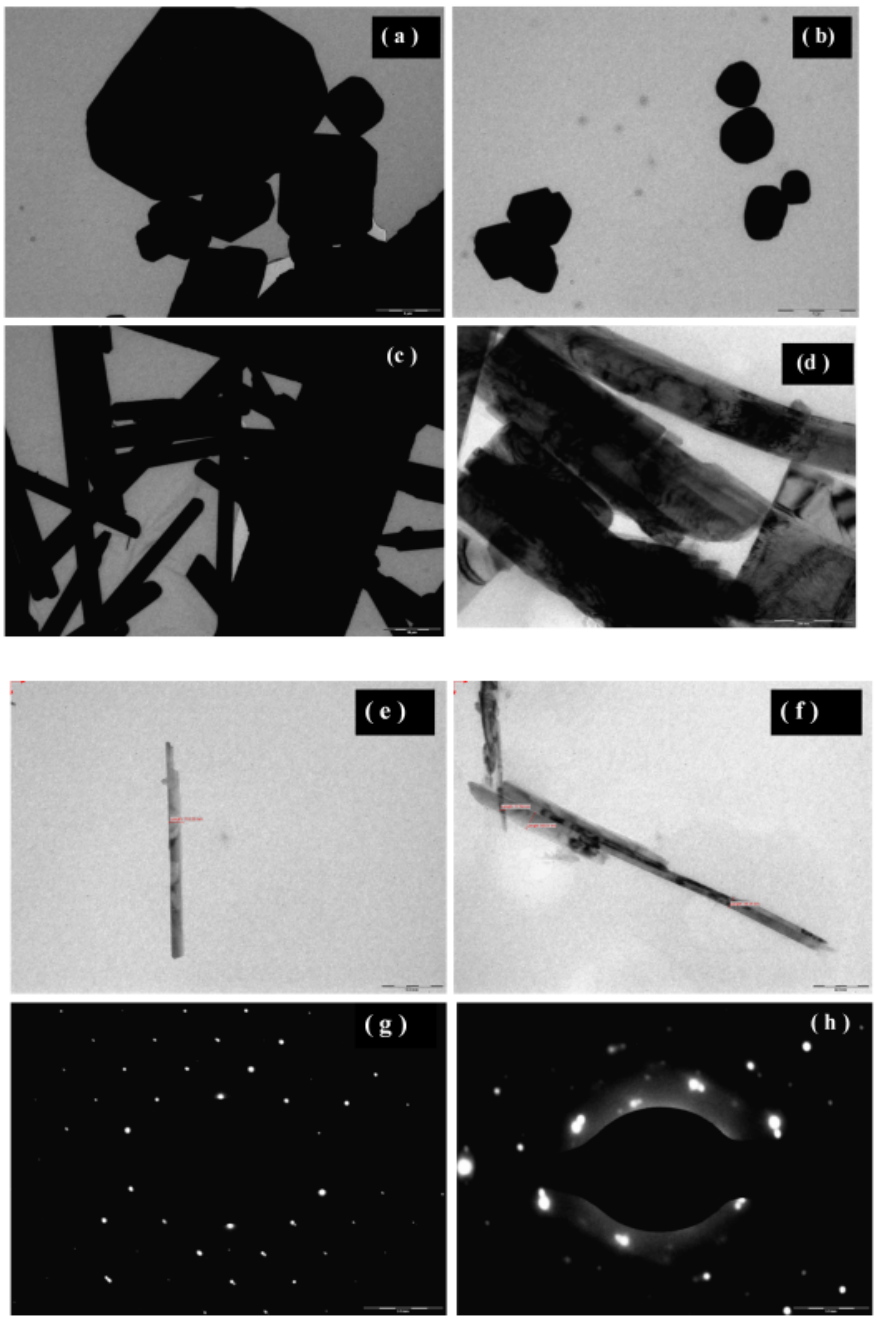


Fig. 2.15 TEM images of $MoO_3$ nanoparticles at 14 mA & 18 mA current density (a),(b) before heated and (c), (d) after heated at 500ºC,(e) cylindrical rod, (e) belt like nanorods & SAED pattern (g) & (h).

## 2.6 Section III Copper-Molybdenum nanoparticles

### 2.6.1 Introduction

The bimetallic nanoparticles are basically composed of two different elements i.e. two kinds of metals are combined in one particle. Bimetallic nanoparticles composed of two different metal elements are of greater interest than monometallic ones from both the scientific and technological views, for the improvement of the catalytic properties of metal particles [51-53]. This is because bimetallization can improve catalytic properties of the original single metal catalyst and create a new property, which may not be achieved by monometallic catalyst. Schaak and coworkers have performed numerous studies on atomically ordered bimetal intermetallic nanomaterials such as PdZn, CuZn, AuCu and others [54-56]. The copper based nanomaterials have been attracted a lot of attention in the past due to their non-toxicity, interesting electronic structures and promising applications in photovoltaic and solar energy cells [57-79]. Also they have full miscibility and high chemical stability so that they can be used in almost any environment with no risk of rapid chemical reactions.

Molybdenum and molybdenum based materials have been widely used in chemical industry, metallurgy, aerospace industry etc. for the properties of high yield, strength and hardness at high temperature, good erosion resistance, excellent thermal and electrical conductivity [80-81]. Metallic molybdenum is widely used in alloy, electrode, metal particle toughened ceramic matrix composites and catalysts [82-91]. Here we describe the electrochemical reduction method for preparation of Cu-Mo bimetallic oxide nanoparticles.

### 2.6.2 Visual inspection

The inset of Fig. 2.16 shows sample bottles (1-4) of the colloids of Cu-Mo bimetallic oxide nanoparticles after the reaction at different interval of time. After 10 min. the color of reaction mixture changes from colorless to brown red and after 2 hours, the dark brown black Cu-Mo bimetallic oxide nanoparticles were formed in colloidal form.

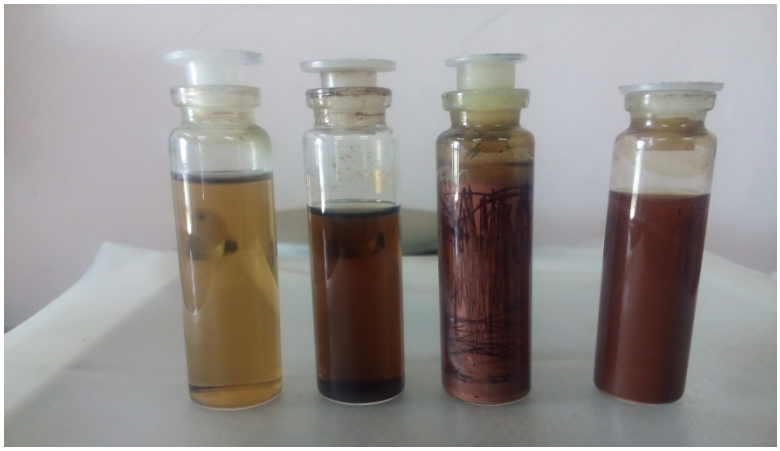

Fig. 2.16 Visual inspection of Cu-Mo bimetallic nanoparticles

### 2.6.3 UV-visible spectroscopy

The property most immediately observable for metal nanoparticles dispersion of certain metals is their color. Comparisons of spectra of bimetallic nanoparticles with the spectra of the respective monometallic nanoparticles dispersions can confirm a bimetallic structure for the nanoparticles [92]. The electrochemical synthesis of Cu-Mo bimetallic nanoparticles capped with different capping agents (TEAB/TPAB/TBAB) at 14 mA/cm$^2$ current density has been carried out in the present study. In Fig. 2.17 a-c the absorption spectrum of the alloy Cu-Mo oxide nanoparticles exhibits distinct peaks at 521-523 nm and 726-731 nm. The reported values for copper nanoparticles show the absorption band at 500-600 nm and molybdenum nanoparticles show the absorption band in the range of 600-700 nm. Thus the peaks in Fig 2.17a-c clearly indicate the formation of bimetallic Cu-Mo oxide nanoparticles.

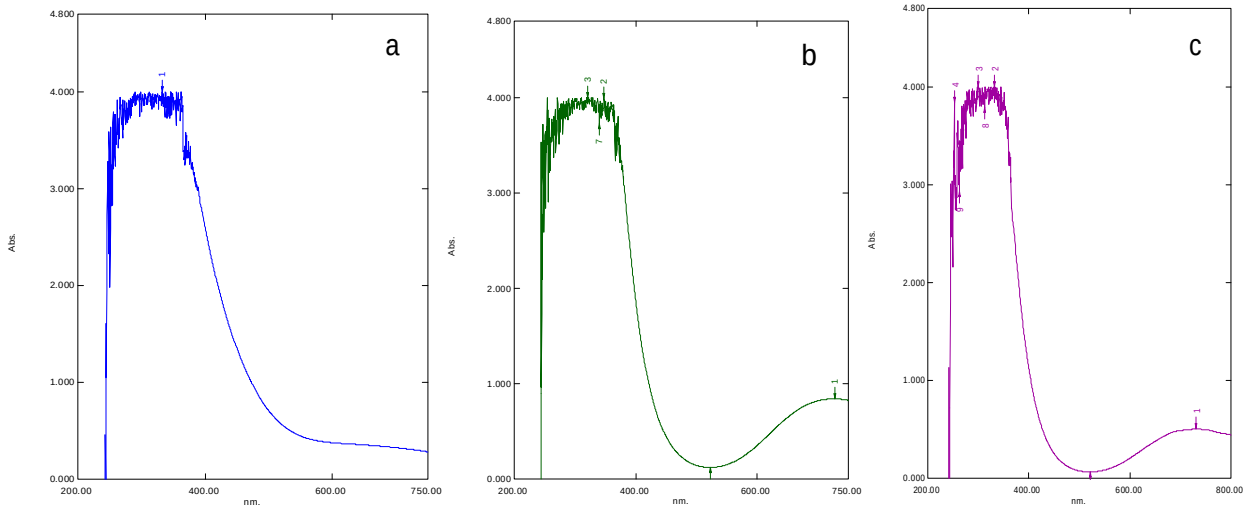


Fig. 2.17 UV-Visible absorption spectra of the Cu-Mo bimetallic oxide nanoparticles at 14 mA/cm$^2$ current density capped with a) TEAB, b) TPAB and c) TBAB respectively

### 2.6.4 FTIR spectroscopy

The analysis of the prepared sample of Cu-Mo bimetallic nanoparticles capped with tetra alkyl ammonium salt (TEAB, TPAB and TBAB) reveal the chemical properties of nanoparticles. On the basis of the FTIR spectra we have obtained the results for the surface chemistry of the nanoparticles. The tetra alkyl ammonium bromide used as a capping agent form a protective layer on the surface of the nanoparticles. These capping agents are organic in nature and possess a number of characteristic functional groups. The frequencies for the different functional groups have been reported [42-44]. The position and the presence of these functional groups can be detected by the FTIR technique.

The Fig.2.18a shows the IR spectrum of the as prepared sample of Cu-Mo bimetallic nanoparticles capped with TEAB. The important peak observed in the IR spectrum of the prepared samples is at 3736cm$^{-1}$ which corresponds to the O-H stretching band. This arises due to the absorption of water molecules by the sample during storage. The broad peak at 3036cm$^{-1}$ and a narrow peak at 2879cm$^{-1}$ correspond to the C-H stretching vibrations. The peak at 1784cm$^{-1}$ corresponds to the $CO_2$ which is absorbed by the sample. The peak at 1684cm$^{-1}$ is related to the symmetrical ammonium ion ($N^+R_4$). The frequency at 1491cm$^{-1}$, 1442cm$^{-1}$ and 1354cm$^{-1}$ corresponds to the C-H bending vibrations. The C-N linkage in the $N^+R_4$ gives a medium band at 1236cm$^{-1}$ and 1134cm$^{-1}$, which are due to the stretching vibrations. The peak at 833cm$^{-1}$ and 690cm$^{-1}$ corresponds to the $CH_2$ rocking. These results indicate that the capping agent TEAB has been adsorbed on the surface of the Cu-Mo bimetallic nanoparticles.

The FTIR spectra for the prepared Cu-Mo bimetallic samples capped with TPAB and TBAB are shown in Fig. 2.18b and Fig. 2.18c respectively. These spectra show the presence of characteristics functional groups present in the ligand at the expected frequencies which indicate that the proper capping of the Cu-Mo bimettalic nanoparticles by the ligand has been achieved.

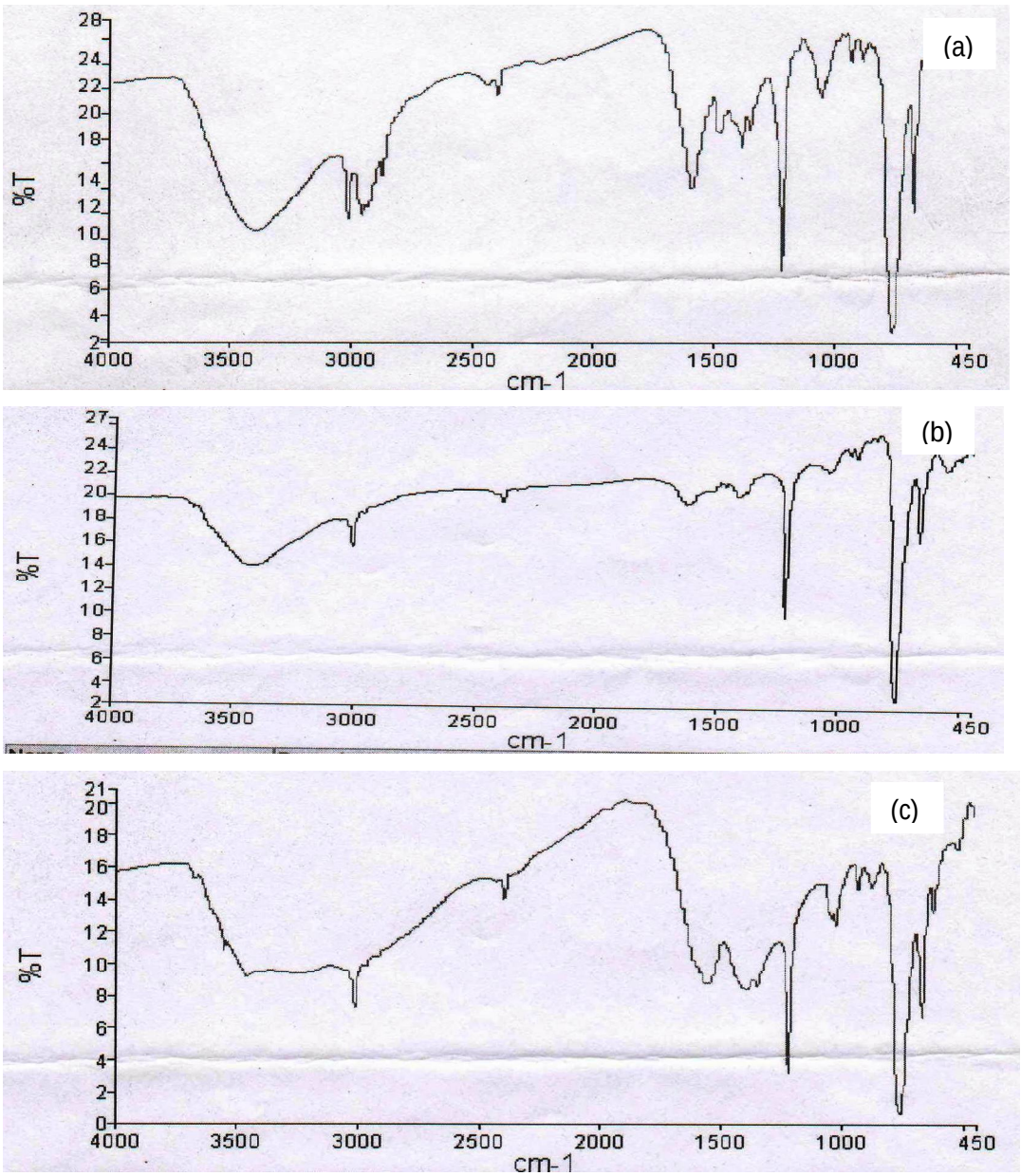


2.18 FTIR spectra of the Cu-Mo bimetallic oxide nanoparticles at 14 mA/cm$^2$ current density capped with a) TEAB, b) TPAB and c) TBAB respectively.

### 2.6.5 X-ray diffraction pattern

The X-ray diffraction pattern of the Cu-Mo bimetallic nanoparticles synthesized with TEAB, TPAB and TBAB capping agent at 14mA/cm$^{-2}$ is shown in Fig. 2.19a-c which indicates the crystalline nature of particles. The peaks at 2θ values of corresponding plane (010), (011), (111), (201), (211), (003) and (312) show the monoclinic structure of copper oxide nanoparticles (ASTM No. 7421).

The peaks at planes (020), (030), (101), (011), (221), (270), (162) and (232) indicate the orthorhombic structure of molybdenum oxide nanoparticles. The data is matched with ASTM card no. 76-1003. The peak at 31.162° that is the strongest peak of copper is overlapped with the peak of molybdenum can be assigned (011) plane of the orthorhombic structure of Mo. The mean size of Cu-Mo nanoparticles obtained from the half width of the (011) peak using the Scherrer equation is about 12.50 nm.

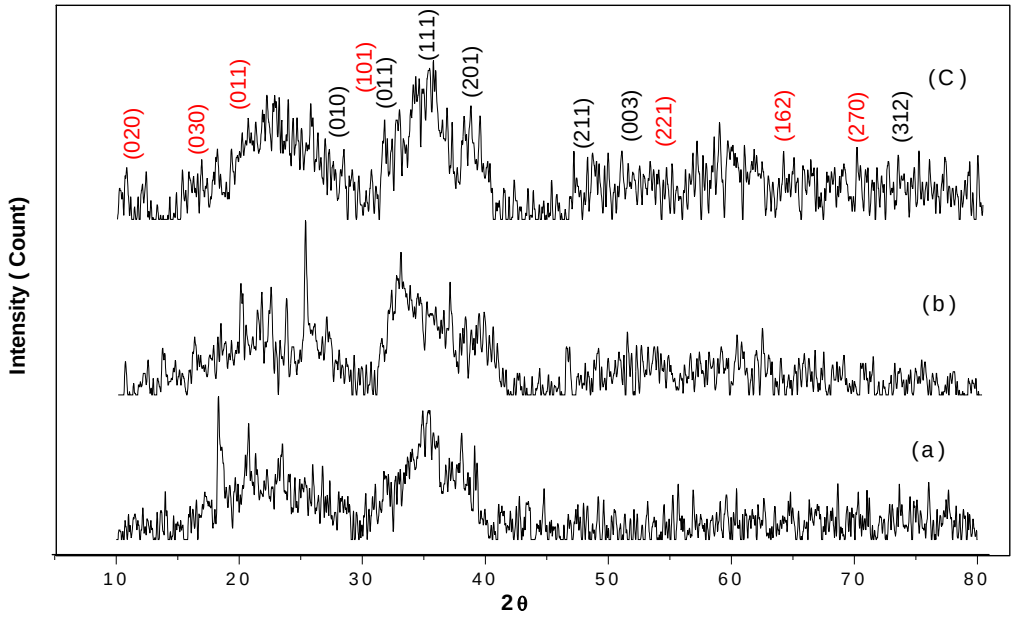


2.19 XRD pattern of the Cu-Mo bimetallic oxide nanoparticles at 14 mA/cm$^2$ current density capped with a) TEAB, b) TPAB and c) TBAB respectively

**2.6.7 Scanning electron microscopy**

The evaluated morphology of Cu-Mo bimetallic nanoparticles capped with TEAB, TPAB and TBAB by SEM is shown in Fig. 2.20a-c. The scanning electron microgram and the particle size distribution for the sample of Cu-Mo bimetallic nanoparticles capped with TEAB, TPAB and TBAB at current density 14 mA/cm$^2$ is obtained for various resolutions.

To study the surface morphology and elemental composition, the SEM with EDS were investigated systematically. Fig. 2.20a-c show that nanoparticles have irregular shape and the distribution was not uniform which was probably due to the partial solubility of the surfactant in the solvent in experimental condition. Fig.2.20a-b show presence of porous nanoparticles that agglomerated irregularly. Fig.2.20c show SEM microstructure of Cu-Mo bimetallic nanoparticles

capped with TBAB with dense agglomerations. This is probably due to the partial solubility of the surfactant in the solvent under the given experimental conditions. Fig. 2.20a-c shows the presence of porous nanoparticles that are agglomerated irregularly. For the purpose of identifying the shapes of the Cu-Mo bimetallic nanoparticles by using the SEM micrographs were studied. However such shape or surface could not be found in any of the reference.

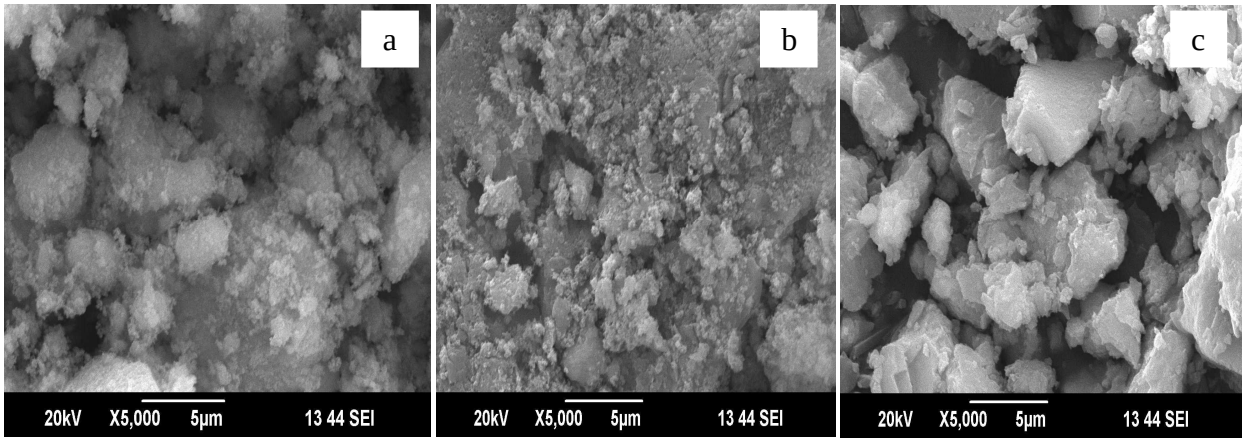


Fig. 2.20 SEM micrographs of the Cu-Mo bimetallic oxide nanoparticles at 14 mA/cm$^2$ current density capped with a) TEAB, b) TPAB and c) TBAB respectively.

**Energy dispersive spectroscopy**

The EDS spectrum of bimetallic oxide nanoparticles in Fig. 2.21a-c prepared by using capping agent TEAB, TPAB and TBAB respectively at 14mA/cm$^2$ current density, shows peaks corresponding to Cu, Mo, C, N, O and Br. The analysis of spectra gives wt% and atom% of each element present in sample. The content of elements according to their wt% and atom% is shown in Table 2.5a-c.

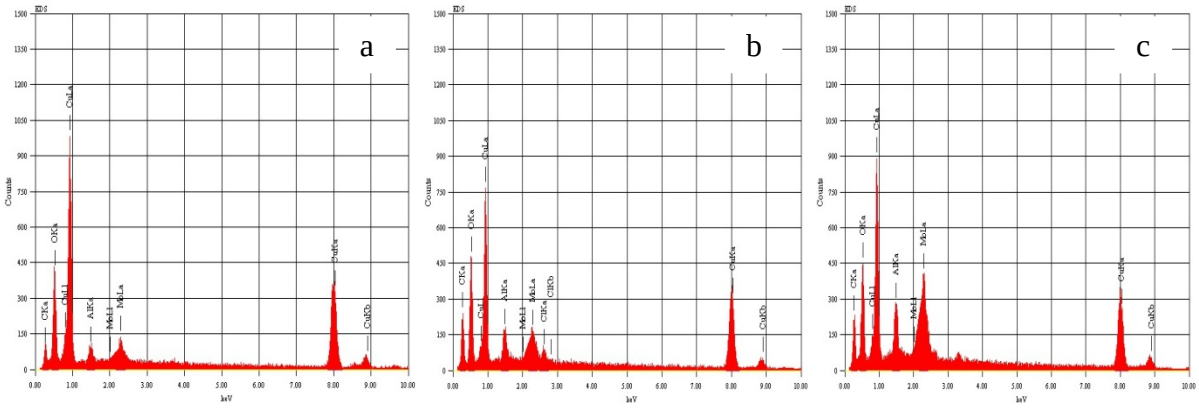


Fig. 2.21 EDS spectra of the Cu-Mo bimetallic oxide nanoparticles at 14 mA/cm$^2$ current density capped with a) TEAB, b) TPAB and c) TBAB respectively.

**Table -2.5a** Elemental compositions of Cu-Mo nanoparticles capped with TEAB

| Elements | KeV | Mass% | Atom% |
|---|---|---|---|
| C | 0.277 | 17.17 | 41.51 |
| O | 0.525 | 14.11 | 25.6 |
| Cu | 8.04 | 58.33 | 26.65 |
| Mo | 1.480 | 5.76 | 1.74 |

**Table -2.5b** Elemental compositions of Cu-Mo nanoparticles capped with TPAB

| Elements | KeV | Mass% | Atom% |
|---|---|---|---|
| C | 0.277 | 7.93 | 26.29 |
| O | 0.525 | 13.44 | 30.9 |
| Cu | 8.04 | 67.82 | 39.24 |
| Mo | 2.293 | 9.34 | 3.58 |

**Table -2.5c** Elemental compositions of Cu-Mo nanoparticles capped with TBAB

| Elements | KeV | Mass% | Atom% |
|---|---|---|---|
| C | 0.277 | 15.36 | 41.18 |
| O | 0.525 | 11.13 | 22.42 |
| Cu | 8.840 | 47.4 | 24.03 |
| Mo | 1.480 | 21.91 | 7.35 |

### 2.6.7 Transmission electron microscope

Fig.2.22a-f display TEM images of Cu-Mo bimetallic nanoparticles prepared with TEAB, TPAB and TBAB as a capping agent at 10 and 14 mA current densities. These particles have size of 5-80 nm and exhibit a broad size distribution. Once the surfactant TEAB, TPAB and TBAB were employed in the system the mean size of Cu nanoparticles reduced to 20-60 nm, 10-30 nm and 5-15 nm respectively. This indicates that the size of metal nanoparticles and its distribution are dramatically reduced with the presence of TBAB in appropriate amounts. It is observed that they are composed of bead like structures of about 5nm in size. The general feature of the precipitated metal in this case is that it is of cotton like structure. The random distribution of metal nanoparticles aggregates is still clearly seen here.

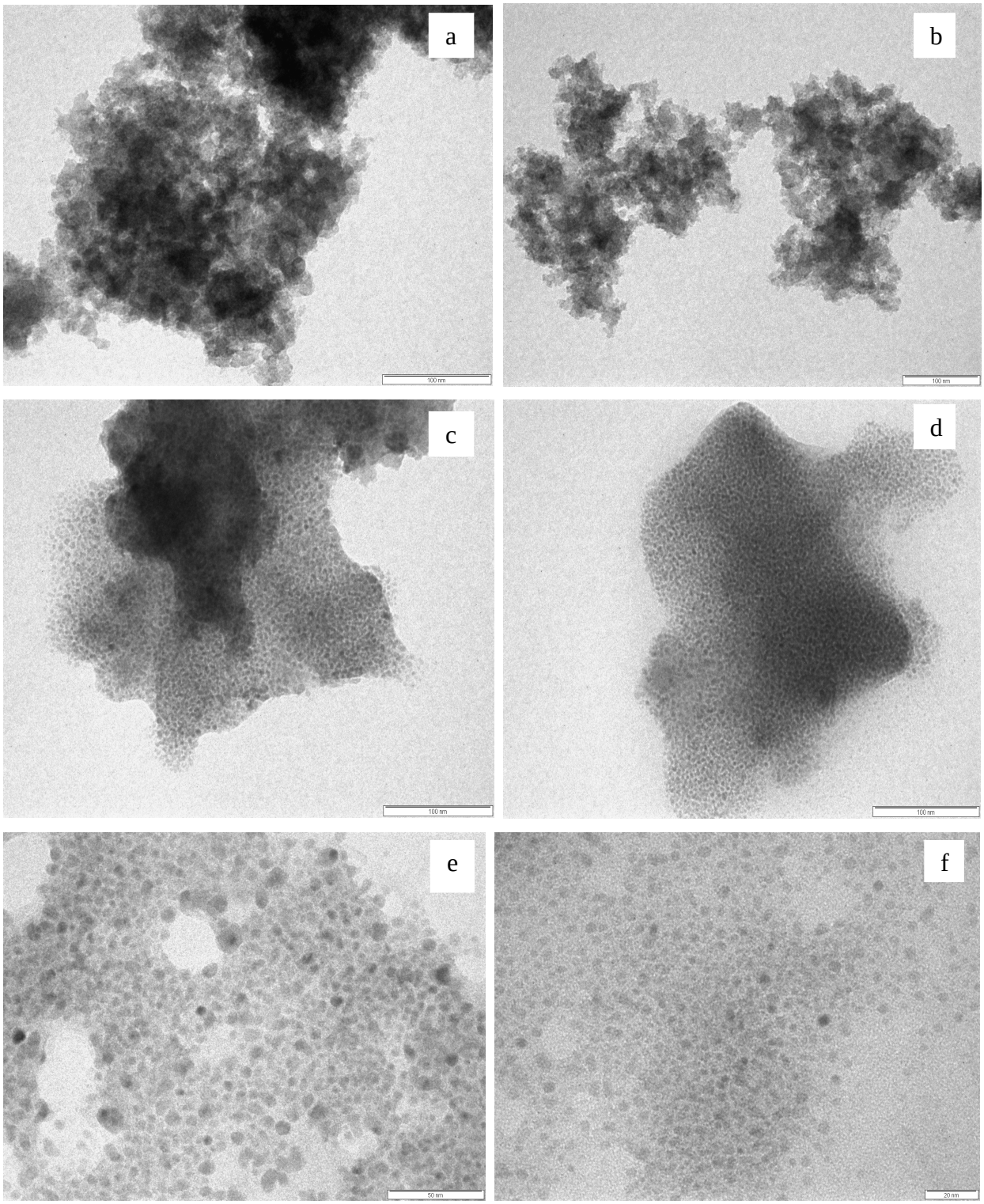


Fig. 2.22 TEM micrographs of the Cu-Mo bimetallic oxide nanoparticles at 14 mA/cm$^2$ current density capped with a-b) TEAB, c-d) TPAB and e-f) TBAB respectively.

The selected area electron diffraction (SAED) pattern of Cu-Mo bimetallic oxide nanoparticles at 14 mA/cm$^2$ current density capped with TEAB, TPAB and TBAB respectively. The SAED pattern appear ring to confirms that the Cu-Mo bimetallic oxide nanoparticles were polycrystaline nature.

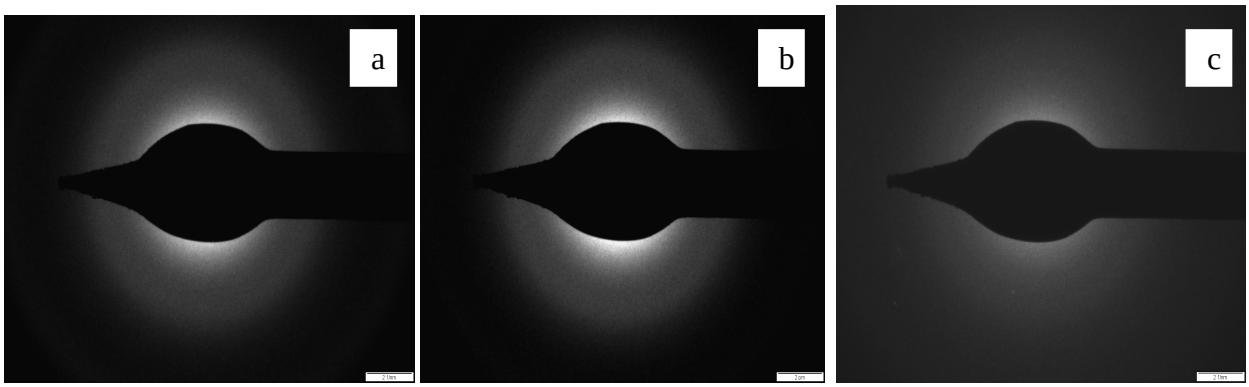


Fig. 2.23 SAED pattern of the Cu-Mo bimetallic oxide nanoparticles at 14 mA/cm$^2$ current density capped with a) TEAB, b) TPAB and c) TBAB respectively.

## 2.6.8 Reference


1. Rbain R., Othman M. & Palaniandy S., *Minerals Engineering*, **(2011)**, 24, 1-9.
2. Pérez-Tijerina E., Gracia Pinilla M., Mejía-Rosales S., Ortiz- Méndez U., Torres A. & José-Yacamán M. *Faraday Discuss.*, **(2008)**, 138, 353.
3. Song K.C., Lee S.M., Park T.S. & Lee B.S., *Korean J. Chem. Eng.*, **(2009)**, 26, 153-155.
4. Ghosh S.K., Kundu S., Pal T., *Bull. Mater. Sci.*, **(2002)**, 25, 581- 582.
5. Mohanty U.S., *J. Appl.Electrochem.*, **(2011)**, 41, 257-270.
6. Hayashi H. & Hakuta Y., *Materials*, **(2010)**, 3, 3794-3817.
7. Sonawane R.S. & Dongare M.K., *J. Molat. A*, **(2006)**, 243, 68–76.
8. Chou K.S., Lai Y.S., *Mater. Chem. Phys*., **(2004)**, 83, 82.
9. Wu S. P., Meng S.Y., *Mater. Chem. Phys*., **(2005)**, 89, 423.
10. Reetz M.T., Helbig W., *J. Am. Chem. Soc.*, **(1994)**, 116, 7401.
11. Hanemann S., Grunwalat J.D., Krumeich F., Kappen P., Baiker A., *Apple. Surf. Sci*., **(2006)**, 252, 7862.
12. Reetz M.T., Breinbauer R., Wanninger K., *Tetrahedron Lett.*, **(1996)**, 37, 4499.
13. Stoimenov P.K., Klinger R.L., Marchin G.L., Klabunde K.J., *Langmuir*, **(2002)**, 18, 6679-6686.
14. Seifi M., Sheibani H., *Catal Lett* **(2008)**, 126, 275–279.
15. Reddy Chintareddy V., Lakshmi Kantam M., *Catal Surv Asia*, **(2011)**, 15, 89–110.
16. Bell A.T., *Science*, **(2003)**, 299, 1688.
17. Schlogl R., Abd Hamid S.B., *Angew Chem Int Ed*, **(2004)**, 43, 1628.
18. Bernardotto G., Menegazzo F., Pinna F., Signoretto M., Cruciani G., Strukul G., *Appl Catal A*, **(2009)**, 358(2), 129–135.
19. Marx S., Baiker A., *J Phys Chem C*, **(2009)**, 113(15), 6191–6201.

20. Mertens P.G.N., Corthals S.L.F., Ye X., Poelman H., Jacobs P.A., Sels B.F., Vankelecom I.F.J., De Vos D.E., *J Mol Catal A Chem,* **(2009)**, 313 (1–2), 14–21.
21. Mizukoshi Y., Okitsu K., Maeda Y., Yamamoto T.A., Oshima R., Nagata Y., *J Phys Chem B,* **(1997)**, 101(36), 7033–7037.
22. Patel K., Kapoor S., Dave D., Mukherjee T., *Res Chem Intermed,* **(2006)**, 32(2), 103–113.
23. Korbekandi H., Iravani S., Abbasi S.,*Crit Rev Biotechnol*, **(2009)**, 29(4), 279.
24. Narayanan K.B., Sakthivel N., *Adv Colloid Interface Sci,* **(2010)**, 156(1–2), 1–13.
25. Davis S.C., Klabunde K.J., *Chem Rev*., **(1982)**, 82, 153.
26. Reetz M.T., Helbig W., Quaiser S.A., Stimming U., Breuer N., Vogel R., *Science* **(1995)** 267, 367.
27. Reetz M.T., Hebig W., Quaiser S.A., *Chem. Mater.*, **(1995)**, 7, 2227.
28. Dang, T.M.D.; T Le, .T.T.; Fribourg-Blanc, E.; Dang, M.C. *Adv. Nat. Sci: Nanosci. Nanotechnol*. **2011**, *2*, 015009
29. Singh, P.; Katyal, A.; Kalra, R.; Chandra, R. *Tetrahedron Lett.* **2008**, *49*, 727.
30. J. Lindley, *Tetrahedron*, 1984, **40**, 1433-1456.
31. A. Klapars, J. C. Antilla, H. Huang and S. L. Buchwald, *J. Am. Chem. Soc.*, 2001, **123**, 7727-7729.
32. Valverde-Alguilar, G.; Garcia-Macedo, J. A.; Renteria-Tapia, V.; *J. Nano. Research* **2008**, *3*, 103.
33. Yao, W., Yu, S., Zhou, Y., Jiang, J., Wu, Q., Zhang L., Jiang, J. *Journal of Physical Chemistry B* (109)2005: pp. 14011-16.
34. Klug, H., Alexander**,** L. X-ray diffraction Procedures, Wiley, New York, **1962**.
35. Chen, H.; Lee, J. H.; Kim, Y. H.; Dong, W. S.; Park, S. C.; Meng, X.; Yoo, J. B. *J. Nanoscience and Nanotechnology* **2010**, *10*, 629.
36. Raja, M.; Subha, J.; Ali, F. B.; Ryu, S. H. *Materials and Manufacturing Process* **2010**, *23*, 782.
37. Das, N. A.; Gedaken, A. *Chem. Mater.***1997**, *9*, 3144.
38. Anpo, M.; Kondo, M.; Louis, C.; Che, M. *J. Chem. Soc. Faraday Trans.* **1988**, *184*, 2771.
39. Liu, Y.; Qian, Y.; Zhang, M.; Chen, Z.; Wang, C. *Mater. Res. Bull.* **1996**, *31*, 1029.
40. Zhou, J.; Xu, N. S.; Deng, S. Z.; Chen, J.; She, J. C. *Chem. Phys. Lett.* **2003**, *382*, 443.
41. King, S. T. *J. Catal.* **1991**, *131*, 215.
42. Yao, J. N.; Hashimoto, K.; Fujishima, A. *Nature* **1991**, *335*, 624.
43. Svachula, J.; Tichy, J. J. *J. Catal. Lett.* **1989**, *3*, 257.
44. Honma, I.; Zhou, H. S. *Chem. Mater.* **1998**, *10*, 103.
45. Janaur, G. G.; Dobley, A.; Guo, J. D.; Zavalij, P.; Whittingham, M. S. *Chem. Mater.* **1996**, *8*, 2096.
46. Durr, H.; Fauchet, P. M. *Appl. Phys. Lett.***1997**, *71*, 380.
47. Mortimer, R. *J. Chem. Soc. Rev.* **1997**, *26*, 147.
48. Yao, J. N.; Hashimoto, K.; Fujishima, A. *Nature* **1992**, *355*, 624.
49. Shoutian, Li; Germanenko, I. N.; EI-Shell, M. S. *J. Cluster Science* **1999**, 10.
50. L. Mai, B. Hu, W. Chen, Y. Qi, C. Lao, R. Yand, Y. Dai, Z. Wang, Adv Mater. 19, 3712(2007)
51. Sinfelt, J. H. *J. Catal.* **1973**, *29*, 308.
52. Sinfelt, J. H. *Acc. Chem. Res.* **1987**, *20*,134.
53. Toshima, N. *J. Macromol. Sci. Chem.* **1990**, *A27*, 1225.
54. Schaak, R. E.; Sra, A. K.; Leonard, B. M.; Cable, R. E.; Bauer, J. C.; Han, Y.F.; Means, J.; Teizer, W. *J. Am. Chem. Soc.* **2005**, *127*, 3506.
55. Cable, R.; Schaak, R. *Chem. Mater.* **2007**, *19*, 4098.

56. Vasquez, Y.; Luo, Z.; Schaak, R. *J. Am. Chem. Soc*. **2008**, *130*, 11866.
57. Klimov, V.; Bolivar, P. H.; Kurz, H.; Karavanskii, V. ; Krasovskii, V.; Korkishko, Y. *Appl. Phys. Lett.* **1995**, *67*, 653.
58. Klimov, V. I.; Haring-Bolivar, P. H.; Kurz, Karavanskii, V. A. *Superlatt. Microstruct*. **1996**, *20*, 395.
59. Klimov, V. I.; Karavanskii, V. A. *Phys. Rev. B* **1996**, *5*4, 8087.
60. Brelle, M. C.; Torres-Martinez, C. L.; McNulty, J. C.; Mehra, R. K. ; Zhang, J. Z. *Pure Appl. Chem*. **2000**, *72*, 101.
61. Loferski, J. J.; Shewchun, J.; Mitlerman, S. D.; De Meo, E. A.; Arnott, R.; Hwang, H. L.; Beauliew, R. ; Champman, G. *Solar Energy Mater*. **1979**, *1*, 157.
62. Ghijsen, J.; Tjeng, L. H.; Elp, J. V.; Eskes, H.; Westerink, J. Sawatzky, G. A. *Phys. Rev. B* **1988**, *38*, 11322.
63. Ching, W. Y.; Xu, Y. N.; Wong, K. W. *Phys. Rev. B* **1989**, *40*, 7684.
64. Kellersohn, A.; Knoezinger, E; Langel W.; Giersig, M. *Adv. Mater*. **1995**, *7*, 652.
65. Ito, T.; Yamaguchi, H.; Masumi, T.; Adachi, S. *J. Phys. Soc. Jpn*. **1998**, *67*, 3304.
66. Nair, M. T. S.; Guerrero, L.; Nair, P. K. *Semicond. Sci. Technol*. **1998**, *13*, 1164.
67. Chandra, R.; Taneja, P.; Ayyub, P. *Nanostruct. Mater.* **1999**, *11*, 505.
68. Borgohain, K.; Singh, J. B.; Rao, M. V. R.; Shripathi. T.; Mahamuni, S. *Phys. Rev. B* **2000**, *61*, 11093.
69. Banerjee, S.; Chakravorty, D. *Europhys. Lett.* **2000**, *52*, 468.
70. Borgohain, K.; Murase, N.; Mahamuni, S. *J. Appl. Phys*. **2002**, *92*, 1292.
71. Reijnen, L.; Meester, B.; Goossens, A.; Schoonman, J. *Mater. Sci. Eng. C* **2002**, *19*, 311.
72. Wang, W. Z.; Wang, G. H.; Wang, X. S.; Zhan, Y. J.; Liu, Y. K.; Zheng, C. L. *Adv. Mater*. **2002**, *14*, 67.
73. Liu, G.; Schulmeyer, T.; Brotz, J. A.; Klein Jaegermann, W. *Thin Solid Films* **2003**, *431*, 477.
74. Michael, J.; Sigman, B.; Ghezelbash, A.; Hanrath, T. A.; Saunders, E.; Lee, F.; Korgel, B. A. *J. Am. Chem. Soc.* **2003**, *125*, 16050.
75. Chen, L.; Chen, Y. B.; Wu, L. M. *J. Am. Chem. Soc.* **2004**, *126*, 16334.
76. Li, Z.; Yang, H.; Ding, Y.; Xiong, Y.; Xie,Y. *Dalton Trans*. **2006**, *149*.
77. Larsen, T. H.; Sigman, M.; Ghezeibash, A.; Doty, R. C.; Korgel, B. A. *J. Am. Chem. Soc.* **2003**, *125*, 5638.
78. Sigman, M. B.; Ghezelbash, A.; Hanrath, T.; Saunders, A. E.; Lee, F.; Korgel, B. A. *J. Am. Chem. Soc.* **2003**, *125*, 16050.
79. Wen, X.; Yang, S. *Nano. Lett*. **2002**, *2*, 451.
80. McLeod, P. S.; Partain, L. D.; Sawyer D. E.; Peterson, T. M. *Appl. Phys. Lett.* **1984**, *45*, 472.
81. Braithwaite, E.R.; Haber, J. *Elseveir New York* **1994**.
82. Shields, J. A.; Baker, E. L. *Adv. Mater. Processes I* **1991**, *61*.
83. Fustier, G.; Langeron, J. P.; DE LA Bastie, J.; Carlizza, J. *US Patent, US4, 115,113.*
84. Iordanova, I.; Forcey, K. S.; Gergov, B.; Bojinov, V. *Surf. Coating Tech.* **1995**, *72*, 23.

85. Mchugh, C. O.; Whalen, T. J.; Humenik, M. *J. Am. Ceram. Soc*. **1966**, *49*, 486.
86. Rankin, D. T.; Stiglich, J. J.; Ruh, R. *J. Am. Ceram. Soc*. **1966**, *49*, 486.
87. Nawa, M.; Sekino, T.; Niihara, K. *J. Mater. Sci*. **1994**, *29*, 3185.
88. Wei, W. C. J.; Wang, S.; Cheng, F. H. *Nanostruct. Mater*. **1998**, *10*, 965.
89. Tang, B. Z.; Xu, H. Y. *Macromolecules* **1999**, *32*, 2369.
90. Xu, H. Y.; Tang, B. Z. *Polym. Mater. Sci. Eng*. **1999**, *80*, 215.
91. Beckoff, W. E.; Mceuen, J. M. *US Patent, US3, 424, 813*.
92. Miner, R. S.; Namba, S.; Turkevich, J. *Proceeding of the VII Int. Congress on Catalysis, Tokyo* **1981**, 160.

Recently transition metals, metal oxide, metal salts, mixed metal oxides in the form of nanoparticles have emerged as viable alternative to conventional materials in various field of chemistry [1]. The nanocatalysts plays dual role as heterogeneous as well homogeneous catalysis and have beneficial physical and chemical properties. Nanocatalysis is a phenomenon of significant fundamental research and important practical applications in a variety of fields such as chemistry, physics and material science, environmental and atmospheric sciences in addition to its traditional significance in advancing the petroleum field. It encompasses supported or unsupported nanometer scale metal catalytic structure (spherical nanoparticles, nanorods, nanoplates, nanocubes, nanotubes etc.) where the catalytic phenomena are specific to that length scale and in general are related to the high surface area [2]. Nanophase metal and metal oxide catalysts with controlled particle size, high surface area and more densely populated unsaturated surface co-coordinated sites could potentially provide significantly improved catalytic performance over conventional catalysts.

Potential for increased efficiency from nanoparticles catalysts in combination with advantages of such heterogeneous supports increases the green approach of the process with higher selectivity, yield and catalyst recovery being proposed advantageous and targets. Supported metallic nanoparticles with their potential in a wide range of current and future applications is one of the fastest growing research field [3]. Such supported nanoparticles materials have attracted much attention over the past decades due to the potential for enhanced selectivity of the size/shape selective catalysts and activity as well as advantage of nanoparticles aggregation inhibition provided by immobilization/separation on the heterogeneous support.

**3.1 Scope and application**

Nanoparticles have been widely applied in different areas including, medicine, sensor and catalysis. In our study we have concentrated our work towards the application of the metal nanoparticles in the field of catalysis. Several reports can be found on wide range of application of various supported metal nanoparticles in catalysis including Au, Ag, Pt, Cu, Cd, Ni, Mo etc. metals in the form of reduced metals and in compounds forms as heterogeneous catalysis. The efficiency of heterogeneous catalysis can be improved by employing nano sized catalysts because of their extremely small size and large surface to volume ratio. Heterogeneous catalysts are easily removable from reaction medium and are reusable. Nanoparticles have potential for improving the efficiency, selectivity and yield of catalytic processes. In particular the

nanoparticles have ability to disperse into the solution and provide higher surface to volume ratio while participating in the reaction. Higher selectivity of the nanoparticles towards reaction proceeds through less waste and fewer impurities which could lead to safer technique and reduced environmental impact.

Metal nanoparticles are known to be promising material in the field of heterogeneous catalysts in variety of organic transformations such as oxidation of CO, alcohol, alkenes, hydrogenation of alkenes and dienes, alkynes, aromatic compounds, allylic alcohols, in C-C coupling reactions like Heck, Suzuki, Sonogashira, Negishi and Kumanda reactions and hydro chlorination [4-6]. There are many other types of chemical reactions that have been conducted using supported transition metal nanoparticles in heterogeneous catalysis [7, 8].

Nanomaterials containing high surface area and reactive morphologies have been studied as effective catalysts for organic synthesis. Furthermore, the nanomaterial catalyzed reactions provide the advantages of high atom efficiency, simplified isolation of product, and easy recovery and recyclability of the catalysts. In preliminary communication, we reported the catalysis of CuO nanoparticles for the cross-coupling reactions of amines and thiols with iodobenzene. The reactions were simple, general, and ligand-free, and the CuO nanoparticles were recyclable. These features led us to further study the scope of the CuO nanoparticles for the catalysis of the C-N, C-O, and C-S cross-coupling reactions. The $MoO_3$ nanoparticles has been applied to a wide range of applications such as their unique redox chemistry resulting from its high reduction potential and $MoO_3$ is known to be an important catalyst or a catalyst precursor in a number of industrially relevant reactions. Its catalytic efficiency has long been known e.g. in alcohol and methane. Recently, molybdenum has been examined as heterogeneous catalysts because their activity is often similar to that of the platinum group metals.

The significant catalytic properties together with operational simplicity, high reactivity, environmental friendliness, reduce reaction time and reusability of nanoparticles confides us to work on nanocatalysis. In this thesis we have focused on the organic reactions that are catalyzed using CuO, $MoO_3$ and Cu-Mo heterogeneous transition metal nanocatalysts.

## Section A- Copper nanoparticles catalyzed organic transformation

## 3.2 Solvent free green synthesis of 5-arylidine barbituric acid derivatives catalyzed by copper oxide nanoparticles

### 3.2.1 Introduction

Barbituric acid is a strong acid in aqueous medium with an active methylene group and can be involved in knoevenagel type condensation reaction [9]. The barbiturates are associated with a number of biological activities such as antibacterial, hypotensive, sedative and local anesthetic drugs [10-11] to the more recent report indicating that they have applications in antitumor[12], anti-cancer[13], analeptics[14], anti-AIDS [15] and anti-osteoporosis[16] treatments and are used as oxidants for mild oxidation of thiols [17] and alcohols[18].

Owing to the wide range of biological and medicinal activities the synthesis of 5-arylidine barbituric acid compounds by the use of barbituric acid and 2-thio barbituric acid as starting compound have become an important target in recent years.

### 3.2.2 Literature review

Numerous synthetic method have been reported for the synthesis of synthesis of 5-arylidine barbituric acid derivatives by solvent free grinding, using $NH_2SO_3H$[19], infra red promoted[20], microwave irradiation[21], ionic liquid mediated condensation[22], and uses variety of catalysts such as $ZnCl_2$ [23], $CdI_2$ [24], Ni-$SiO_2$ [25], KF–$Al_2O_3$ [26], natural phosphate [(NP)/KF or NP/$NaNO_3$] [27] and synthetic phosphate ($Na_2CaP_2O_7$) [28], $K_2NiP_2O_7$ [29], dry condensation with acidic clay catalysts [30], Ni nanoparticles [31] and $CoFe_2O_4$ nanoparticles [32] etc. However these methods are plagued by limitation of longer reaction time, effluent pollution, bis-addition and self condensation, lower yield. Owning to the importance of barbituratic acid derivatives especially 5-arylidine barbiturates, there is needed to develop efficient method for the Knovengel Condensation at mild conditions.

Solvent free organic reaction have drawn great interest, particularly from the viewpoint of green chemistry as organic solvent are toxic and flammable. Solid state reactions are simple to handle, reduce pollution and comparatively cheaper to operate. Heterogeneous catalysts offer several intrinsic advantages over their homogeneous counterparts such as easy removal of catalyst, operational simplicity and reusability.

The use of metal nanoparticles in the field of catalysis is of great interest since they have a large surface-to-volume ratio compared to bulk materials. Recently, there has been growing interest in using copper nanoparticles in organic synthesis because of their potent catalytic activity, high stability and non toxic.

### 3.2.3 Present work

Electrochemically prepared CuO nanoparticles were tested on the synthesis of 5-arylidine barbituric acid derivatives. The short reaction time, solvent free reaction condition, consistent yield and minimum environmental effect were important features of the reaction (**Scheme1**).

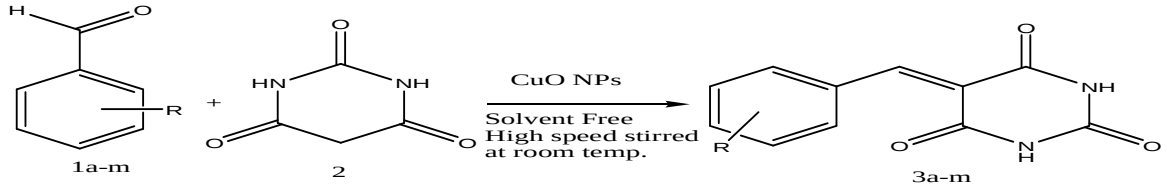


**Scheme 1** CuO nanoparticles catalyzed knoevenagel condensation of aldehydes and barbituric acid

### 3.2.4 Experimental

The uncorrected melting points of compounds were taken in an open capillary in a paraffin bath. IR spectra were recorded on a Jasco FTIR-4100 spectrophotometer. $^{1}H$ NMR spectra were recorded on an 400 MHz FT-NMR spectrometer in $CDCl_3$ as a solvent and chemical shift values were recorded in units δ (ppm) relative to tetramethylsilane ($Me_4Si$) as an internal standard.

**General procedure**

A mixture of aromatic aldehyde(1mmol), barbituric acid(1mmol)(solid aromatic aldehyde wetted with ethanol) and CuO nanoparticles (100mg) was stirred with high speed at room temperature till the completion of reaction monitored by TLC( ethyl acetate and n-hexane 7:3). After completion of reaction solid product obtained was dissolved in 10ml ethyl acetate and concentrated on rotavapor. Finally pure product was obtained by recrystalization and authentic samples were characterized by FTIR, $H^1$NMR and $C^{13}$NMR.

### 3.2.5 Spectral data of representative compound

**i) 5(4-Cl-Benzylidene)- Barbituric acid(3b):** [IR (KBr) $\nu_{max}/cm^{-1}$]: 3404, 3214, 2970, 1755, 1703, 1570 $cm^{-1}$; $^{1}H$ NMR (DMSO) δ ppm:7.53(d, 2H, Ar-H), 8.08(2d, 2H, Ar-H), 8.25(s, 1H, HC=C), 11.25(s, H, NH), 11.40(S, 1H, NH); $^{13}C$ NMR($CDCl_3$) δ ppm; 117.46, 127.76, 128.29, 133.25, 133.50, 148.70, 150.16, 165.10.

**ii) 5(2-Cl-Benzylidene)- Barbituric acid(3c):** [IR (KBr) $\nu_{max}/cm^{-1}$]: 3460, 3120, 2981, 1754, 1569, 1454, 1079, 910, 782; $^1$H NMR ($CDCl_3$) δ ppm: 7.36 (t, 1H Ar-H), 7.47 (t, 1H, Ar-H), 7.53 (d, 1H, Ar-H), 7.73 (d, 1H, Ar-H), 8.29 (s, 1H, HC=C), 11.25(s,1H, NH), 11.47(s, 1H,NH); $^{13}$C NMR($CDCl_3$,ppm) δ= 121.76, 126.29, 128.29, 131.88, 132.25, 133.15, 146.70, 150.16, 160.85, 162.60 .

**iii) 5(4-OH-Benzylidene)- Barbituric acid(3i):** [IR (KBr) $\nu_{max}/cm^{-1}$]: 3420, 3214, 2970, 1755, 1703, 1570 $cm^{-1}$; $^1$H NMR (DMSO) δ ppm:6.86(d, 2H, Ar-H), 8.32(2d, 2H, Ar-H), 8.24(s, 1H, HC=C), 10.68(S, 1H, OH), 11.13(s, H, NH), 11.25(S, 1H, NH).

### 3.2.6 Result discussion

The catalytic activity of the synthesized CuO nanoparticles was investigated in the synthesis of arylidene barbituric acid derivatives at room temperature. To study the efficiency of the CuO nanocatalyst, 4-chlorobenzaldehyde (**1b**) and barbituric acid (**2**) were used as the model substrate. We also carried out the reaction without any catalyst, but the product isolated gave poor yield (25%). In optimizing the reaction conditions, the amount of catalyst was the major factor. The model reaction was studied using 25, 50, 75, 100 and 125 mg of a reaction of 4-chlorobenzaldehyde (1b). The results revealed that best yield was obtained by using 100mg catalyst. With increase in the catalyst concentration, the yield of the desired product was found to be constant. The results obtained are summarized in Table-3.2.2. It is evident that the aromatic aldehyde carrying electron-donating or electron-withdrawing groups as well as heterocyclic system such as Furan-2-carboxyaldehyde reacted smoothly to produce high yield of products. The results with different aromatic aldehydes are summarized in Table-3.2.1.

**Table-3.2.1 Synthesis of 5-arylidine barbituric acid derivatives catalyzed by CuO Nanoparticles.**

| Sr. No. | Reactant | Products[a] | Time (min) | Yield (%) | Melting point (°C) | |
|---|---|---|---|---|---|---|
| | | | | | Found | Reported |
| 1 | $C_6H_5$ | 3a | 15 | 97 | 264 - 266 | 263-265[32] |
| 2 | 4-$ClC_6H_4$ | 3b | 12 | 98 | 298 - 299 | 298[32] |
| 3 | 2-$ClC_6H_4$ | 3c | 13 | 95 | 250-252 | 252-254[32] |
| 4 | 4-$NO_2C_6H_4$ | 3d | 09 | 94 | 268-270 | 272-274[19] |
| 5 | 3-$NO_2C_6H_4$ | 3e | 07 | 95 | 230-231 | 231-233[19] |
| 6 | 4-$CH_3C_6H_4$ | 3f | 15 | 96 | 290-291 | 297-298[19] |
| 7 | 2,4-$Cl_2C_6H_3$ | 3g | 13 | 94 | 268-270 | 269-271[19] |
| 8 | 4-$OMeC_6H_4$ | 3h | 10 | 93 | 296-298 | 298-300[32] |
| 9 | 4-$OHC_6H_4$ | 3i | 15 | 94 | >300 | >320[32] |
| 10 | 2-furfural | 3j | 20 | 95 | 262-263 | 264[31] |
| 11 | 4-$FC_6H_4$ | 3k | 12 | 95 | >300 | 309-10[20] |
| 12 | 4-$BrC_6H_4$ | 3l | 15 | 92 | 288-290 | 292-293[20] |

| | | | | | | |
|---|---|---|---|---|---|---|
| 13 | $C_6H_5CH=CH$ | 3m | 18 | 93 | 267-268 | 270[21] |

[a]Reaction condition: aldehyde (2mmol), barbituric acid (2mmol), and 100mg of CuO nanoparticles solvent free stirred at room temp.

**Table-3.2.2 Screening of catalyst CuO NPs for the synthesis of 5-arylidine barbituric acid**

| Entry[a] | Catalyst amount(mg) | Time(min) | Yield(%)[b] |
|---|---|---|---|
| 1 | 25 | 60 | 38 |
| 2 | 50 | 40 | 82 |
| 3 | 75 | 25 | 90 |
| 4 | 100 | 12 | 98 |
| 5 | 125 | 12 | 98 |

[a]Reaction condition: aldehyde (2mmol), barbituric acid (2mmol), and 100mg of CuO nanoparticles solvent free stirred at room temp. [b]isolated yield

In this study, the catalyst was recovered and reused in another run. The catalyst was recovered by simple work-up using centrifugation method, washed with ethanol and reused for three successive reaction corresponding yields for each cycle were mentioned in Table-3.2.3.

**Table-3.2.3 Studies on reusability of CuO nanoparticles in the preparation of 3b**

| No of Cycles | Fresh | 1 | 2 | 3 |
|---|---|---|---|---|
| Yield(%) | 98 | 94 | 91 | 85 |

[a]Reaction condition: aldehyde (2mmol), barbituric acid (2mmol), and 100mg of CuO nanoparticles solvent free stirred at room temp. [b]isolated yield

To compare the merits of our work to the other reported procedure; the results of the synthesis of arylidene barbituric acid derivatives in the presence of different reported catalysts with respect to time and yield of the product are listed in Table-3.2.4. These results show that our catalyst CuO nanoparticles are more stable in air, nontoxic, give good yield in short time than other catalysts and there is no use of any hazardous solvent.

**Table-3.2.4Comparisation result of CuO nanoparticles with other catalysts reported in the literature**.

| Sr. No. | Catalyst | Reaction condition | Yield (%) | Literature |
|---|---|---|---|---|
| 1 | $NH_2SO_3H$ | Grinding/10 min | 47 | 19 |
| 2 | KSF clay | MW, 560 W/7 min | 70 | 20 |
| 3 | PVPNi Nanoparticles | Ethyleneglycol, 50$^oC$/10–15 min | 91 | 31 |
| 4 | CuO nanoparticles | Solvent free/ R.T./7 min | 95 | This work |

Thus, we report fast, clean and highly competent methodology for the Knoevenagel condensation of aromatic aldehydes with barbituric acids catalyzed by CuO nanoparticles to give 5-arylidene barbituric acids as the desired products in short time span and in quantitative yields by a simple high speed stirring at room temperature. The reaction time, yield and reusability of catalysts make the present protocol a useful and important addition to the present methodologies for the synthesis of 5-arylidine barbituric acid derivatives.

### 3.2.7 Conclusion

We have reported mild, easy and green method for the synthesis of 5-arylidine barbituric acid derivatives using recyclable CuO Nps as heterogeneous catalysts at room temperature under solvent free condition. Short reaction time, appropriate yield and clean reaction make this procedure an attractive alternative to the existing methods. Furthermore, this method is of interest in the perspective of environmentally greener and safer method.

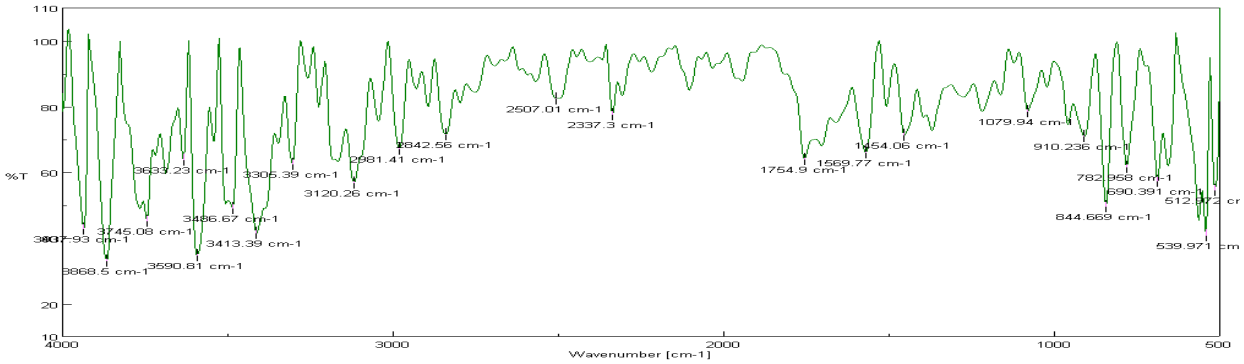


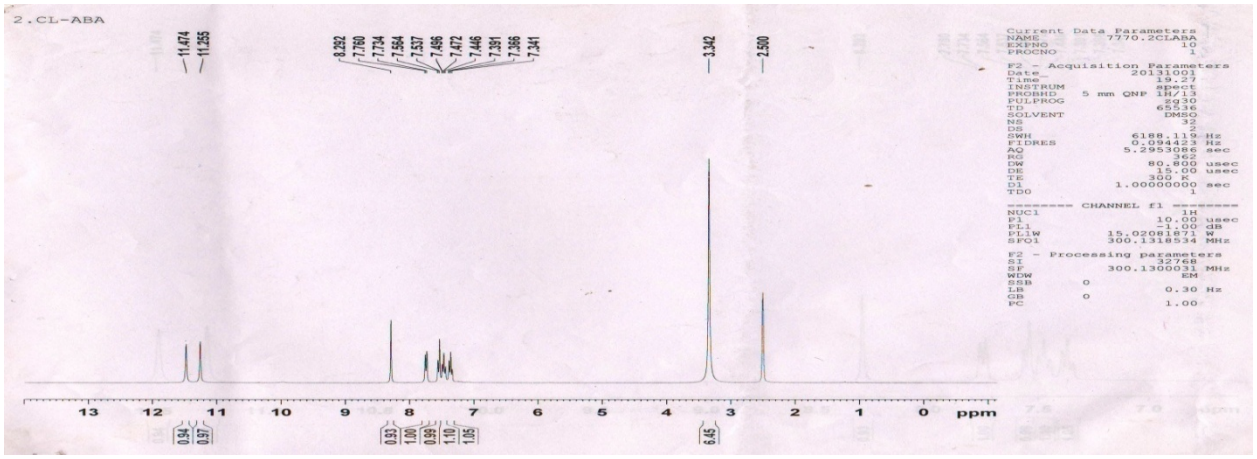


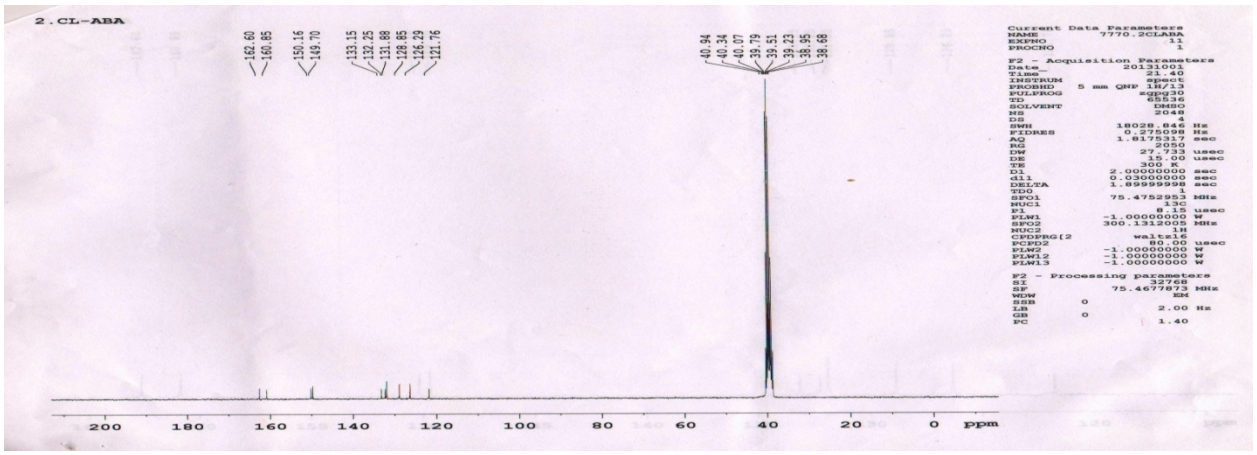

## 3.3 Synthesis of 2-benzylidenemalononitrile catalyzed by copper oxide nanoparticles

### 3.3.1 Introduction

Chemistry of multiple bonds has achieved a dramatic development in the past decades because these compounds have been used as substrates in the synthesis of industrial and biologically active compounds [33-35]. Moreover, the compounds containing carbon-nitrogen, carbon –oxygen and carbon-carbon double bond are known to possess biological activities [36] such as antimicrobial, antifungal, antitumor and nematicidal. Carbon-carbon bond formation reaction is one of the most important reactions in organic synthesis. Knoevenagel condensation is one of such reaction between an aldehyde and active methylene compounds. Owing to its applicability in the synthesis of various chemicals and chemical intermediates [37] coumarin derivatives have found applications in the field of cosmetics, perfumes and pharmaceuticals [38-39], fine chemical industry such as polymers [40], and synthesis of carboxylic as well as heterocyclic compounds [41] of biological significance. The products of Knoevenagel condensation have found increasing applications in industry, agriculture, medicine and biological science [42-43]. Substituted cinnamic acids possess a wide range of activities such as anti-allergic [44] and in the synthesis of substituted styrene [45].

### 3.3.2 Literature review

Numerous reagents have been reported for Knoevenagel condensation in literature such as triethylbenzylammonium chloride (TEBA) [46], $NH_4OAc$-AcOH [47], zinc acetate [48], triethylamine and catalytic amount of magnesium bromide diethyl etherate [49], lithium perchlorate and lithium bromide [50], $K_2CO_3$ and $P_2O_5$ [51], K montmorillonite [52], fluorapatite (FAP)/sodium nitrate [53], calcium oxide [54], rhenium complex [55], $Al_2O_3$, Ni-Mg Ferrite, hydrotalcite in ionic liquid, CsNaX-$NH_2$, polyacrylamide, natural phosphate doped with potassium fluoride , anionexchange resin, 12-tungstophophoric acid [56-62]. The usual catalysts are ammonia and ammonium salts, primary and secondary amines and their salts [63]. Recently silica gel functionalized with amine groups have been used under heterogeneous catalysis conditions [64].

But most of the reported reagents are associated with certain disadvantages such as tedious work-up, expensive, toxic nature etc. In order to cumbersome these problems, emphasis has been laid on the use of supported reagents. The major advantage of supported reagent is the reusability of the catalyst which makes the process inexpensive. Moreover, it also contributes

towards the area of "Green Chemistry". The catalytic behavior of CuO nanoparticles is studied in the synthesis of 2-benzylidene malononitriles by the condensation of aromatic aldehydes and malononitrile with solvent free condition (Scheme 2). The catalyst/product(s) separation could be easily achieved with a simple decantation and more than 95% of catalyst could usually be recovered from each reaction.

### 3.3.3 Present work

Electrochemically prepared CuO nanoparticles were tested on the synthesis of 5-benzylidine malononitrile derivatives (Scheme 2). The short reaction time, solvent free reaction condition, consistent yield and minimum environmental effect are important features of the reaction.

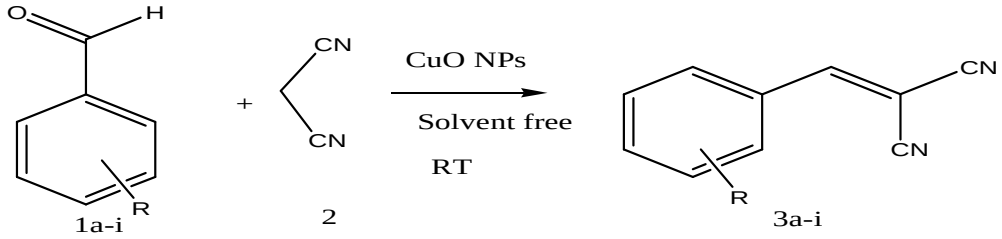


**Scheme 2**

### 3.3.4 Experimental

The melting points of compounds were taken in an open capillary in a paraffin bath. IR spectra were recorded on a Jasco FTIR-4100 spectrophotometer. $^{1}H$ NMR spectra were recorded on an 400 MHz FT-NMR spectrometer in $CDCl_3$ as a solvent and chemical shift values were recorded in units δ (ppm) relative to tetramethylsilane ($Me_4Si$) as an internal standard.

**General procedure**

A mixture of aromatic aldehyde (1mmol), malononitrile (1mmol) and CuO nanoparticles (100mg) was stirred with high speed at room temperature till the completion of reaction monitored by TLC( ethyl acetate and n-hexane 7:3). After completion of reaction, solid product obtained was dissolved in 10ml ethyl acetate and concentrated on rotavapor. Finally pure product was obtained by recrystalization and authentic samples were characterized by FTIR, $H^{1}NMR$ and $C^{13}NMR$.

### 3.3.5 Spectral data of representative compound

3a: 5-(Benzylidine) malanonitrile: FTIR (KBr $cm^{-1}$ ) - 2220, 2922, 1587, 1485, 956, 673 $cm^{-1}$.

$^{1}H$ NMR (400 MHz in $CDCl_3$) δ ppm: 7.24 (t, 1 H), 7.62 (d, 2H), 7.78 (d, 2H), 8.02 (s, 1H).

$^{13}C$ NMR (100 MHz in $CDCl_3$) δ ppm:82.84, 112.60, 113.79, 130.76, 134, 160.03

3b: 5-(4-Cl-Benzylidine) malanonitrile: IR (KBr)- 2221, 1576, 1483, 1363, 850 $cm^{-1}$. $^1$HNMR ($CDCl_3$) 7.45 (d, 2H), 7.78 (d, 2H), 7.86(s, 1H).

### 3.3.6 Result discussion

The catalytic activity of the synthesized CuO nanoparticles was investigated in the synthesis of 5-benzylidene malononitrile derivatives at room temperature. To study the efficiency of the CuO nanocatalyst, 4-chlorobenzaldehyde (**1b**) and malononitrile (**2**) were used as the model substrate. We have also carried out the reaction without any catalyst, but the product isolated gave poor yield (25%). In optimizing the reaction conditions, the amount of catalyst was the major factor. The model reaction was studied using 10, 20, 30, 50 and 60 mg of catalyst in the reaction of 4-chlorobenzaldehyde (1b) and malononitrile (2). The results revealed that best yield was obtained by using 50 mg catalyst. With increase in the catalyst concentration, the yield of the desired product was found to be constant. Therefore, the catalyst plays a crucial role in the success of the reaction in term of yields of the product. The results obtained are summarized in Table-3.3.2. It is evident that the aromatic aldehyde carrying electron-donating or electron-withdrawing groups reacted smoothly to produce high yield of products. The results with different aromatic aldehydes are summarized in Table-3.3.1.

**Table-3.3.1 Synthesis of 5-benzylidine malononitrile derivatives catalyzed by CuO Nanoparticles.**

| Sr. No. | Reactant | Products[a] | Time (min) | Yield[b] (%) | Melting point (°C) | |
|---|---|---|---|---|---|---|
| | | | | | Found | Reported |
| 1 | $C_6H_5$ | 3a | 18 | 96 | 82 | 82-82 |
| 2 | 4-$ClC_6H_4$ | 3b | 12 | 99 | 161-162 | 161-163 |
| 3 | 2-$ClC_6H_4$ | 3c | 13 | 94 | 93-94 | 92-94 |
| 4 | 4-$NO_2C_6H_4$ | 3d | 10 | 96 | 158-159 | 159-160 |
| 5 | 3-$NO_2C_6H_4$ | 3e | 10 | 95 | 103-105 | 103-105 |
| 6 | 4-$CH_3C_6H_4$ | 3f | 20 | 92 | 132-133 | 134-135 |
| 7 | 4-$CH_3OC_6H_4$ | 3g | 22 | 90 | 112-113 | 113-114 |
| 8 | 4-$OHC_6H_4$ | 3h | 15 | 94 | 185-187 | 187-188 |
| 9 | 4-$FC_6H_4$ | 3i | 12 | 95 | 130-131 | 131-133 |
| 10 | 4-$BrC_6H_4$ | 3j | 15 | 94 | 167-168 | 168-170 |

[a] Reaction condition: Aldehyde (1mmol), malononitrile (1mmol) and 50mg of CuO NPs solvent free at RT.
[b]isolated yield

**Table-3.3.2 Screening of catalyst CuO NPs for the synthesis of5-benzylidine malononitrile**

| Entry[a] | Catalyst amount(mg) | Time(min) | Yield(%)[b] |
|---|---|---|---|
| 1 | 10 | 60 | 48 |
| 2 | 20 | 40 | 78 |
| 3 | 30 | 25 | 88 |
| 4 | 50 | 12 | 99 |
| 5 | 60 | 12 | 99 |

[a]Reaction condition: 4 Cl benzaldehyde (1mmol), malononitrile (1mmol) and 50mg of CuO NPs solvent free at RT.
[b]isolated yield

In this study, the catalyst was recovered and reused in another run. The catalyst was recovered by simple work-up using centrifugation method, washed with ethanol and reused for three successive reaction corresponding yield for each cycle as mentioned in Table-3.3.3.

**Table-3.3.3 Reusability of CuO nanoparticles in the preparation of 5-benzylidine malononitrile**

| No of Cycles[a] | Fresh | 1 | 2 | 3 |
|---|---|---|---|---|
| Yield(%)[b] | 99 | 97 | 91 | 86 |

[a] Reaction condition: Aldehyde (1mmol), malononitrile (1mmol) and 50mg of CuO NPs solvent free at RT.
[b]isolated yield

To compare the merits of our work to the other reported procedure; the results of the synthesis of 5-benzylidene malononitrile derivatives in the presence of different reported catalysts with respect to time and yield of the product are listed in Table-3.3.4. These results show that our catalyst CuO nanoparticles are stable in air, nontoxic, give good yield in short time than other catalysts and there is no use of any hazardous solvent.

**Table-3.3.4Comparisation result of CuO nanoparticles with other catalysts reported in the literature**.

| Sr. No. | Catalyst | Reaction condition | Yield (%) | Literature |
|---|---|---|---|---|
| 1 | Ni-Mg Ferrite | Stirr/RT/15 min | 90 | 47 |
| 2 | $SiO_2$-$NH_4OAc$ | 60°C/ 7 Hr | 87 | 56 |
| 3 | $Al_2O_3$ | 100°C/ 15 min | 85 | 57 |
| 4 | CuO nanoparticles | Solvent free/ RT/10 min | 99 | This work |

### 3.3.7 Conclusion

Thus, we report fast, clean and highly competent methodology for the Knoevenagel condensation of various aromatic aldehydes with malononitrile catalyzed by CuO nanoparticles to give 5-benzylidene malononitrile derivatives. The desired products were obtained in short reaction time with quantitative yields by a simple high speed stirring at room temperature. The reaction time, yield of products and reusability of catalysts make the present protocol a useful and important addition to the present methodologies for the synthesis of 5-benzylidene malononitrile derivatives.

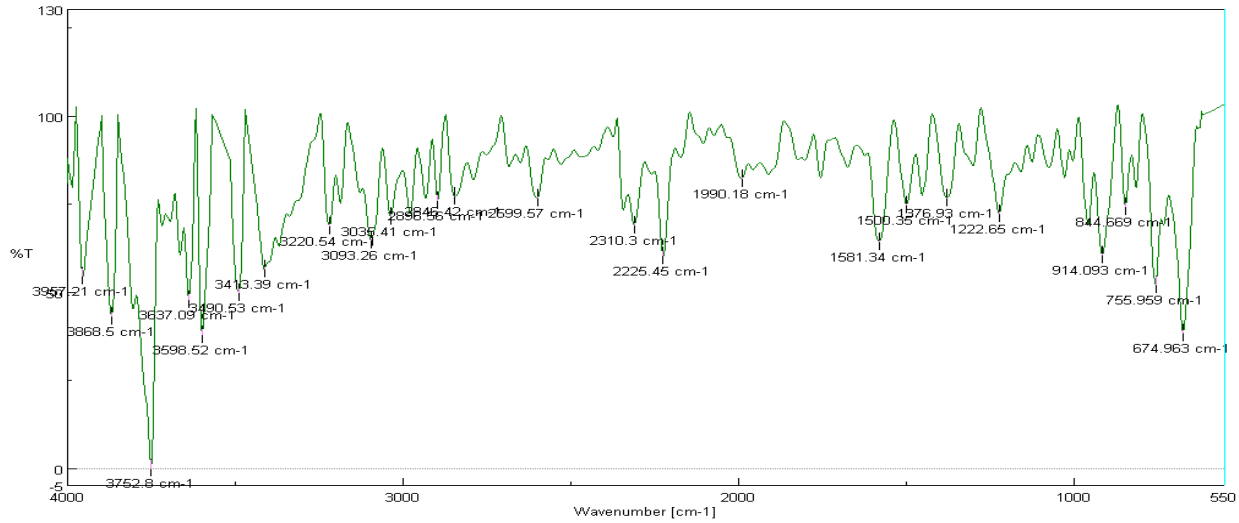


B-CN

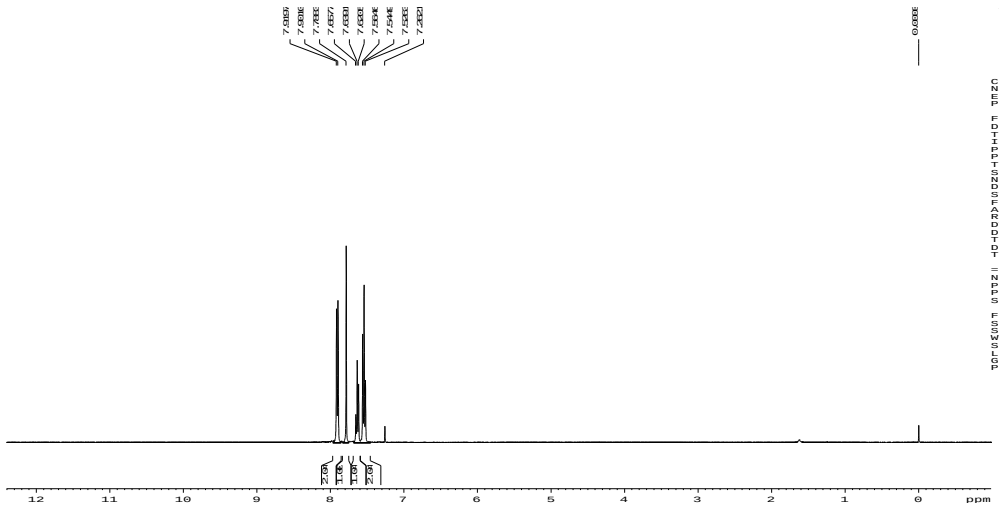

BRUKER
AVANCE II 400 NMR
Spectrometer
SAIF
Panjab University
Chandigarh

```
Current Data Parameters
NAME        Apr22-2014-Administrator
EXPNO                 10
PROCNO                 1

F2 - Acquisition Parameters
Date_              20140422
Time                18.12
INSTRUM             spect
PROBHD   5 mm PABBO BB-
PULPROG             zg30
TD                 65536
SOLVENT            CDCl3
NS                     8
DS                     2
SWH             12019.230 Hz
FIDRES              0.183399 Hz
AQ                2.7263477 sec
RG                   203
DW                  41.600 usec
DE                   6.00 usec
TE                 296.6 K
D1                1.00000000 sec
TD0                    1

======== CHANNEL f1 ========
NUC1                  1H
P1                 10.90 usec
PL1                -3.00 dB
SFO1          400.1324710 MHz

F2 - Processing parameters
SI                 32768
SF            400.1300098 MHz
WDW                   EM
SSB                    0
LB                  0.30 Hz
GB                     0
PC                  1.00
```

avtar_saifpu@yahoo.co.in

B-CN

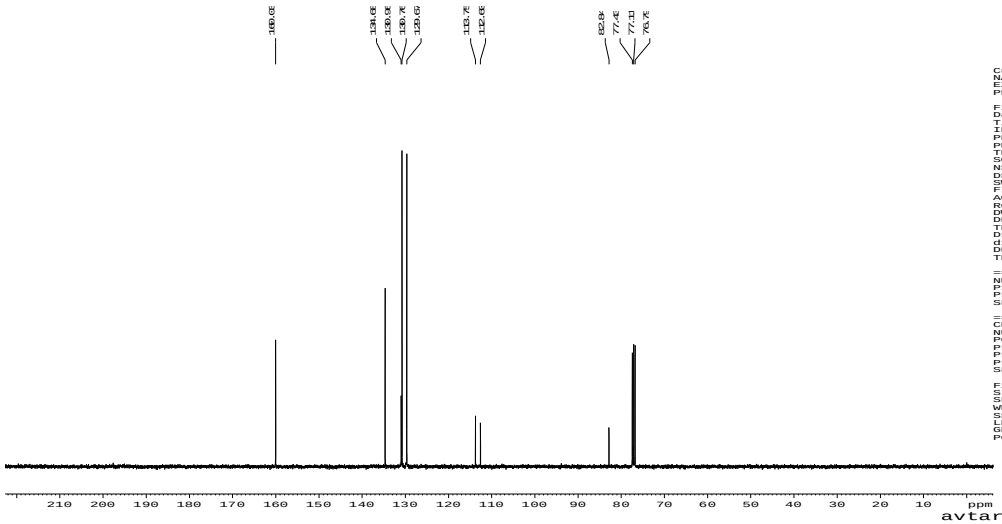

BRUKER
AVANCE II 400 NMR
Spectrometer
SAIF
Panjab University
Chandigarh

```
Current Data Parameters
NAME        Apr22-2014-Administrator
EXPNO                 11
PROCNO                 1

F2 - Acquisition Parameters
Date_              20140422
Time                18.22
INSTRUM             spect
PROBHD   5 mm PABBO BB-
PULPROG           zgpg30
TD                 65536
SOLVENT            CDCl3
NS                   140
DS                     4
SWH             29761.904 Hz
FIDRES              0.454131 Hz
AQ                1.1010548 sec
RG                   575
DW                  16.800 usec
DE                   6.00 usec
TE                 297.3 K
D1              2.00000000 sec
d11             0.03000000 sec
DELTA           1.89999998 sec
TD0                    1

======== CHANNEL f1 ========
NUC1                 13C
P1                  9.60 usec
PL1                 2.00 dB
SFO1          100.6228298 MHz

======== CHANNEL f2 ========
CPDPRG2          waltz16
NUC2                  1H
PCPD2              80.00 usec
PL2                -3.00 dB
PL12               14.31 dB
PL13               18.00 dB
SFO2          400.1316005 MHz

F2 - Processing parameters
SI                 32768
SF            100.6127690 MHz
WDW                   EM
SSB                    0
LB                  1.00 Hz
GB                     0
PC                  1.40
```

avtar_saifpu@yahoo.co.in

## 3.4 **Synthesis of 1, 2-dibenzylidenehydrazine derivatives catalyzed by copper oxide nanoparticles**

### 3.4.1 Introduction

Azines, N-N linked diimines, are extremely useful compounds and recently they have received attention because of their utility in a number of interesting reactions [65], their biological properties and their potential application in bond formation, liquid crystals, nonlinear optical materials [66]. The azines are an important class of molecules because many compounds of pharmacological interest can be synthesized from them [67]. Azines are useful for the isolation, purification, and characterization of carbonyl compounds [68]. There are several advantages to make derivatives or protection of azines: (1) economic advantage resulting from the low cost of only one-half equivalent of protective group, (2) easy isolation of the products resulting from the symmetrical structure with high melting points and (3) easy identification of the products resulting from the fully conjugated and colorful structures [69-70]. Applications of azines include possible nonlinear optical materials [71] and conducting polymers (polyazine) [72]. Azine derivatives display important biological properties and are important for drug development [66]. Complexes of titanium [73], zirconium [74], cobalt [75], uranium [76], and iron [77] are capable of cleaving the N-N bond in azines. They have considerable interest for their properties and useful applications in coloring and dyeing processes [78].

Azines, $R_1R_2C=N–N=CR_1R_2$, have attracted great attention in organic synthesis as they are good synthons for obtaining various heterocyclic compounds [79-80]. These compounds constitute an important class of compounds with unexpected biological activities [81-82].

### 3.4.2 Literature review

Different synthetic pathways can be employed to prepare azines. Symmetrical azines have been synthesized by the condensation of aldehydes or ketones with hydrazine in ethanol solution under reflux conditions [83]. In the past few years, the study of new procedures in chemical industries that are less hazardous to human health and the environment has received extensive attention. We report herein our progress toward the establishment of a new protocol for preparation of azines with common additives.

Commercially available $BiCl_3$ had been widely used as a Lewis acid catalyst for aldol reaction, hetero Diels-Alder reaction, ring opening of epoxides with aromatic amines, deoxygenative allylation of substituted benzylic alcohols with allyltrimethylsilane, and for three-component

synthesis of β-amino carbonyl compounds. But $BiCl_3$ is highly hygroscopic and difficult to handle as it is toxic and causes irritation to the gastrointestinal and respiratory tract. In addition, this catalyst cannot be reused. Bismuth chloride is to be loaded on a support material for easy handling and utilization. Clays function as efficient catalysts for various organic transformations due to their Bronsted and Lewis acidities in their natural and ion-exchanged forms.

Commercially available montmorillonite K10 (Mont K10) clay is one suchmaterial that can fulfill these requirements. Mont K10 is an environmentally benign and economically feasible solid cayalyst that offer several advantages, such as ease of handling, non-corrosiveness, low cost, and regeneration. Its high surface area makes it as a useful and active catalyst. Its structural feature and synthetic potential have been extensively studied. Mont K10 is a layered alumino-silicate with a dioctahedral layer sandwiched between two tetrahedral layers. Due to strong catalytic activity as solid acid, Mont K10 clay has been used extensively as a catalyst for many organic transformations [84-87].

The usual method for the preparation of azines involves treatment of carbonyl compounds with hydrazine hydrate and acetic acid in ethanol [88]. A number of methods have been reported for the synthesis of azines under various conditions [89-92] but most of them require elevated temperatures and complex catalysts. Hence, there is a need to develop a simple, eco- friendly method under mild conditions for the preparation of azines. In this work on the synthesis of azine derivatives with CuO nanoparticles in ethanol solvent, herein we report a recyclable, easily separable, ecofriendly and highly effective catalytic system CuO nanoparticles loaded.

### 3.4.3 Present work

Electrochemically prepared CuO nanoparticles were tested on the synthesis of 1,2-dibenzylidenehydrazine derivatives (Scheme 3). The short reaction time, green solvent ethanol at reflux condition, high yield and minimum environmental effect were important features of the reaction.

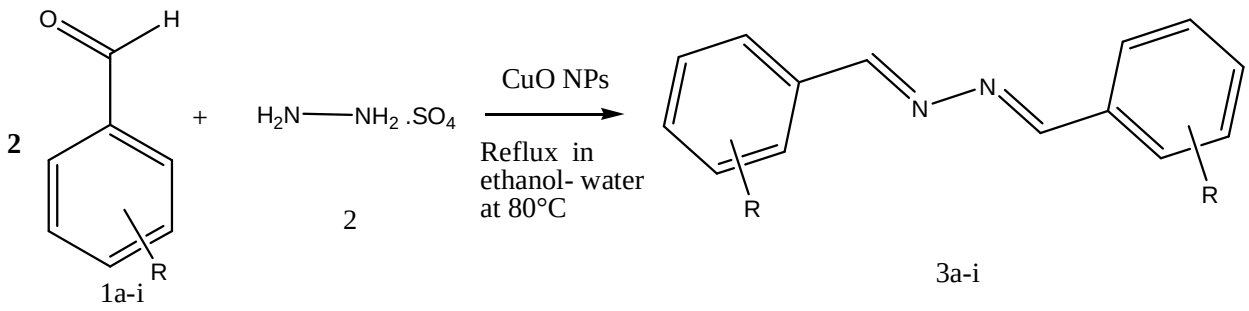


**Scheme 3**

### 3.4.4 Experimental

The melting points of compounds were taken in an open capillary in a paraffin bath. IR spectra were recorded on a Jasco FTIR-4100 spectrophotometer. $^1$H NMR spectra were recorded on an 400 MHz FT-NMR spectrometer in $CDCl_3$ as a solvent and chemical shift values were recorded in units δ (ppm) relative to tetramethylsilane ($Me_4Si$) as an internal standard.

**General procedure**

A mixture of aromatic aldehyde (2mmol), hydrazine hydrate sulphate (1mmol) and CuO nanoparticles (100mg) (Scheme 3) was reflux in ethanol:water(1:1) at 80 ºC till the completion of reaction monitored by TLC( ethyl acetate and n-hexane 7:3). After completion of reaction solid product obtained was dissolved in 10ml ethyl acetate and concentrated on rotavapor. Finally pure product was obtained by recrystalization and authentic samples were characterized by FTIR, $H^1$NMR and $C^{13}$NMR.

### 3.4.5 Spectral data of representative compound

1] (1E,2E)-1,2-Dibenzylidenehydrazine 3a. $^1$H NMR(400 MHz, $CDCl_3$): d 7.07 (1H, mm, CH), 7.28 (1H, m, CH), 7.49 (1H, m, CH), 7.65 (1H, t, CH), 8.28 (1H, m, CH), 8.48 (1H, s, CH=N); 13C NMR (100 MHz, $CDCl_3$): d 128.41 (CH of Ar), 128.72 (CH of Ar), 130.76 (CH of Ar), 132.31 (C of Ar) 164.80 (C of CN).

2] (1E,2E)-1,2-Bis(3-nitrobenzylidene)hydrazine 3c. FTIR (KBr $\nu_{max}$/$cm^{-1}$):3153, 1662, 1598, 1448, 1314, 1283,1217,1163, 1054, 1007, 923, 858, 832, 787 and 665 $cm^{-1}$.$^1$H NMR(400 MHz, CDCl3) δ ppm : 7.77 (t, 2H, CH of Ar), 8.28(d, 2H, CH of Ar), 8.35 (d,2H, CH of Ar), 8.74 (S,2H, CH of benzylidenimin), 8.86(s, 2H, CH of Ar), 8.49 (1H, m, CH), 8.56 (1H, s, CH=N); 13C NMR (100MHz, CDCl3) δ ppm: d 122.41(CH of Ar), 125.35(CH of Ar), 130.07 (CH of Ar), 134.31 (C of Ar), 135.23 (CH of Ar), 148.12 (C of Ar), 160.09 (C of CN).

### 3.4.6 Result discussion

We reveal herein for the first time, the CuO nanoparticles catalyzed 1,2-dibenzylidenehydrazine with a variety of aldehydes by simple reflux at 80ºC in ethanol-water(1:1) greener solvent. In the present work, attempt is made to optimize the reaction condition by using 3 nitro-benzaldehyde and hydrazine hydrate sulphate as a model reaction at different solvents and amount of catalyst used. From Table 3.4.1, it can be seen that the best ratio of CuO nanoparticles to starting material is 100mg. There is considerable increase in the yield of product when the concentration of CuO nanoparticles increases from 20mg to 100mg. But when we increased catalyst quantity to 120 mg there is no considerable change in reaction time and yield of product

**Table 3.4.1** Screening of catalyst CuO NPs for the synthesis of 1, 2-dibenzylidenehydrazine

| Entry[a] | Catalyst amount(mg) | Time(min) | Yield[b](%) |
|---|---|---|---|
| 1 | 20 | 30 | Trace |
| 2 | 40 | 30 | 36 |
| 3 | 60 | 30 | 66 |
| 4 | 80 | 30 | 92 |
| 5 | 100 | 30 | 96 |
| 6 | 120 | 30 | 96 |

[a]3 Nitro- benzaldehyde(2mmol), hydrazine hydrate sulphate (1mmol) and CuO NPs (100mg) in ethanol:water(1:1) reflux at 80 ºC. [b] Isolated yield

In this study, the effect of different solvent was investigated and given in Table 3.4.2. The choice of solvent proved critical. We observed that polar solvents such as methanol, ethanol, acetonitrile, afford better yield than nonpolar ones and mixture of ethanol-water (1:1) is most effective solvent affording maximum yield of product.

**Table 3.4.2** Optimization of solvent in synthesis of 1,2-dibenzylidenehydrazine

| Entry[a] | Solvent | Time(min) | Yield[b](%) |
|---|---|---|---|
| 1 | ACN | 180 | 54 |
| 1 | Toluene | 180 | 32 |
| 2 | THF | 180 | 35 |
| 4 | Methanol | 120 | 72 |
| 5 | Ethanol | 60 | 86 |
| 6 | Ethanol:water (1:1) | 30 | 94 |

[a]3 Nitro- benzaldehyde (2mmol), hydrazine hydrate sulphate (1mmol) and CuO NPs (100mg) in ethanol:water(1:1) reflux at 80ºC. [b] Isolated yield

After optimizing the conditions, the generality of this method was examined by the reaction of cyclohexanone with several aldehydes bearing electron withdrawing groups (such as nitro, chloro and hydroxyl) and electron donating groups (such as methyl, methoxy and N-dimetyl). The entire product reacted in a similar manner producing moderate to good yield of expected product. The para substituted aromatic aldehyde reacted in a shorter reaction time as compared with ortho and meta substituted aromatic aldehyde and electron donating substituted aldehyde required more time and comparative less yield result summarized in Table 3.4.3.

**Table3.4.3.** Synthesis of 1, 2-dibenzylidenehydrazine derivatives using CuO NPs catalyst

| Products[a] | R | Time (min) | Yield[b] (%) | Melting point (°C) | |
|---|---|---|---|---|---|
| | | | | Found | Reported |
| 3a | H | 45 | 90 | 93-94 | 92-93 |
| 3b | 4-Cl | 35 | 95 | 207-209 | 208-210 |
| 3c | 2-Cl | 40 | 91 | 141-142 | 142-144 |
| 3d | 4-$NO_2$ | 30 | 94 | 297-299 | 299-300 |
| 3e | 3-$NO_2$ | 30 | 96 | 195-196 | 198-199 |
| 3f | 2-OH | 35 | 94 | 213-214 | 216-217 |
| 3g | 4-$N(CH_3)_2$ | 40 | 91 | 214-215 | 215-216 |
| 3h | 4-$CH_3$ | 50 | 88 | 156-158 | 159-160 |
| 3i | 4-OMe | 45 | 89 | 166-168 | 166-169 |

[a] Aromatic aldehyde(2mmol), hydrazine hydrate sulphate (1mmol) and CuO NPs (100mg) in ethanol:water (1:1) reflux at 80°C. [b] Isolated yield.

In this study, the catalyst was recovered and reused. The catalyst was recovered by a simple work-up using centrifugation and then it was washed with ethanol and reused. The reused catalyst gave excellent yield and was used in mentioned reaction for three times, the observations in Table 3.4.4 reveal that as the number of the cycles of catalyst increases the activity decreases.

**Table3.4.4.** Reusability of CuO NPs catalyst in synthesis of 1,2-dibenzylidenehydrazine

| **Cycle** | **Fresh** | **First** | **Second** | **Third** |
|---|---|---|---|---|
| [a]Yield (%)[b] | 96 | 94 | 90 | 85 |

[a]3 Nitro- benzaldehyde(2mmol), hydrazine hydrate sulphate (1mmol) and CuO NPs (100mg) in ethanol water(1:1) reflux at 80°C. [b] Isolated yield

### 3.4.7 Conclusion

The results of the synthesis of 1,2-dibenzylidenehydrazine derivatives in the presence of different reported catalyst with respect to time and yield of the product. These results show that

our catalyst, CuO nanoparticles were efficient, stable, nontoxic and reusable. They give good yield of product in shorter reaction time in presence of green solvent ethanol: water.

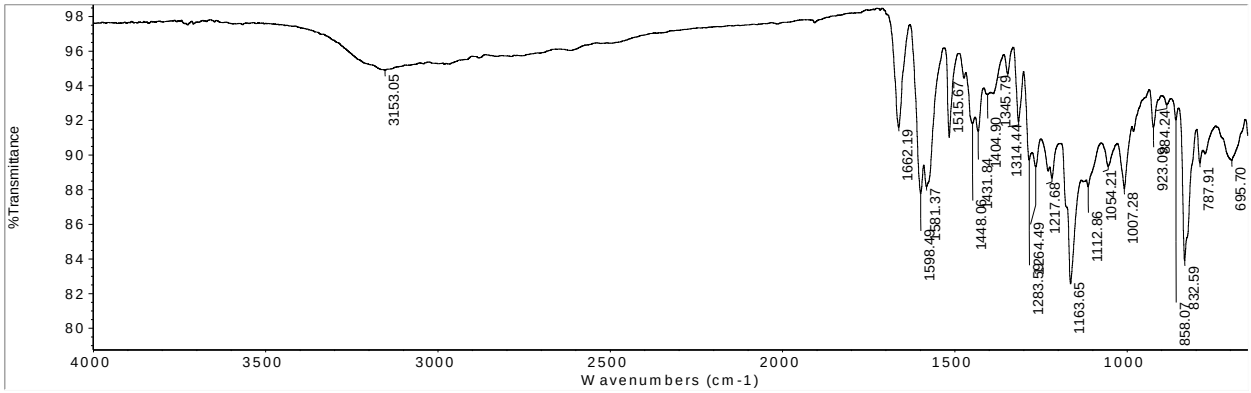


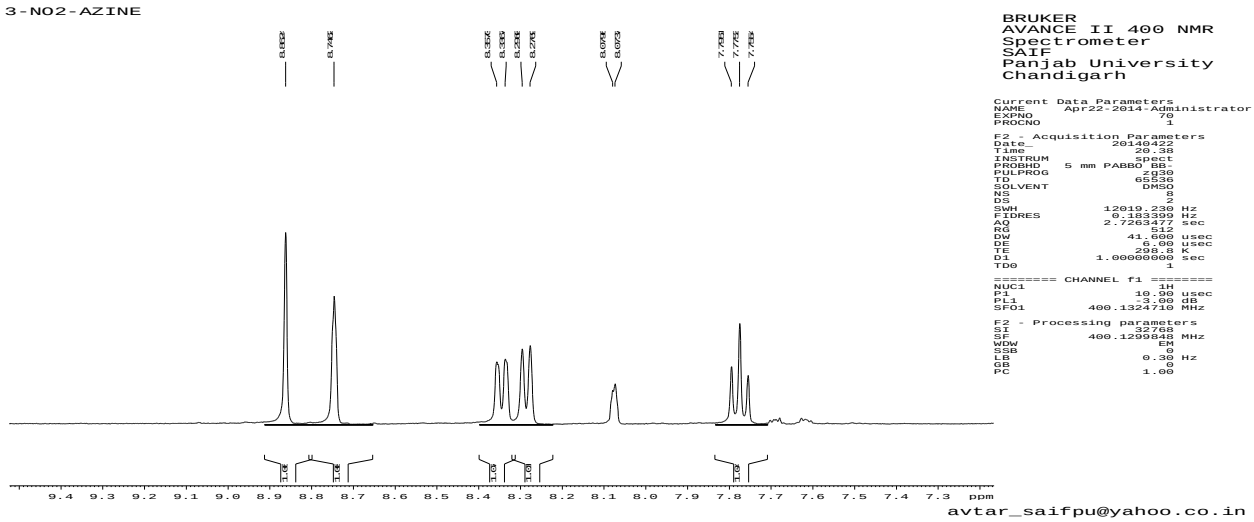


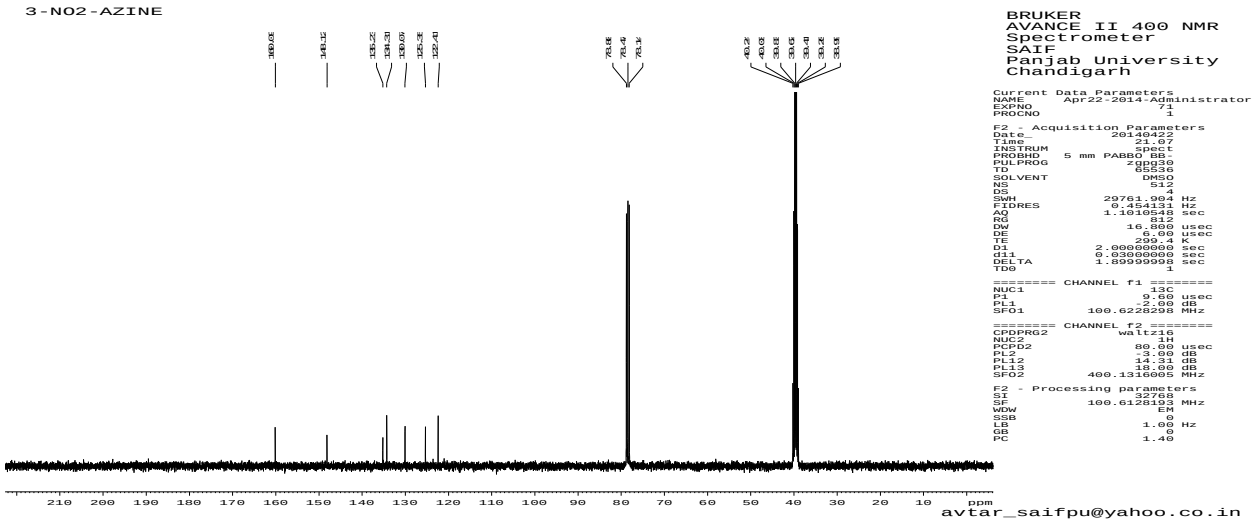

## Section B- $MoO_3$ nanoparticles catalyzed organic transformation reactions

### 3.5 Synthesis of 2, 6-bis (benzylidene) cyclohexanones derivatives catalyzed by $MoO_3$ nanoparticles

#### 3.5.1 Introduction

The α,α'-unsaturated ketones have been attracting much more attention particularly the α,α'-unsaturated derivatives of cyclohexanone, such as 2,6-bis(benzylidene)cyclohexanone [93] not only due to their intriguing biological activities such as antiangiogenic [94] , cytotoxic [95], cholesterol-lowering activity[96] but also their potential for nonlinear optical materials [97]. Arylidene cycloalkanones are useful intermediates for synthesis of bioactive pyrimidine [98], perfumes [99], bis-spiroisoxazolines [100], liquid crystalline polymers [101] and pharmaceutical applications, especially as HIV-1 integrase inhibitors. [102]. Due to their wide importance as precursors of potentially bioactive pyrimidine derivatives, α,α' bis(substituted benzylidene) cycloalkanones have attracted considerable attention. Bis-benzylidene cycloalkanones display a significant range of properties such as cytotoxicity and histone acetyl transferase (HAT) inhibitory activities. Moreover, these compounds find several applications not only in non linear optics but also in agrochemical industries as well as liquid crystalline polymers.

#### 3.5.2 Literature review

Owing to the importance of these compounds various methods for synthesis of this type of compound have been developed. The typical methods for the preparation of 2,6-bis(benzylidene)cyclohexanone generally involve cross-aldol condensation of cyclohexanone with aldehydes in presence of strong acid or bases [103]. However acid or base catalyzed reactions resulted in low yield of product due to reverse & side reactions [104]. Coordination complexes with a variety of metals have been introduced to replace acid or base, but there is no satisfactory effect on the yield of product in most cases [105]. Continuing efforts to find new catalysts have resulted in the introduction of various reagents such as $RuCl_3$ , $KF/Al_2O_3$, KOH, NaOH, $I_2$, SSA, $Yb(OTf)_3$, $Cu(OTf)_2$, $CH_3CO_2Na/CH_3CO_2H$, $PEG/AlCl_3$ and $Fe_2O_3$ nanoparticles [106-116] . The other synthetic method for preparation of these compounds involves microwave radiation [117] and ultrasound irradiation [118]. However, these methods suffer from one or more disadvantages such as use of toxic organic solvents or toxic catalyst and in many cases after the completion of the reaction, the catalyst system cannot be recycled. Considering the

importance for the preparation of 2, 6-bis (benzylidene)cyclohexanone & disadvantages in the current reported method, it is important to exploit a simple, efficient & clean procedure for the synthesis of these compound without using hazardous solvents, using less toxic, inexpensive and reusable catalyst.

### 3.5.3 Present work

Electrochemically prepared $MoO_3$ nanoparticles were tested on the synthesis of 2, 6- Bis (benzylidene) cyclohexanones derivatives (Scheme-4). The short reaction time, clean reaction condition, consistent yield and minimum adverse environmental effect were important features of the reaction.

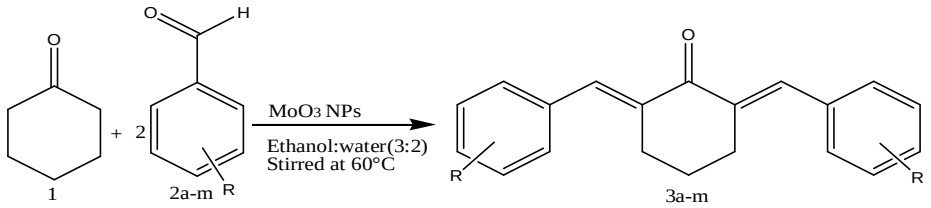


**Scheme 4** synthesis of 2, 6- Bis (benzylidene) cyclohexanones derivatives

### 3.5.4 Experimental

The melting points of compounds were taken in an open capillary in a paraffin bath. IR spectra were recorded on a Jasco FTIR-4100 spectrophotometer. $^1$H NMR spectra were recorded on an 400 MHz FT-NMR spectrometer in DMSO as a solvent and chemical shift values were recorded in units δ (ppm) relative to tetramethylsilane ($Me_4Si$) as an internal standard.

**General procedure**

A mixture of aromatic aldehyde (10 mmol), cyclohexanone (5 mmol) and $MoO_3$ nanoparticles (60mg) in 5 ml ethanol: water (3:2) was stirred at 60ºC till the completion of reaction (monitored by TLC). After cooling solid product obtained was filtered, washed with water and recrystallized with ethanol to obtained pure product. The hot reaction mixture was centrifuged for recovery of catalyst. The recovered catalyst washed with ethanol, dried and reused three times in same reaction.

### 3.5.5 Spectral data of representative compound

2,6-bis(benzylidene)cyclohexanone (3a) Colour- Yellow crystals M.P: 115-116°C

IR(KBr) $V_{max}/cm^{-1}$ : 3020, 2902, 1658, 1607, 1573,1486, 970, 750, $^1$H-NMR (300.13 MHz, $CDCl_3$, δ ppm):- 1.73-1.81(m, 2H, $CH_2$), 2.90-2.93(t, 4H, $2CH_2$), 7.24-7.55(m, 10H, Ar-H),

7.80(S, 2H, 2=CH). $^{13}$C-NMR (75.46 MHz, $CDCl_3$, δ ppm): 23.19($CH_2$), 28.62-29.09($2CH_2$), 128.08(4CH of Ar), 128.55(4CH of Ar-H) 135.80(2CH), 136.17(2C-Ar), 136.38(2C=C), 190.50(C=O). MS (EI) m/z 275($M^+$)

2,6-bis(p-chlorobenzylidene)cyclohexanone (3b) Colour- brown solid; MP 149-151

IR(KBr) $V_{max}/cm^{-1}$: 2930,1665, 1606, 1576, 1350, 810 $cm^{-1}$. $^1$H-NMR (300.13 MHz, $CDCl_3$, δ ppm): 1.82-1.88(m, 2H, $CH_2$), 2.96(t, 4H, $2CH_2$), 7.60-8.22(m, 8H Ar-H), 8.30(s, 2H, 2=CH). $^{13}$C-NMR 26.72($CH_2$), 27.46($2CH_2$), 126.4(4 CH-Ar), 128.70(4 CH of Ar), 135.20(2C-Ar), 137.20(2C=C), 145.40(2CH=C), 187.20(C=O).

2,6-bis(p-nitrobenzylidene)cyclohexanone (3d)Colour –yellow solid; MP- 158-160

IR(KBr) $V_{max}/cm^{-1}$: 3081, 2925,1660, 1606, 1575, 1260, 828 $cm^{-1}$. $^1$H-NMR (300.13 MHz, $CDCl_3$, δ ppm): 1.75-1.82(m, 2H, $CH_2$), 2.92(t, 4H, $2CH_2$), 7.35-7.44(m, 8H Ar-H), 7.72(s, 2H, 2=CH). $^{13}$C-NMR 26.72($CH_2$), 27.46($2CH_2$), 121.10(4 CH-Ar), 127.30(4 CH of Ar), 137.20(2C-Ar), 141.30(2C=C), 145.40(2CH=C), 181.20(C=O).

### 3.5.6 Result discussion

We reveal herein for the first time, the $MoO_3$ nanoparticles catalyzed aldol condensation of cyclohexanone with a variety of aldehydes by simple stirring at 60ºC. In the present work, attempt is made to optimize the reaction condition by using 4 nitro-benzaldehyde and cyclohexanone as a model reaction at different solvents and amount of catalyst used. From Table 3.5.1 it can be seen that the best ratio of $MoO_3$ nanoparticles to starting material is 60mg. There is considerable increase in the yield of product when the concentration of $MoO_3$ nanoparticles increases from 10mg to 60mg. But when we increased catalyst quantity to 70mg there is no considerable change in reaction time and yield of product

**Table 3.5.1.** Screening of catalyst $MoO_3$ for the synthesis of 2,6- Bis (benzylidene) cyclohexanones

| Entry[a] | Catalyst amount(mg) | Time(min) | Yield[b](%) |
|---|---|---|---|
| 1 | 10 | 240 | Trace |
| 2 | 20 | 160 | 36 |
| 3 | 40 | 120 | 66 |
| 4 | 50 | 90 | 92 |
| 5 | 60 | 90 | 94 |
| 6 | 70 | 90 | 95 |

[a]Reaction condition: aldehyde (2mmol), cyclohexanone (1mmol), and 60mg of $MoO_3$ nanoparticles stirred at 60°C
[b] Isolated yield

In this study, the effect of different solvent was investigated and given in Table 3.5.2. The choice of solvent proved critical. We observed that polar solvents such as methanol, ethanol, acetonitrile afford better yield than nonpolar ones and mixture of water(2ml) & ethanol(3ml) is most effective solvent affording maximum yield of product.

**Table 3.5.2** Optimization of solvent in synthesis of 2,6- Bis (benzylidene) cyclohexanones by$MoO_3$ NPs catalyst

| Entry | Solvent | Time(hrs) | Yield[b](%) |
|---|---|---|---|
| 1 | ACN | 3 | 54 |
| 1 | Toluene | 3 | 32 |
| 2 | THF | 3 | 35 |
| 4 | Methanol | 3 | 62 |
| 5 | Ethanol | 3 | 76 |
| 6 | Ethanol:water (3:2) | 2 | 94 |

[a]Reaction condition: aldehyde (2mmol), cyclohexanone (1mmol), and 60mg of $MoO_3$ nanoparticles stirred at 60°C
[b] Isolated yield

After optimizing the conditions, the generality of this method was examined by the reaction of cyclohexanone with several aldehydes bearing electron withdrawing groups (such as nitro, chloro, bromo, fluoro, and hydroxyl) and electron donating groups (such as methyl, methoxy). The entire product reacted in a similar manner producing moderate to good yield of expected product. The para substituted aromatic aldehyde reacted in a shorter reaction time as compared with ortho and meta substituted aromatic aldehyde in Table 3.5.3.

**Table3.5.3.** Synthesis of 2,6-bis(benzylidene)cyclohexanone derivatives using $MoO_3$NPs catalyst

| Products[a] | R | Time (min) | Yield[b] (%) | Melting point (°C) | |
|---|---|---|---|---|---|
| | | | | Found | Reported |
| 3a | H | 120 | 91 | 115-116 | 115-118[106] |
| 3b | 4-Cl | 95 | 95 | 145-147 | 147-148[106] |
| 3c | 2-Cl | 130 | 92 | 103-105 | 102-106[115] |
| 3d | 4-$NO_2$ | 90 | 94[b], 91[c], 89[c], 84[c] | 158-160 | 160-163[106] |
| 3e | 3-$NO_2$ | 130 | 95 | 191-192 | 188-190[113] |
| 3f | 4-$CH_3$ | 100 | 90 | 160-162 | 170-171[106] |
| 3g | 2,4-$Cl_2$ | 140 | 89 | 166-167 | 163-164[108] |
| 3h | 4-OMe | 95 | 93 | 160-161 | 161-163[115] |
| 3i | 4-OH | 100 | 94 | 172-174 | - |
| 3j | 4-F | 105 | 94 | 156-157 | 156-158[109] |
| 3k | 4-Br | 110 | 92 | 162-163 | 163-165[115] |
| 3l | 2-furfuralde | 145 | 85 | 140-142 | 140-142[113] |
| 3m | Cinnamalde | 130 | 88 | 180-181 | 180[106] |

[a]Reaction condition: aldehyde (2mmol), cyclohexanone (1mmol), and 60mg of $MoO_3$ nanoparticles stirred at 60°C.
[b] Isolated yield, [c] Isolated yield reused of catalyst 1st, 2nd& 3rd cycle respectively.

In this study, the catalyst was recovered and reused. The catalyst was recovered by a simple work-up using centrifugation, and then it was washed with ethanol and reused. The reused catalyst gave excellent yield and was used in mentioned reaction for three times, the observation in Table 3.5.4 revealed that as the number of the recycle of catalyst increases the activity decreases.

**Table 3.5.4** Reusability of $MoO_3$NPs catalyst for synthesis of 2,6-bis(benzylidene)cyclohexanone

| **Cycle** | **Fresh** | **First** | **Second** | **Third** |
|---|---|---|---|---|
| Yield (%)[b] | 94 | 91 | 89 | 84 |

[a]Reaction condition: aldehyde (2mmol), cyclohexanone (1mmol), and 60mg of $MoO_3$ nanoparticles stirred at 60°C.
[b] Isolated yield,

To compare the merits of our work with the other reported procedure in Table 3.5.5; it shows the results of the synthesis of 2,6-bis(benzylidene)cyclohexanone derivatives in the presence of different reported catalyst with respect to time and yield of the product. These results show that our catalyst $MoO_3$ nanoparticles are more stable in air and nontoxic. It gives good yield in short reaction time.

**Table 3.5.5** Comparison $MoO_3$ nanoparticles with other catalysts reported in the literature.

| Sr. No. | Catalyst | Reaction condition/time in hr | Yield (%) | Literature |
|---|---|---|---|---|
| 1 | $RuCl_3$ | 120ºC sealed/ 12 | 94 | 106 |
| 2 | KOH | 0ºC ethanol room temp/ 4 | 90 | 108 |
| 3 | $I_2$ | $CH_2Cl_2$ room temp./4.5 | 92 | 110 |
| 4 | $Yb(OTf)_3$ | Flourous solvent 120ºC/12 | 95 | 112 |
| 5 | $Cu(OTf)_2$ | Solvent free 80ºC/6 | 94 | 113 |
| 6 | NaOAc/HOAc | 120ºC/7 | 86 | 114 |
| 7 | $MoO_3$ nanoparticles | Ethanol:water(3:2) 60ºC/ 1.5 | 94 | Present work |

### 3.5.7 Conclusion

$MoO_3$ nanoparticles are inexpensive and efficient reusable catalyst for the synthesis of 2, 6-bis (benzylidene) cyclohexanone derivatives. The advantages offered by this method are simple workup, short reaction times, ease of product isolation and high yields. We believed that this method is a useful addition to the present methodology for the synthesis of 2, 6-bis (benzylidene) cyclohexanone.

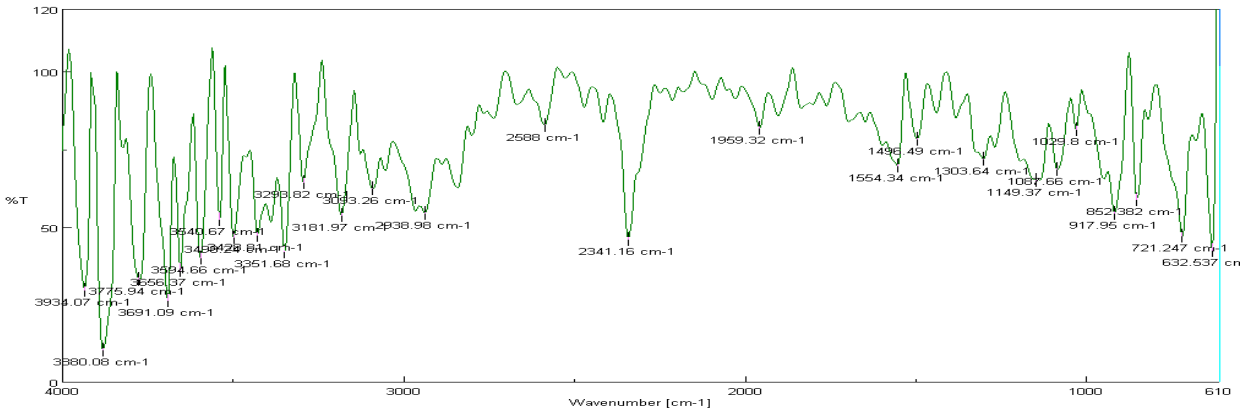
%T
Wavenumber [cm-1]
3380.08 cm-1
3934.07 cm-1
3775.94 cm-1
3691.09 cm-1
3594.66 cm-1
3556.37 cm-1
3351.68 cm-1
3181.97 cm-1
3033.26 cm-1
2938.98 cm-1
2588 cm-1
2341.16 cm-1
1959.32 cm-1
1554.34 cm-1
1496.49 cm-1
1303.64 cm-1
1149.37 cm-1
1029.8 cm-1
917.95 cm-1
852.382 cm-1
721.247 cm-1

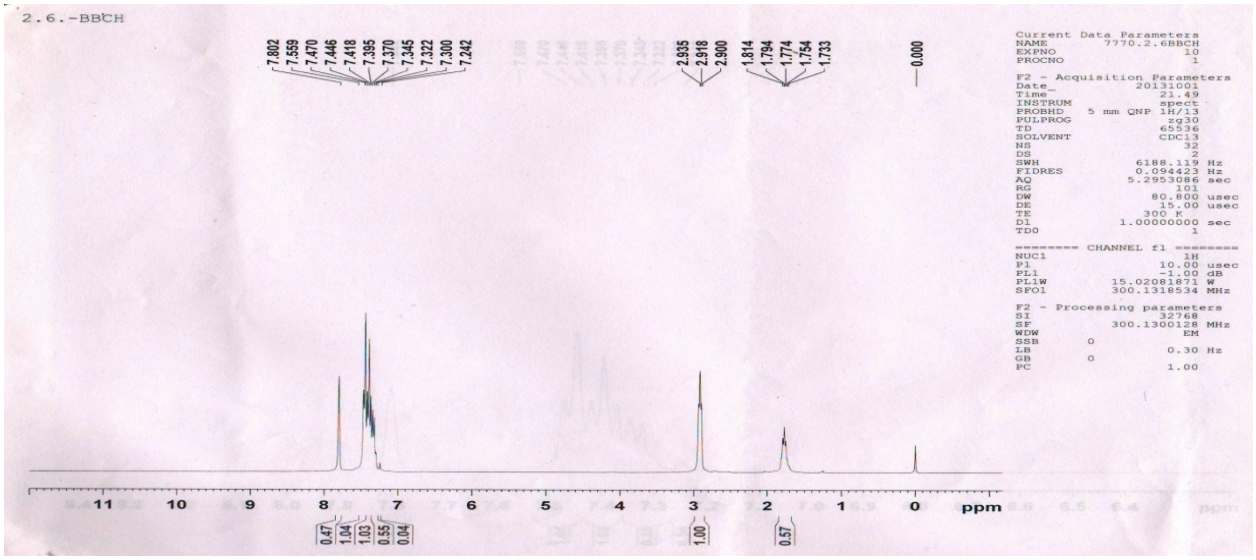
2.6.-BBCH
7.802
7.559
7.470
7.446
7.418
7.395
7.370
7.345
7.322
7.300
7.242
2.935
2.918
2.900
1.814
1.794
1.774
1.754
1.733
0.000
ppm

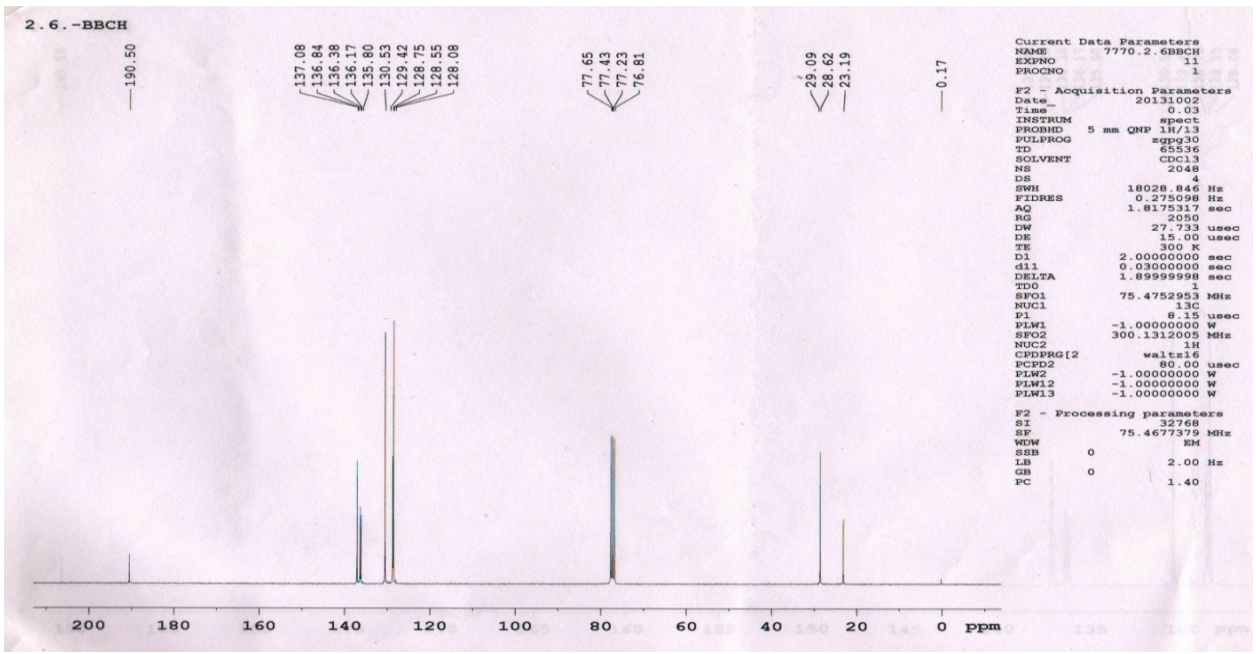
2.6.-BBCH
190.50
137.08
136.84
136.38
136.17
135.80
130.53
129.42
128.75
128.55
128.08
77.65
77.43
77.23
76.81
29.09
28.62
23.19
0.17
ppm

## 3.6 Synthesis of (1E,4E)-1,5-diphenylpenta-1,4-dien-3-one derivatives catalyzed by $MoO_3$ nanoparticles

### 3.6.1 Introduction

Aldol condensation reaction is usually performed to synthesize unsaturated αβ-carbonyl compounds with various advantageous such as chalcone, benzalacetone, etc. Synthesis of analogeous dibenzalacetone by reacting acetone and benzaldehyde and its derivatives is a well-known reaction [119-120]. Acetone which has Hα in both sides can be reacted in condensation with the same or different aldehyde. By the scheme, previous research investigated ultrasound-induced crossed aldol condensation of benzalacetone and several derivatives to obtain 1,5-dibenzalaceton [121] . The 1,5-diaryl-1,4-pentadien-3-ones are used as precursors to potentially bioactive pyrimidine derivatives [122] , intermediates of spiro prostaglandin analog which might act as a mediator in many physiological activities[123] and optically active poly(g-ketosulfide)s [124] . Preparation of 1,5-diaryl-1,4-pentadien-3-ones is usually completed via Claisen-Schmidt condensation between acetone and aromatic aldehydes using conventional stirring or heating method [125-127] . However, there was some shortcoming in terms of long reaction time or low yield. Gupta et al. have reported that the preparation of 1,5-diaryl-1,4-pentadien-3-ones catalyzed by sodium hydroxide under microwave gave good yield [128]. Further there are no reports to our knowledge about the use of $MoO_3$ Nps for the condensation between acetone or benzalacetone with aromatic aldehydes.

### 3.6.2 Literature review

Eventhough the reaction is an efficient reaction but it is time consuming as two steps of reaction are required. In a simpler way, previous experiment was conducted by using acetone and two different aldehydes and derivatives but with low yield [129]. Reference of these works, is observed as an efficient and novel method for producing high yield and purity of 1,5-dibenzalacetone is presented. Cross aldol condensation can be conducted under both acid and base condition and homogeneous form of catalyst [130]. Recently, heterogeneous catalyst has been attempted to replace the homogeneous catalyst as it has more selectivity, stability and reusable characters [131-132]. In this purpose hydrotalcite was used as the most popular catalyst based on its anionic surface properties [133]. Started from this point of more advantage in using heterogeneous catalyst, many researches pay more attention to look for other solid catalyst instead of hydrotalcite.

Zirconium dioxide is a promising heterogeneous catalyst due to its thermal stability and reduction-oxidation properties. Potassium-modified $ZrO_2$ is heterogeneous base catalyst while in pillared form into montmorillonite has acid properties [134-135]. Due to surface acidity and its potential application as environmental friendly catalyst, it is interesting to take advantageous from immobilized $ZrO_2$ in montmorilonite. Refer to aldol condensation conducted by Ordomsky et al.(2010), an effort to use the active sites of immobilized $ZrO_2$ in montmorilonite can be achieved. Bifunctional catalysis of Lewis acid and Broensted base of $ZrO_2/SiO_2$ was reported to accelerate the reaction by abstracting Hα from an aldehyde to form an enol structure for further reaction with C carbonyl from another acetaldehyde.

Ultrasound has been used more and more frequently in organic synthesis in recent three decades [136]. Compared with traditional methods, this method is more convenient and easily controlled. Many organic reactions can be carried in higher yield, shorter reaction time or milder conditions under ultrasound irradiation. Recently, our laboratory has reported the Claisen-Schmidt condensation of furfural with cycloalkanones catalyzed by NaOH under ultrasound irradiation and the results are better than that under conventional heating condition [137]. In continuation of broad programme being pursued in our laboratory on ultrasound-induced organic reactions, herein we report a facile sonochemical synthesis of 1,5-diaryl-1,4-pentadien-3-ones catalyzed by $MoO_3$ nanoparticles.

### 3.6.3 Present work

Electrochemically prepared $MoO_3$ nanoparticles were tested on the synthesis of (1E,4E)-1,5-diphenylpenta-1,4-dien-3-one derivatives (Scheme-5). The short reaction time, clean reaction condition, consistent yield and minimum environmental effect are important features of the reaction.

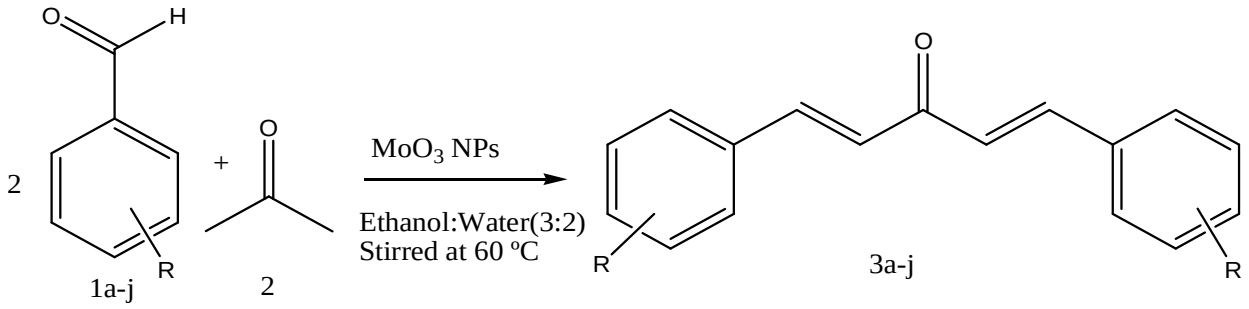


**Scheme 5**

### 3.6.4 Experimental

The melting points of compounds were taken in an open capillary in a paraffin bath. IR spectra were recorded on a Jasco FTIR-4100 spectrophotometer. $^{1}H$ NMR spectra were recorded on an 400 MHz FT-NMR spectrometer in DMSO as a solvent and chemical shift values were recorded in units δ (ppm) relative to tetramethylsilane ($Me_4Si$) as an internal standard.

**General procedure**

A mixture of aromatic aldehyde (10 mmol), acetone (5 mmol) and $MoO_3$ nanoparticles (60mg) in 5 ml ethanol: water (3:2) was stirred at 60ºC till the completion of reaction monitored by TLC. After cooling, solid product obtained was filtered, washed with water and recrystallized with ethanol to obtain pure product. The hot reaction mixture was centrifuged for recovery of catalyst. The recovered catalyst was washed with ethanol, dried and reused three times in same reaction.

### 3.6.5 Spectral data of representative compound

1) Bis (4-$CH_3$ Phenyl) Methelidine 3e: FTIR ( KBr in $cm^{-1}$): 2913, 1666, 1617, 1581, 1507, 1410, 1180, 10923, 964, 887, 842 and 726 $cm^{-1}$. $^{1}$HNMR-(400 MHz, $CDCl_3$, δ ppm) 2.38(s, 6H, aliphatic), 7.05(d, 2H, CH of Ar), 7.21(d, 4H, Ch of Ar), 7.51( D, 4H, Ch of Ar), 7.77 (d, 2H, Ch of Ar); $^{13}$C NMR( 100 MHz $CDCl_3$, δ ppm) 21.54 ( CH aliphatic), 124.61 ( CH of Ar), 128.41 ( CH of Ar), 129.72(Ch of Ar), 132.15 ( C of Ar), 140.96 ( C of Ar), 143.16 (CH of aliphatic ) 189.06 ( C of C=O).

2) Bis( 2-Cl Phenyl) Methelidine:$^{1}$HNMR-(400 MHz, $CDCl_3$, δ ppm) 7.06 (d, 2H, aliphatic C=C), 7.26-733 (m, 4H, CH of Ar), 8.13(d, 2H, aliphatic C=C)

### 3.6.6 Result discussion

We reveal herein for the first time, the $MoO_3$ nanoparticles catalyzed condensation of acetone with a variety of aromatic aldehydes by simple stirring at 60ºC. In the present work, attempt is made to optimize the reaction condition by using 4 nitro-benzaldehyde and acetone as a model reaction at different solvents and amount of catalyst used. From Table 3.6.1 it can be seen that the best ratio of $MoO_3$ nanoparticles to starting material is 60mg. There is considerable increase in the yield of product when the concentration of $MoO_3$ nanoparticles increases from 10mg to 60mg. But when we increased catalyst quantity to 70 mg there is no considerable change in reaction time and yield of product

**Table 3.6.1.** Screening of catalyst $MoO_3$ for the synthesis of (1E,4E)-1,5-diphenylpenta-1,4-dien-3-one

| Entry[a] | Catalyst amount(mg) | Time(min) | Yield[b](%) |
|---|---|---|---|
| 1 | 10 | 240 | Trace |
| 2 | 20 | 160 | 36 |
| 3 | 40 | 120 | 66 |
| 4 | 50 | 90 | 92 |
| 5 | 60 | 90 | 94 |
| 6 | 70 | 90 | 95 |

[a]Reaction condition: 4 nitrobenzaldehyde (2 mmol), acetone (1 mmol), and 60mg of $MoO_3$ NPs stirred at 60°C.
[b] Isolated yield

In this study, the effect of different solvent was investigated and given in Table 3.6.2. The choice of solvent proved critical. We observed that polar solvents such as methanol, ethanol, acetonitrile, afford better yield than nonpolar ones and mixture of water(2ml) & ethanol(3ml) is most effective solvent affording maximum yield of product.

**Table 3.6.2** Optimization of solvent in synthesis of (1E,4E)-1,5-diphenylpenta-1,4-dien-3-one

| [a]Entry | Solvent | Time(hrs) | Yield[a](%) |
|---|---|---|---|
| 1 | ACN | 3 | 54 |
| 2 | Toluene | 3 | 32 |
| 3 | THF | 3 | 35 |
| 4 | Methanol | 3 | 62 |
| 5 | Ethanol | 3 | 76 |
| 6 | Ethanol:water (3:2) | 2 | 94 |

[a]Reaction condition: 4 nitro benzaldehyde (2mmol), acetone (1mmol), and 60mg of $MoO_3$ NPs stirred at 60°C.
[a] Isolated yield

After optimizing the conditions, the generality of this method was examined by the reaction of cyclohexanone with several aldehydes bearing electron withdrawing groups (such as nitro, chloro, bromo, fluoro, and hydroxyl) and electron donating groups (such as methyl, methoxy). The entire product reacted in a similar manner producing moderate to good yield of expected product. The para substituted aromatic aldehyde reacted in a shorter reaction time as compared with ortho and meta substituted aromatic aldehyde in Table 3.6.3.

**Table3.6.3.** Synthesis of (1E,4E)-1,5-diphenylpenta-1,4-dien-3-one derivatives using $MoO_3$NPs catalyst

| Products[a] | R | Time (min) | Yield[b] (%) | Melting point (°C) | |
|---|---|---|---|---|---|
| | | | | Found | Reported |
| 3a | H | 120 | 91 | 110-111 | 112-113 |
| 3b | 4-Cl | 95 | 95 | 190-190 | 192-194 |
| 3c | 2-Cl | 130 | 92 | 125-126 | 125-126 |
| 3d | 3-$NO_2$ | 130 | 95 | 238-239 | 238-240 |
| 3e | 4-$CH_3$ | 100 | 90 | 176-177 | 175 |
| 3f | 4-OMe | 95 | 93 | 127-129 | 129-130 |
| 3g | Ar-CH=CH | 100 | 94 | 142-143 | 142-144 |
| 3h | 4-F | 105 | 94 | 91-92 | 92-94 |
| 3i | 4-Br | 110 | 92 | 212-213 | 213-214 |
| 3j | 2,4$Cl_2$ | 120 | 88 | 168-169 | 168-170 |

[a]Reaction condition: aldehyde (2mmol), acetone(1mmol) and 60mg of $MoO_3$ nanoparticles stirred at 60°C.
[b] Isolated yield.

In this study, the catalyst was recovered and reused. The catalyst was recovered by a simple work-up using centrifugation, and then it was washed with ethanol and reused. The catalyst was removed in excellent yields and was used in mentioned reaction for three times, the observation Table 3.6.4 revealed that as the number of the recycle of catalyst increases the activity decreases.

**Table 3.6.4.** Reusability of $MoO_3$NPs in synthesis of (1E,4E)-1,5-diphenylpenta-1,4-dien-3-one

| **Cycle** | **Fresh** | **First** | **Second** | **Third** |
|---|---|---|---|---|
| [a]Yield (%)[b] | 94 | 91 | 89 | 84 |

[a]Reaction condition: aldehyde (2mmol), acetone(1mmol) and 60mg of $MoO_3$ nanoparticles stirred at 60°C.
[b] Isolated yield.

### 3.6.7 Conclusion

$MoO_3$ nanoparticles are inexpensive and efficient reusable catalyst for the synthesis of (1E,4E)-1,5-diphenylpenta-1,4-dien-3-one derivatives. The advantages offered by this method are simple workup, short reaction times, ease of product isolation and high yields. We believed that this method is a useful addition to the present methodology for the synthesis of (1E,4E)-1,5-diphenylpenta-1,4-dien-3-one derivatives.

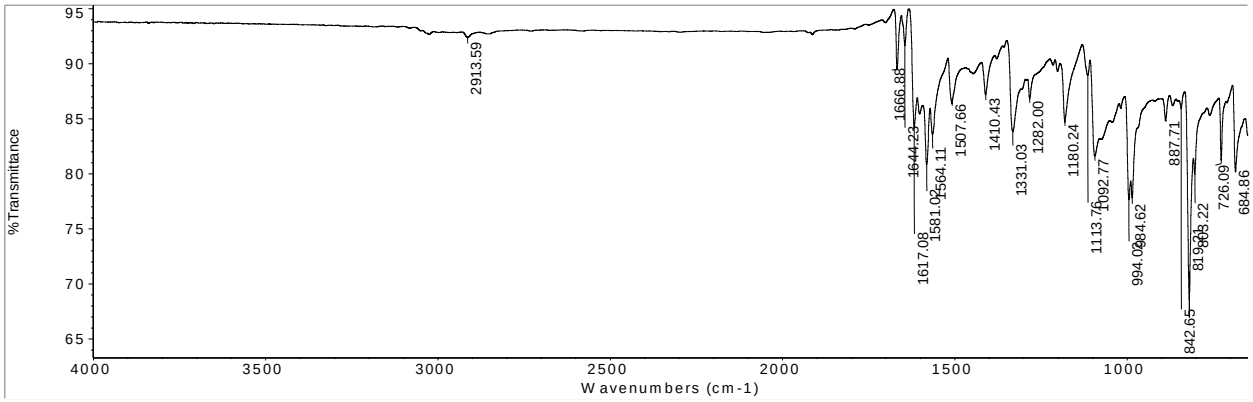


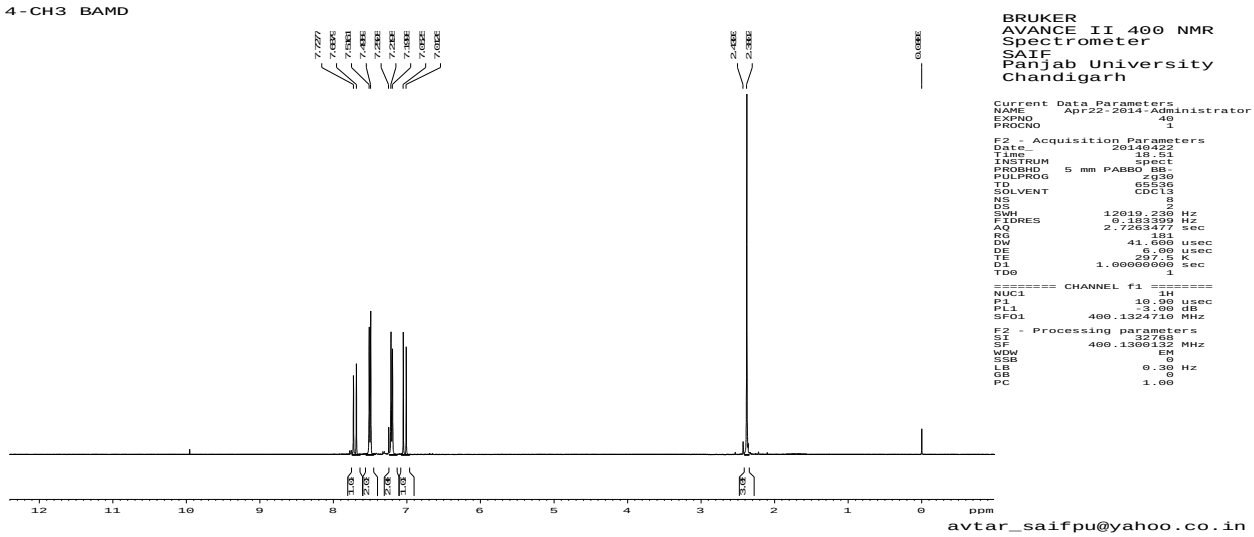


avtar_saifpu@yahoo.co.in

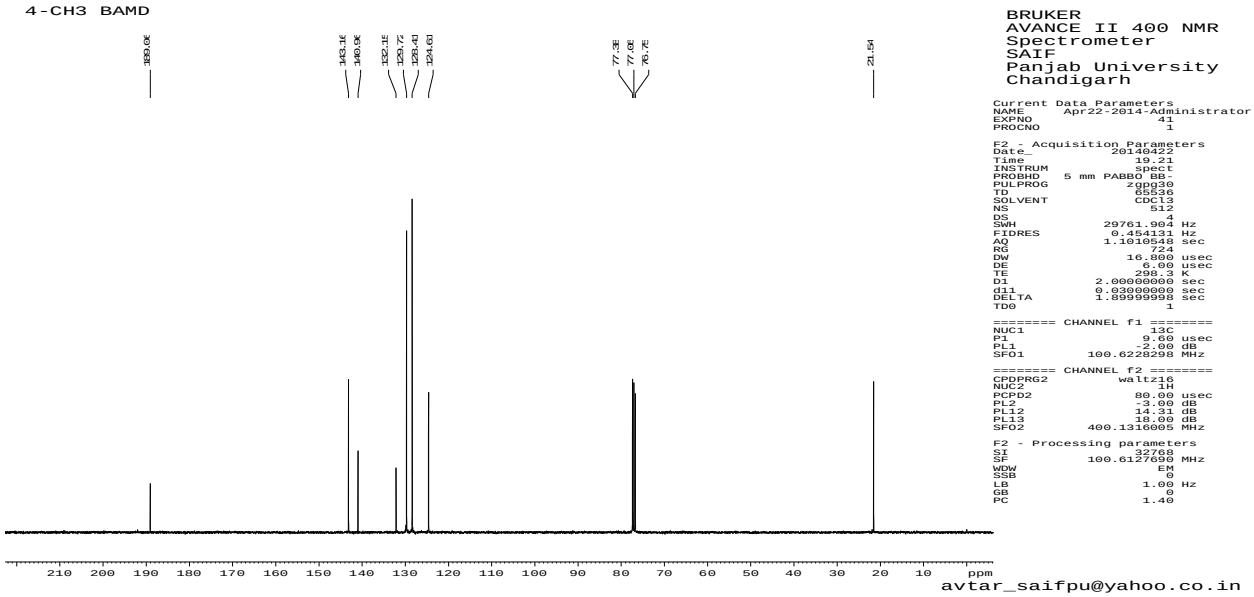


avtar_saifpu@yahoo.co.in

## 3.7 Green synthesis of 2-phenylbenzo[d]thiazole derivatives catalyzed by $MoO_3$ nanorods

### 3.7.1 Introduction

2-Aryl benzothiazole and their derivatives exhibit a wide range of biological properties which have led to continuous interest in the field of medicinal chemistry. 2-Aryl benzothiazole exhibit antimicrobial [138-139], antibiotic [140], antiviral [141], anti-inflammatory [142], antifungal [143], antitumor [144], anticonvulsant [145], antiparasitic [146], antagonists[147] and treatment of Alzheimer diseases [148]. They exhibit nanomolar inhibitory activity against human cancer cell [149] and several enzymes such as aldoses reducates [150], $H^+$-$K^+$ ATPase [151], protease [152] and carbonic anhydrase [153]. Benzothiazoles also exhibit physiological activities like H37Rv inhibitory [154], elastase inhibitory [155] and cytotoxicity towards $P_{338}$ cells [156].

### 3.7.2 Literature review

The synthesis of 2-aryl benzothiazole involves condensation of 2-aminothiophenol with aldehyde, acid chloride, carboxylic acid, ester, aryl bromide and coupling with aryl boronic acid. The condensation of 2-aminothiophenol and aldehyde have been reported by using various catalysts such as $NiO_2$ [157], Cu NPs [158], CuCl [159], $MnO_2/SiO_2$ [160] and ceric ammonium nitrate etc [161].

However most of these procedures of synthesis of benzothiazoles are associated with some disadvantages such as tedious reaction, expensive catalyst, multistage processes and loss of catalyst, the use of hazardous and carcinogenic solvents like nitrobenzene & dioxane which are harmful to environment and also to the human. Therefore, it is necessary to study the reaction by some green methods which is efficient and simple. The present study involves synthesis of 2-aryl benzothiazole by using $MoO_3$ nanorods, which is efficient simple environmentally begin.

### 3.7.3 Present work

Electrochemically prepared $MoO_3$ nanoparticles were tested on the synthesis of 2-aryl benzothiazole derivatives (Scheme-6). The short reaction time, clean reaction condition, consistent yield and minimum environmental effect were important features of the reaction.

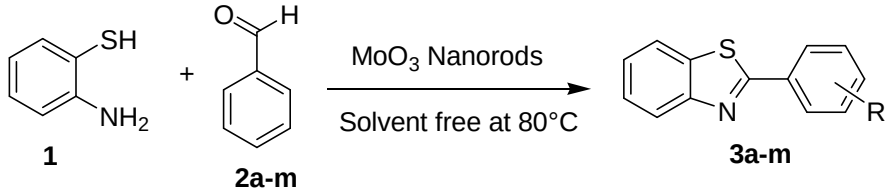


**1** **2a-m** **3a-m**

**Scheme 6**

### 3.7.4 Experimental

The melting points of compounds were taken in an open capillary in a paraffin bath. IR spectra were recorded on a Jasco FTIR-4100 spectrophotometer. $^1$H NMR spectra were recorded on an 400 MHz FT-NMR spectrometer in $CDCl_3$ as a solvent and chemical shift values were recorded in units δ (ppm) relative to tetramethylsilane ($Me_4Si$) as an internal standard.°

**General procedure**

A mixture of 2-aminothiophenol (1mmol), aromatic aldehyde (1 mmol) & $MoO_3$ nanorods (100 mg) was stirred at 80°C for 2 hrs to obtain 2-aryl benzothiazole crude product. The progress of reaction was monitored by TLC. After completion of reaction, the crude product was dissolved by adding ethanol and the $MoO_3$ nanorods were separated by centrifuging, followed by decantation. $MoO_3$ nanorods were dried in vacuum desiccators and crude product recrystallized in ethanol. The recrystallized product analysis by FTIR, $^1$H NMR and $^{13}$C NMR spectra was recorded.

### 3.7.5 Spectral data of representative compound

3a) 2-Aryl benzothiazole FTIR (KBr, $cm^{-1}$): 3062, 1590, 1556, 1510, 1435, 1245, 960, 766 $cm^{-1}$ $^1$H NMR (400.13 MHz, $CDCl_3$, δ ppm): 7.34 (t, 1H, CH of Ar), 7.88(d, 2H, CH of Ar), 8.06(d, 1H CH of Ar), 8.07(d, 1H, CH of Ar), 8.09(d, 1H, CH of Ar).$^{13}$C NMR (100.61 MHz, $CDCl_3$, δ, ppm): 121.89(CH of Ar), 121.91(CH of Ar), 125.20(CH of Ar), 125.90(CH of Ar), 127.51(2CH of Ar), 128.80(CH of Ar), 129.32(2CH of Ar), 133.50(C of Ar), 135.80, 154.42), 166.60.

3b) 2(4-Bromo -aryl) benzothiazole FTIR (KBr, $cm^{-1}$): 3056, 1582, 1545, 1505, 1474, 1247, 969, 854, 751 $cm^{-1}$;$^1$H NMR (400.13 MHz, $CDCl_3$, δ ppm): 7.38(t, 1H, CH of Ar), 7.48(t, 1H, CH of Ar), 7.60(d, 2H, CH of Ar), 7.88(d, 1H, CH of Ar), 7.90(d, 2H, CH of Ar), 8.06(d, 1H, CH of Ar); $^{13}$C NMR (100.61 MHz, $CDCl_3$ δ ppm): 121.68(CH of Ar), 123.34(CH of Ar), 125.43(C-N), 125(CH of Ar), 126.52(CH of Ar), 128.91(2 CH of Ar), 132.56(2 CH of Ar), 135.06, 154.9, 166.69.

3c) 2(4- Chloro -aryl) benzothiazole; FTIR (KBr, $cm^{-1}$): 3056, 1582, 1545, 1505, 1474, 1247, 969, 854, 751 $cm^{-1}$; $^1$H NMR (400.13 MHz, $CDCl_3$, δ ppm): 7.38(t, 1H, CH of Ar), 7.48(t, 1H, CH of Ar), 7.60(d, 2H, CH of Ar), 7.88(d, 1H, CH of Ar), 7.90(d, 2H, CH of Ar), 8.06(d, 1H, CH of Ar); $^{13}$C NMR (100.61 MHz, $CDCl_3$ δ ppm): 121.68(CH of Ar), 123.34(CH of Ar),

125.43(C-N), 125(CH of Ar), 126.52(CH of Ar), 128.91(2 CH of Ar), 132.56(2 CH of Ar), 135.06, 154.9, 166.69.

### 3.7.6 Result discussion

We report here a very simple process for the synthesis of 2- aryl benzothiazoles by condensation of 2-aminothiophenol with aromatic aldehyde under solvent free conditions catalyzed by $MoO_3$ nanorods. In the present work, an attempt has been made to optimize the reaction conditions by using 2-aminothiophenol (1mmol) **1** and 4-bromo benzaldehyde (1 mmol) **2b** as model reaction at different solvents and amount of catalyst used. In order to investigate the best results in terms of yield & reaction time, we have examined the efficiency of different reaction media and the amount of catalyst required. From Table 3.7.1, it can be seen that loading of 100mg of $MoO_3$ nanorod catalyst were adequate for smooth condensation of 2 aminothiophenol and 4-bromobenzaldehyde under solvent free condition at 80°C. There is considerable increase in the yield of product when amount of catalyst is increased from 50 mg to 100 mg; above 100 mg, no considerable change in reaction time and yield of the product was observed.

**Table 3.7.1** Screening of catalyst $MoO_3$ nanorods for the synthesis of 2- aryl benzothiazoles.

| Entry[a] | Catalyst Amount (mg) | Time (Min) | Yield[b] (%) |
|---|---|---|---|
| 1 | 00 | 180 | Trace |
| 2 | 40 | 160 | 35 |
| 3 | 60 | 120 | 64 |
| 4 | 80 | 90 | 78 |
| 5 | 100 | 45 | 95 |
| 6 | 120 | 45 | 95 |

[a]Reaction condition: 4-bromobenzaldehyde(1mmol), 2-amino thiophenol(1mmol),$MoO_3$ nanorods
[b]Isolated Yield

The catalyst was recovered by simple work-up using centrifugation method, washed with ethanol and reused for three successive reactions. The corresponding yield for each cycle was mentioned in Table 3.7.2.

Table 3.7.2 Reusability of catalyst $MoO_3$ nanorods for synthesis of 2- aryl benzothiazoles.

| Entry[a] | 1 | 2 | 3 | 4 |
|---|---|---|---|---|
| No. of recycle | Fresh | I | II | III |
| Yield[b] (%) | 95 | 94 | 92 | 89 |

[a]Reaction condition: 4-bromobenzaldehyde(1mmol), 2-amino thiophenol(1mmol), $MoO_3$ nanorods
[b]Isolated Yield

Under optimization reaction condition, we obtained 95% yield of 2(4-bromo-aryl) benzothiazole within 40 mins. In Table 3.7.3, the reaction time & the product yield depends on the substituents introduced on substrates. For instance, the condensation of 2-aminothiophenol having strong electron withdrawing groups (F, Cl, Br, $NO_2$, OH) in para position gave the desired product with good yield and shorter reaction time than meta substituted product and electron donor groups($CH_3$, $OCH_3$).

Table 3.7.3 Synthesis of 2-aryl benzathiazole derivative using $MoO_3$ nanorods

| Products[a] | R | Time (min) | Yield[b](%) | Melting point(°C) | |
|---|---|---|---|---|---|
| | | | | Found | Reported |
| 3a | H | 70 | 88 | 112-114 | 112-114 |
| 3b | 4-Br | 45 | 95 | 131-132 | 132 |
| 3c | 4-Cl | 50 | 92 | 114-116 | 115-117 |
| 3d | 4-$NO_2$ | 50 | 94 | 180-182 | 181-182 |
| 3e | 4-$CH_3$ | 100 | 85 | 82-84 | 84-86 |
| 3f | 4-$OCH_3$ | 110 | 86 | 120-122 | 120-121 |
| 3g | 4-OH | 60 | 90 | 224-227 | 225-227 |
| 3h | 4-F | 60 | 80 | 100-102 | 101-102 |
| 3i | 3-$NO_2$ | 80 | 87 | 180-182 | 181-182 |
| 3k | 2-OH | 90 | 88 | 128-129 | 129-130 |
| 3l | 2-$OCH_3$ | 80 | 90 | 103-104 | 103-105 |
| 3m | 2-Furfurald | 100 | 85 | 100-102 | 103-104 |

[a]Reaction condition: 4-bromobenzaldehyde(1mmol), 2-amino thiophenol(1mmol), $MoO_3$ nanorods
[b]Isolated Yield

### 3.7.7 Conclusion

We have developed efficient $MoO_3$ nanorods catalysts for the synthesis of 2-aryl benzothiazole with high yield of product in short reaction time and very less amount of catalyst. This catalyst showed excellent activity during four consecutive runs without appreciable loss of activity. Furthermore, this method is of interest in the context to environmentally greener and safer processes.

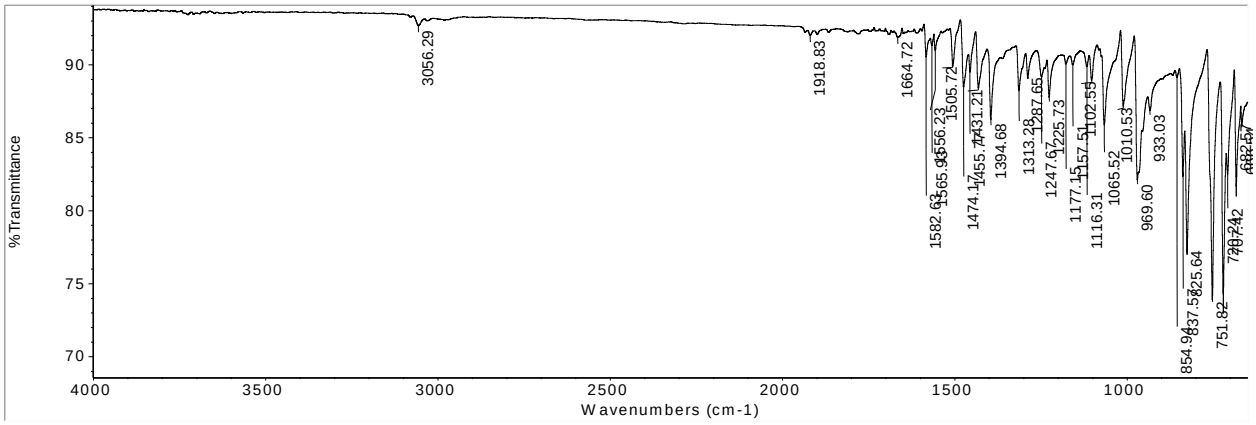


4-Br-BTZ

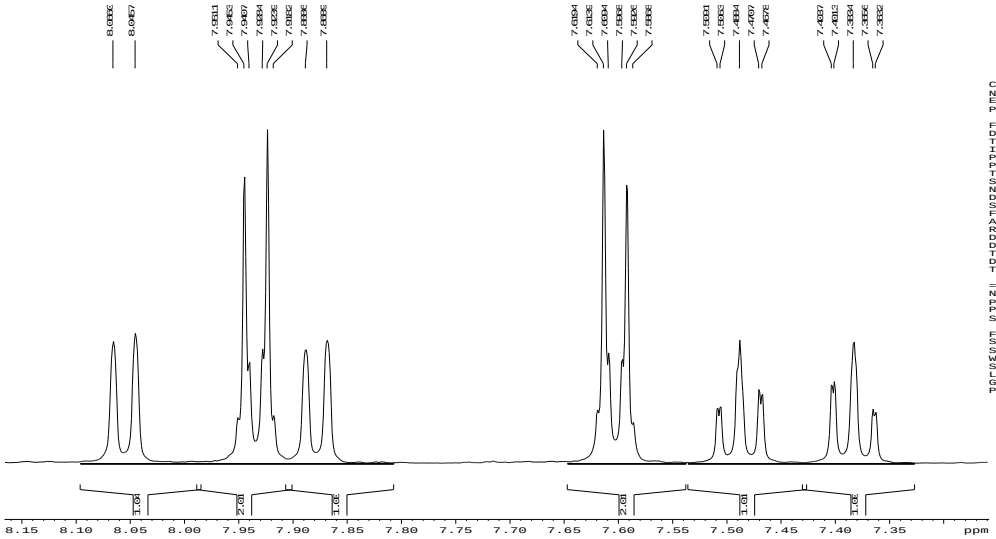


BRUKER
AVANCE II 400 NMR
Spectrometer
SAIF
Panjab University
Chandigarh

```
Current Data Parameters
NAME      Apr22-2014-Administrator
EXPNO                 20
PROCNO                 1

F2 - Acquisition Parameters
Date_              20140422
Time                 18.27
INSTRUM              spect
PROBHD   5 mm PABBO BB-
PULPROG              zg30
TD                  65536
SOLVENT             CDCl3
NS                      8
DS                      2
SWH              12019.230 Hz
FIDRES           0.183399 Hz
AQ               2.7263477 sec
RG                    575
DW                 41.600 usec
DE                  6.00 usec
TE                 297.0 K
D1              1.00000000 sec
TD0                     1

======== CHANNEL f1 ========
NUC1                   1H
P1                  10.90 usec
PL1                 -3.00 dB
SFO1          400.1324710 MHz

F2 - Processing parameters
SI                  32768
SF            400.1300138 MHz
WDW                    EM
SSB                     0
LB                   0.30 Hz
GB                      0
PC                   1.00
```

avtar_saifpu@yahoo.co.in

4-Br-BTZ

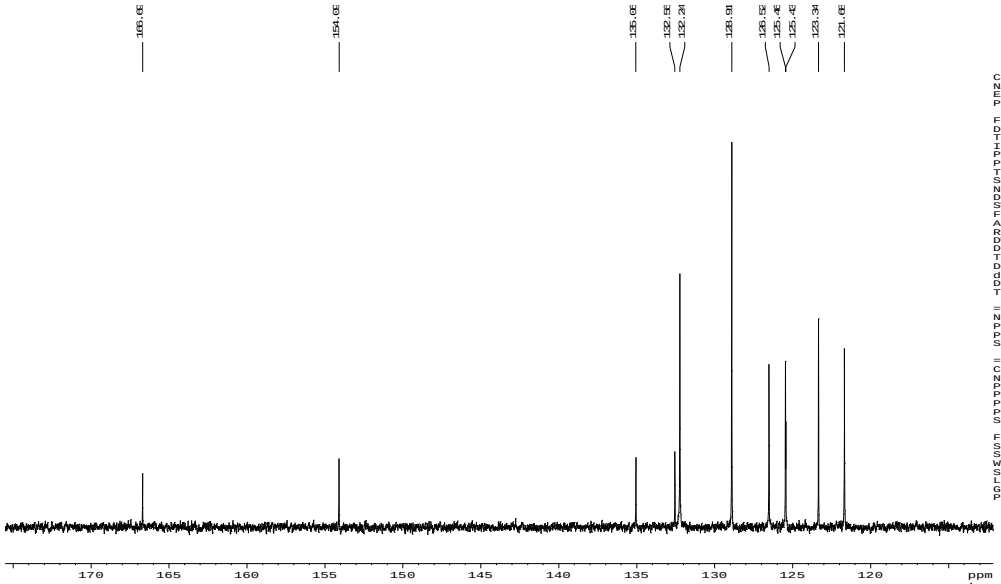


BRUKER
AVANCE II 400 NMR
Spectrometer
SAIF
Panjab University
Chandigarh

```
Current Data Parameters
NAME      Apr22-2014-Administrator
EXPNO                 21
PROCNO                 1

F2 - Acquisition Parameters
Date_              20140422
Time                 18.34
INSTRUM              spect
PROBHD   5 mm PABBO BB-
PULPROG            zgpg30
TD                  65536
SOLVENT             CDCl3
NS                    110
DS                      4
SWH              29761.904 Hz
FIDRES           0.454131 Hz
AQ               1.1010548 sec
RG                    645
DW                 16.800 usec
DE                  6.00 usec
TE                 297.4 K
D1              2.00000000 sec
d11             0.03000000 sec
DELTA           1.89999998 sec
TD0                     1

======== CHANNEL f1 ========
NUC1                  13C
P1                   9.60 usec
PL1                 -2.00 dB
SFO1          100.6228298 MHz

======== CHANNEL f2 ========
CPDPRG2           waltz16
NUC2                   1H
PCPD2               80.00 usec
PL2                 -3.00 dB
PL12                14.31 dB
PL13                18.00 dB
SFO2          400.1316005 MHz

F2 - Processing parameters
SI                  32768
SF            100.6127690 MHz
WDW                    EM
SSB                     0
LB                   1.00 Hz
GB                      0
PC                   1.40
```

avtar_saifpu@yahoo.co.in

## 3.8 Synthesis of 2-phenylbenzo[d]oxazole derivatives catalyzed by $MoO_3$ nanoparticles

### 3.8.1 Introduction

Benzoxazoles are an important class of molecules and are common heterocyclic scaffold in biologically active and medicinally significant compounds. Benzoxazoles are found in a variety of natural products [162] and are important targets in drug discovery [163]. Also, much attention has been paid to benzoxazoles because they have a number of applications such as photoluminescents [164], whitening agents [165] and in dye lasers [165]. They are also used as intermediates for several therapeutic materials [167-168]. Pyrazines are found in the luminescent chromophores or certain marine organisms [169] in cephalostatins isolated from Cephalodiscus gilehrist, which are powerful anticancer agents [170] in the fungal metabolite aspergillic acid [171] and in food in the form of potent flavor compounds [172]. They have been also used as ligands in asymmetric synthesis [173]. Benzoxazole exhibites various pharmaceutical properties such as antiviral [174], antibiotic [175], antimicrobial [176], antitumor [177] and anti-inflammatory [178] activities.

### 3.8.2 Literature review

The classical approach for the synthesis of benzoxazoles involves (i) coupling of carboxylic acids with 2-aminophenols by dehydration catalyzed by strong acid [179], orthoesters [180], acid chlorides [181], nitriles [182], amides [183], aldehydes [184]and esters [185] with o-Aminophenol and (ii) the oxidative cyclization of phenolic Schiff's bases derived from the condensation of 2-aminophenols and aldehydes using various oxidants such as $PhI(OAc)_2$ [186], $Mn(OAc)_3$ [187], $ThClO_4$ [188], $(MnO_4)_2$ [189], $NiO_2$ [190], $Pb(OAc)_4$ [191], DDQ [192], NiS [193], Cu-np [194], aerial oxidation in the presence of activated carbon (Darco KB) [195], CuCl [196] and Pd/Pt-C [197]. Other synthetic routes for benzoxazole include microwaveassisted reaction of *N*-acyl-aminophenol [198], iron catalysed intramolecular *O*-arylation of 2-haloacetanilides [199] and cyclization of phenolic Schiff base under UV irradiation [200]. Apart from these methodologies, there have been many precedents for the synthesis of 2-aryl benzothiazoles and benzoxazoles via palladium catalysed cross-coupling reactions disclosed in the literature [201].

However, most of these procedures have some drawbacks such as long reaction times, low yield of products and the use of expensive, toxic or non-reusable catalysts, high

temperatures, harsh reaction conditions and use of toxic solvents and/or co-occurrence of several side reactions. In some cases more than one step is required for the synthesis of these heterocycles. Therefore, it is necessary to find a better catalyst for the synthesis of benzoxazoles in terms of operational simplicity, non-toxicity, reusability and environmental and economical acceptability. Herein we report a new and efficient route for the one-pot synthesis of substituted benzoxazoles from substituted benzaldehydes and 2-aminophenoles. When substituted benzaldehyde and 2-aminophenole is treated with $MoO_3$ nanorods, rapid and efficient oxidative cyclisation takes place as shown in Scheme-7. Easy handling, cheapness, efficiency, non-toxicity make this catalyst eco-friendly, synthetically acceptable and economically viable.

### 3.8.3 Present work

Electrochemically prepared $MoO_3$ nanoparticles were tested on the synthesis of 2-aryl benzoxazole derivatives (Scheme-7). The short reaction time, clean reaction condition, consistent yield and minimum environmental effect were important features of the reaction.

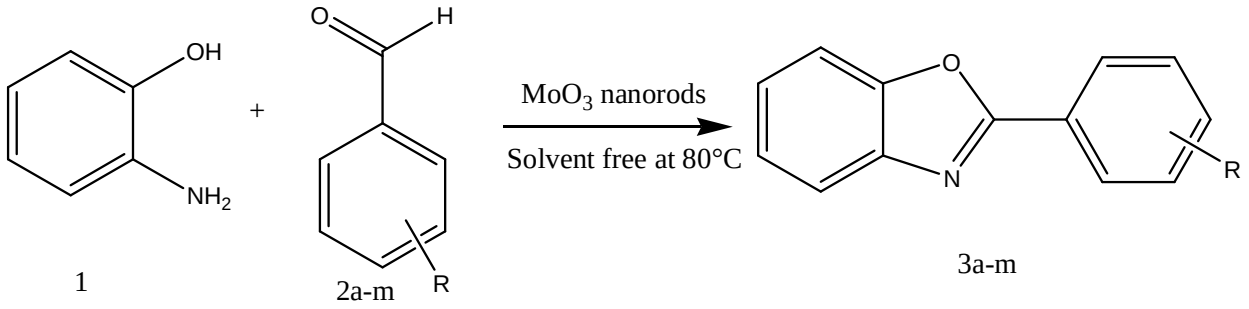


**Scheme -7**

### 3.8.4 Experimental

The melting points of compounds were taken in an open capillary in a paraffin bath. IR spectra were recorded on a Jasco FTIR-4100 spectrophotometer. $^1$H NMR spectra were recorded on an 400 MHz FT-NMR spectrometer in DMSO as a solvent and chemical shift values were recorded in units δ (ppm) relative to tetramethylsilane ($Me_4Si$) as an internal standard.

**General procedure**

A mixture of 2-aminophenol (1mmol), aromatic aldehyde (1 mmol) & $MoO_3$ nanoparticles (100 mg) was stirred at 60°C for 2 hrs to obtain 2-aryl benzoxazole crude product. The progress of reaction was monitored by TLC. After completion of reaction, the crude product was dissolved by adding ethanol and the $MoO_3$ nanoparticles were separated by centrifuging, followed by decantation. $MoO_3$ nanoparticles were dried in vacuum desiccators and crude product

recrystallized in ethanol. The recrystallized product analysis by FTIR, $^{1}H$ NMR and $^{13}C$ NMR spectra was recorded.

### 3.8.5 Spectral data of representative compound

2-(4-Bromophenyl)benzo[d]oxazole: IR (KBr): 1581, 1501,1269, 1052, 944, 830, 799 $cm^{-1}$

$^{1}H$ NMR (400 MHz,CDCl3)δH 7.30–7.37 (m, 2H, Ar-H); 7.50–7.55 (m, 1H, Ar-H); 7.60–7.65 (m, 2H, Ar-H); 7.70–7.75 (m, 1H, Ar-H); 8.05–8.10 (m, 2H, Ar-H).$^{13}C$ NMR (400 MHz,$CDCl_3$ ) δC110.5, 120.0, 124.6, 125.5, 126.1, 126.3,128.9, 132.3, 142.0, 150.5, 161.9.

### 3.8.6 Result discussion

We report here a very simple process for the synthesis of 2- aryl benzoxazoles by condensation of 2-aminophenol with aromatic aldehyde under solvent free conditions catalyzed by $MoO_3$ nanoparticles. In the present work, an attempt has been made to optimize the reaction conditions by using 2-aminophenol (1mmol) **1** and 4-bromo benzaldehyde(1 mmol) **2b** as model reaction at different solvents and amount of catalyst used. In order to investigate the best results in terms of yield & reaction time, we have examined the efficiency of different reaction media and the amount of catalyst required. From Table 3.8.1, it can be seen that loading of 100mg of $MoO_3$ nanoparticles catalyst were adequate for smooth condensation of 2-aminophenol and 4-bromobenzaldehyde under solvent free condition at 60°C. There is considerable increase in the yield of product when amount of catalyst is increased from 50 mg to 100 mg; above 100 mg, no considerable change in reaction time and yield of the product was observed.

Table 3.8.1 Screening of catalyst $MoO_3$ nanoparticles amount for the synthesis of 3b.

| Entry[a] | Catalyst Amount (mg) | Time (Min) | Yield[b] (%) |
|---|---|---|---|
| 1 | 00 | 180 | Trace |
| 2 | 40 | 150 | 32 |
| 3 | 60 | 120 | 66 |
| 4 | 80 | 90 | 77 |
| 5 | 100 | 50 | 96 |
| 6 | 120 | 50 | 95 |

[a]Reaction condition: 4-bromobenzaldehyde(1mmol), 2-amino phenol(1mmol),$MoO_3$ nanoparticles
[b]Isolated Yield

The catalyst was recovered by simple work-up using centrifugation method, washed with ethanol and reused for three successive reactions. The corresponding yield for each cycle was mentioned in Table 3.8.2.

Table 3.8.2 Reusability of catalyst $MoO_3$ nanoparticles

| Entry[a] | 1 | 2 | 3 | 4 |
|---|---|---|---|---|
| No. of recycle | Fresh | I | II | III |
| Yield[b] (%) | 96 | 94 | 91 | 89 |

[a]Reaction condition: 4-bromobenzaldehyde(1mmol), 2-aminophenol(1mmol), $MoO_3$ nanoparticles
[b]Isolated Yield

Under optimization reaction condition, we obtained 95% yield of 2(4-bromo-aryl) benzoxazole within 40 mins. In Table 3.8.3, the reaction time & the product yield depends on the substituents introduced on substrates. For instance, the condensation of 2-aminophenol having strong electron withdrawing groups (F, Cl, Br, $NO_2$, OH) in para position gave the desired product with good yield and shorter reaction time than meta substituted product and electron donor groups($CH_3$, $OCH_3$).

Table 3.8.3 Synthesis of 2-aryl benzathiazole derivative using $MoO_3$ nanoparticles

| Products[a] | R | Time (min) | Yield[b](%) | Melting point(°C) | |
|---|---|---|---|---|---|
| | | | | Found | Reported |
| 3a | H | 70 | 88 | 101 | 102 |
| 3b | 4-Br | 45 | 95 | 131-132 | 132 |
| 3c | 4-Cl | 50 | 92 | 146 | 147 |
| 3d | 4-$NO_2$ | 50 | 94 | 266-267 | 266-268 |
| 3e | 4-$CH_3$ | 100 | 85 | 113 | 113-114 |
| 3f | 4-$OCH_3$ | 110 | 86 | 102 | 101-103 |
| 3g | 4-OH | 60 | 90 | 224-227 | 225-227 |
| 3h | 4-F | 60 | 80 | 100-102 | 101-102 |
| 3i | 3-$NO_2$ | 80 | 87 | 241 | 242-243 |
| 3k | 2-OH | 90 | 88 | 128-129 | 129-130 |

[a]Reaction condition: 4-bromobenzaldehyde(1mmol), 2-aminophenol(1mmol), $MoO_3$ nanorods
[b]Isolated Yield

### 3.8.7 Conclusion

We have developed efficient $MoO_3$ nanoparticles catalysts for the synthesis of 2-aryl benzoxazole with high yield of product in short reaction time and very less amount of catalyst. This catalyst showed excellent activity during four consecutive runs without appreciable loss of activity. Furthermore, this method is of interest in the context to environmentally greener and safer processes.

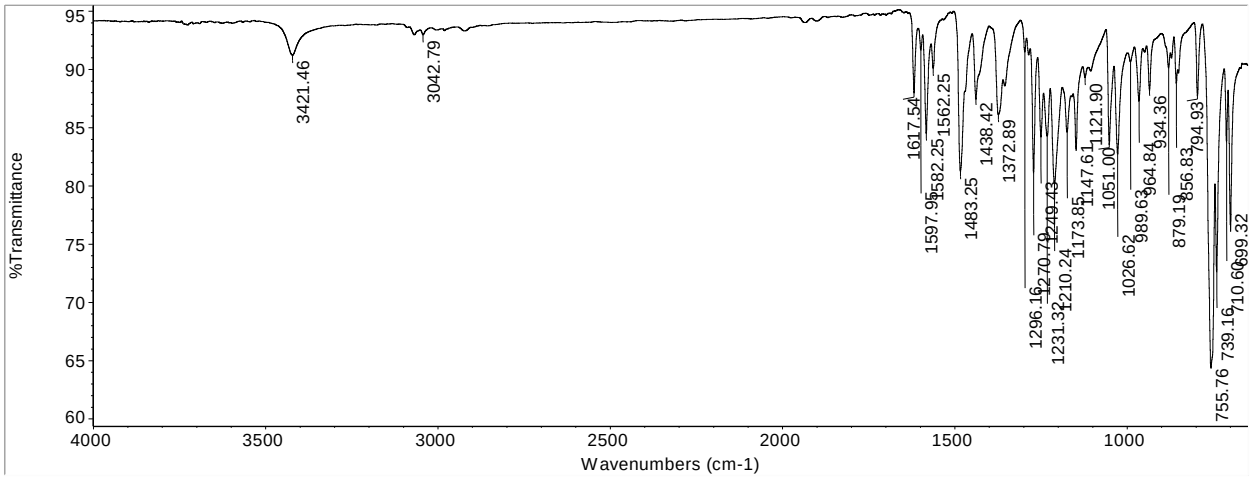


4-Br-BOZ

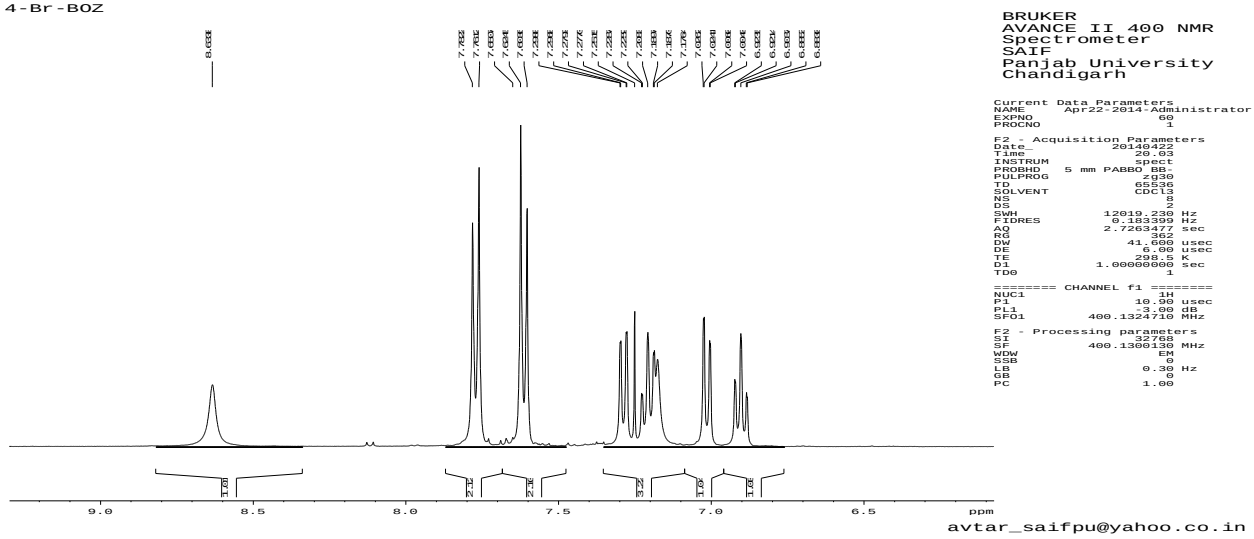


BRUKER
AVANCE II 400 NMR
Spectrometer
SAIF
Panjab University
Chandigarh

```
Current Data Parameters
NAME          Apr22-2014-Administrator
EXPNO                60
PROCNO                1

F2 - Acquisition Parameters
Date_          20140422
Time              20.03
INSTRUM           spect
PROBHD    5 mm PABBO BB-
PULPROG           zg30
TD                65536
SOLVENT           CDCl3
NS                    8
DS                    2
SWH           12019.230 Hz
FIDRES            0.183399 Hz
AQ            2.7263477 sec
RG                  362
DW               41.600 usec
DE                6.00 usec
TE               298.5 K
D1            1.00000000 sec
TD0                   1

======== CHANNEL f1 ========
NUC1                 1H
P1                10.90 usec
PL1               -3.00 dB
SFO1         400.1324710 MHz

F2 - Processing parameters
SI                32768
SF           400.1300130 MHz
WDW                  EM
SSB                   0
LB                 0.30 Hz
GB                    0
PC                 1.00
```

avtar_saifpu@yahoo.co.in

4-Br-BOZ

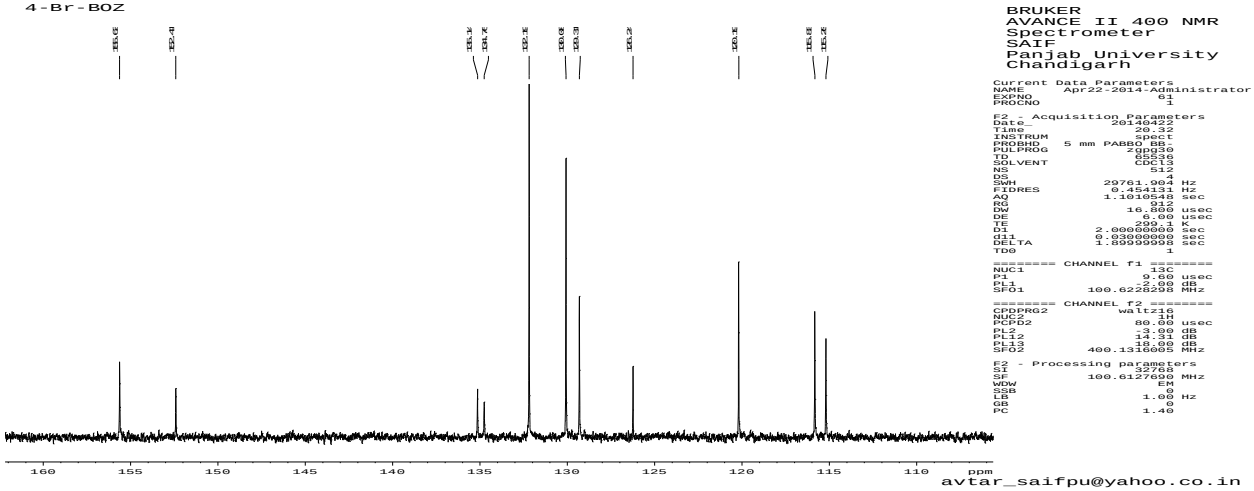


BRUKER
AVANCE II 400 NMR
Spectrometer
SAIF
Panjab University
Chandigarh

```
Current Data Parameters
NAME          Apr22-2014-Administrator
EXPNO                61
PROCNO                1

F2 - Acquisition Parameters
Date_          20140422
Time              20.32
INSTRUM           spect
PROBHD    5 mm PABBO BB-
PULPROG         2qpg30
TD                65536
SOLVENT           CDCl3
NS                  512
DS                    4
SWH           29761.904 Hz
FIDRES            0.454131 Hz
AQ            1.1010548 sec
RG                  912
DW               16.800 usec
DE                6.00 usec
TE               299.1 K
D1            2.00000000 sec
d11           0.03000000 sec
DELTA         1.89999998 sec
TD0                   1

======== CHANNEL f1 ========
NUC1                 13C
P1                 9.60 usec
PL1               -2.00 dB
SFO1         100.6228298 MHz

======== CHANNEL f2 ========
CPDPRG2          waltz16
NUC2                 1H
PCPD2             80.00 usec
PL2               -3.00 dB
PL12              14.31 dB
PL13              18.00 dB
SFO2         400.1316005 MHz

F2 - Processing parameters
SI                32768
SF           100.6127690 MHz
WDW                  EM
SSB                   0
LB                 1.00 Hz
GB                    0
PC                 1.40
```

avtar_saifpu@yahoo.co.in

## Section C- Cu-Mo nanoparticles catalyzed organic transformation reactions

### 3.9 Synthesis of 2-phenylbenzo[d]imidazole derivatives catalyzed by Cu-Mo nanoparticles

#### 3.9.1 Introduction

Benzimidazoles are very useful intermediates/subunits for the development of molecules of pharmaceutical or biological interest [202]. Benzimidazole and its derivatives are an important class of bioactive molecules in the field of drugs and pharmaceuticals [203]. Benzimidazole derivatives have found applications in diverse therapeutic areas including anti-ulcers, anti-hypertensives, anti-virals, anti-fungals, anti-cancers, and anti-histaminic [203]. Moreover, these fused heterocycles have been studied as new non-nucleoside topoisomerase-I poisons, human immunodeficiency virus-1 reverse transcriptase inhibitors, and/or potent DNA gyrase inhibitors [204]. They can act as ligands to transition metals for modeling biological systems [205]. There is a continuing interest in preparing of benzimidazole containing structures. Benzimidazoles have been used as antitumor [206], antimicrobial agents [207], antivirus [208], topoisomerase I inhibitors [209], selective neuropeptide Y Y1 receptor antagonists [210-211] and angiotensin II inhibitors [212] while benzothiazoles are important as antitumor [213], antimicrobial agents [214] and $LTD_4$ receptor antagonist [215]. In addition, benzimidazoles are very important intermediates in organic reactions [216].

#### 3.9.2 Literature review

The literature assay shows that two general methods for the synthesis of benzimidazoles are the acidic cyclocondensation of o-phenylenediamine with carboxylic acids or their derivatives and oxidative cyclo-dehydrogenation of o-phenylenediamin with aldehydes [217]. Various oxidative reagents such as DDQ [218] , $NaHSO_3$(aq) [219] , nitrobenzene [220], $MnO_2$ [221], 1,4-benzoquinone [222], benzofuroxan [223], tetracyanoethylene [224], $Pb(OAc)_4$ [225] and Oxone have been employed for the synthesis of benzimidazoles and benzothiazoles. Various catalyzed syntheses of benzimidazole derivatives are known, by condensation of *o*-phenylenediamine with aldehydes [226].Condensation of *o*-phenylenediamine with *ortho*-esters in the presence of various Lewis acid catalyst is also known *viz.* $ZrCl_4$, $SnCl_4.5H_2O$, $TiCl_4$, $BF_3.Et_3O$, $ZrOCl_2.8H_2O$ and $HfCl_4$ [227]. Phthalic acid attached to polyethylene glycol ether and polymer supported 4-fluoro-3-nitrobenzoic acid in solid phase have been used as precursor for 2-

substituted benzimidazoles, benzoxazoles and benzothiazoles [228]. However, a number of these methods have some drawbacks such as low yield, long reaction times, drastic reaction conditions, tedious work-up procedures and co-occurrence of several side reactions. Promoted by the need for finding another new and efficient method for the synthesis of these heterocyclic compounds, we became interested in the synthesis of 2-substituted benzimidazoles by the condensation of o-phenylenediamine with various aldehydes in the presence of Cu-Mo nanoparticles catalyst.

### 3.9.3 Present work

Electrochemically prepared Cu-Mo bimetallic nanoparticles were tested on the synthesis of 2-aryl benzimidazoles derivatives (Scheme -8). The short reaction time, clean reaction condition, consistent yield and minimum environmental effect are important features of the reaction.

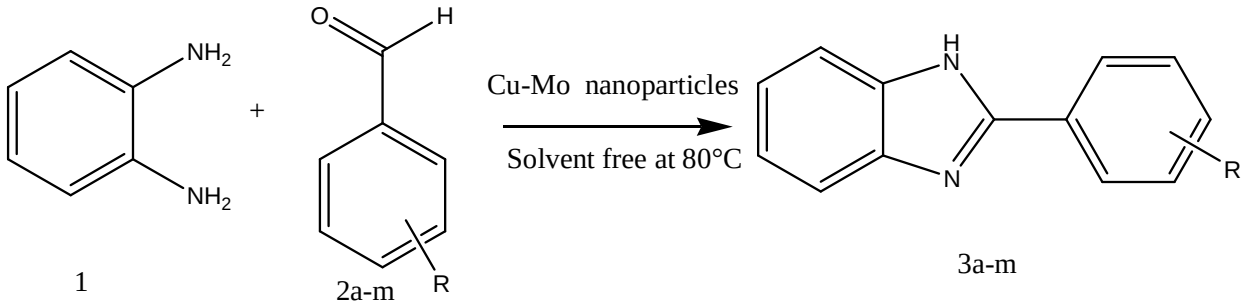


**Scheme -8**

### 3.9.4 Experimental

The melting points of compounds were taken in an open capillary in a paraffin bath. IR spectra were recorded on a Jasco FTIR-4100 spectrophotometer. $^{1}$H NMR spectra were recorded on an 400 MHz FT-NMR spectrometer in DMSO as a solvent and chemical shift values were recorded in units δ (ppm) relative to tetramethylsilane ($Me_4Si$) as an internal standard.

**General procedure**

A mixture of 2-aminophenol (1mmol), aromatic aldehyde (1 mmol) & Cu-Mo bimetallic nanoparticles (100 mg) was stirred at 80°C in solvent free condition to obtain 2-aryl benzimidazoles derivatives crude product. The progress of reaction was monitored by TLC. After completion of reaction, the crude product was dissolved by adding ethanol and the Cu-Mo bimetallic nanoparticles were separated by centrifuging, followed by decantation. Cu-Mo bimetallic nanoparticles were dried in vacuum desiccators and crude product recrystallized in

ethanol. The recrystallized product analysis by FTIR, $^{1}$H NMR and $^{13}$C NMR spectra was recorded.

### 3.9.5 Spectral data of representative compound

2-Phenyl-1H-benzimidazole ; IR (KBr) 3566, 2360, 1748,1716, 1698, 1683, 1652, 1616 $cm^{-1}$; $^{1}$HNMR (DMSO-d6, 400MHz, δ ppm ) 12.92 (s, 1H), 8.19 (d,J=8.0Hz,2H),7.61–7.55(m,4H), 7.52–7.48 (m, 1H), 7.23–7.19 (m, 2H);$^{13}$CNMR (DMSO-d6,100MHz, δ ppm)151.7, 144.3, 135.5, 130.7, 130.3, 129.4, 126.9,123.0, 122.1, 119.4, 111.8

2-(4-Chlorophenyl)-1H-benzimidazole; IR(KBr) 3606, 3001, 2818, 2310, 1700, 1513, 735$cm^{-1}$; $^{1}$HNMR(DMSO-d6,400MHz, δ ppm)13.00(s,1H),8.20(d, J=8.4Hz, 2H),7.64(d, J=8.4Hz, 4H),7.24–7.21 (m,2H); $^{13}$CNMR (DMSO-d6,100MHz, δ ppm )150.6, 144.3, 135.0, 134.8, 129.5, 128.6, 128.2,122.9, 122.5, 119.4, 111.9

### 3.9.6 Result discussion

In order to get best results of synthesized catalytic material, we have carried out the model reaction of o-phenylenediamine and benzaldehyde in presence of Cu-Mo bimetallic nanoparticles (0.1 g) stirred at 80 °C solvent free condition. To examine the solvent effect from this study,the reactions were carried out in various solvents such as water. Methanol(MeOH), Acetonitrile(MeCN), Tetrahydrofuran(THF), Ethanol (EtOH), n-hexane and solvent free. From the results, it is observed that solvent free condition found to be the best to carry out the synthesis of desired compounds shown in Table 3.9.1.

**Table 3.9.1** Comparative study of synthesis benzaimidazole with different solvent**.**

| Entry[a] | Solvent | Time(min) | Yield[b](%) |
|---|---|---|---|
| 1 | ACN | 180 | 54 |
| 1 | Toluene | 240 | 32 |
| 2 | THF | 200 | 35 |
| 4 | Methanol | 180 | 62 |
| 5 | Ethanol | 150 | 76 |
| 6 | Solvent free | 120 | 94 |

[a]Reaction condition: o-phenyldiamine(1mmol), Benzaldehyde (1mmol) and 100mg of Cu-Mo NPs stirred at 80°C in solvent free condition. [b] Isolated yield.

We report here a very simple process for the synthesis of 2- aryl benzaimidzoles by condensation of o-phenylenediamine with aromatic aldehyde under solvent free conditions catalyzed by CuMo nanoparticles. In the present work, an attempt has been made to optimize the reaction conditions by using o-phenylenediamine (1mmol) **1** and benzaldehyde (1 mmol) **2a** as

model reaction at different solvents and amount of catalyst used. In order to investigate the best results in terms of yield & reaction time, we have examined the efficiency of different reaction media and the amount of catalyst required. From Table 3.9.2, it can be seen that loading of 100mg of CuMo nanoparticles catalysts were adequate for smooth condensation of o-phenylenediamine and benzaldehyde under solvent free condition at 80°C. There is considerable increase in the yield of product when amount of catalyst is increased from 50 mg to 100 mg; above 100 mg, no considerable change in reaction time and yield of the product was observed.

Table 3.9.2 Screening of catalyst CuMo NPs for the synthesis of 2-aryl benzimidazoles.

| Entry[a] | Catalyst Amount (mg) | Time (Min) | Yield[b] (%) |
|---|---|---|---|
| 1 | 00 | 180 | Trace |
| 2 | 40 | 150 | 32 |
| 3 | 60 | 120 | 66 |
| 4 | 80 | 90 | 85 |
| 5 | 100 | 50 | 94 |
| 6 | 120 | 50 | 94 |

[a]Reaction condition: o-phenyldiamine(1mmol), Benzaldehyde (1mmol) and 100mg of Cu-Mo NPs stirred at 80°C in solvent free condition. [b] Isolated yield.

The catalyst was recovered by simple work-up using centrifugation method, washed with ethanol and reused for three successive reactions. The corresponding yield for each cycle was mentioned in Table 3.9.3.

Table 3.9.3 Reusability of catalyst CuMo nanoparticles

| Entry[a] | 1 | 2 | 3 | 4 |
|---|---|---|---|---|
| No. of recycle | Fresh | I | II | III |
| Yield[b] (%) | 94 | 91 | 88 | 85 |

[a]Reaction condition: o-phenyldiamine(1mmol), Benzaldehyde (1mmol) and 100mg of Cu-Mo NPs stirred at 80°C in solvent free condition. [b] Isolated yield.

Under optimization reaction condition, we obtained 94% yield of 2 aryl benzimidazole within 50 mins. In Table 3.9.4, the reaction time & the product yield depends on the substituents introduced on substrates. For instance, the condensation of o-phenyldiamine having strong electron withdrawing groups (F, Cl, Br, $NO_2$, OH) in para position gave the desired product with good yield and shorter reaction time than meta substituted product and electron donor groups($CH_3$, $OCH_3$).

Table3.9.4 Synthesis of 2-aryl benzimidazole derivative using CuMo nanoparticles

| Products[a] | R | Time (min) | Yield[b](%) | Melting point(°C) | |
|---|---|---|---|---|---|
| | | | | Found | Reported |
| 3a | H | 50 | 94 | 132-134 | 132 |
| 3b | 4-Cl | 50 | 92 | 138-140 | 137 |
| 3c | 4-$NO_2$ | 50 | 94 | 119-120 | 118 |
| 3d | 4-$CH_3$ | 100 | 85 | 126-128 | 126 |
| 3e | 4-$OCH_3$ | 110 | 86 | 130-131 | 131 |
| 3f | 4-OH | 60 | 90 | 250-253 | 254-256 |
| 3g | 4-$(CH_3)_2N$- | 100 | 82 | 292-294 | 294-296 |
| 3h | 2-$NO_2$ | 80 | 87 | 169-170 | 168-170 |
| 3i | 2-OH | 90 | 88 | 205-208 | 207-208 |
| 3k | 2-Cl | 70 | 87 | 158-159 | 155 |
| 3l | 2-Furyl | 90 | 85 | 96-98 | 96 |
| 3m | 3-$NO_2$ | 80 | 90 | 185-187 | 184-187 |

[a]Reaction condition: o-phenyldiamine(1mmol), Benzaldehyde (1mmol) and 100mg of Cu-Mo NPs stirred at 80°C in solvent free condition. [b] Isolated yield.

### 3.9.7 Conclusion

The present work offers a simple procedure promoted by inexpensive, non-toxic, reusable and heterogenous Cu-Mo nanoparticles catalyst as an efficient methodology for the synthesis of 2-aryl-benzimidazoles via condensation of aromatic aldehydes with o-phenylenediamine under solvent free condition. A mild, manipulatable procedure, eco-friendly and green aspects avoiding hazardous solvents, shorter reaction times and high yield of the products are the advantages of this method

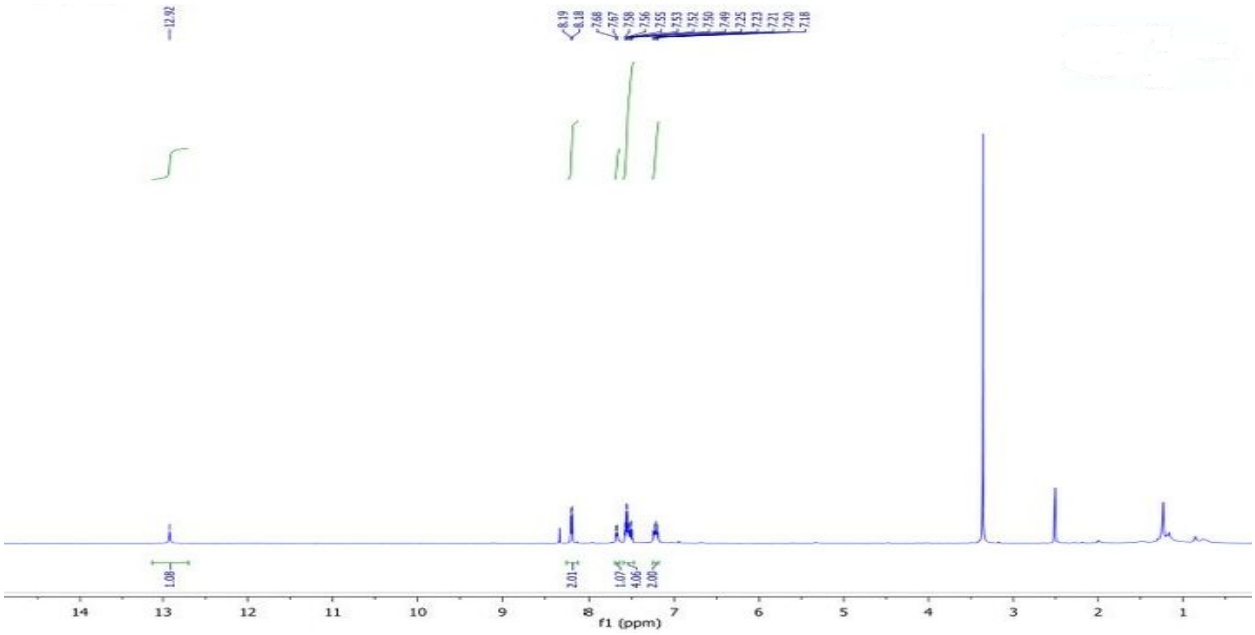
12.92
8.19
8.18
7.68
7.67
7.58
7.56
7.55
7.53
7.52
7.50
7.49
7.25
7.23
7.21
7.20
7.18
1.08
2.01
1.07
4.06
2.00
f1 (ppm)

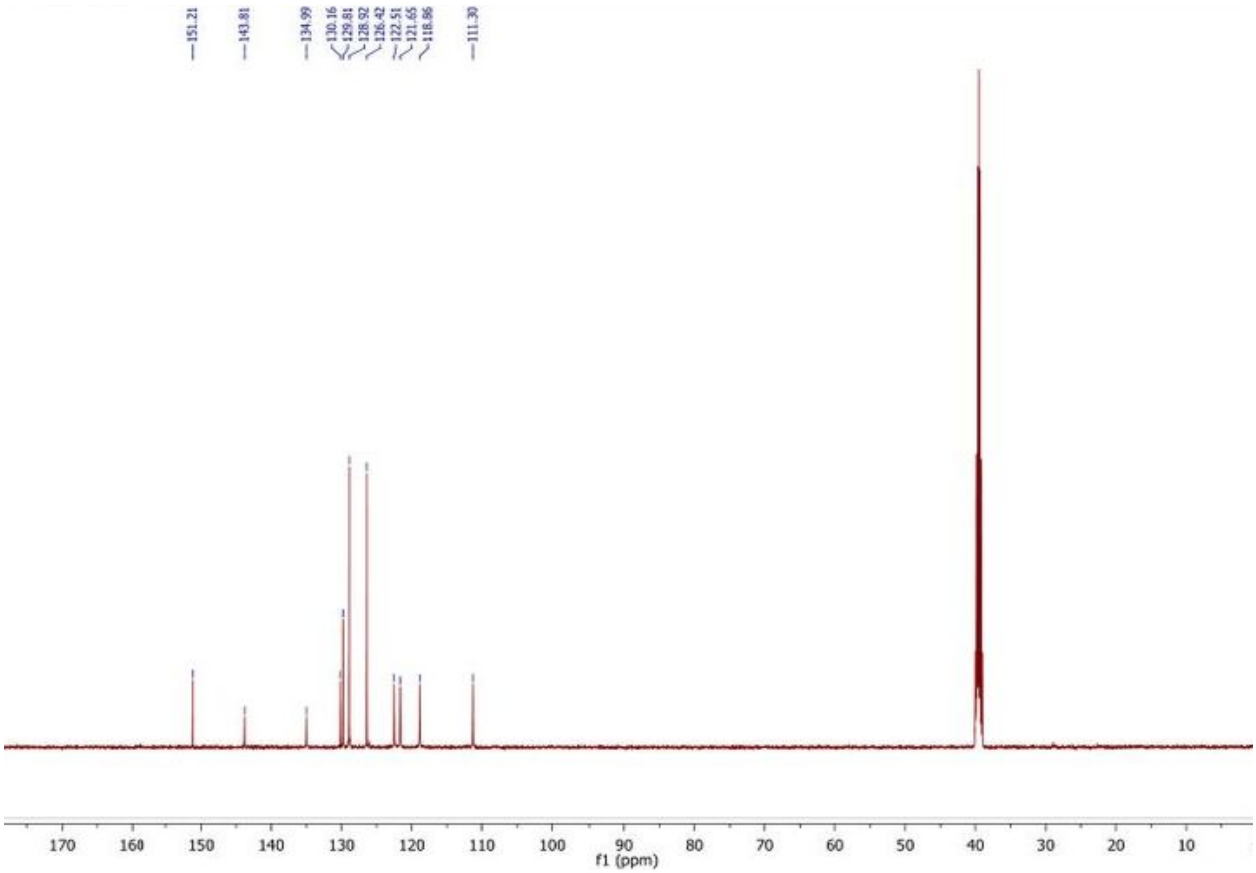
151.21
143.81
134.99
130.16
129.81
128.92
126.42
122.51
121.65
118.86
111.30
f1 (ppm)

## 3.10 Synthesis of 2-phenylbenzo[d]oxazole derivatives catalyzed by Cu-Mo nanoparticles

### 3.10.1 Introduction

Benzoxazoles are an important class of molecules and are a common heterocyclic scaffold in biologically active and medicinally significant compounds. Benzoxazoles are found in a variety of natural products [162] and are important targets in drug discovery [163]. Also, much attention has been paid to benzoxazoles because they have a number of applications such as photoluminescents [164], whitening agents [165] and in dye lasers [166]. They are also used as intermediates for several therapeutic materials [167-168]. Pyrazines are found in the luminescent chromophores or certain marine organisms [169] in cephalostatins isolated from Cephalodiscus gilehrist, which are powerful anticancer agents [170], in the fungal metabolite aspergillic acid [171] and in food in the form of potent flavor compounds [172]. They have been also used as ligands in asymmetric synthesis [173]. Benzoxazole is heterocyclic moiety which exhibited various pharmaceutical properties such as antiviral [174], antibiotic [175], antimicrobial [176], antitumor [177] and anti-inflammatory [178] activities.

### 3.10.2 Literature review

The classical approach for the synthesis of benzoxazoles involves (i) coupling of carboxylic acids with 2-aminophenols by dehydration catalyzed by strong acid [179], orthoesters [180], acid chlorides [181], nitriles [182], amides [183], aldehydes [184] and esters [185] with o-Aminophenol and (ii) the oxidative cyclization of phenolic Schiff's bases derived from the condensation of 2-aminophenols and aldehydes, using various oxidants such as $PhI(OAc)_2$ [186], $Mn(OAc)_3$ [187], $ThClO_4$ [188], $(MnO_4)_2$ [189], $NiO_2$ [190], $Pb(OAc)_4$ [191], DDQ [192], NiS [193], Cu-np [194], aerial oxidation in the presence of activated carbon (Darco KB) [195], CuCl [196] and Pd/Pt-C [197]. Other synthetic routes for benzoxazole include microwaveassisted reaction of *N*-acyl-aminophenol [198], iron catalysed intramolecular *O*-arylation of 2-haloacetanilides [199] and cyclization of phenolic Schiff base under UV irradiation [200]. Apart from these methodologies, there have been many precedents for the synthesis of 2-aryl benzothiazoles and benzoxazoles via palladium catalysed cross-coupling reactions that have been disclosed in the literature [201].

However, most of these procedures have some drawbacks such as long reaction times, low yields of products, the use of expensive, toxic or non-reusable catalysts, high temperatures,

harsh reaction conditions and use of toxic solvents and/or co-occurrence of several side reactions. In some cases more than one step is required for the synthesis of these heterocycles. Therefore, it is necessary to find a better catalyst for the synthesis of benzoxazoles in terms of operational simplicity, non-toxicity, reusability and environmental and economical acceptability. Herein, we report a new and efficient route for the one-pot synthesis of substituted benzoxazoles from substituted benzaldehydes and 2-aminophenoles. When substituted benzoic acid and 2-aminophenole is treated with Cu-Mo nanoparticles, rapid and efficient oxidative cyclisation takes place as shown in Scheme-10. Easy handling, cheapness, efficiency, non-toxicity make this catalyst eco-friendly, synthetically acceptable and economically viable.

### 3.10.3 Present work

Electrochemically prepared Cu-Mo nanoparticles were tested on the synthesis of 2-aryl benzoxazole derivatives (Scheme-9). The short reaction time, clean reaction condition, consistent yield and minimum environmental effect are important features of the reaction.

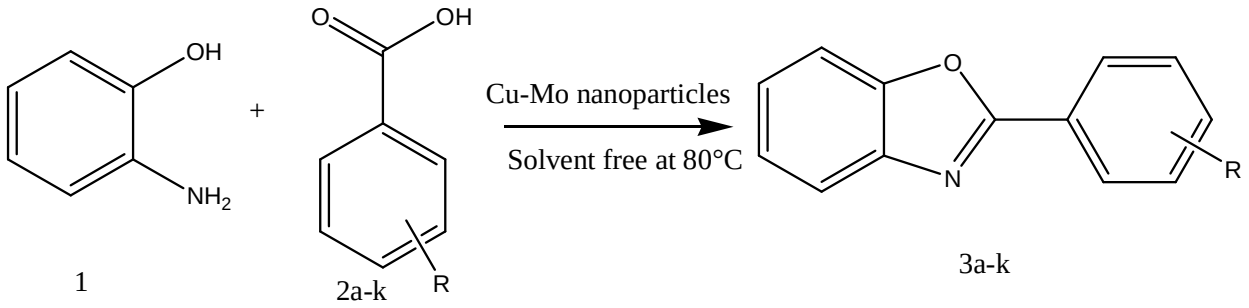


**Scheme-9**

### 3.10.4 Experimental

The melting points of compounds were taken in an open capillary in a paraffin bath. IR spectra were recorded on a Jasco FTIR-4100 spectrophotometer. $^{1}$H NMR spectra were recorded on an 400 MHz FT-NMR spectrometer in DMSO as a solvent and chemical shift values were recorded in units δ (ppm) relative to tetramethylsilane ($Me_4Si$) as an internal standard.

**General procedure**

A mixture of 2-aminophenol (1mmol), aromatic acid (1 mmol) & Cu-Mo bimettalic nanoparticles (100 mg) was stirred at 80°C for 2 hrs to obtain crude product (3a-m, Scheme 1). The progress of reaction was monitored by TLC. After completion of reaction, the crude product was dissolved by adding ethanol and the Cu-Mo bimetallic nanoparticles were separated by

centrifuging, followed by decantation. Cu-Mo bimetallic nanoparticles were dried in vacuum desiccators and crude product recrystallized in ethanol. The recrystallized product analysis by FTIR, $^{1}H$ NMR and $^{13}C$ NMR spectra was recorded.

### 3.10.5 Spectral data of representative compound

2-(4-chlorophenyl)benzo[d]oxazole (Entry 3).IR (KBr, cm-1):3032, 1641, 1609, 1515,1433, 1304, 1295, 1258, 828, 777, 743.1H NMR (400 MHz, $CDCl_3$, δ ppm): 7.30 (m, 4H), 7.55 (d, 2H, 9.0 Hz), 7.75 (d, 2H, 9.0 Hz) .13C NMR (100 MHz $CDCl_3$ δ ppm):108.5, 118.8, 121.7, 123.1, 124.1, 129.29, 130.0, 132.1, 139.5, 148.8, 162.7

### 3.10.6 Result discussion

We report here a very simple process for the synthesis of 2- aryl benzoxazoles by condensation of 2-aminophenol with aromatic acid under solvent free conditions catalyzed by Cu-Mo bimetallic nanoparticles. In the present work, an attempt has been made to optimize the reaction conditions by using 2-aminophenol (1mmol) **1** and 4-chloro benzoic acid (1 mmol) **2b** as model reaction at different solvents and amount of catalyst used. In order to investigate the best results in terms of yield & reaction time, we have examined the efficiency of different reaction media and the amount of catalyst required. From Table 3.10.1, it can be seen that loading of 100mg of Cu-Mo bimetallic nanoparticles catalyst were adequate for smooth condensation of 2 aminophenol and 4-chloro benzoic acid under solvent free condition at 60°C. There is considerable increase in the yield of product when amount of catalyst is increased from 50 mg to 100 mg; above 100 mg, no considerable change in reaction time and yield of the product was observed.

Table 3.10.1 Screening of catalyst Cu-Mo NPs amount for the synthesis of 2- aryl benzoxazoles.

| Entry[a] | Catalyst Amount (mg) | Time (Min) | Yield[b] (%) |
|---|---|---|---|
| 1 | 00 | 180 | Trace |
| 2 | 40 | 150 | 32 |
| 3 | 60 | 120 | 66 |
| 4 | 80 | 90 | 77 |
| 5 | 100 | 50 | 96 |
| 6 | 120 | 50 | 95 |

[a]Reaction condition: 4-chloro benzoic acid (1mmol), 2-amino phenol(1mmol), Cu-Mo bimetallic nanoparticles
[b]Isolated Yield

The catalyst was recovered by simple work-up using centrifugation method, washed with ethanol and reused for three successive reactions. The corresponding yield for each cycle was mentioned in Table 3.10.2.

Table 3.10.2 Reusability of catalyst Cu Mo nanoparticles

| Entry[a] | 1 | 2 | 3 | 4 |
|---|---|---|---|---|
| No. of recycle | Fresh | I | II | III |
| Yield[b] (%) | 96 | 94 | 91 | 89 |

[a]Reaction condition: 4-chloro benzoic acid(1mmol), 2-aminophenol(1mmol), Cu-Mo bimetallic nanoparticles
[b]Isolated Yield

Under optimization reaction condition, we obtained 95% yield of 2(4-chloro-aryl) benzoxazole within 50 mins. In Table 3.10.3, the reaction time & the product yield depends on the substituents introduced on substrates. For instance, the condensation of 2-aminophenol having strong electron withdrawing groups (F, Cl, Br, $NO_2$, OH) in para position gave the desired product with good yield and shorter reaction time than meta substituted product and electron donor groups($CH_3$, $OCH_3$).

Table 3.10.3 Synthesis of 2-aryl benzaoxazole derivative using $MoO_3$ nanoparticles

| Products[a] | R | Time (min) | Yield[b](%) | Melting point(°C) | |
|---|---|---|---|---|---|
| | | | | Found | Reported |
| 3a | H | 70 | 88 | 101 | 102 |
| 3b | 4-Br | 55 | 95 | 131-132 | 132 |
| 3c | 4-Cl | 50 | 92 | 146 | 147 |
| 3d | 4-$NO_2$ | 50 | 94 | 266-267 | 266-268 |
| 3e | 4-$CH_3$ | 100 | 85 | 113 | 113-114 |
| 3f | 4-$OCH_3$ | 110 | 86 | 102 | 101-103 |
| 3g | 4-OH | 60 | 90 | 224-227 | 225-227 |
| 3h | 4-F | 60 | 80 | 100-102 | 101-102 |
| 3i | 3-$NO_2$ | 80 | 87 | 241 | 242-243 |
| 3k | 2-OH | 90 | 88 | 128-129 | 129-130 |

[a]Reaction condition: 4-chloro benzoic acid (1mmol), 2-aminophenol(1mmol), Cu-Mo bimetallic nanorods
[b]Isolated Yield

### 3.10.7 Conclusion

We have developed efficient Cu-Mo bimetallic nanoparticles catalysts for the synthesis of 2-aryl benzoxazole with high yield of product in short reaction time and very less amount of catalyst. This catalyst showed excellent activity during four consecutive runs without appreciable loss of activity. Furthermore, this method is of interest in the context to environmentally greener and safer processes.

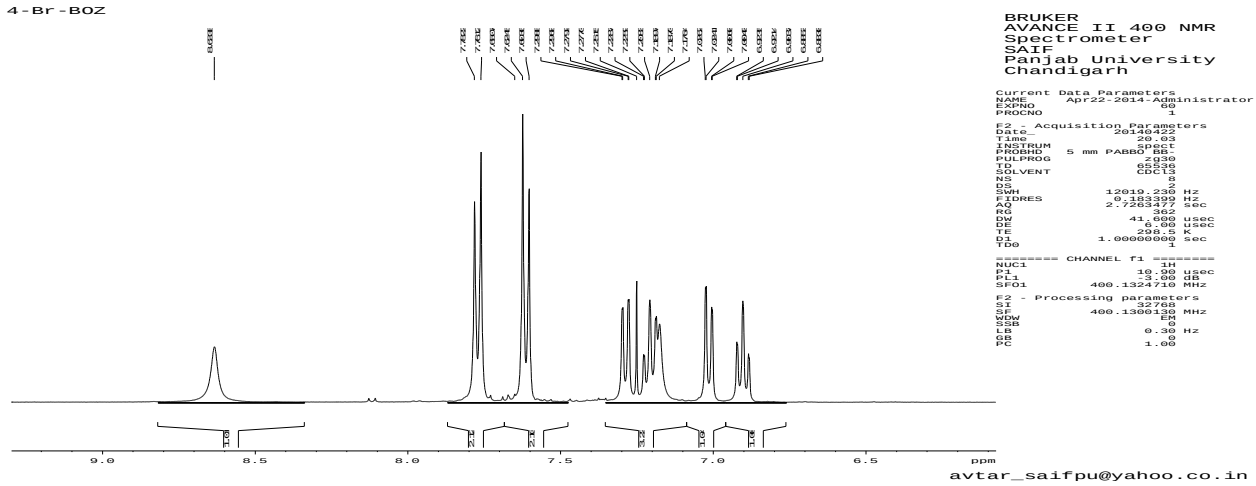


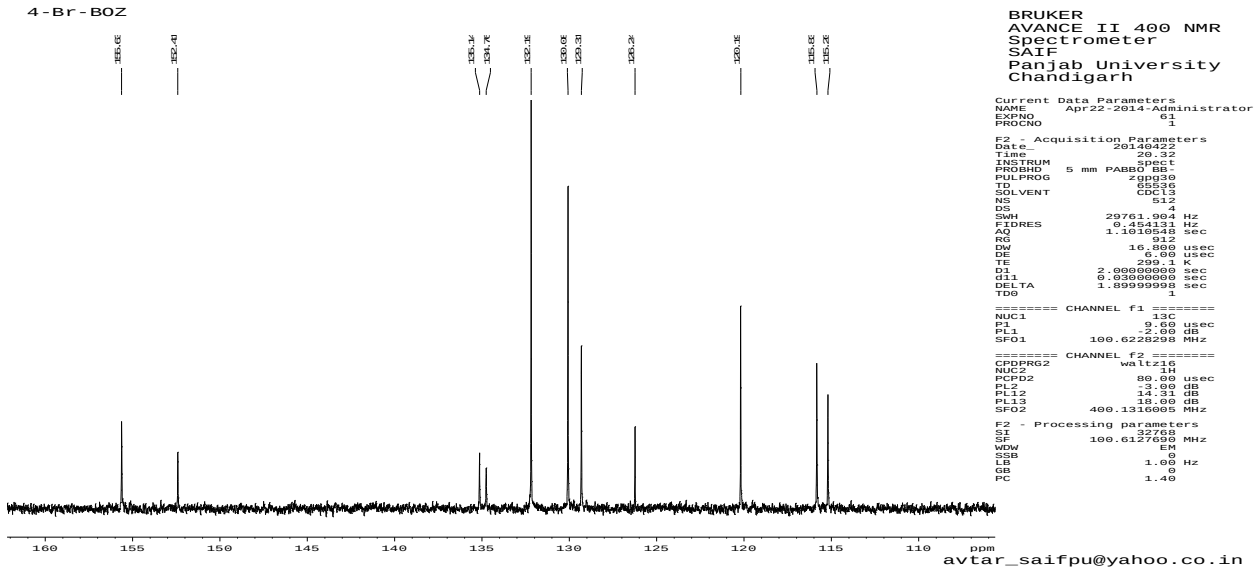

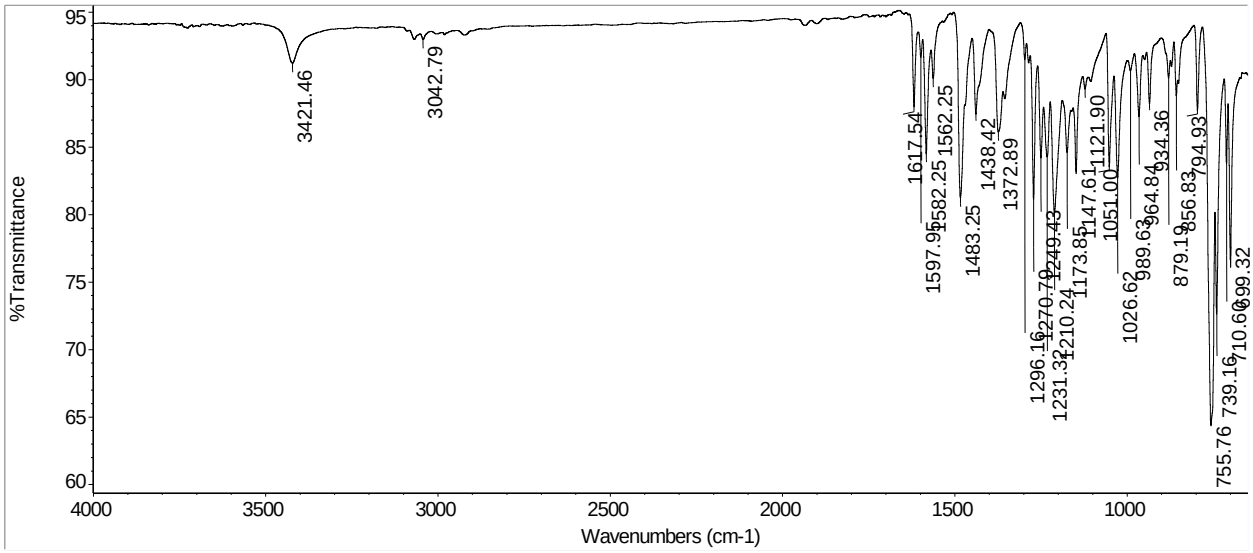


2-CL-BOZ

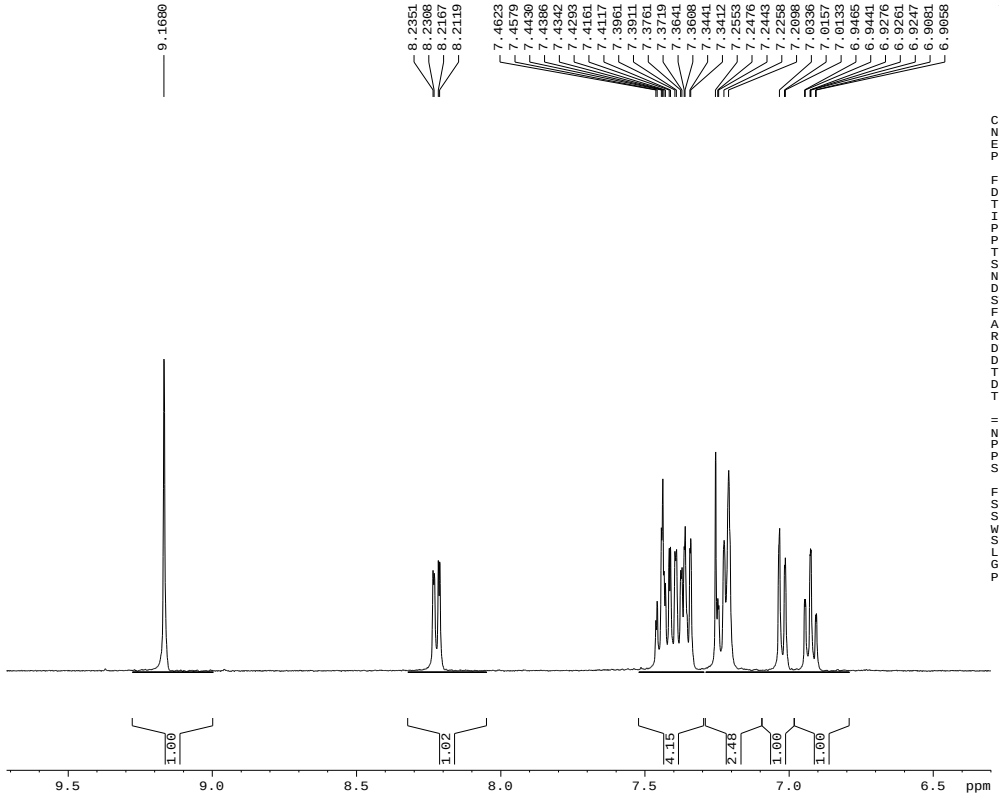


BRUKER
AVANCE II 400 NMR
Spectrometer
SAIF
Panjab University
Chandigarh

```
Current Data Parameters
NAME      Apr22-2014-Administrator
EXPNO                  140
PROCNO                   1

F2 - Acquisition Parameters
Date_               20140422
Time                  22.45
INSTRUM               spect
PROBHD   5 mm PABBO BB-
PULPROG                zg30
TD                    65536
SOLVENT               CDCl3
NS                        8
DS                        2
SWH               12019.230 Hz
FIDRES             0.183399 Hz
AQ                2.7263477 sec
RG                      912
DW                   41.600 usec
DE                    6.00 usec
TE                   299.5 K
D1               1.00000000 sec
TD0                       1

======== CHANNEL f1 ========
NUC1                    1H
P1                   10.90 usec
PL1                  -3.00 dB
SFO1           400.1324710 MHz

F2 - Processing parameters
SI                    32768
SF               400.1300117 MHz
WDW                      EM
SSB                       0
LB                    0.30 Hz
GB                        0
PC                    1.00
```

avtar_saifpu@yahoo.co.in

## 3.11 Green synthesis of 2-phenylbenzo[d]thiazole derivatives catalyzed by Cu-Mo bimetallic nanoparticles

### 3.11.1 Introduction

2-Aryl benzothiazole and their derivatives exhibit a wide range of biological properties which have led to continuous interest in the field of medicinal chemistry. 2-Aryl benzothiazole exhibits antimicrobial [138-139], antibiotic [140], antiviral [141], anti-inflammatory [142], antifungal [143], antitumor [144], anticonvulsant [145], antiparasitic [146], antagonists [147] and treatment of Alzheimer diseases [148]. They exhibit nanomolar inhibitory activity against human cancer cell [149] and several enzymes such as aldose reducates [150], $H^+$-$K^+$ ATPase [151], protease [152] and carbonic anhydrase [153]. Benzothiazoles also exhibit physiological activities like $H_{37}$Rv inhibitory [154], elastase inhibitory [155] and cytotoxicity towards $P_{338}$ cells [156].

### 3.11.2 Literature review

The synthesis of 2-aryl benzothiazole involves condensation of 2-aminothiophenol with aldehyde, acid chloride, carboxylic acid, ester, aryl bromide and coupling with aryl boronic acid. The condensation of 2-aminothiophenol and aromatic acid have been reported by using various methods such as solid phase[157], liquid phase [158], microwave irradiation [159] and multisubstituted derivatives etc[160].

However most of these procedures of synthesis of benzothiazoles are associated with some disadvantages such as tedious reaction, expensive catalyst, multistage processes and loss of catalyst, the use of hazardous and carcinogenic solvents like nitrobenzene & dioxane which are harmful to environment and also to the human. Therefore, it is necessary to study the reaction by some green methods which is efficient and simple. The present study involves synthesis of 2-aryl benzothiazole by using Cu-Mo bimetallic nanoparticles which are efficient, simple and environmentally begin.

### 3.11.3 Present work

Electrochemically prepared Cu-Mo bimetallic nanoparticles were tested on the synthesis of 2-aryl benzothiazole derivatives (Scheme -10). The short reaction time, clean reaction condition, consistent yield and minimum adverse environmental effect were important features of the reaction.

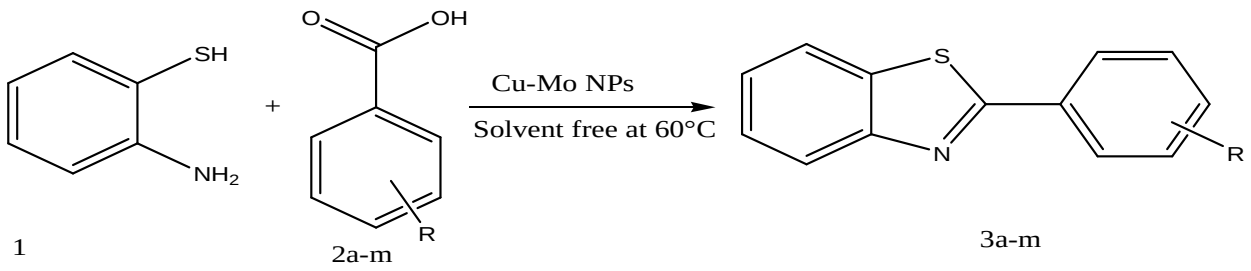


**Scheme 10**

### 3.11.4 Experimental

The melting points of compounds were taken in an open capillary in a paraffin bath. IR spectra were recorded on a Jasco FTIR-4100 spectrophotometer. $^{1}$H NMR spectra were recorded on an 400 MHz FT-NMR spectrometer in DMSO as a solvent and chemical shift values were recorded in units δ (ppm) relative to tetramethylsilane ($Me_4Si$) as an internal standard.°

**General procedure**

A mixture of 2-aminothiophenol (1mmol), aromatic acid (1 mmol) & Cu-Mo bimetallic nanoparticles (100 mg) was stirred at 60°C for 2 hrs to obtain 2-aryl benzothiazole crude product.The progress of reaction was monitored by TLC. After completion of reaction, the crude product was dissolved by adding ethanol and the Cu-Mo bimetallic nanoparticles were separated by centrifuging followed by decantation. Cu-Mo bimetallic nanoparticles were dried in vacuum desiccators and crude product recrystallized in ethanol. The recrystallized product analysis by FTIR, $^{1}$H NMR and $^{13}$C NMR spectra were recorded.

### 3.11.5 Spectral data of representative compound

3a) 2-Aryl benzothiazole: FTIR (KBr, $cm^{-1}$): 3062, 1590, 1556, 1510, 1435, 1245, 960, 766 $cm^{-1}$ $^{1}$H NMR (400.13 MHz, $CDCl_3$, δ ppm): 7.34 (t, 1H, CH of Ar), 7.88(d, 2H, CH of Ar), 8.06(d, 1H CH of Ar), 8.07(d, 1H, CH of Ar), 8.09(d, 1H, CH of Ar). $^{13}$C NMR (100.61 MHz, $CDCl_3$, δ, ppm): 121.89(CH of Ar), 121.91(CH of Ar), 125.20(CH of Ar), 125.90(CH of Ar), 127.51(2CH of Ar), 128.80(CH of Ar), 129.32(2CH of Ar), 133.50(C of Ar), 135.80, 154.42), 166.60,

3b) 2(4-Bromo -aryl) benzothiazole: FTIR (KBr, $cm^{-1}$): 3056, 1582, 1545, 1505, 1474, 1247, 969, 854, 751 $cm^{-1}$. $^{1}$H NMR (400.13 MHz, $CDCl_3$, δ ppm): 7.38(t, 1H, CH of Ar), 7.48(t, 1H, CH of Ar), 7.60(d, 2H, CH of Ar), 7.88(d, 1H, CH of Ar), 7.90(d, 2H, CH of Ar), 8.06(d, 1H, CH of Ar). $^{13}$C NMR (100.61 MHz, $CDCl_3$ δ ppm): 121.68(CH of Ar), 123.34(CH of Ar),

125.43(C-N), 125(CH of Ar), 126.52(CH of Ar), 128.91(2 CH of Ar), 132.56(2 CH of Ar), 135.06, 154.9, 166.69.

3m) 2(2,3-di Bromo -aryl) benzothiazole: $^{1}$H NMR (400.13 MHz, $CDCl_3$, δ ppm): 6.46(t, 1H, CH of Ar), 6.77(d, 1H, CH of Ar), 7.05(d, 1H, CH of Ar), 7.1(d, 1H, CH of Ar), 7.89(d, 2H, CH of Ar), 8.06(d, 1H, CH of Ar). $^{13}$C NMR (100.61 MHz, $CDCl_3$ δ ppm): 109.65(CH of Ar), 114.42(CH of Ar), 117.12.(C-N), 115.57(CH of Ar), 116.51(CH of Ar), 130-131(2 CH of Ar), 135.56(2 CH of Ar), 139.60( CH of Ar), 149.02, 157.29, 170.58.

**3.11.6 Result discussion**

We report here a very simple process for the synthesis of 2- aryl benzothiazoles by condensation of 2-aminothiophenol with aromatic acid under solvent free conditions catalyzed by Cu-Mo bimetallic nanoparticles. In the present work, an attempt has been made to optimize the reaction conditions by using 2-aminothiophenol(1mmol) **1** and 4-chloro benzoic acid (1 mmol) **2b** as model reaction at different solvents and amount of catalyst used. In order to investigate the best results in terms of yield & reaction time, we have examined the efficiency of different reaction media and the amount of catalyst required. From Table 3.11.1, it can be seen that loading of 100mg of Cu-Mo bimetallic nanoparticles catalyst were adequate for smooth condensation of 2 aminothiophenol and 4-chlorobenzoic acid under solvent free condition at 60°C. There is considerable increase in the yield of product when amount of catalyst is increased from 50 mg to 100 mg; above 100 mg, no considerable change in reaction time and yield of the product was observed.

Table 3.11.1 Screening of catalyst Cu-Mo NPs amount for the synthesis of 2-aryl benzothiazoles.

| Entry[a] | Catalyst Amount (mg) | Time (Min) | Yield[b] (%) |
|---|---|---|---|
| 1 | 00 | 180 | Trace |
| 2 | 40 | 160 | 35 |
| 3 | 60 | 120 | 64 |
| 4 | 80 | 90 | 78 |
| 5 | 100 | 45 | 95 |
| 6 | 120 | 45 | 95 |

[a]Reaction condition: 4-chlorobenzoic acid (1mmol), 2-amino thiophenol(1mmol), Cu-Mo bimetallic nanoparticles
[b]Isolated Yield

The catalyst was recovered by simple work-up using centrifugation method, washed with ethanol and reused for three successive reactions. The corresponding yield for each cycle was mentioned in Table 2.

Table 3.11.2 Reusability of catalyst Cu-Mo NPs 2-aryl benzothiazoles

| Entry[a] | 1 | 2 | 3 | 4 |
|---|---|---|---|---|
| No. of recycle | Fresh | I | II | III |
| Yield[b] (%) | 95 | 94 | 92 | 89 |

[a]Reaction condition: 4-chlorobenzoic acid (1mmol), 2-amino thiophenol(1mmol), Cu-Mo bimetallic nanoparticles
[b]Isolated Yield

Under optimization reaction condition, we obtained 95% yield of 2(4-chloro-aryl) benzothiazole within 50 mins. In Table 3.11.3, the reaction time & the product yield depends on the substituents introduced on substrates. For instance, the condensation of 2-aminothiophenol having strong electron withdrawing groups (F, Cl, Br, $NO_2$, OH) in para position gave the desired product with good yield and shorter reaction time than meta substituted product and electron donor groups($CH_3$, $OCH_3$).

Table 3.11.3 Synthesis of 2-aryl benzathiazole derivative using Cu-Mo NPs

| Products[a] | R | Time (min) | Yield[b](%) | Melting point(°C) | |
|---|---|---|---|---|---|
| | | | | Found | Reported |
| 3a | H | 70 | 88 | 112-114 | 112-114 |
| 3b | 4-Br | 45 | 95 | 131-132 | 132 |
| 3c | 4-Cl | 50 | 92 | 114-116 | 115-117 |
| 3d | 4-$NO_2$ | 50 | 94 | 180-182 | 181-182 |
| 3e | 4-$CH_3$ | 100 | 85 | 82-84 | 84-86 |
| 3f | 4-$OCH_3$ | 110 | 86 | 120-122 | 120-121 |
| 3g | 4-OH | 60 | 90 | 224-227 | 225-227 |
| 3h | 4-F | 60 | 80 | 100-102 | 101-102 |
| 3i | 3-$NO_2$ | 80 | 87 | 180-182 | 181-182 |
| 3k | 2-OH | 90 | 88 | 128-129 | 129-130 |
| 3l | 2-$OCH_3$ | 80 | 90 | 103-104 | 103-105 |
| 3m | 2-Furfurald | 100 | 85 | 100-102 | 103-104 |

[a]Reaction condition: Benzoic acid derivative (1mmol), 2-amino thiophenol(1mmol), Cu-Mo bimetallic nanoparticles
[b]Isolated Yield

### 3.11.7 Conclusion

We have developed efficient Cu-Mo bimetallic nanoparticles catalysts for the synthesis of 2-aryl benzothiazole with high yield of product in short reaction time and very less amount of catalyst. This catalyst showed excellent activity during four consecutive runs without appreciable loss of

activity. Furthermore, this method is of interest in the context to environmentally greener and safer processes.

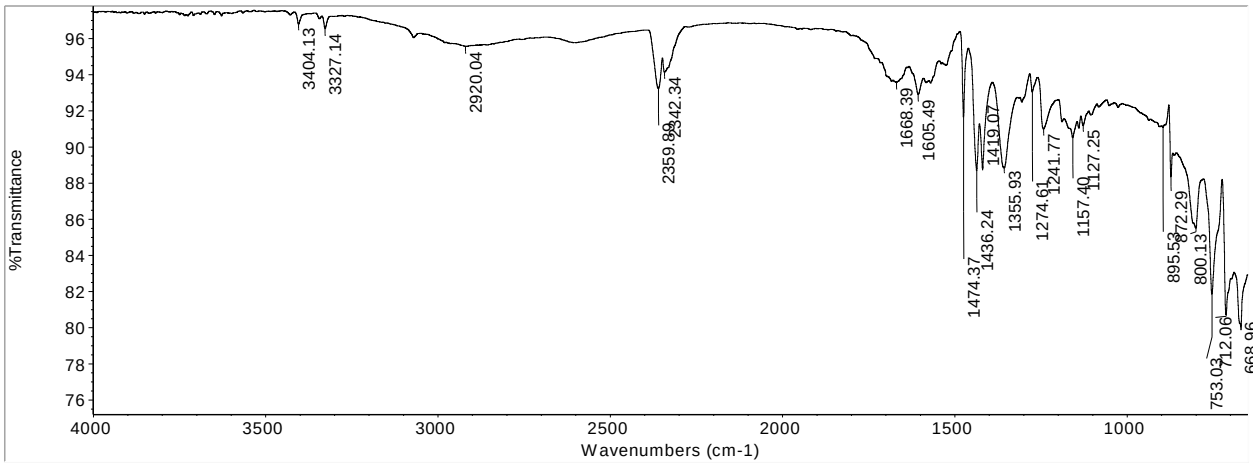


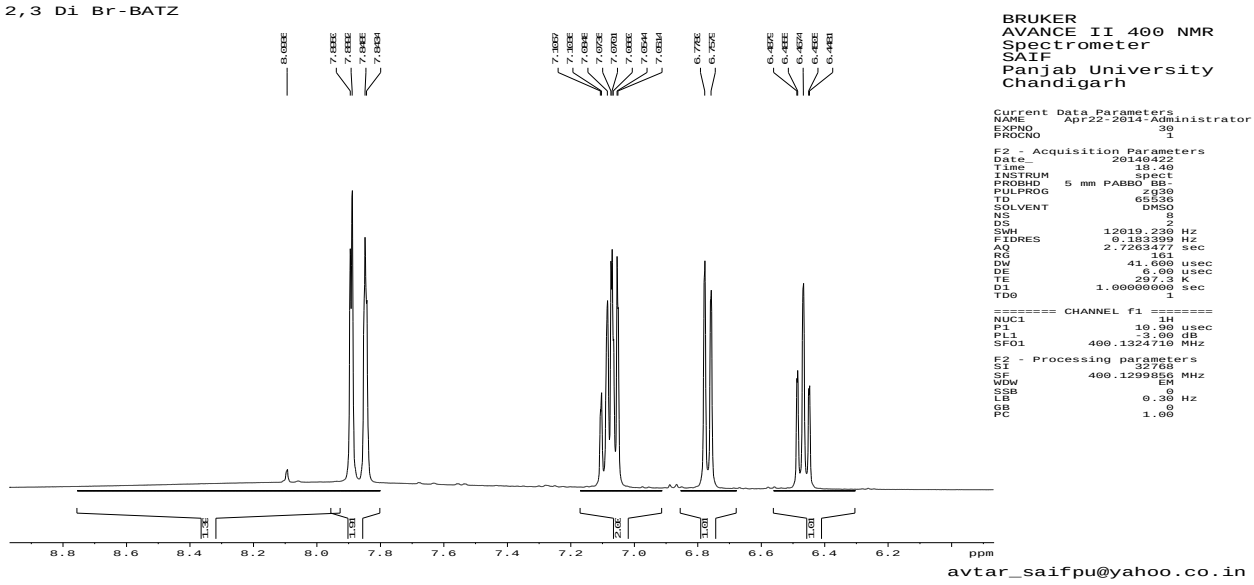


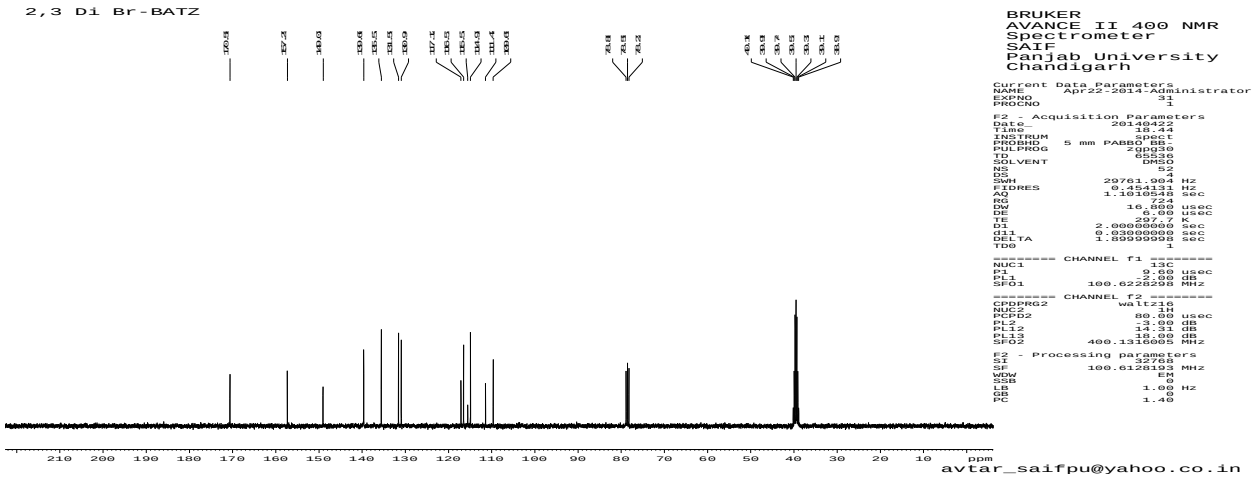

## 3.12 **Synthesis of (Z)-5-benzylidenethiazolidine-2,4-dione derivatives catalyzed by Cu-Mo nanoparticles**

### 3.12.1 Introduction

There are numerous biologically active molecules which contain various heteroatoms such as nitrogen, sulphur and oxygen have always drawn the attention of chemist over the years mainly because of their biological importance. Thiazolidinediones (TZD's) or glitazones forms a significant class of drugs which exhibits various biological activities. 1, 3-thiazolidine 2, 4-Dione contains basic skeleton of thiazole or thiazolidine [229]. Presence of one carbonyl group in thiazole at $4^{th}$ position makes it thiazolidine-4-one which is known for various activities such as antiinflammatory and presence of another carbonyl group at $2^{nd}$ position makes it thiazolidine-2, 4 Dione which is basically known for its antidiabetic activity. Its derivatives constitute an interesting class of compounds due to their synthetic versatility and effective biological activity Thiazolidinones are thiazolidine derivatives and have an atom of sulfur at position 1, an atom of nitrogen at position 3 and a carbonyl group at position 2, 4, or 5. However, its derivatives belong to the most frequently studied moieties and its presence in penicillin was the first recognition of its occurrence in nature [230-231]. Similarly 1,3-thiazolidin-4-ones are heterocyclic nucleus that have an atom of sulfur and nitrogen at position 1 and 3, respectively and a carbonyl group at position 4 have been subjected to extensive study in the recent years. The 4-thiazolidinone scaffold is very versatile and has featured in a number of clinically used drugs. 4-Thiazolidinone derivatives are an important group of heterocyclic compounds possessing a variety of biological effects [232], including antitumor [233-235], anti-inflammatory [236], antimicrobial [237], antiviral [238], anticonvulsant [239], antifungal [240], antibacterial [241] activities and and as antiviral agents, especially as anti-HIV agents.

It has been extensively reported that presence of arylazo [242], sulfamoylphenylazo [243] or phenylhydrazono [244] moieties at different positions of the thiazolidone ring enhanced anti-microbial activity and its antibacterial activity may be due to its inhibitory activity of enzyme MurB which is precursor acting during the biosynthesis of peptidoglycan [245]. Numerous reports have appeared in the literatures which highlight their chemistry and pharmacological uses [246-248].

### 3.12.2 Literature review

Several methods for the synthesis of 4-thiazolidinones are widely reported in the literature. The main synthetic routes to 1,3-thiazolidin-4-ones involve three components that is an amine, a carbonyl compound, and a mercapto-acid. The classical synthesis reported can be either a one-pot three-component condensation or a two-step process. The reactions begin by formation of an imine (the nitrogen of amine attacks the carbonyl of aldehyde or ketone) which undergoes attack by generated sulfur nucleophile followed by intramolecular cyclization on elimination of water [249-251]. Eltsov et al. reported an convenient one-step cyclization reaction protocol wherein the reaction of ethyl 5-phenyl-thioureido-3H-imidazole-4-carboxylate with bromoacetic acid afforded (imidazolylimino) thiazolidinones. The cyclization reaction proceeds by one of the nitrogen atoms of the nucleophilic centers in derivatives of 5-thioureido-3H-imidazole-4-carboxylic acid give the desired thiazolidinone [252]. Furthermore, novel route to the synthesis of 2-isopropyl-3-benzyl-1,3-thiazolidin-4-ones and 2-phenyl-3-isobutyl-1,3-thiazolidin-4-ones by using 1:1:3 mole ratio of valine, arenealdehyde and mercaptoacetic acid was reported by Cunico et al.[253] and suggested that the insertion of strong withdrawing group, $NO_2$, present on benzaldehydes favored the synthesis of hetero-cycle in good yield, whereas the methoxy and fluoro groups produces the type 2 thiazolidinones.

In continuation of research, authors reported solvent-free synthesis of five-membered heterocyclic thiazolidinones from phenylhydrazine and 2,4-dinitrophenylhydrazine as the amino cores [254]. Pratap et al.[255] have reported another method of synthesis of 2,3-diaryl-4-thiazolidinones wherein Saccharomyces cerevisiae (baker's yeast) that contained enzyme lipase was used as a catalyst which accelerated the formation of imines as well as cyclo-condensation of the aryl aldehydes, amines, and thioglycolic acid Various quinazolinyl azomethines on treatment with mercaptoacetic acid in the presence of silica chloride that was used as a heterogeneous catalyst to accelerate the intra-molecular cyclocondensation under solvent-free condition, yield 4-thiazolidinones.Furthermore, the reaction of aryl or alkyl isothiocyanate with a primary amine furnished the corresponding thiourea derivative, which was directly cyclized by treating with halo acetic acid to the corresponding two isomeric 2-imino-thiazolidin-4-ones of the general structures[256]. Also, coupling reaction between a chloro amide derivatives with isothiocyanate in the presence of a mild base afforded the iminothiazolidinone derivatives[157]. Bolognese et al.[258] prepared a range of 1,3-thiazolidin-4-one derivatives by the microwave-

assisted reaction between benzylidene-anilines and mercaptoacetic acid in benzene at 30°C for 10 min. After purification by chromatography, the 1,3-thiazolidin-4-ones are isolated in 65–90% yield.

### 3.12.3 Present work

Electrochemically prepared Cu-Mo bimetallic nanoparticles were tested on the synthesis of (Z)-5-benzylidenethiazolidine-2,4-dione derivatives (Scheme -11). The short reaction time, solvent free reaction condition, consistent yield and minimum environmental effect were important features of the reaction.

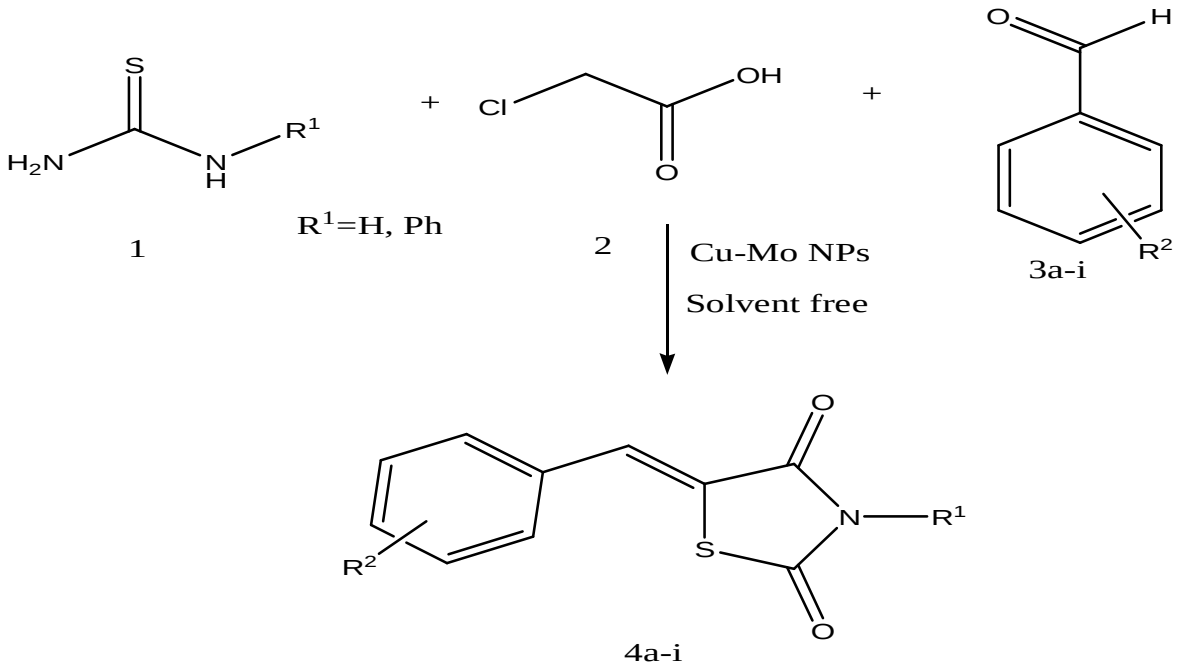


**Scheme 11**

### 3.12.4 Experimental

The melting points of compounds were taken in an open capillary in a paraffin bath. IR spectra were recorded on a Jasco FTIR-4100 spectrophotometer. $^{1}$H NMR spectra were recorded on an 400 MHz FT-NMR spectrometer in DMSO as a solvent and chemical shift values were recorded in units δ (ppm) relative to tetramethylsilane ($Me_4Si$) as an internal standard.

**General procedure**

A mixture of thiourea or phenyl thiourea (1mmol), chloro acetic acid (1 mmol), aromatic aldehyde (1 mmol) & Cu-Mo bimetallic nanoparticles (100 mg) was stirred at 80°C in solvent free condition to obtain (Z)-5-benzylidenethiazolidine-2,4-dione crude product. The progress of reaction was monitored by TLC. After completion of reaction, the crude product was dissolved

by adding ethanol and the Cu-Mo bimetallic nanoparticles were separated by centrifuging, followed by decantation. Cu-Mo bimetallic nanoparticles were dried in vacuum desiccators and crude product recrystallized in ethanol. The recrystallized product analysis by FTIR, $^{1}$H NMR and $^{13}$C NMR spectra was recorded.

**3.12.5 Spectral data of representative compound**

5-(4 Br benzylidenethiazolidine-2,4-dione) : FTIR (KBr, $cm^{-1}$) 2917, 2851, 1663, 1583, 1508, 1473, 1329, 1272, 1073,1017, 973,851,750,722 $cm^{-1}$; $^{1}$HNMR (400 MHz, DMSO, δ ppm); 7.0 (d, 2H), 7.20(t, 2H), 7.38(t, 5H), 7.51(d, 1H), 7.58(t, 2H) 7.67(d, 2H), 7.82(d, 1H); $^{13}$CNMR (400 MHz, DMSO, δ ppm): 30.8, 78.5, 131.50, 135.6, 138.5, 141.6, 144.2, 160

**3.12.6 Result discussion**

We report here a very simple one pot synthesis of (Z)-5-benzylidenethiazolidine-2,4-dione derivatives by condensation of thiourea or phenylthiourea, chloro acetic acid with aromatic aldehyde under solvent free conditions catalyzed by Cu-Mo bimetallic nanoparticles. In the present work, an attempt has been made to optimize the reaction conditions by using thio urea(1mmol) **1,** chloro acetic acid(1 mmol) **2** and benzaldehyde (1 mmol) **3a** as model reaction at different solvents and amount of catalyst used. In order to investigate the best results in terms of yield & reaction time, we have examined the efficiency of different reaction media and the amount of catalyst required. From Table 3.12.1, it can be seen that loading of 100mg of Cu-Mo bimetallic nanoparticles catalyst were adequate for smooth condensation of 2 aminothiophenol and 4-chlorobenzoic acid under solvent free condition at 60°C. There is considerable increase in the yield of product when amount of catalyst is increased from 50 mg to 100 mg; above 100 mg, no considerable change in reaction time and yield of the product was observed.

Table3.12.1 Screening of catalyst Cu-Mo NPs for synthesis of (Z)-5-benzylidenethiazolidine-2,4-dione.

| Entry[a] | Catalyst Amount (mg) | Time (Min) | Yield[b] (%) |
|---|---|---|---|
| 1 | 00 | 180 | - |
| 2 | 40 | 120 | 25 |
| 3 | 60 | 110 | 54 |
| 4 | 80 | 80 | 84 |
| 5 | 100 | 50 | 93 |
| 6 | 120 | 50 | 93 |

[a]Reaction condition: benzaldehyde (1mmol), chloro acetic acid (1mmol), thiourea (1mmol) and Cu-Mo NPs
[b]Isolated Yield

The catalyst was recovered by simple work-up using centrifugation method, washed with ethanol and reused for three successive reactions. The corresponding yield for each cycle was mentioned in Table 3.12.2.

Table 3.12.2 Reusability of catalyst Cu-Mo bimetallic nanoparticles

| Entry[a] | 1 | 2 | 3 | 4 |
|---|---|---|---|---|
| No. of recycle | Fresh | I | II | III |
| Yield[b] (%) | 95 | 94 | 92 | 89 |

[a]Reaction condition: benzaldehyde (1mmol), chloro acetic acid (1mmol), thiourea (1mmol) and Cu-Mo NPs
[b]Isolated Yield

Under optimization reaction condition, we obtained 93% yield of (Z)-5-benzylidenethiazolidine-2,4-dione within 50 mins. In Table 3.12.3, the reaction time & the product yield depends on the substituents introduced on substrates. For instance, one pot synthesis of (Z)-5-benzylidenethiazolidine-2,4-dione derivatives having strong electron withdrawing groups (F, Cl, Br, $NO_2$, OH) in para position gave the desired product with good yield and shorter reaction time than meta substituted product and electron donor groups($CH_3$, $OCH_3$).

Table 3.12.3 Synthesis of (Z)-5-benzylidenethiazolidine-2,4-dione derivative using Cu-Mo NPs

| Products[a] | $R^1$ | $R^2$ | Time (min) | Yield[b](%) | Melting point(°C) | |
|---|---|---|---|---|---|---|
| | | | | | Found | Reported |
| 3a | H | 4-Cl | 50 | 95 | 238-240 | 238-242 |
| 3b | H | 4-$NO_2$ | 50 | 94 | 265-266 | 266-268 |
| 3c | H | 2-$CH_3$ | 100 | 85 | 240-242 | 240-242 |
| 3d | H | 4-$OCH_3$ | 110 | 86 | 240-241 | 240-242 |
| 3e | H | 4-F | 60 | 80 | 130-132 | 130-135 |
| 3f | H | 3-$NO_2$ | 80 | 87 | 188-190 | 189-192 |
| 3g | H | 2-OH | 90 | 88 | 232-233 | 232-235 |
| 3h | Ph | H | 85 | 88 | 267-270 | 268-270 |
| 3i | Ph | 4-Br | 90 | 90 | 294-295 | 298 |

[a]Reaction condition: benzaldehyde (1mmol), chloro acetic acid (1mmol), thiourea (1mmol) and Cu-Mo NPs
[b]Isolated Yield

### 3.12.7 Conclusion

We have developed efficient Cu-Mo bimetallic nanoparticles catalysts for the one pot solvent free synthesis of (Z)-5-benzylidenethiazolidine-2,4-dione with high yield of product in short reaction time and very less amount of catalyst. This catalyst showed excellent activity during four consecutive runs without appreciable loss of activity. Furthermore, this method is of interest in the context to environmentally greener and safer processes.

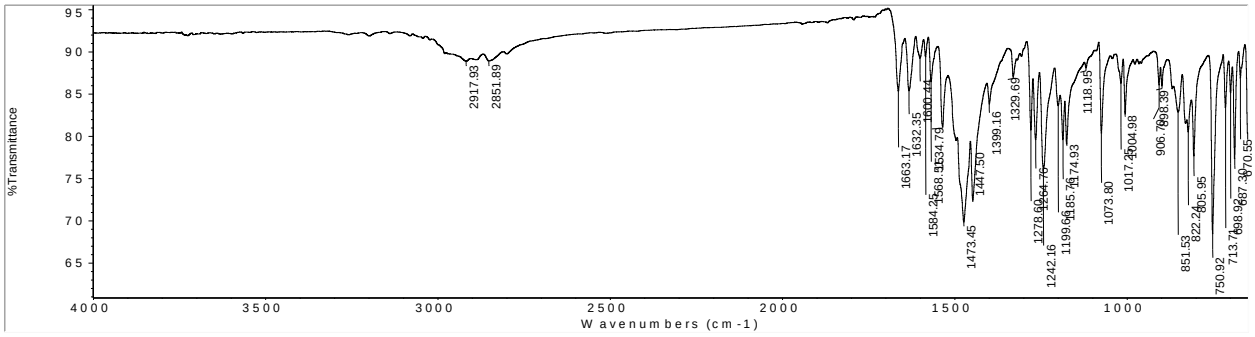


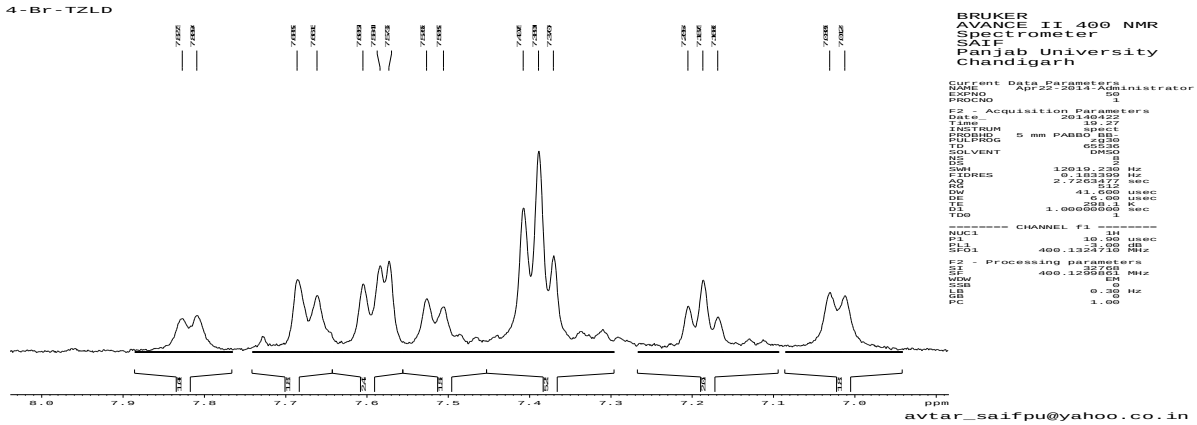


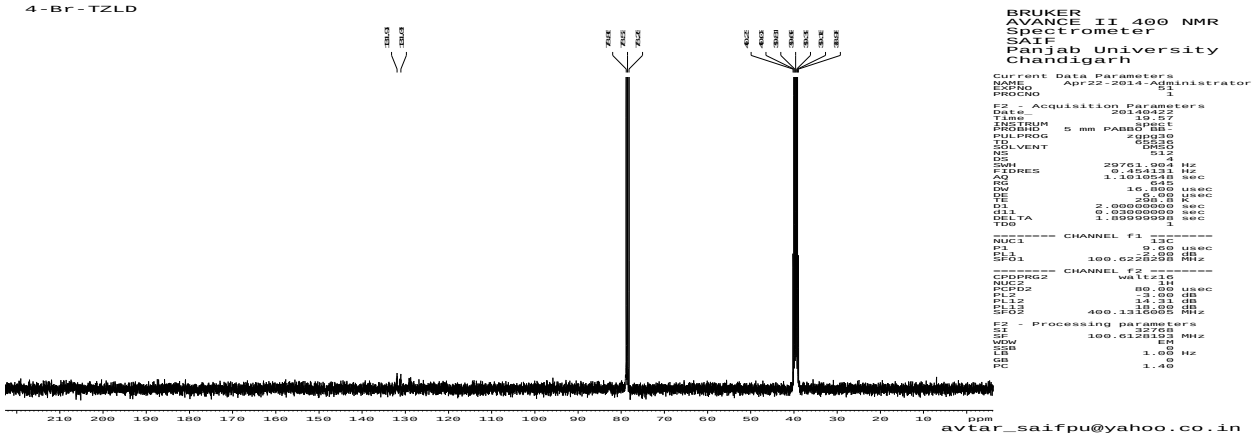


## 3.12.8 Reference:


1. Herzing A.A., Kiely C.J., Carley A.F., Landon P., Hutchings G.J., *Science*, **(2008),** 321,1331.
2. Beatriz R.C., *Thin Solid Films*, **(2010)**, 518, 3127–3150.
3. Narayanan R., in "Shape-dependent Nanocatalysis and the effect of catalysis on the shape and size of colloidal metal nanoparticles" thesis submitted to *Georgia Institute of Technology,* **(2005)**.
4. (a) Liew K.H., Loh P.L., Juan J.C., Yarmo M.A., Yusop R.M., *The Scientific World Journal*, **(2014)**, doi: dx.doi.org/10.1155/2014/796196. (b) Schmid G.and Corain B., *Eur. J. Inorg. Chem.*, (**2003)**, 3081-3098.

5. Hou W., Dehm N.A. and Scott R.W.J., *J. Catal.*, (**2008)**, 253, 22-27.
6. (a) Shi F., Man K.T., Pohl M-M, Brückner A., Zhang S., Angew M.B. *Chem. Int. Ed.* **(2007)**, 46, 8866 –8868.(b) Martínez M., Ocampo R., Rios L.A., Ramírez A. and Giraldo O., *J. Braz. Chem. Soc.*, **(2011)**, 22(12), 2322.
7. Shobeiri Z., Pourayoubi M., Heydari A., et al, *C. R. Chimie*, **(2011)** 14597–603 (b) Ma L, Peng Q, He D. *Catal Lett*, **(2009)**, 130, 137.
8. Safari J., Khalili S.D., Rezaei M., Banitaba S.H., Meshkani F. *Monatsh Chem*, **(2010)**, 141, 1339.
9. Tietze L.F. and Beifuss U., Comprehesive organic synthesis, by Trost B. M., Flaming I. and Heathcock C. H., *Pergoman Press Oxford*, **2**, 341-394 (**1919**)
10. Borjarski J. T., Mokros J. L., Barton H. J. and Paluchowska M. H., *Adv. Heterocyc. Chem*, **38,** 229-297(**1985**)
11. Cheng X., Tanaka K. and Yoneda F., *Chem. Pharm. Bull.*, **38,** 307-311 (1990)
12. Gulliya K. S., Uses for barbituric acid analogs, *US Patent*, 5869494A, (**1999**)
13. Gulliya K. S., Anti-cancer uses for barbituric acid analogs, *US Patent*, 5674870, (**1997**)
14. Naguib F. N. M., Levesque D. L., Wang E. C., Panzica R. P. and Kouni El. M. H., *Biochem. Pharmacol*, **46**, 1273-1283 (**1993**)
15. Grams F., Brandstetter H. and D'Alo S., *Biol. Chem*., **382**,1277-1285 (**2001**)
16. Sakai K. and Satoh Y *International Patent*, W09950252A3, (**2000**)
17. Tanaka K., Chen X., Kimura T. and Yoneda F., *Tetrahedron Lett.*, **28**, 4173-4176 (**1987)**
18. Tanaka K., Chen X., Kimura T. and Yoneda F., *Chem. Pharm. Bull.*, **34**, 3945-3948 (**1986**)
19. Li J. T., Dai H. G., Liu D. and Li T. S., , *Synth. Commun*., **36**, 789-794 (**2006**)
20. Alarreca G., Sanabria R., Miranda R., Arroyo G., Tamariz J. and Delgado F., *Synth. Commun*., **30**, 1295-1301 (**2000**)
21. Dewan S. and Singh R., *Synth. Commun.*, **33**, 3081-3084 (**2003**)
22. Wang C., Ma J., Zhou X., Zang X., Wang Z. Gao Y. and Cui P., *Synth. Commun.*, **35**, 2759-2764 (**2005**)
23. Rao P. S. and Venkataratnam R. V., *Tetrahedron Lett.*, **32**, 5821-5822,(**1991**)
24. Prajapati D. and Sandhu J. S., *J. Chem. Soc. Perkin Trans.*, **1**, 739-740 (**1993)**
25. Pullabhotla Rajasekhar V. S. R., Rahman A. and Jonnalagadda S. B., *Catal. Commun.*, **10**, 365-369 (**2009**)
26. Dai G., Shi D., Zhou L. and Huaxue Y., *Chin. J. Appl. Chem.*, **12**, 104-108 (**1995**)
27. Sebti S., Smahi A. and Solhy A *Tetrahedron Lett.*, **43**, 1813-1816 (**2002**)
28. Bennazha J., Zahouily M., Boukhari A. and Holt E. M., *Catal. Commun.*, **2**, 101-104 (**2001**)
29. Maadi El. A., Matthiesen C. L., Ershadi P., Baker J., Herron D. M., Holt E. M., *J. Chem. Cryst.*,**33**,757 (2003)
30. Deb M. L. and Bhuyan P. J., *Tetrahedron Lett.*, **46**, 6453-6456 (**2005**)
31. Khurana J. M. and Vij K., *Catal. Lett.*, **138**, 104-110 (**2010**)
32. Kaur J. R. and Kaur G., *Chinese Journal of Catalysis*, **34**, 1697-1704 (**2013**)
33. Chen G. M., Brown H.C., *J. Am Chem. Soc.* 112, 2000, 4217.
34. Hothi H. S., Makkar A., Sharma J.R., Manrao M.R., *Eur J Med. Chem*. 42, 2006,253.
35. Sidhu A., Rai M. *Ind. J. Chem B* 47, 2008,778.
36. Sandhar R.K., Sharma J. R., Manrao A. R. *J. Ind. Chem. Soc*.,85, 2008, 220.
37. Jones G. Inorganic Reaction, Wiley, New York, Volume 15: 204,1967.
38. Reeves RL and Patai S. Interscience publishers, New York, 567 1996.
39. Tietze LF, Beifuss U, Trost BM, Fleming I and Heathcock CH. comprehensive organic. synthesis pergamon press, oxford Volume 2: 341 1991.
40. Martin CA and Aranda RM. Appl. Catal. A 1993; 105: 271-279.
41. Tietze LF. Chem Rev., 1996; 96: 115.
42. Freeman, F. *Chem. Rev.* **1981**, *80*, 329.
43. Fatiadi, A. J. *Synthesis* **1978**, 165 and 241

44. *Japan Pharmaceutical References*, First ed.; 1989-90; p 144.
45. Abbott, T.; Johnson, J. *Org. Synth.* Coll.; John Wiley and Sons: New York, 1941; Vol. I, p 440.
46. Rong, L.; Li, X.; H, Li.; Wang, D. S.; Tu, S.; Zhuang, Q. *Synth. Commun*. **2006**, *36*, 2407.
47. Dave, C. G.; Augustine, C. *Indian J. Chem.* **2000**, *39B*, 403.
48. Liu, X.-W.; Jiang, H.; Gong, H. *Chinese J. Org. Chem*. **2007**, *27*,131
49. Abaee, M. S.; Mojtahedi, M. M.; Zahedi, M. M.; Khanalizadeh, G. *Arkivoc* **2006**, *xv*, 48
50. Bandgar, B. P.; Uppalla, L. S.; Sadavarte, V. S. *J. Res* (*S*) **2002**, 40.
51. Kidwai, M.; Sapra, P.; Bhushan, K. R. *J. Indian Chem. Soc.***2002**, *79*, 596.
52. Shi, D. Q.; Wang, X. S.; Yao, C. S.; Mu, L. *J. Chem. Res* (*S*) **2002**,344.
53. Sebti, S.; Nazith, R.; Tahir, R.; Saber, A. *Synth. Commun.* **2001**,*31*, 993.
54. Peng, Y.; Song, G. *Indian J. Chem.* **2003**, *42B*, 924.
55. Zuo, W. Z.; Hua, R.; Qiu, X. *Synth. Commun.* **2004**, *34*, 3219.
56. Reddy, K. R.; Maheshwari, C. U.; Lakshmikantam,M. *New J. Chem.* **2006**, *30*, 1549.
57. Khan, F. A.; Dash, J.; Satapathy, R.; Upadhay, S. K. *Tetrahedron Lett.* **2004**, *45*, 3055.
58. Zhng, X.; Lai, E. M.; Aranda, R. M.; Yeung, K. L. *Appl. Catal. A:Gen.* **2004**, *261*, 109.
59. Tamami, B.; Fadavi, A. *Iranian Poly. J.* **2006**, *15*, 331.
60. Sebti, S.; Smahi, A.; Solhy, A. *Tetrahedron Lett.* **2002**, *43*, 1813.
61. Jin, T. S.; Zhang, J.-S.; Wang, A.-Q.; Li, T.-S. *Synth. Commun.***2004**, *34*, 2611.
62. Oskooie, H. A.; Heravi, M. M.; Derikvand, F.; Khorasani, M.*Synth. Commun.* **2006**, *36*, 2819.
63. Jones, G. Organic Reactions, Wiley, New York, 1967; Vol. 15, P.204.
64. Angeletti, I.; Canepa, C.: Martinetti, G.; Venturello, P.Tetrahedron Letts.. 1988, 29, 2261.
65. Hopkins, J. M.; Bowdridge, M.; Robertson, K. N.; Cameron, T. S.; Jenkins, H. A.;Clyburne, J. A. C. J. Org. Chem. 2001,66, 5713–5716.
66. Wu, C. Y.; Chen, Y.; Jing, S. Y.; Hwang, W. S. Polyhedron 2006, 25, 3053–3065.
67. Machado, H. J. S.; Hinchliffe, A. J. Mol. Struct.1995,339, 255–258.
68. Greene, T. W.; Wuts, P. G. Protective Groups in Organic Synthesis, 2nd ed.; Wiley:New York,1999; p. 24.
69. Tajbakhsh, M.; Hosseinzadeh, R.; Ramazanian-Lahmali, F.; Sadatshahabi, M.J. Chin. Chem. Soc.2005,52, 1005–1009.
70. Bandgar, B. P.; Makone, S. S. J. Chin. Chem. Soc.2000,47,575–577.
71. Nalwa, H. S.; Kakatu, A.; Mukoh, J. Appl. Phys.1993,73, 4743.
72. Kesslen, E. C.; Euler, W. B. Chem. Mater.1999,11, 336.
73. Rep, M.; Kaagman, J.-W. F.; Elsevier, C. J.; Sedmera, P.; Hiller, J.; Thewalt, U.;
74. Horacek, M.; Mach, K. J. Organomet. Chem.2000,597, 146–156.
75. Zippel, T.; Arndt, P.; Ohff, A.; Spannenberg, A.; Kempe, R.; Rosenthal, U. organometallics1998,17,4429–4437.
76. Kiplinger, J. L.; Morris, D. E.; Burns, C. J. Organometallics2002,21(15), 3073–3075.
77. Zimniak, A.; Bakalarski, G. J. Mol. Struct.2001,597, 211–221.
78. Ammar, A. H.; El-Sayed, B. A.; El-Sayad, E. A. J. Mat. Sci.2002,37, 3255–3260.
79. R. M. Mohareb, J. Z. Ho, and F. O. Alfarouk Journal of the Chinese Chemical Society, vol. 54, no. 4, pp. 1053–1066, 2007.
80. R. Manikannan, R. Venkatesan, S. Muthusubramanian, P. Yogeeswari, and D. Sriram Bioorganic and Medicinal Chemistry Letters, vol. 20, no. 23, pp. 6920–6924, 2010.
81. V. M. Kolb, D. H. Hua, and W. L. Duax, J.of Org.Chem., vol. 52, no.14, pp. 3003–3010, 1987.
82. V. M. Kolb and D. H. Hua, Journal of Organic Chemistry, vol. 49, no. 20, pp. 3824–3828, 1984
83. Sanz, D.; Ponce, M. A.; Claramunt, R. M.; Fernandez-Castano, C.; Foces-Foces, C.;Elguero, J. J. Phys. Org. Chem.1999,12, 455–469.
84. T. K. Huang, R. Wang, L. Shi, and X. X. Lu, Catalysis Communications,vol. 9, no. 6, pp. 1143–1147, 2008.
85. T. Joseph, G. V. Shanbhag, D. P. Sawant, and S. B. Halligudi,Journal of Molecular Catalysis A, vol. 250, no. 1-2, pp.210–217, 2006.

86. F. R. Crisóstomo, R. Carrillo, T. Martın,andV.S.Martın,Tetra.Lett., 46 (16), 2829–2832,2005.
87. T. Kawabata, T. Mizugaki, K. Ebitani, K. Kaneda, Tetra. Lett., 44(51) 9205–9208, 2003.
88. A. I. Vogel,Text book of Prac. Org. Chem., ELBS Longman, London, UK, 4th edition, 1978.
89. H. M. Nanjundaswamy and M. A. Pasha, Synth. Commun., 36(21) 3161–3165, 2006.
90. S. N. Shah and N. K. Chudgar, Molecules, vol. 5, no. 4,pp. 657–664, 2000.
91. H. Eshghi and M. Hosseini, Journal of the Chinese Chem. Soc., . 55, 3,636–638, 2008.
92. J. Safari and S. Gandomi-Ravandi, Synthetic Communications,vol.41,no.5,pp.645–651, 2011
93. Reeves RL In: S. Patai (Ed.), Chem. of Carbonyl Group, Wiley Interscience, New York, 1966.
94. Robinson T.P., Ehlers T., Hubbard R.B., Bai X., Arbiser J.L., Goldsmith D.J., Bowena J.P., Bioorg. Med. Chem. Lett., 13 (2003),115.
95. Dimmock J.R., Padmanilayam M.P., Zello G.A., Nienaber K.H., Allen T.M., Santos C.L., De Clercq E., Balzarini J., Manavathu E.K., Stables J. P., Eur. J. Med. Chem., 38(2003), 169.
96. Piantadosi C., Hall I.H., Irvine J.L., Carlson G.L., J. Med. Chem. 16(1973), 770.
97. Kawamata J., Inoue K., Inabe T., Kiguchi M., Kato M., Taniguchi Y., Chem Phys Lett 249(1996), 29.
98. Deli J., Lorand J., Szabo D., Foldesi A., Pharmazie, 39(1984), 539.
99. Ogawa M., Ishili Y., Nakano T., Irifune S., Japan Kohai Tokyo JP 63192446 A2, 1988.
100. Xiaofang L., Xianyong Y., Yaqing F., Chin. J. Chem. 27(2009), 1531.
101. Kaushal G. K., Polymer, 36(1995), 1903.
102. Artico M., Santo R.D., Costi R., Novellino E., Greco G., Massa S., Tramontano E., Marogiu M.F., Montis A.D., Colla P.L., J. Med. Chem., 41(1998),3948.
103. Sinisterra J.V., Garcia-Raso A., Synthesis, (1984) 502.
104. Hathaway B. A., J. Chem. Edu. 64(1987), 367.
105. Irie K., Watanabe K., Bull. Chem. Soc. Jpn., 53(1980), 1366.
106. Zheng M, Wang L, Shao J, Zhong Q. Synth Commun, 27(1997),351
107. Yadav J.S., Reddy B.V.S., Nagaraju A., Sarma J.A.R.P., Synth. Commun., 32(2002), 893.
108. Mahdavinia G.H., Mirzazadeh M., E- Journal of chemistry 9(1) (2012), 49.
109. Ziani N., Lamara K., Sid A., Willem Q., Dassonneville B., Demoneceau A., Eur. Journal of Chemistry, 4(2) (2012),176.
110. Das B., Thirupathi P., Mahender I., Reddy K.R., J. Mol. Catal. A: Chem., 247(2006), 182.
111. Salehi P., Dabiri M., Zolfigol M.A., Bodaghi Fard M.A., J. Braz. Chem. Soc. 15(2004), 773.
112. Wang L.M., Sheng J., Tian H., Han J.W., Fan Z.Y., Qian C., Synthesis, 18 (2004) 3060.
113. Jianjun L., Weike S., Ning L., Synthetic Communications, 35(2005), 3037.
114. Zhou J.F., Sun X.J., Zhu F.X., Li Y.L., Gong G.X., Synth. Commun., 38(2008), 4182.
115. Amoozadeh A., Rahmani S., Nemati F., S. Afr. J. Chem., 63(2010), 72.
116. Girija D., Halehatty BhojyaNaik S., VinayKumar B., Sudhamani C.N., Am. Chem. Sci. Journal, 1(3) (2011), 97.
117. Babu G., Perumal P.T., Synth. Commun., 27(1997), 3677
118. Li J., Yang W., Chen G., Li T., Synth. Commun. 33(2003), 2619.
119. Handayani, S dan Arty, I.S., Journal of Physical Chemistry, 19(2), 2008,62.
120. Motohashi, N., Ashisara, Y., Yamagami, C., and Saito, Y., Mutation Research/Fundamental and Molecular Mechanism of Mutagenesis, 474, 2001, 113.
121. Guofeng, C., Jitai, L., Huiyun, D and Tongshuang, L. Chem. Journal on Internet, 6(1), 2004, 7.
122. Reddy D B, Padmavathi V, Ramana Reddy P V. Indian J. Chem., 1992, 31B: 774.
123. Hamanaka N, Nakai H, Kurono M. Bull. Chem. Soc. Jpn., 1980, 53: 2327.
124. Angiolini L, Caretti D, Carlini C et al. Polymer, 1995, 36 (5): 1071.
125. Hathaway B A. J. Chem. Edu., 1987, 64 (4): 367.
126. Hull L A. J. Chem. Edu., 2001, 78 (2): 226.
127. Wattanasin S, Murphy W S. Synthesis, 1980, 8: 647.
128. Gupta R, Gupta A K, Paul S et al. Indian J. Chem.,1995, 34B: 61.
129. Handayani,S., Proceeding of Chemistry, Biology and Environmental Engineering, 2009,1423

130. Pudjono, Sismindari and Widada, H,Majalah Farmasi Indonesia, 19(1),2008, 48.
131. Ordomsky, V.V., Sushkevich, V.L. and Ivanova, I.I. Journal of Molecular Catalyst A: Chemical, 2010,333.
132. Kustrowski, P., Sulkowska, D., Chmielarz, L. and Dziembaj, R.Applied Catalysis A: General, 302, 2006, 317.
133. Cavani, F., Trifiro, F., Vaccari, A., Catalysis Today, 11, 1991,173.
134. Li, Z., Novel Solid Base Catalyst for Michael Additions : Synthesis, Chac. and Application, Dissertation, 2005, Humboldt-Universitat zu Berlin, Germany
135. Fatimah,I., Wijaya, K. Setyawan, K.H., Bulletin of Reaction Eng. and Catalyst, 2, 2008, 9.
136. Li J T, Li L J, Li T S et al. Indian J. Chem., 1998, 37B: 298.
137. Li J T, Chen G F, Wang J X et al. Synth. Commun., 1999, 29 (6): 965
138. Palmer P.J., Trigg R.B., Warrington J. V., Benzothiazoline as antituberculous agents. J. Med. Chem. 1971, 14, 248-251.
139. Ertan T., Yildiz I, Tekiner-Gulbas B. Bolelli K., temiz-Arpaci O., Ozlan S. Kaynak F. Yelcin I., Aki E., Eur. J. Med. Chem. 2009, 44, 501.
140. Evans, D. A.; Sacks, C. E.; Kleschick, W. A.; Taber, T. R. *J. Am. Chem. Soc.* **1979,** *101,* 6789.
141. Paget C. J., Kisner K. Stone R. L., Delong D.C., J. Med. Chem. 1969, 12, 1016-1018.
142. a) Srinivas A., Sagar J. V. Srangapani M. J. Chem. Pharma. Res. 2010, 2, 319. b) D. Ravi Sankar Reddy R. L. Priyadarshine. Der Pharma Chemica, 2013, 5(4):207-212
143. Yamato, M. *Yakugaku Zasshi* **1992**, *112*, 81.
*144.* C-O Leong, M Gaskell, E A Martin, R T Heydon, P B Farmer, M C Bibby, P A Cooper, J A Double, T D Bradshaw, M F G Stevens Br. J. Cancer. 2003 Feb 10; 88(3): 470–477.
*145.* Beneteau, V.; Besson, T.; Guillard, J.; Leonce, S.; Pfeiffer, B. *Eur.J. Med. Chem*. **1999**, *34*, 1053
146. Benazzouz, A.; Boraud, T.; Dubèdat, P., Boireau, A.; Stutzmann, J.-M.; Gross, C. *Eur. J. Pharmacol*. **1995**, *284*, 299.
147. R. Caujolle, P. Loiseau, M. Payard, P. Gayral, Ann Pharm Fr. 1989: 47(2), 68-73.
148. Yamamoto K, Fujita M, Tabashi K, Kawashima Y, Kato E, Oya M, Iso T, Iwao J. J. Med. Chem. (1988) 31:919-930
149. Ivanov S. K., Vuritsyn V. S. Neftekhimiya 1971, 11, 99-107
150. Kotani T, Nagaki Y, Ishii A, Konishi Y, Yago H, Suehiro S, Okukado N and Okamoto K 1997 *J. Med. Chem.* **40** 684
151. Sohn S K, Chang M S, Choi W S, Kim K B, Woo T W, Lee S B and Chung Y K 1999 *Can. J. Physiol. Pharmacol.* **77** 330
152. Caccese R G, DiJoseph J F, Scotnicki J S, Borella L E and Adams L M 1991 *Agents Actions* **34** 223
153. Paramashivappa R, Kumar P P, Rao P V S and Rao A S 2003 *Bioorg. Med. Chem. Lett.* **13** 657
154. Deluca M R and Kerwin S M 1997 *Tetrahedron Lett.* **38** 199
155. Edwards P D, Meyer E F, Vijayalakshmi J, Tuthill P A, Andisik D A, Gomes B and Strimpler A 1992 *J. Am.Chem. Soc.* **114** 1854
156. Rodriguez A D, Ramrez C, Rodiguez I I and Gonzalez E 1999 *Org. Lett.* **1** 527
*157.* Nakagawa K, Onoue H and Sugita J 1964 *Chem. Pharm. Bull.* **12** 1135
158. Kidwai M, Bansal V, Saxena A, Aerry S and Mozumdar S 2006 *Tetrahedron Lett.* **47** 8049
159. Speier G *J. Mol. Catal.* 1987**41** 253
160. Bougrin, K.; Loupy, A.; Soufiaoui, M. *Tetrahedron* **1998**, *45*, 8055- 8064.
161. Al-Qalaf, F.; Mekheimer, R.A.; Sadek, K.U *Molecules* **2008**, *13*, 2908–2914
162. Michael OC, Paul VD, Noel DJ, John LO. J Am Chem Soc 1974; 96: 1932-1933.
163. (a) Brown RN, Cameron R, Chalmers DK, Hamilton S, Luttick A, Krippner GY, McConnell DB, Watson KG, Bioorg Med Chem Lett 2005; 15: 2051
164. Clussen U, Harnisch H. Eur Pat Appl 1981; 25:136.
165. Stendby S. Surfactant Sci Ser 1981; 5: 729.

166. Reser A, LeyshonL J, Saunders D, Mijovic MV, Bright A, Bogie J. J Am Chem Soc 1972; 94: 2414-2421.
167. Roussilhe J, Fargin E, Despax B, Lopez A, Despax B, Pailous N. J Org Chem 1983; 48: 3736-3741.
168. (a) Evans DA, Sacks CE, Kleschick WA, Taber TR. J Am Chem Soc 1979; 101: 6789-6791.(b) Houpis IN, Molina A, Lynch J, Rramer RA, Volante RP, Reider PJ. J Org Chem 1993; 58: 3176-3178.
169. (a) Jones K, Keenan M, Hibbert F. Synlett. 1996; 6:509-510. (b) Cavalier J, Marchand G, Rees J, Marchand-Brynaert J. Synthesis 2001; 5:768-772.
170. Lotowski Z, Gryszkiewiez A, Borowiecka JB, Nikitiuk A, Morzyeki JW. J Chem Res 1999; 11: 662-663.
171. Vazquez J, Gonzalez JL, Marquez F, Pongor G, Boogs JE. J Phus Chem 2000; 104: 2599-2612.
172. Fourrey JL, Beauhaire J, Yuan CW. J Chem Soc, Perkin Trans-1 1987; 1841-1843.
173. Figge A, Altenbach HJ, Braauer DJ, Tielmann P. Tetrahedron: Asymmetry-13 2002; 13(2): 137-144.
174. Yildiz-Oren I, Yalcin I, Aki-Sener E, Ucarturk N, Eur. J. Med. Chem. 2004, 39,291.
175. Ireland R E, Daub J.P., Tetrahedron Letters, 1982, 23(34), 3471-3474.
176. Zhang P., Du C Y, Li Y. Acta Cryst. 2006,E62, 5862-5863.
177. Leurs R., Chazot P.L., Shenton FC et al. Br. J. Pharmacol. 2009,157(1), 14-23.
178. Azarifar D, Maleki B. Setayeshanazar M. Phos. Sulf. & Slicon Related Element. 2009,184(8) 2097-2102.
179. Terashima M and Ishii M 1982 *Synthesis* 1484
180. Villemin D, Hammadi M, Martin B. Synth Commun 1996; 26: 2895-2899.
181. Pottorf RS, Chadha NK, Katkevics M, Ozola V, Suna E, Ghane H, Regberg T, Player MR. Tetrahedron Lett 2003; 44:175-178.
182. Hein DW, Alheim RJ, Leavitt JJ. J Am Chem Soc 1957; 79:427-429.
183. Terashima M, Ishii M. Synthesis 1982; 6: 484-485.
184. Beaulieu PL, Haché B, von Moos E. Synthesis 2003; 11: 1683-1692.
185. Chakraborti AK, Rudrawar S, Kaur G Sharma L. Synlett 2004; 9:1533-1536; b) Dolbier Jr WR, Burkholder CR, Médebielle M. J Fluorine Chem 1999;95:127-130.
186. (a) Varma R S, Saini R K and Prakash O 1997 *Tetrahedron Lett.* **38** 2621; (b) Prakash O, Pannu K and Kumar A 2006 *Molecules* **11** 43
187. Varma R S and Kumar D 1998 *J. Heterocycl. Chem.* **35** 1539
188. Park K H, Jun K, Shin S R and Oh S W 1996 *Tetrahedron Lett.* **37** 8869
189. Srivastava R G and Venkataramani P S 1988 *Synth. Commun.* **18** 1537
190. Nakagawa K, Onoue H and Sugita J 1964 *Chem. Pharm. Bull.* **12** 1135
191. Stephens F F and Bower J D 1949 *J. Chem. Soc.* 2971
192. Chang J, Zhao K and Pan S 2002 *Tetrahedron Lett.* **43** 951
193. Talapatra S K, Chaudhuri P and Talapatra B 1980 *Heterocycles***14** 1279
194. Kidwai M, Bansal V, Saxena A, Aerry S and Mozumdar S 2006 *Tetrahedron Lett.* **47** 8049
195. Kawashita Y, Nakamichi N, Kawabata H and HayashiM 2003 *Org. Lett.* **5** 3713
196. Speier G 1987 *J. Mol. Catal.* **41** 253
197. Haginiwa J, Higuchi Y and Ohtsuka H 1976 *Yakugaku Zasshi* **96** 209
198. (a) Huxley A 2006 *Synlett* 2658; (b) Pottorf R S, Chadha N K, Katkevics M, Ozola V, Suna E, Ghane H, Regberg T and Player M R 2003 *Tetrahedron Lett.* **44** 175
199. Bonnamour J and Bolm C 2008 *Org. Lett.* **10** 2665
200. Chen Y and Xie N 2006 *J. Photochem. Photobiol.A; Chem.* **179** 320; (b) Chen Y and Zeng De X 2004 *J.Org. Chem.* **69** 5037; (c) Li Z-X, FuW-F, YuM-M, Zhao X-J and Chen Y 2007 *Dyes Pigments* **75** 516;

201. (a) Chen W H and Pang Y 2009 *Tetrahedron Lett.* **50** 6680; (b) Gottumukkala A L, Derridj F, Djebbar S and Doucet H 2008 *Tetrahedron Lett.* **49** 2926; (c) Alagille D, Baldwin R M and Tamagnan G D 2005 *Tetrahedron Lett.* **46** 1349;
202. Gravatt, G. L.; Baguley, B. C.; Wilson, W. R.; Denny, W. A. *J. Med. Chem.* **1994**, *37*, 4338.
203. Ravindra, K. C.; Vagdevi, H. M.; Vaidya, V. P. *ARKIVOC* **2008**, *(xi)*, 1.
204. Hubschwerlen, C.; Pflieger, P.; Specklin, J. L. *J. Med. Chem.* **1992**, *35*, 1385.
205. Zhan, Z. H.; Liang, Y.; Yong, W. M. *Catal. Commun.* **2007**, *8*, 1126
206. Denny, W. A.; Rewcastle, G. W.; Baguley, B. C. J. Med. Chem.1990, 33, 814.
207. Fonseca, T.; Gigante, B.; Gilchrist, T. L. Tetrahedron 2001, 57,1793.
208. Porcari, A. R.; Devivar, R. V.; Kucera, L. S.; Drach, J. C.;Townsend, L. B. J. Med. Chem. 1998, 41, 1252
209. Kim, J. S.; Gatto, B.; Yu, C.; Liu, A.; Liu, L. F.; LaVoie, E. J. Med.Chem. 1996, 39, 992.
210. Zarrinmayeh, H.; Zimmerman, D. M.; Cantrell, B. E.; Schober, D. A.; Bruns, R. F. Bioorg. Med. Chem. Lett. 1999, 9, 647.
211. Zarrinmayeh, H.; Nunes, A.; Ornstein, P.; Zimmerman, D.; Arnold,B.; Schober, D.; Gackenheimer, S.; Bruns, R.; Hipskind, P.; Britton,T.; Cantrell, B.; Gehlert, D. J. Med. Chem. 1998, 41, 2709.
212. Kohara, Y.; Kubo, K.; Imamiya, E.; Wada, T.; Inada, Y.; Naka, T. J. Med. Chem. 1996, 39, 5228.
213. Bradshaw, T. D.; Wrigley, S.; Shi, D. F.; Schulz, R. J.; Paull, K. D.; Stevens, M. F. G. Br. J. Cancer 1998, 77, 745.
214. Palmer, P. J.; Trigg, R. B.; Warrington, J. V. J. Med. Chem. 1971,14, 248.
215. Lau, C. K.; Dufresne, C.; Gareau, Y.; Zamboni, R.; Labelle, M.; Young, R. N.; Metters, K. M.; Rochette, C.; Sawyer, N.; Slipetz, D. M.; Charette, L.; Jones, T.; McAuliffe, M.; McFarlane, C.
216. Ford-Hutchinson, W. Bioorg. Med. Chem. 1995, 5, 1615.
217. Chakraborti, A. K.; Selvam, C.; Kaur, G.; Bhagat, S. Synlett 2004,851.
218. Lee, K. J.; Janda, K. D. Can. J. Chem. 2001, 79, 1556.
219. Weidner-Wells, M. A.; Ohemeng, K. A.; Nguyen, V. N.; Fraga-Spano, S.; Macielag, M. J.; Werblood, H. M.; Foleno, B. D.; Webb, G. C.; Barrett, J. F.; Hlasta, D. J. Bioorg. Med. Chem. Lett. 2001, 11, 1545.
220. (a) Yadagiri, B.; Lown, J. W. Synth. Commun. 1990, 20, 955.
221. (b) Harapanhalli, R. S.; McLaughlin, L. W.; Howell, R. W.; Rao, D. V.; Adelstein, S. J.; Kassis, A. I. J. Med. Chem. 1996, 39, 4804.
222. Bhatnagar, I.; George, M. V. Tetrahedron 1968, 24, 1293.
223. Verner, E.; Katz, B. A.; Spencer, J. R.; Allen, D.; Hataye, J.;Hruzewicz, W.; Hui, H. C.; Kolesnikov, A.; Li, Y.; Luong, C.; Martelli, A.; Radika, K.; Rai, R.; She, M.; Shrader, W.; Sprengeler, P. A.; Trapp, S.; Wang, J.; Young, W. B.; Mackman, R. L. J. Med.Chem. 2001, 44, 2753.
224. Patzold, F.; Zeuner, F.; Heyer, T. H.; Niclas, H. J. Synth. Commun. 1992, 22, 281.
225. Chikashita, H.; Nishida, S.; Morita, Y.; Itoh, K.Bull. Chem. Soc. Jpn. 1987, 60, 737.
226. Stephens, F. F.; Bower, J. D. J. Chem. Soc. 1949, 2971.
227. (a) Chikashita, H.; Nishida, S.; Miyazaki, M.; Morita, Y.; Itoh, K. *Bull. Chem. Soc. Jpn.* **1987**, *60*, 737. (b) Kumar, S.; Kansal, V.; Bhaduri, A. *Indian J. Chem.* **1991**, *20B*, 254. (c) Lombardy, R. L.; Tanious, F. A.; Ramachandran, K.; Tidwell, R. R.; Wilson, W. D. *J. Med. Chem.* **1996**, *39*, 1452. (d) Beaulieu, P. L.; Hache, B.; von Moos, E. *Synthesis* **2003**, 1683.
228. (a) Zhang, Z. H.; Yin, L.; Li, Y.; Wang, Y. M. *Catal. Commun.* **2007**, *8*, 1126. (b) Zhang, Z. H.; Yin, L.; Li, Y.; Wang, Y. M. *Tetrahedron Lett.* **2005**, *46*, 889.
229. (a) Chen, C.; Chen, Y. J. *Tetrahedron Lett.* **2004**, *45*, 113. (b) Mayer, J. P; George, S.; Lewis, C. M.; Danute, B. D. *Tetrahedron Lett.* **1998**, *39*, 6655.
230. Sachin M Kumar.U, Prabhat, Sandeep M,Sachin, Int. Journal of PharmTech Research,3[1],2011,62-75

231. Singh, S. P.; Parmar, S. S.; Raman, K.; Stenberg, V. I.Chem. Rev.1981,81, 175.
232. Brown, F. C.Chem. Rev.1961,61, 463.
233. T. Tomasic , L. P. Masic, Curr. Med. Chem., 2009,16,1596.
234. R. Lesyk, B. Zimenkovsky, D. Atamanyuk, F. Jensen, K. Kiec-Kononowicz, A. Gzell,Bioorg. Med. Chem.,2006,14,5230.
235. D. Havrylyuk, B. Zimenkovsky, O. Vasylenko, L. Zaprutko, A. Gzella, R. Lesyk, Eur. J. Med. Chem.,2009, 44, 1396.
236. D.Kaminskyy, B.Zimenkovsky, R. Lesyk, Eur. J.Med.Chem.,2009, 44, 3627.
237. R. Ottana, R. Maccari, M.L. Barreca, G. Bruno, A. Rotondo, A. Rossi, G. Chiricosta, R. Di Paola, L. Sautebin, S. Cuzzocrea, M.G. Vigorita, Bioorg. Med. Chem., 2005, 13, 4243.
238. P. Vicini, A. Geronikaki, M. Incerti, F. Zani, Bioorg. Med. Chem.,2006, 14, 3859.
239. A.A. Elbarbary, A.I. Khodair, E.B. Pedersen, C.Nielsen, Monatsh. Chem.,1994,125, 593.
240. E. Rydzik, A. Szadowska, A. Kaminska, Acta Pol. Pharm.,1984, 41, 459-464.
241. H.L. Liu, Z.C. Li, T. Anthonsen, Molecules, 2000, 5, 1055.
242. B. Samir, K. Wesam, A.F. Ahmed, Eur. J. Med. Chem.,2007, 42, 948.
243. Samarin, A. S.; Loslcutov, V. A.Tr Tomsk. Gos. Utiiv. Ser. Khim.1965,1706, 157.
244. Meher, S. S.; Naik, S.; Behera, R. K.; Nayak, A.J. Indian Chem. Soc.1981,58, 274.
245. Mandlik, J. V.; Patwardham, V. A.; Nargund, K. S.J. Univ. Poona. Sci. Technol.1966,32, 39.
246. Bronson, J. J.; DenBleyker, K. L.; Falk, P. J.; Mate, R. A.; Ho, H. T.; Pucci, M. J.;Snyder, L. B.Bioorg. Med. Chem. Lett.2003,13, 873.
247. Cunico, W.; Gomes, C. R. B.; Vellasco, W. T., Jr.Mini Rev. Org. Chem.2008,5,336.
248. Verma, A.; Saraf, S. K.Eur. J. Med. Chem.2008,43, 897.
249. Hamama, W. S.; Ismail, M. A.; Shaaban, S.; Zoorob, H. H.J. Heterocycl. Chem.2008,45,1
250. Arkovic, R.; Stodanovic, M.Heterocycles2005,56, 2635.
251. Pawar, R. B.; Mulwad, V. V.Chem Heterocycl. Compd.2004,40, 219.
252. Ocal, N.; Aydogan, F.; Yolacan, C.; Turgut, Z. J. Heterocycl. Chem.2003,40, 721.
253. Cunico, W.; Gomes, C. R. B.; Ferreira, M.; Capri, L. R.; Soares, M.; Wardell, S. M.S. V. Tetrahedron Lett.2007,48, 6217.
254. Neuenfeldt, P. D.; Drawanz, B. B.; Siqueira, G. M.; Gomes, C. R. B.; Wardell, S. N.S. V.; Flores, A. F. C.; Cunico, W.Tetrahedron Lett.2010,51, 3106.
255. Pratap, U. R.; Jawale, D. V.; Bhosle, M. R.; Mane, R. A.Tetrahedron Lett.2011,52,1689.
256. Bolli, M. H.; Abele, S.; Binkert, C.; Bravo, R.; Buchmann, S.; Bur, D.; Gatfield, J.;Hess, P.; Kohl, C.; Mangold, C.; Mathys, B.; Menyhart, M.; Meuller, C.; Nayler,O.; Scherz, M.; Schmidt, G.; Sippel, V.; Treiber, A.;Weller, T. J. Med. Chem.2010,53, 4198.
257. Moghaddam, F. M.; Hojabri, L. J. J. Heterocycl. Chem.2007,44, 35.
258. Bolognese, A.; Correale, G.; Manfra, M.; Lavecchia, A.; Novellino, E.; Barone, V. Org. Biomol. Chem.2004, 2, 2809.

**SIGNATURE OF PRINCIPAL INVESTIGATOR** **REGISTRAR**

**UNIVERSITY GRANTS COMMISSION**
**BAHADUR SHAH ZAFAR MARG**
**NEW DELHI – 110 002**

# Summary of Major Research Project

**UGC Reference No.:39-832/2010 (SR)**

**Title of research project**: **Synthesis of nanostructured mono and bimetallic cluster of Cu and Mo and their application as catalyst in various organic reactions.**

The work embodied in this project, with respect to the electrochemical synthesis and characterization of mono and bimetallic nanoclusters of copper and molybdenum is being summarized. This is discussed in three parts namely:

i) Synthesis of mono and bimetallic nanoclusters

ii) Characterization of mono and bimetallic nanoclusters

iii) Catalytic Application mono and bimetallic nanoclusters

## I) Synthesis of mono and bimetallic nanoparticles

The electrochemical reduction method used in the synthesis was found to be highly suitable in the present study. It has allowed the variation in the current density (For Cu 6 & 10 $mA/cm^2$, for Mo 14 & 18 $mA/cm^2$ and for Cu-Mo 10 & 14 $mA/cm^2$) as well as the use of different capping agents (TEAB/TPAB/TBAB). The progress in the electrochemical synthesis of the copper, molybdenum and copper-molybdenum bimetallic colloids and nanoparticles could be visualized. The observations are:

The progress in the electrolysis was visualized by a change in the colour of the reaction mixture which occurred within 20 minutes. A wide range of colors were observed. These were dependent upon the nature of the anode, the capping agent and the current density.

i) The colour exhibited by the copper colloids was dark brown to black.

ii) The molybdenum colloids were yellow in colour.

iii) The Cu-Mo bimetallic colloidal solution showed dark brown black colour.

**II) Characterization mono and bimetallic nanoparticles**

**A) Copper Nanoparticles:**

i) The UV-visible study of the Cu colloids collected after 20 minutes of electrolysis at 6 and 10mA/cm2 current density showed a variation in the optical response. The colloids obtained at 6mA/$cm^2$ of current density show a surface absorbance resonance band in the range of 550 to 700 nm. The sharp peak at 638-642 nm confirms the formation of copper nanoparticles.

ii) The FTIR spectroscopic study of the Cu nanoparticles confirmed the presence of the capping agent in the nanoparticles as a protective covering.

iii) The XRD analysis of the different Cu nanoparticles showed the presence of the characteristic peaks for copper and copper oxide. The 'd' values confirmed that the Cu nanoparticles have a monoclinic structure. The average particle size obtained from the XRD pattern was found to vary with the current density and the nature of the capping agent. The general trend observed was that, with increase in the current density the particle size was found to decrease. The effect of the nature of the capping shows that with the increase in the bulkiness (size) of the capping agent the size of the nanoparticles was found to decrease.

iv) The SEM analysis of Cu nanoparticles revealed the surface as agglomerated and porous.

v) EDS analysis shows the formation of copper oxide nanoparticles.

vi) The TEM analysis of the Cu nanoparticles helped to determine the shape and size of the nanoparticles. The TEM photographs showed that the nanoparticles have a nearly spherical shape, with edges in some case. The size of the various Cu nanoparticle samples was found to be in the range of 4 to 20 nm. It was observed that the size of the nanoparticles decrease with the increase in current density, as well as with the increase in the size of the capping agent.

**B) Molybdenum Nanoparticles:**

i) The UV-visible study of the Mo colloids collected after 20 minutes of electrolysis showed a variation in the optical response. The colloids show a surface absorbance resonance band in the range of 600 to 850 nm.

ii) The FTIR spectroscopic study of the Mo nanoparticles confirmed the presence of the capping agent in the nanoparticles as a protective covering.

iii) The XRD analysis of different Mo nanoparticles showed the presence of the characteristic peaks for molybdenum and molybdenum oxide. The'd' values confirmed that the Mo nanoparticles has orthorhombic structure.

iv) The SEM analysis of molybdenum oxide nanoparticles revealed the surface morphology change after calcination at 500°C.

v) EDS analysis showed the formation of molybdenum oxide nanoparticles.

vi) The TEM analysis of the molybdenum oxide nanoparticles showed that the nanoparticles have square, cubical and rod shape. The size of the various Mo nanoparticle samples was found to be in the range of 20 to 100 nm.

**C) Cu-Mo Bimetallic Nanoparticles:**

i) The coloured Cu-Mo colloids prepared using TEAB/TPAB/TBAB as capping agents and current density of 10 and 14mA/cm2 showed formation of the Cu-Mo samples in the alloy form.

ii) The FTIR spectra of Cu-Mo bimetallic nanoparticles confirmed that capping took place during synthesis of these nanoparticles.

iii) The XRD study showed characteristics peaks for Cu-Mo phase in the form of an alloy.

iv) The surface structure of the Cu-Mo bimetallic nanoparticles studied by SEM showed agglomerated particles with irregular shape.

v) EDS confirmed the formation of Cu-Mo bimetallic nanoparticles.

vi) TEM studies of the Cu-Mo bimetallic nanoparticles revealed the shape as nearly spherical and the size was found in the range of 5.0 nm to 60.0 nm.

**III) CATALYTIC APPLICATION OF MONO AND BIMETALLIC NANOPARTICLES**

The Cu monometallic nanoparticles were used as catalysts in various organic reactions. The Cu nanoparticles were used as catalysts in Knoevenagel condensation reaction of aromatic aldehyde and barbituric acid solvent free as room temperature, synthesis of 2-benzylidenemalononitrile and synthesis of 1,2-dibenzylidenehydrazine. These reactions required simple work set and shorter reaction time. The Cu nanoparticles were efficient, stable and reusable catalysts. The representative products of organic reactions were characterized by using FTIR, $^{1}$H-NMR, and $^{13}$C-NMR analysis.

The synthesized Mo monometallic nanoparticles were used in organic reaction as catalysts in synthesis of α,α' Bis ( substituted arylidene ) cyclohexanone [(2E,6E)-2,6-

dibenzylidenecyclohexanone], synthesis of (1E,4E)-1,5-diphenylpenta-1,4-dien-3-one, synthesis of 2-phenylbenzo[d]thiazole and 2-phenylbenzo[d]oxazole. These reactions required simple workup process and short reaction time. Mo nanoparticles act as very efficient, stable and reusable catalyst. The representative product of organic reactions were characterized by using FTIR, $^{1}$H-NMR and $^{13}$C-NMR analysis.

The synthesized CuMo bimetallic nanoparticles were used in organic reaction as catalysts in synthesis of 2-phenylbenzo[d]thiazole, 2-phenylbenzo[d]imidazole, 2-phenylbenzo[d]oxazole and (2Z,5E)-2,5-dibenzylidenethiazolidin-4-one. These reactions required simple workup process and short reaction time. CuMo nanoparticles were very efficient, stable and reusable catalysts. The representative product of organic reaction characterized by using FTIR, $^{1}$H-NMR, $^{13}$C-NMR and Mass spectroscopic analysis.

**SIGNATURE OF PRINCIPAL INVESTIGATOR** **REGISTRAR**

## List of Publication

1. Sunita Jadhav, Priyanka L. Anandgaonker, Ganesh Kulkarni, Suresh T. Gaikwad, **Anjali S. Rajbhoj**, Microwave-Assisted One-Pot Synthesis of Octahydroquinazolinone Derivatives Using Molybdenum Oxide Nanoparticles in Solvent-Free Condition. ***Journal of Cluster Science***, 25, pp. 1389-1399, 2014, DOI 10.1007/s10876-014-0716-2. **Impact Factor: 1.664**
2. Dighore N.R., Anandgaonker P.L., Gaikwad S.T. and **Rajbhoj A.S**., Solvent free green Synthesis of 5-arylidine Barbituric acid Derivatives Catalyzed by Copper oxide Nanoparticles. ***Research Journal of Chemical Sciences,*** Vol. 4(7), pp. 93-98, (2014). **Impact Factor: 0.654**
3. N. R. Dighore, S. P. Jadhav, S. T. Gaikwad, **A. S. Rajbhoj**, Electrochemical Synthesis of MoO3 Nanoparticles Effect of Temperature Convert to MoO3 Nanorods. ***Int. Journal of Engineering Research and Applications,*** Vol. 4, Issue 7(5), pp.135-139, 2014. **Impact Factor: 1.69**
4. N. R. Dighore, S. P. Jadhav, S. T. Gaikwad, **A. S. Rajbhoj**, Nanosized $MoO_3$ as a reusable heterogeneous catalyst for the Synthesis of α,α- Bis (substituted-benzylidene) cyclohexanones. ***Material Science-Poland*** Vol. 33(1), pp. 163-168, 2015. **Impact Factor: 0.533**
5. N. R. Dighore, S. P. Jadhav, S. T. Gaikwad, **A. S. Rajbhoj**, Copper Oxide Nanoparticles synthesis by electrochemical method. ***Material Science*** Vol. 22 (2), pp. 170-173, 2016. **Impact Factor: 0.62**
6. Dighore N.R., Anandgaonker P.L., Gaikwad S.T. and **Rajbhoj A.S** Green synthesis of 2-aryl benzothiazole heterogenous catalyzed by $MoO_3$ nanorods. ***Green processing and Synthesis***, Vol. 5(2), pp.139-143, 2016. **Impact Factor: 1.291**
7. N. R. Dighore, S. P. Jadhav, S. T. Gaikwad, **A. S. Rajbhoj,** Molybdenum Oxide Nanoparticles as Antimicrobial Agents ***Journal of Cluster Science***, June 2016 DOI 10.1007/s10876-016-1048-1. **Impact Factor: 1.664**